Expression of alternative oxidase (AOX) in the filamentous fungus *Neurospora crassa.*

by

Nishka Kishore

A thesis submitted in partial fulfillment of the requirements for the degree of

Master of Science

in
Molecular Biology and Genetics

Department of Biological Sciences
University of Alberta

Abstract

When chemical inhibitors or mutations impair the standard mitochondrial electron transport chain (sETC) in *Neurospora crassa*, alternative oxidase (AOX) is induced. AOX transfers electrons directly from coenzyme Q to oxygen, thus bypassing the later steps of the sETC. In *N. crassa* AOX is encoded by the nuclear *aod-1* gene. Over the years, some genes playing a role in the expression of AOX have been identified using traditional genetic screens. More recently, the gene knockout (KO) library of *N. crassa* was screened for mutants unable to grow in the presence of antimycin A (AA), an inhibitor of Complex III of the sETC. AOX levels in such mutants were determined using western blotting following growth in the presence of chloramphenicol (Cm, inhibitor of mitochondrial translation).

Eight new mutants with severe AOX deficiencies were identified. As part of this thesis, in an attempt to further characterize two of these strains, it was found that the AOX deficiency in them could not be rescued by transformation with the wild-type gene thought to be affected in each strain. This led to a detailed analysis of all eight AOX deficient KO mutants. PCR amplification analysis, Southern blotting and crossing the KO mutants with wild-type strains suggested the presence of additional secondary random mutation(s), in the genome of seven of the eight KO mutant strains tested. Sequencing the *aod-1* gene from the remaining seven strains suggested the presence of an identical frame-shift mutation in the coding region of the *aod-1* gene in two of these KO strains. This frame-shift leads to production of a truncated AOX protein due to the occurrence of a premature stop codon. The other five KO strains have a wild-type *aod-1* gene. Thus, they likely carry secondary mutation(s) in a regulatory gene for AOX production.

The KO mutant library screen also identified strains that showed very poor or no growth in the presence of AA but had virtually normal levels of AOX protein under Cm inducing conditions. The proteins affected in these mutants were thought to play a role in assembly of AOX into a functional protein or its insertion into the MIM. As part of this thesis, five such KO strains were tested by carbonate extraction to determine the possibility of aberrant membrane association of AOX in these mutants. No conclusions could be reached based on these experiments.

Acknowledgements

I would like to express my sincere gratitude to my supervisor Dr. Frank Nargang for his guidance, encouragement and constant support throughout the course of my degree.

I am grateful to my examination committee, Dr. Martin Srayko, Dr. John Locke and Dr. Andrew Waskiewicz for their valuable time and support. I am also grateful to Dr. John Locke for providing me with positively charged nylon membrane for Southern blotting, Dr.Richard Rachubinski and late Mr. Rick Poirier (former lab technician in the Rachubinski lab) for help with cytochrome spectra generation and analysis, Dr. Kirst King-Jones for granting me access to the RT-PCR machine and members of the King-Jones lab for their technical insights and support.

I would also like to thank the past and present members of the Nargang lab including Zhigang Qi, Natasa Bosnjak, Sebastian Lakey, Beau Desaulniers and Jeremy Wideman for their advice and technical assistance. Special thanks to Kelly Adames for designing several plasmids that I used throughout my study. I am extremely thankful to Kelly Adames and Annie Wong for helping me out and training me when I was new to the lab. I would also like to thank the staff at the Molecular Biology Services Unit (MBSU) including Cheryl Nargang, Sophie Dang and Troy Locke for all their help and technical assistance.

I would like to acknowledge my entire family including, my father Deepak Kishore, mother, Vibha Kishore, sister Vartika Kishore and brother-in-law Harshit Jaiswal for always supporting me, encouraging me and motivating me to perform to the best of my abilities. I would also like to express my sincere gratitude to all my friends, who were my family away from home, and were always there for me through good times and bad.

Table of Contents

List of Figures

List of Tables

List of Abbreviations

Δ	deletion
°C	degree Celsius
µg	microgram
µL	microliter
µm	micrometer
A	adenine or alanine
AA	antimycin A
AMP	adenosine monophosphate
Amp	ampicillin
Amp^R	ampicillin resistance
AOX	alternative oxidase
ATP	adenosine triphosphate
Bm	bleomycin
Bm^R	bleomycin resistance (conferred by the *ble* gene)
C	cytosine
cDNA	complementary DNA
cfu	colony forming units
CJ	cristae junction
cm	centimeter
Cm	chloramphenicol
CM	cristae membrane
CoQ	coenzyme Q/ ubiquinone
Cys	cysteine
dH_2O	distilled water
DIC	differential interference contrast
DNA	deoxiribonucleic acid
E	glutamic acid
$FADH_2$	flavin adenine dinucleotide
g	gram(s)
G	guanine

GFP	green fluorescent protein
GMP	guanosine monophosphate
GTP	guanosine triphosphate
H	histidine
HA	hemaglutinin
hr	hour(s)
Hyg^R	hygromycin resistance (conferred by the *hph* gene)
IBM	inner boundary membrane
IMS	intermembrane space region
Kb	kilobasepair(s)
kDa	kilodalton(s)
KO	knockout
L	liter
LB	luria Bertani medium
M	molar
MBSU	molecular biology services unit
mg	microgram(s)
MICOS	mitochondrial contact site and cristae organizing system
MIM	mitochondrial inner membrane
min	minute(s)
mL	milliliter
mM	millimolar
MMP	mitochondrial membrane potential
MOM	mitochondrial outer membrane
MOPS	4-morpholinepropanesulfonic acid
mRNA	messenger RNA
mtDNA	mitochondrial DNA
$NaCO_3$	sodium carbonate
NADH	nicotinamide adenine dinucleotide reduced form
ng	nanogram(s)
nM	nanomolar

PAGE	polyacrylaminde gel electrophoresis
PCR	polymerase chain reaction
PMSF	phenylmethylsulfonyl fluoride
qPCR	quantitative real time PCR
RNA	ribonucleic acid
RNAase	ribonuclease
rRNA	ribosomal RNA
RT-PCR	reverse transcriptase PCR
SDS	sodium dodecyl sulfate
sETC	standard electron transport chain
T	thymine
TCA cycle	tricarboxylic acid cycle
TCA	Trichloroacetic acid
TIM	translocase of the inner membrane
TMD	transmembrane domain
TOM	translocase of the outer membrane
tRNA	transfer RNA
VSuTB	Vogel's sucrose medium

Chapter 1: Introduction

1.1 Mitochondrial structure, morphology and dynamics

Mitochondria are multifunctional organelles found in almost all eukaryotic cells. Although mitochondria vary in size, depending on cell type and physiological conditions, they generally have a diameter of 0.5-1μm (GRIPARIC and VAN DER BLIEK 2001). They are made up of two membranes, termed the mitochondrial inner membrane (MIM) and the mitochondrial outer membrane (MOM). The existence of the two membranes divides the mitochondria into four functionally distinct regions: the MIM, MOM, the intermembrane space region (IMS) and the matrix.

The MIM is a highly convoluted structure and forms invaginations called cristae. The MIM can be further subdivided into the inner boundary membrane (IBM) and the cristae membrane (ZICK *et al.* 2009). The IBM is the part of the MIM that is in parallel to the outer membrane while the MIM that forms the cristae is known as the cristae membrane (CM). The composition of these two forms of the MIM is known to differ (VAN DER LAAN *et al.* 2012). The outer membrane and the inner membrane also form contact sites (CSs). These are regions where the two membranes are in close proximity to each other. These contact regions are thought to facilitate protein import. The translocases of the MOM and MIM, the TOM (translocase of the outer membrane) and TIM23 (translocase of the inner membrane) complexes respectively, seem to be in close contact at these sites (LOGAN 2006; VAN DER LAAN *et al.* 2012; PFANNER *et al.* 2014). These features are shown in Fig. 1.

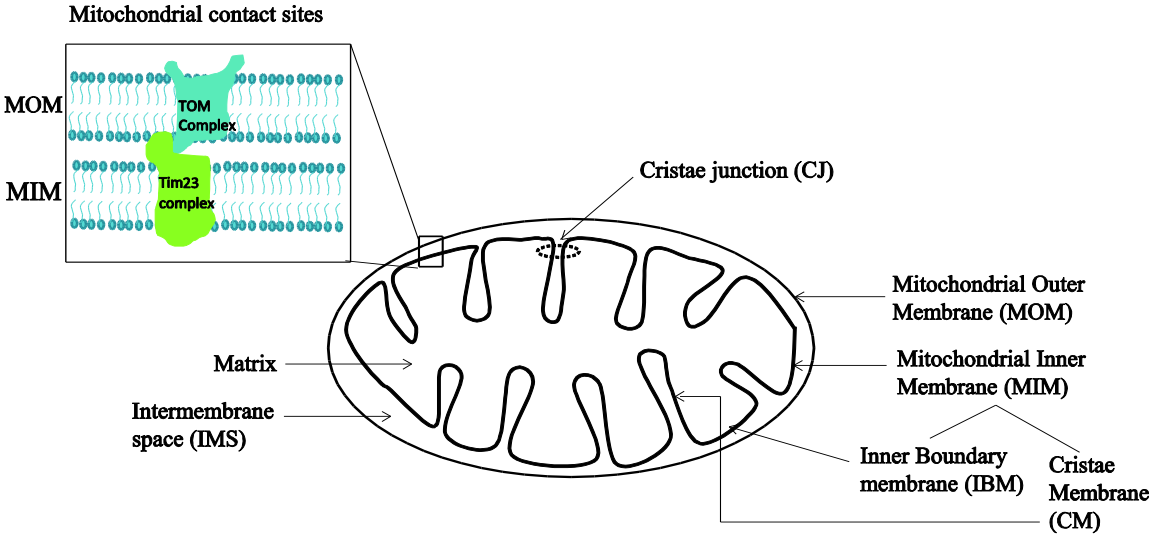

Figure 1. Mitochondrial structure and subcompartmentalization. The presence of two membranes divides the mitochondria into four sub-compartments: the MOM, the MIM, the IMS and the matrix. The MIM is further subdivided into the IBM and the CM. The cristae are connected to the IBM via narrow tubular regions called the CJs. The MOM and the MIM also form regions of close proximity termed contact sites. The TOM and TIM23 complexes seem to be in close contact at these sites facilitating efficient transport of precursor proteins into the mitochondria.

Electron microscopy images have revealed that cristae are not merely wide in-foldings or invaginations of the MIM (as proposed by the 'baffle model'), but are microcompartments that are connected to the IBM via narrow tubular regions termed cristae junctions (CJs) (LOGAN 2006; MANNELLA 2008). One proposed functional consequence of the cristae junction is that these narrow tubular regions may limit metabolite diffusion into and out of the cristae thus playing a regulatory role in certain mitochondrial processes (MANNELLA 2006; ZICK *et al.* 2009; HERRMANN and RIEMER 2010).

A highly conserved (from yeast to humans) hetero-oligomeric protein complex of the MIM, the mitochondrial contact site and cristae organizing system (MICOS) complex (PFANNER *et al.* 2014), exists predominantly at the CJs. The complex has been shown to play a role in formation and maintenance of CSs and maintenance of CJs (MUN *et al.* 2010; HARNER *et al.* 2011; HEAD *et al.* 2011; HERRMANN 2011; HOPPINS *et al.* 2011; VON DER MALSBURG *et al.* 2011; PFANNER *et al.* 2014; HORVATH *et al.* 2015). The MICOS complex has also been shown to interact with proteins and protein complexes of the MOM (HARNER *et al.* 2011; HOPPINS *et al.* 2011; KÖRNER *et al.* 2012; ZERBES *et al.* 2012; PFANNER *et al.* 2014; HORVATH *et al.* 2015).

The MOM houses protein complexes, such as the TOM complex, that play an important role in import of nuclear encoded mitochondrial proteins into the mitochondria (GELLERICH *et al.* 2000; SCHMITT *et al.* 2006; LISTER *et al.* 2007; BECKER *et al.* 2009; ENDO and YAMANO 2010; DUDEK *et al.* 2013). Other proteins embedded in the MOM are involved in maintenance of mitochondrial morphology, lipid homeostasis, apoptosis, fission and fusion processes and in the transport of metabolites into the mitochondria

(KORNMANN and WALTER 2010; FRIEDMAN *et al.* 2011; LINDSAY *et al.* 2011; OSMAN *et al.* 2011; MISHRA and CHAN 2014). The inner membrane (MIM) is a protein rich compartment, housing proteins known to play a role in protein import, such as the TIM23 complex (enriched in the IBM), components of the respiratory chain and ATP synthase (enriched in the CM), and many proteins involved in transport of metabolites (BECKER *et al.* 2009). The intermembrane space contains several soluble proteins. This compartment includes proteins involved in shuttling MIM or matrix targeted proteins to the import machinery of the MIM, proteins involved in exchange of metals and proteins that play a role in lipid homeostasis or exchange of lipids between the mitochondrial membranes (HERRMANN and RIEMER 2010; AFRODITI and KOSTAS 2013). The IMS also houses Mia40 and Erv1 which are involved in the disulfide relay system for import of a structurally related class of proteins into the IMS (HERRMANN and RIEMER 2012). The mitochondrial matrix is the site of several important metabolic processes such as the citric acid cycle. The matrix also harbors the mtDNA (mitochondrial DNA) and mitochondrial ribosomes as well as the enzymes involved in transcription and translation of mtDNA genes (GRIFFITHS *et al.* 1995).

Mitochondria are highly dynamic organelles and undergo constant fusion, fission and movement along the cytoskeletal network. These dynamic changes are influenced by the cell type, the metabolic state of the cell and the organelle, and by environmental conditions (VAN DER BLIEK *et al.* 2013).

Fusion of mitochondria and formation of large interconnected networks seems to be important in cells that have a high demand for ATP (i.e. metabolically active cells). Fused mitochondria also seem to play a role in calcium signaling and in mixing contents

of mitochondria, which may be beneficial in alleviating errors caused by accumulating mtDNA damage in certain mitochondria (WESTERMANN 2008). Mitochondrial fission on the other hand seems to play a role in apoptosis, as prior to cytochrome c release, mitochondria in the cell appear to undergo rapid fragmentation by fission (YOULE and KARBOWSKI 2005).

A delicate balance between biogenesis, fission and fusion determines the number, size and shape of mitochondria in a cell. If this balance is perturbed the mitochondria can become fragmented (if fusion is reduced) or can become highly fused and form elongated, interconnected networks (if fission is reduced) (CHAN 2006; BERMAN *et al.* 2008; WESTERMANN 2008; CHAN 2012). Defects in fission or fusion proteins have been linked to human diseases and lethality during gestation in knockout mice (CHEN and CHAN 2010; CHAN 2012).

Mitochondria move throughout the cell and interact with each other (via fission and fusion) using the cytoskeletal elements and their associated motor proteins in the cell (BOLDOGH and PON 2007). Association of mitochondria to the cytoskeletal elements is also important for efficient inheritance of mitochondria by daughter cells. The inheritance of mitochondria by daughter cells has been studied in great detail in the budding yeast *Saccharomyces cerevisiae* and actin microfilaments seem to play a major role in this process. Mitochondria in this budding yeast appear to move in an anterograde (movement towards the developing bud) and a retrograde manner (movement towards the mother cell) (FREDERICK and SHAW 2007; WU *et al.* 2013) .

Microtubules play a major role in the movement of mitochondria in fission yeasts, in pollen tubes (in higher plants), neurons and also in filamentous fungi (FREDERICK and

SHAW 2007). Microtubule-associated motor proteins, kinesins and dyneins are involved in movement of mitochondria along the microtubules (SAXTON and HOLLENBECK 2012; MISHRA and CHAN 2014). Kinesins help transport mitochondria in an anterograde fashion, whereas dyneins transport mitochondria in a retrograde manner. Several adaptor and linker proteins have been proposed to be involved in mitochondrial motility along cytoskeletal tracks.

1.2 Mitochondrial origin

The endosymbiotic origin of plastids was first speculated upon in 1905 by Konstantin Mereschkowski. In 1923, Ivan Wallin proposed that mitochondria have bacterial origins (WALLIN 1923; MARTIN and KOWALLIK 1999; MCINERNEY *et al.* 2014). However, this idea that mitochondria have bacterial origins and the general theory of endosymbiosis were not well accepted until the concepts were reintroduced by Lynn Margulis in 1967 (SAGAN 1967; MARGULIS 1970; ARCHIBALD 2011).

It is now well accepted that mitochondria originated from an endosymbiotic relationship between a bacterium and a host cell more than 1.5 billion years ago (DYALL *et al.* 2004; GROSS and BHATTACHARYA 2009; MCINERNEY *et al.* 2014). Various lines of evidence support the theory that the mitochondrial ancestor was most likely an α-proteobacterium. Sequencing data for the large and small subunit rRNAs from several eukaryotic mitochondrial and bacterial species, suggests that ancestors of the mitochondria probably originated from the order Rickettsiales within the α-proteobacterium class of bacteria (YANG *et al.* 1985; GRAY 2012). In addition, the lifestyle of several α-proteobacterium species suggests possible mechanisms that led to their acquisition as mitochondria. The class α-proteobacteria consists of several species

that form intracellular associations with several simple and complex eukaryotes (BATUT *et al.* 2004). An unusual example of such an interaction is the association of *Holospora obtuse* with a *Paramecium*. The endosymbiont migrates into the macronucleus of the *Paramecium* and once it has multiplied and matured it leaves the host cell without causing any apparent damage to the cell (LANG 2014). Just as in mitochondria, several Rickettsiales species have undergone reductive genome evolution, or loss of genes over evolutionary time, further supporting the idea that the mitochondrial ancestor was most likely an α-proteobacterium (BATUT *et al.* 2004). In case of the mitochondria, genes encoded originally by the ancestral mitochondrial endosymbiont are believed to have been transferred to the nucleus by EGT (endosymbiotic gene transfer) (TIMMIS *et al.* 2004; O'MALLEY 2010)).

Although the idea of mitochondria originating from an α-proteobacterial endosymbiont is widely accepted, the nature of the host, the nature of the association between host and endosymbiont, and the timeline of the transition of this endosymbiotic cell into a eukaryote is still unclear and highly debated (O'MALLEY 2010; VAN DER GIEZEN 2011; MCINERNEY *et al.* 2014). Many hypotheses have been suggested to explain the evolution of eukaryotes. These include the 'three domain hypothesis' which suggests that eukaryotes, eubacteria and archaebacteria are monophyletic lineages with the eukaryotes and archaebacteria sharing a common ancestor (WOESE 1987; MCINERNEY *et al.* 2014). Another hypothesis proposed by LAKE *et al.* (1984) called the 'eocyte hypothesis' suggests that eukaryotes evolved from a branch of archaebacteria called eocytes (MCINERNEY *et al.* 2014). RIVERA and LAKE (2004) further postulated the 'ring of life hypothesis' which suggests that eukaryotes arose from the merger of a

eubacterium with an eocyte. Several lines of evidence, including the observation that the eukaryotic nuclear genome appears to be a mix of genes having both archaebacterial and bacterial origin (RIBEIRO and GOLDING 1998; ANDERSSON 2013; MCINERNEY *et al.* 2014), point towards eukaryogenesis resulting from the merger of two prokaryotes. However, debate on the nature and origin of the first eukaryote continues (MCINERNEY *et al.* 2014).

1.3 Mitochondrial DNA

Mitochondria contain their own DNA called mitochondrial DNA (mtDNA). The mtDNA of all eukaryotes seems to encode two categories of products. The first are genes that play a role in protein synthesis machinery of the mitochondria (e.g., tRNA genes and mitochondrial rRNA genes). The second category includes genes for proteins that are subunits of the complexes of the oxidative phosphorylation process (SACCONE 2011). mtDNA in most species is a circular double stranded molecule, but several species containing other mtDNA organizations have also been observed. These genome organizations include single or multiple linear chromosomes. Examples of organisms possessing a single linear mtDNA molecule include some fungi, apicomplexans, most ciliates and many cnidarians (BURGER *et al.* 2003; SACCONE 2011; BERNT *et al.* 2013). mtDNA in the fungus *Spizellomyces punctatus* and the animal species *Globodera* and *Dicyema* exists as a population of multiple circular DNA molecules with different circular molecules encoding a different set of mitochondrial proteins (WATANABE *et al.* 1999; ARMSTRONG *et al.* 2000; BURGER *et al.* 2003; BURGER and LANG 2003). Other organisms (e.g. trypanosomatid parasites) have been observed to possess both maxi and mini circular molecules (BURGER *et al.* 2003). Trypanosomatid mtDNA is called

kinetoplastid DNA (kDNA) and is a network of topologically interlocked maxi circles (encoding typical mitochondrial proteins and rRNA, but not tRNA) and mini circles (encoding guide RNAs that play a role in editing maxicircle mRNAs) (SHAPIRO and ENGLUND 1995; MORRIS *et al.* 2001; SHLOMAI 2004).

The size of the mitochondrial genome varies considerably among eukaryotes. The average mtDNA molecule is about 15-60 Kb depending on the organism (BURGER *et al.* 2003). However, the possible range in size of the mitochondrial genome is large. For example, that of *Plasmodium falciparum* is only 6 Kb while that of many land plants approaches 1 Mb (ROUSSEAU-GUEUTIN *et al.* 2012; BERNT *et al.* 2013). The average size of fungal mtDNA ranges from 18-175 Kb (BURGER *et al.* 2003). *Neurospora crassa* contains a single circular 64,840 bp mtDNA molecule that encodes 28 proteins, 28 tRNA molecules and 2 rRNA molecules (BORKOVICH *et al.* 2004; MCCLUSKEY 2012).

1.4 Mitochondrial functions

Mitochondria are most notably known for the role they play in the production of energy in the form of ATP by the process of oxidative phosphorylation. Most of the substrates for this process are produced via the Krebs cycle.

The Krebs cycle (also known as the citric acid cycle or the tricarboxylic acid (TCA) cycle) takes place in the mitochondrial matrix. Acetyl-CoA generated by glycolysis, β-oxidation of fatty acids or breakdown of certain amino acids undergoes condensation with oxaloacetate (OAA) to generate citrate (OSELLAME *et al.* 2012). The Krebs cycle proceeds through several oxidation steps that lead to carbon dioxide production, regeneration of OAA, production of electron donors $NADH+H^+$ and $FADH_2$, and phosphorylation of GDP to GTP (Fig. 2). Some Krebs cycle intermediates can serve as

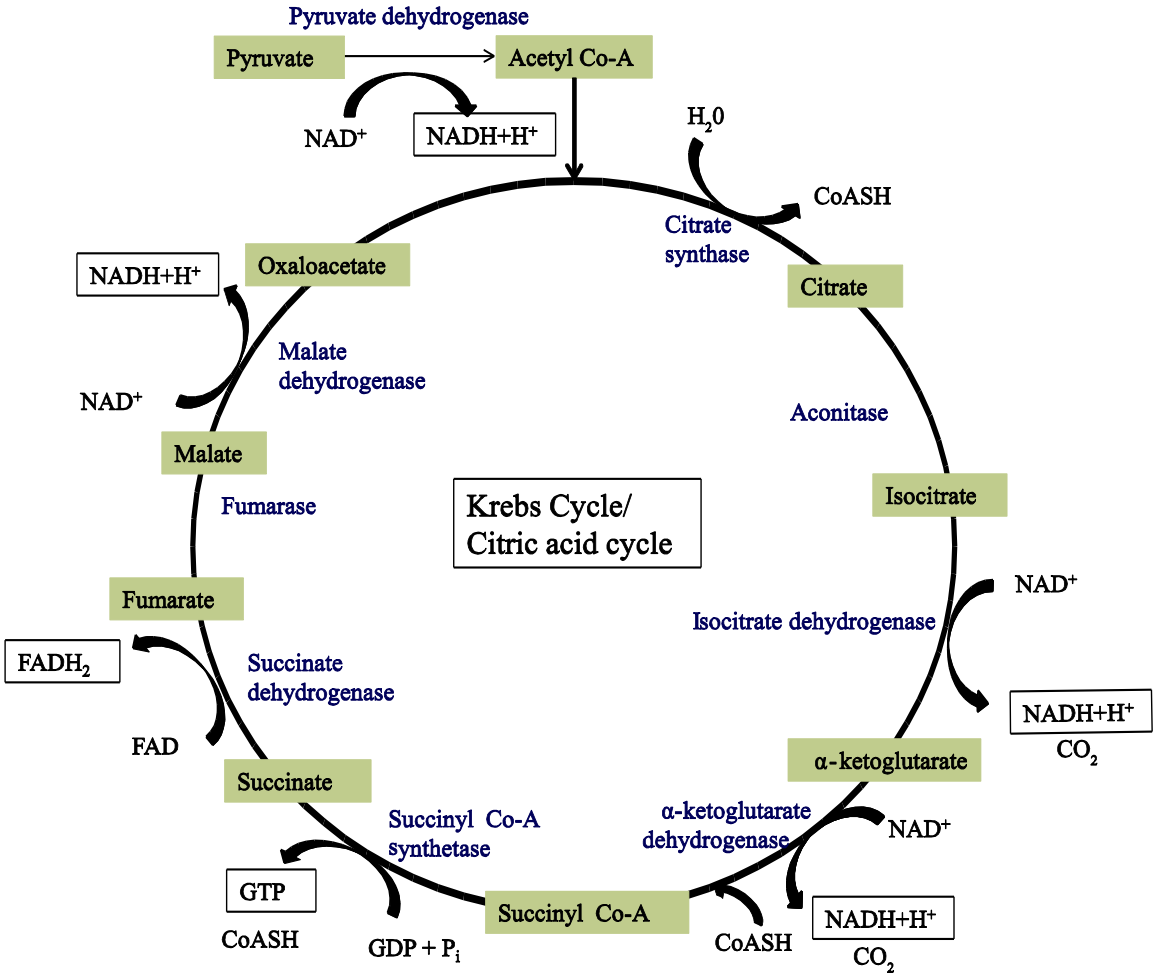

Figure 2. Basic schematic of the Krebs cycle. The Krebs cycle takes place in the mitochondrial matrix. Glycolysis, β-oxidation of fatty acids or breakdown of certain amino acids generates acetyl-CoA which undergoes condensation with oxaloacetate (OAA) to generate citrate. Regeneration of OAA and production of electron donors $NADH+H^+$ and $FADH_2$ as well as CO_2 and GTP takes place as a consequence of TCA cycle operation (Fig. adapted from RUSTIN *et al.* (1997); SCHEFFLER (2008)).

building blocks for synthesis of amino acids, fatty acids and glucose (OWEN *et al.* 2002; SWEETLOVE *et al.* 2010).

Oxidative phosphorylation is the process whereby electron transfer is coupled to the establishment of a chemiosmotic gradient of protons that leads to production of ATP in the mitochondria (SCHULTZ and CHAN 2001; LENAZ and GENOVA 2010; PAPA *et al.* 2012; GENOVA 2014). The Krebs cycle and glycolysis generate $NADH+H^+$ and $FADH_2$ molecules that act as electron donors for the standard electron transport chain (sETC). Under normal conditions, the reduced electron carriers $NADH+H^+$ and $FADH_2$, donate electrons to complex I (NADH-ubiquinone oxidoreductase) and complex II (succinate-ubiquinone oxidoreductase) of the electron transport chain, respectively. These electrons then travel via the sETC in sequence to ubiquinone, complex III (ubiquinol-cytochrome c oxidoreductase), cytochrome c, complex IV (cytochrome c oxidase), and the terminal electron acceptor, molecular oxygen. During electron transfer, complexes I, III and IV pump protons from the matrix to the IMS. The chemisomotic gradient thus generated is harnessed by the F_0F_1 ATP synthase for ATP production.

Apart from the standard NADH-ubiquinone oxidoreductase (complex I), plants, fungi and a few metazoan species (MATUS-ORTEGA *et al.* 2011) also possess alternative NADH dehydrogenases (JOSEPH-HORNE *et al.* 2001; RASMUSSON *et al.* 2004; LENAZ and GENOVA 2010). These MIM proteins can be internal (catalyzing the oxidation of NADH from the mitochondrial matrix side) or external (catalyze the oxidation of NADH from the IMS). They transfer electrons from $NADH+H^+$ to ubiquinone but are not involved in proton pumping across the MIM. *S. cerevisiae* lacks complex I of the respiratory chain and thus in this yeast electron transfer from $NADH+H^+$ to ubiquinone takes place solely

via one internal and two external alternative NADH dehydrogenases (LUTTIK *et al.* 1998; SMALL and MCALISTER-HENN 1998). One internal and three external alternative NADH dehydrogenases have been identified in *Neurospora crassa* (CARNEIRO *et al.* 2007).

Complexes of the sETC and ATP synthase are not arranged in the MIM as randomly dispersed components, as proposed by the 'random diffusion model', (HACKENBROCK *et al.* 1986; LENAZ and GENOVA 2012) but are organized into distinct dynamic supercomplexes. Evidence for the existence of sETC supercomplexes came from electron microscopy and BN-PAGE (blue native polyacrylamide gel electrophoresis) analysis of mitochondria from organisms belonging to different eukaryotic kingdoms (CHABAN *et al.* 2014). Four groups of supercomplexes have been identified thus far, including: I + III_2, III_2 + IV $_{1-2}$, I + III_2 + IV $_{1-4}$ and ATP synthase dimers (CHABAN *et al.* 2014). Fungi have an abundance of the III_2 + IV_2 type supercomplex (HEINEMEYER *et al.* 2007; CHABAN *et al.* 2014). The presence of the I-III-IV type and III-IV type supercomplexes has been observed in *N. crassa* along with complex I dimers (MARQUES *et al.* 2007). One suggested function of these complexes is the efficient transfer of electrons from one complex to another which minimizes the chances of loss of electrons and formation of ROS (reactive oxygen species) (CHABAN *et al.* 2014). Formation of ATP synthase dimers has been suggested to play a role in maintaining cristae morphology by locally bending cristae membranes (STRAUSS *et al.* 2008).

Mitochondria are also involved in maintenance of cellular iron homeostasis and in the assembly of iron-sulfur clusters and heme molecules (AJIOKA *et al.* 2006; STEHLING and LILL 2013; MALLIKARJUN *et al.* 2014). Heme is an important prosthetic group found in proteins like hemoglobin, cytochromes and myoglobin. The biosynthesis of heme

occurs in eight steps, some of which occur in the mitochondria (AJIOKA *et al.* 2006; CHIABRANDO *et al.* 2014). Iron-sulfur clusters biogenesis takes place within the mitochondria. These protein co-factors are important components of several proteins of the mitochondria, cytosol and the nucleus and play an important role in regulatory and catalytic processes, as well as in electron transfer reactions (LILL 2009; STEHLING and LILL 2013). The mechanism and components for the biosynthesis and assembly of iron-sulfur clusters seem to be highly conserved from yeast to humans (STEHLING and LILL 2013; MAIO and ROUAULT 2014). Most components of the iron-sulfur cluster biosynthesis and maturation pathways are essential for the viability of yeast and mammalian cells (LILL 2009; MAIO and ROUAULT 2014).

Mitochondria also play an important role in cellular calcium homeostasis. Calcium ions are essential for several processes such as muscle contraction, mitochondrial metabolism, cell differentiation, fertilization and proliferation (BERRIDGE *et al.* 1998; CLAPHAM 2007; RIZZUTO *et al.* 2012). It has been demonstrated that a rise in cytosolic [Ca^{2+}] promotes the uptake of calcium by the mitochondria via the mitochondrial calcium uniporter (MCU) (CONTRERAS *et al.* 2010; OSELLAME *et al.* 2012; RIZZUTO *et al.* 2012). Calcium is stored mainly in the endoplasmic reticulum (ER). The release of Ca^{2+} from the ER causes microdomains of high Ca^{2+} concentrations at areas of close contact between the mitochondria and the ER called MAMs (Mitochondria associated membranes, (MARCHI *et al.* 2014)), following this the mitochondria imports Ca^{2+} into the matrix (RIZZUTO *et al.* 2012). The accumulation of calcium in the mitochondrial matrix helps in buffering local and bulk calcium levels in the cytosol. Ca^{2+} can also indirectly increase ATP production by activation of dehydrogenases in the matrix (specifically, isocitrate dehydrogenase,

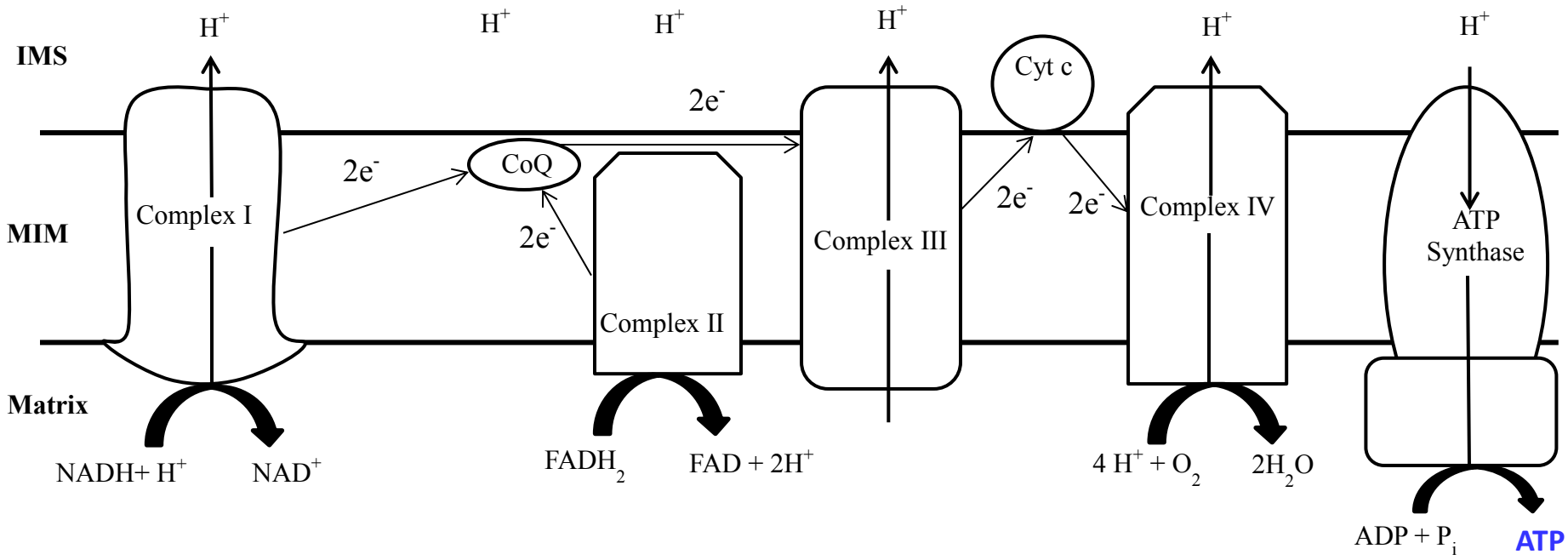

Figure 3. The Electron Transport chain and ATP Synthase. Electrons from NADH $+H^+$ and $FADH_2$ are transferred via complex I and complex II respectively to ubiquinone (coenzyme Q or CoQ). Complex III then transfers them to cytochrome c (Cyt c) and then complex IV, which donates them to molecular oxygen. This movement of electrons is coupled to proton pumping (from the mitochondrial matrix into the intermembrane space (IMS)) across complex I, III and IV creating a chemiosmotic gradient across the MIM. This chemiosmotic gradient is harnessed by ATP synthase for ATP production.

pyruvate dehydrogenase and α-ketoglutarate dehydrogenase). When mitochondria become overloaded with Ca^{2+}, cell death pathways may become activated (PIZZO *et al.* 2012; RIZZUTO *et al.* 2012).

Mitochondria are involved in the MPT (mitochondrial permeability transition) dependent necrosis and also in apoptotic cell death pathways (GALLUZZI *et al.* 2014). Necrosis can occur when the cell experiences severe stress which leads to MPT formation in the MIM, in a cyclophilin D dependent manner (PARSONS and GREEN 2010; GALLUZZI *et al.* 2014). Cyclophilin D is a mitochondrial protein belonging to the peptidyl prolyl-cis, trans-isomerase family of proteins, thought to act as a regulator of MPT formation (GUTIÉRREZ-AGUILAR and BAINES 2014). MPT formation leads to destabilization of membrane potential which can further lead to matrix swelling and rupture of the MOM. The mechanism of MPT formation is still poorly understood.

Intrinsic apoptosis (caused by internal cellular factors such as DNA damage) and extrinsic apoptosis (activated when death receptors, such as Fas, associate with the plasma membrane of a cell) in cells are brought about with the help of caspase signaling (PARSONS and GREEN 2010; TAIT and GREEN 2010). Mitochondria play an essential role in intrinsic apoptosis by releasing apoptogens like cytochrome c and SMAC/DIABLO (second mitochondrial activator of caspases/ direct inhibitor of apoptosis-binding protein with low pI) into the cytosol which can activate the caspase cascade and eventually leads to cell death. The release of apoptogens into the cytosol is mediated by the formation of MOMP (mitochondrial outer membrane permeabilization) (JÄGER and FEARNHEAD 2013). This is brought about by the pro-apoptotic factors Bak and Bax, members of the Bcl-2 family, which reside on the MOM. Upon activation, these proteins form an

oligomer that creates holes in the MOM and leads to permeabilization of the MOM. Caspase-independent cell death is induced by release of the apoptogen AIF (apoptosis inducing factor) into the cytosol, which enters the nucleus and causes chromatin condensation and DNA fragmentation (ZHU *et al.* 2007; JÄGER and FEARNHEAD 2013).

1.5 Role of mitochondria in aging and disease

Aging is a time-dependent degradative and degenerative process caused by accumulated cellular damage, that eventual leads to death as a consequence of tissue failure and cellular dysfunction (LEE and WEI 2012). Mitochondria have been implicated in aging as proposed by the famous 'mitochondrial free radical theory of aging' (MFRTA). This theory suggests that ROS molecules (such as superoxide anions, peroxynitrite anions, hydrogen peroxide and hydroxide ions) generated during transport (mainly at complex I and complex III), are highly toxic and cause damage to various cellular macromolecules which eventually leads to aging (BALABAN *et al.* 2005; MURPHY 2009; BRATIC *et al.* 2013). The MFRTA is supported by the findings that with age, there is a decline in enzymes that scavenge ROS molecules and there is an increase in mtDNA mutations (BRATIC *et al.* 2013). It has also been demonstrated by studies in several models that mitochondrial number and morphology changes as cells age. This is accompanied by an overall decline in mitochondrial functionality (LEE and WEI 2012). However, the finding that ROS molecules can be important signaling molecules have raised doubts about the role of ROS in aging and the MFRTA (COPELAND *et al.* 2009; YANG and HEKIMI 2010).

That mtDNA mutations play a strong role in the aging process was suggested based on studies using mtDNA mutator mice. These mice have homozygous knock-in

mutations causing expression of a proof reading deficient version of the catalytic subunit of mtDNA polymerase (TRIFUNOVIC *et al.* 2004; BRATIC *et al.* 2013). As a consequence these mice accumulate several different types of mtDNA mutations that lead to defects in the respiratory chain subunits and premature aging phenotypes. (EDGAR *et al.* 2009). Further investigations suggested that mutations in respiratory chain subunit genes caused sETC dysfunction in somatic stem cells at an early stage during embryogenesis in these mice (AHLQVIST *et al.* 2012).

Recently, mitochondrial derived peptides (MDPs), a newly identified set of mitochondrial signals generated due to mitochondrial stress, have also been implicated in lifespan extension (HILL and VAN REMMEN 2014). One example of a MDP is humanin, which is a protein of possible mitochondrial origin (its origin is still poorly understood). This protein appears to be released by human cells under stress conditions and plays a role in suppressing apoptosis (LEE *et al.* 2013). Humanin is also present in human plasma and has a neuroprotective role in mice model of diabetes (XU *et al.* 2006).

Several disorders arising from mutations in mtDNA are known to occur in humans. They affect several different organs and can produce symptoms at any age with very broad phenotypic variability (YLIKALLIO and SUOMALAINEN 2012). The progression of several neurological diseases also seems to involve mitochondrial dysfunction, though not necessarily due to mtDNA mutations. These include Parkinson's disease (KAZLAUSKAITE and MUQIT 2014), Huntington's disease (DUAN 2013), Alzheimer's disease (CARLSON *et al.* 2013) and amyotrophic lateral sclerosis (COZZOLINO *et al.* 2013). Several studies have also proposed the involvement of mitochondria in type 2 diabetes mellitus due to an impairment of oxidative function and reduction in mitochondrial mass,

as observed in muscle tissues (KELLEY *et al.* 2002; PATTI and CORVERA 2010; GOODPASTER 2013). Mitochondrial dysfunction and mtDNA mutations have also been linked to carcinogenesis (TOKARZ and BLASIAK 2014).

1.6 Mitochondrial protein import

Based on large scale proteome analysis and other studies, it has been estimated that mammalian mitochondria contain ~ 1100-1500 proteins (PAGLIARINI *et al.* 2008) whereas yeast mitochondria house ~ 1000 proteins (REINDERS *et al.* 2006; MEISINGER *et al.* 2008). Thus, given the small coding capacity of mtDNA (section 1.3) it is estimated that in most eukaryotes ~ 1% of mitochondrial proteins are encoded by the mtDNA. The remaining ~ 99% are encoded by the nuclear genome (SCHMIDT *et al.* 2010). These nuclear encoded mitochondrial proteins are translated on cytosolic ribosomes as precursor proteins, and are imported into the mitochondria via the mitochondrial import machinery (NEUPERT and HERRMANN 2007; DUDEK *et al.* 2013). Import of precursors takes place both post-translationally and co-translationally (YOGEV *et al.* 2007; LESNIK *et al.* 2014). Precursor proteins are targeted to different sub compartments of the mitochondria based on the import signals they carry (SCHMIDT *et al.* 2010). Most mitochondrial precursor proteins contain a cleavable N-terminal targeting presequence. Some others, like the metabolite carrier proteins (e.g. the ADP/ATP carrier, AAC) of the MIM contain internal import signals that are not cleaved and are present in the coding region of the mature protein (DUDEK *et al.* 2013; FERRAMOSCA and ZARA 2013).

Precursor proteins in the cytosol remain associated with chaperones (Hsc70, Hsp90 and other chaperones and co-chaperones) to prevent aggregation and misfolding (YOUNG *et al.* 2003; BHANGOO *et al.* 2007). Almost all protein precursors (except some MOM

proteins with membrane spanning α helical domains) cross the MOM via interactions with the translocase of the outer membrane (TOM) protein complex (DUDEK *et al.* 2013).

Once a precursor protein crosses the MOM, it can interact with several different components of the import machinery depending on the import signal it contains. For example, β-barrel proteins are found only in the MOM (PASCHEN *et al.* 2003) and they are inserted from the IMS side. Once these proteins cross the MOM via the TOM complex, they associate with the small Tim proteins in the IMS (DUDEK *et al.* 2013). The β-barrel precursors are then transferred to the SAM complex (sorting and assembly machinery) which folds and assembles the protein into the MOM (PASCHEN *et al.* 2003; KUTIK *et al.* 2008). The insertion of MOM proteins with α-helical domains is catalyzed by the interaction of the precursor proteins with the Mim1 protein (mitochondrial import protein 1) on the outer surface of the MOM (BECKER *et al.* 2007; PAPIĆ *et al.* 2011; HARBAUER *et al.* 2014).

Proteins that are inserted into the MIM are localized by one of two import pathways, depending on their import signal. Some MIM proteins have an N-terminal, cleavable presequence and use the TIM23 preprotein translocase complex (translocase of the inner membrane, with Tim23 as the central pore component) (BAUER *et al.* 2000; DUDEK *et al.* 2013). The TOM complex and the TIM23 complex are in close proximity to each other at the contact sites of the MIM and MOM and interact with each other via certain subunits of each complex (CHACINSKA *et al.* 2003). MIM-destined presequence-containing proteins pass through the TOM complex to the TIM23 complex, which can laterally insert proteins into the MIM. This is done via a stop transfer mechanism that is activated by hydrophobic transmembrane segment(s) present following the targeting signal in these

MIM-destined proteins (SCHMIDT *et al.* 2010; DUDEK *et al.* 2013). Precursors destined for the matrix use a similar pathway. However these proteins contain no stop transfer signal and continue through the TIM23 complex to the PAM (presequence translocase-associated motor) which is associated with the TIM23 complex on the matrix side (DUDEK *et al.* 2013). Association with PAM aids in translocation of proteins through the MIM into the matrix. In the matrix the presequence is removed by the mitochondrial processing peptidase (MPP). Other modifications of the precursor protein take place in the matrix to ensure generation of a mature and properly folded mitochondrial protein (MOSSMANN *et al.* 2012).

A second import pathway is used by MIM-destined precursors of the carrier protein class. These proteins contain hydrophobic internal import signals and lack the N-terminal presequence. These precursors pass through the MOM via the TOM complex and associate with the small Tims in the IMS to prevent aggregation (KOEHLER *et al.* 1998; DUDEK *et al.* 2013). They are then transferred to the TIM22 (translocase of the inner membrane, with Tim22 as the core pore forming component) complex of the MIM (GEBERT *et al.* 2008; DUDEK *et al.* 2013). The mechanisms of translocation across the TIM22 complex and insertion of proteins into the MIM are not well understood processes (SCHMIDT *et al.* 2010; DUDEK *et al.* 2013).

Proteins that are destined to be located in the IMS contain mitochondrial IMS sorting signals (MISS) that are recognized by the Mia40 protein of the MIA (mitochondrial intermembrane space assembly) machinery that operates the disulfide relay system (DUDEK *et al.* 2013). Mia40 is an oxidoreductase and also serves as a receptor for identification of IMS destined proteins (STOJANOVSKI *et al.* 2012). Mia40 forms transient

disulfide bonds with IMS destined precursor protein and then catalyzes the formation of intramolecular disulfide bonds within the precursor protein, thereby acting like a protein disulfide carrier (SCHMIDT *et al.* 2010; STOJANOVSKI *et al.* 2012). This creates mature folded proteins of the IMS that cannot escape back out into the cytosol. Mia40 is then reoxidized by the Erv1 protein which is a sulphhydryl oxidase that transfers electrons to cytochrome c to achieve its own reoxidation (SCHMIDT *et al.* 2010).

1.7 Mitochondria and cellular signaling

Mitochondria play an essential role as signaling organelles. It is thought that one reason for this is to prevent discrepancy between the metabolic demand of the cell and the capacity of the mitochondria to meet those demands (CHANDEL 2014). One major mechanism by which mitochondria take part in cellular signaling processes is by release of ROS molecules. At low levels, mitochondrial ROS are involved in maintenance of several biological processes such as oxygen sensing, autophagy, immune response, hormone response and epigenetics (HAMANAKA and CHANDEL 2009; LI *et al.* 2011; WEST *et al.* 2011; SCHROEDER *et al.* 2013). Slightly higher levels of ROS are involved with activation of several stress response pathways, while very high levels of ROS lead to cell death via apoptosis (CIRCU and AW 2010; RUNKEL *et al.* 2014). One example of ROS acting as a signaling molecule comes from the observation that hydrogen peroxide can oxidize cysteine residues within proteins causing allosteric changes that alter protein function (FINKEL 2012; SCHIEBER and CHANDEL 2014).

Mitochondria also act as scaffolds for assembly of signaling complexes. It has been demonstrated that A-kinase-anchoring proteins (AKAPs) tether to the MOM (SONG *et al.* 2007; TAYLOR *et al.* 2013). They associate with cAMP-dependent protein kinase A

(PKA) and help in PKA's association to several signaling proteins, thus assembling a signaling hub which brings about PKA dependent signaling within the mitochondria (WONG and SCOTT 2004; FELICIELLO *et al.* 2005; CHANDEL 2014).

1.8 Mitochondrial retrograde regulation

Since the majority of mitochondrial proteins are encoded by the nuclear genome, proper communication from the nucleus to the mitochondria (anterograde signaling) and from the mitochondria to nucleus (retrograde signaling) is important to insure proper organelle function and biogenesis (WOODSON and CHORY 2008). The nuclear genome senses cellular and environmental cues and coordinates expression of nuclear encoded mitochondrial genes as part of anterograde signaling. Mitochondria drive retrograde regulation by conveying their metabolic and developmental status to the nucleus, resulting in altered expression patterns of nuclear encoded mitochondrial proteins (LIU and BUTOW 2006; BLANCO *et al.* 2014).

Mitochondrial retrograde signaling was first studied in detail in the budding yeast *S. cerevisiae*, where a change in expression of several nuclear genes was observed in cells lacking mtDNA (rho^0) as compared to yeast cells with normal mtDNA (rho^+) (BUTOW and AVADHANI 2004; LIU and BUTOW 2006; WOODSON and CHORY 2008; JAZWINSKI and KRIETE 2012; JAZWINSKI 2013). It was initially found that when mitochondria of *S. cerevisiae* became dysfunctional, the expression levels of the *CIT2* gene (encoding the peroxisomal isoform of citrate synthase) was upregulated by 30-fold or more, in comparison to rho^+ yeast cells, depending on the starting strains used (LIAO *et al.* 1991; BUTOW and AVADHANI 2004). Upregulation of *CIT2* is beneficial as it leads to enhanced peroxisomal biogenesis and increased activity of the glyoxylate cycle, which enhances

citrate production (LIU and BUTOW 2006). Citrate is then transported into the mitochondria where it ensures that the production of α-ketogutarate continues. The latter molecule is important as a precursor to glutamate, which is an essential nitrogen donor during biogenesis of amino acids and nucleotides in yeast cells. Upregulation of *CIT2* in rho^0 cells occurs as a consequence of the disruption of the TCA cycle. The TCA cycle cannot occur to completion in rho^0 cells due to accumulation of $NADH + H^+$ and $FADH_2$ and depletion of their oxidized forms, which act as substrates in the cycle (LIU and BUTOW 2006). Thus, a retrograde signaling pathway is activated which enhances transcription of several genes involved in metabolism and stress response, one of which is the *CIT2* gene (EPSTEIN *et al.* 2001; TRAVEN *et al.* 2001).

The upregulation of *CIT2* and other retrograde responsive genes in *S. cerevisiae* is controlled by the retrograde response genes (RTG) *rtg1* and *rtg3,* which require the activity of the *rtg2* gene for proper functioning (LIAO and BUTOW 1993; JIA *et al.* 1997; JAZWINSKI and KRIETE 2012). RTG1 and RTG3 are basic helix-loop-helix leucine zipper family transcription factor proteins that form a heterodimer (JIA *et al.* 1997). Under normal conditions, this heterodimer remains localized in the cytosol with RTG3 phosphorylated at multiple sites. Under conditions that lead to retrograde signaling, the RTG2 protein, which possesses phosphatase activity, partially dephosphorylates RTG3. This leads to the nuclear translocation of the RTG1-RTG3 heterodimer, which binds to the R box (GTCAC) in the promoter of genes involved in the retrograde response and enhances their transcription (SEKITO *et al.* 2000; LIU and BUTOW 2006; JAZWINSKI 2013). Several positive and negative regulators of the RTG pathway have been identified. The RTG pathway also seems to interact with other pathways like the TOR signaling pathway

(TORC1) (KOMEILI *et al.* 2000; JAZWINSKI and KRIETE 2012). The signaling molecule that activates the RTG pathway and the mechanism by which this molecule activates RTG2 is poorly understood. However, it has been shown that loss of mitochondrial membrane potential in yeast cells is essential for activation of the RTG retrograde response (MICELI *et al.* 2011).

Retrograde regulation has also been studied in other organisms. It has been suggested that when some *Caenorhabditis elegans* genes involved in the respiratory chain are compromised, the life span of the worm is extended as a consequence of activation of retrograde responses (JAZWINSKI and KRIETE 2012; HILL and VAN REMMEN 2014; RUNKEL *et al.* 2014). For example, worms with mutations in *isp-1* (encoding a rieske iron sulfur protein of complex III of the sETC) and *clk-1* (encoding a demethoxyubiquinone hydroxylase, involved in ubiquinone biosynthesis) have a gene expression profile similar to yeast rho^0 strains (CRISTINA *et al.* 2009). This suggests that these *C. elegans* mutants have an activated retrograde response(s) to compensate for loss of mitochondrial proteins as observed in the yeast system. In two independent studies where the *cco-1* gene (encoding the COX5B subunit of cytochrome c oxidoreductase) in worms was knocked down, a different set of transcription factors was found to be involved in activation of the retrograde response and extension of lifespan. In one study, aimed at identifying genes that regulate HIF-1 (hypoxia-inducible factor) activity, *cco-1* (RNAi) caused significantly higher levels of GFP tagged HIF-1 (LEE *et al.* 2010). In these worms ROS acted as the signaling molecule and activated HIF-1 that extends lifespan by activating survival genes (LEE *et al.* 2010). In a similar study, extended lifespan of *cco-1* (RNAi) worms was attributed to the role played by ubiquitin like

protein UBL5 and homeobox protein DVE1, these proteins are effectors of mtUPR (mitochondrial unfolded protein response) (DURIEUX *et al.* 2011). In *Drosophila melanogaster* RNAi knockdown of some genes encoding components of the respiratory pathway also leads to extended lifespan (COPELAND *et al.* 2009), as do mutations affecting the *sbo* gene (small boy), which is involved in coenzyme Q biosynthesis (LIU *et al.* 2011).

In mammalian cells, respiratory chain dysfunctions have also shown to enhance nuclear gene expression via possible involvement of the NFκB signaling or the calcium signaling pathway (BUTOW and AVADHANI 2004; JAZWINSKI and KRIETE 2012). The replicative lifespan of human fibroblasts treated with dinitrophenol (a mitochondrial uncoupler) has also been seen to increase as a consequence of decreased mitochondrial membrane potential, which in turn lowers ROS levels and retards telomere shortening. Telomere shortening was observed to be positively correlated to ROS levels in these cells (PASSOS *et al.* 2007). Studies in mice with reduced activity of a protein involved in coenzyme Q biosynthesis (MCLK1) revealed defective electron transport and an extension of lifespan due to activation of a retrograde pathway in a manner similar to the *clk-1* mutant in *C. elegans* (LAPOINTE and HEKIMI 2008).

In plants, the mitochondrial retrograde response may be activated in response to mitochondrial dysfunctions arising from mutations, certain chemicals, biotic or abiotic stress and expression of transgene(s) that alter mitochondrial function (RHOADS 2011). The plant mitochondrial retrograde response has been proposed to involve nuclear transcription factors, calcium signaling and protein kinases (WOODSON and CHORY 2008; LEISTER 2012; NG *et al.* 2014). An example of plant mitochondrial retrograde pathway

activity is observed in NCS (non-chromosomal stripe) mutants of maize (GABAY-LAUGHNAN and NEWTON 2005). These mutant plants have a characteristic striped pattern on their leaves and have a slow growth phenotype due to mtDNA mutations. These mutations cause enhanced expression of several nuclear genes, including the nucleus encoded heat shock proteins (KUZMIN *et al.* 2004; FUJII and TORIYAMA 2009; TOUZET and H. MEYER 2014).

The mtUPR is another mitochondria-to-nucleus signaling pathway. Accumulation of unfolded proteins in the mitochondria leads to enhanced transcription of chaperone genes, proteases, ROS detoxification genes and genes involved in mitochondrial import (HILL and VAN REMMEN 2014; JOVAISAITE *et al.* 2014). Induction of this pathway has been associated with stresses such as chemicals (that lead to ROS production), depletion of the mitochondrial genome, depletion of sETC components, impairment of mitochondrial protease activity and stochastic imbalance between nuclear and mitochondrial sETC complex components (MARTINUS *et al.* 1996; YONEDA *et al.* 2004; ALDRIDGE *et al.* 2007; CRISTINA *et al.* 2009; DURIEUX *et al.* 2011; HOUTKOOPER *et al.* 2013).

1.9 Alternative oxidase (AOX)

Alternative oxidase (AOX) is a terminal ubiquinol oxidase that is present in all higher plants, several fungi, some protists, a few bacterial species and a few animal species (MCDONALD and VANLERBERGHE 2006; MCDONALD 2008; MCDONALD *et al.* 2009). In several organisms, expression of AOX can be induced (as is the case in *N. crassa*) as a consequence of mitochondrial dysfunction. This makes the protein a good

model for understanding the molecular mechanisms and signaling molecules involved in mitochondrial retrograde responses.

AOX is an interfacial membrane protein that associates with the inner leaflet of the mitochondrial inner membrane (BERTHOLD *et al.* 2000; BERTHOLD and STENMARK 2003). AOX provides a branch point from the standard electron transport chain (sETC) at the ubiquinol pool. It catalyzes the oxidation of ubiquinol (Fig. 4) and transfers electrons directly to molecular oxygen, reducing it to water (RICH and MOORE 1976; MOORE *et al.* 2013). Unlike complex I, III and IV of the sETC, AOX does not pump protons across the MIM to the IMS (MOORE *et al.* 1978). The activity of AOX is inhibited by hydroxamic acids (e.g. salicylhydroxamic acid, SHAM). It is insensitive to cyanide and antimycin A (AA), which inhibit complex IV and III of the sETC, respectively (SCHONBAUM *et al.* 1971; MCDONALD and VANLERBERGHE 2006).

1.9.1 Taxonomic distribution of AOX

The taxonomic distribution of AOX is extremely wide. AOX is present in some organisms in all kingdoms of life, except Archaebacteria (MCDONALD 2008). AOX is present in many basal plant groups and is widespread in angiosperms. The presence of AOX has been reported in several eubacterial species, but is restricted to proteobacteria (e.g. *Novosphingobium aromaticivorans*). Many Ascomycota (e.g. *N. crassa*) and Basidiomycota (e.g. *Cryptococcus neoformans*) fungal species contain AOX and it also seems to be present is some basal Zygomycota (e.g. *Rhizopus oryzae*) and Chytrid fungal species (e.g. *Spizellomyces punctacus*) (MCDONALD and VANLERBERGHE 2006). Twenty eight species in the animal kingdom have also been shown to possess AOX (e.g. the sea squirt *Ciona intestinalis* belonging to the phylum chordate) (MCDONALD *et al.* 2009).

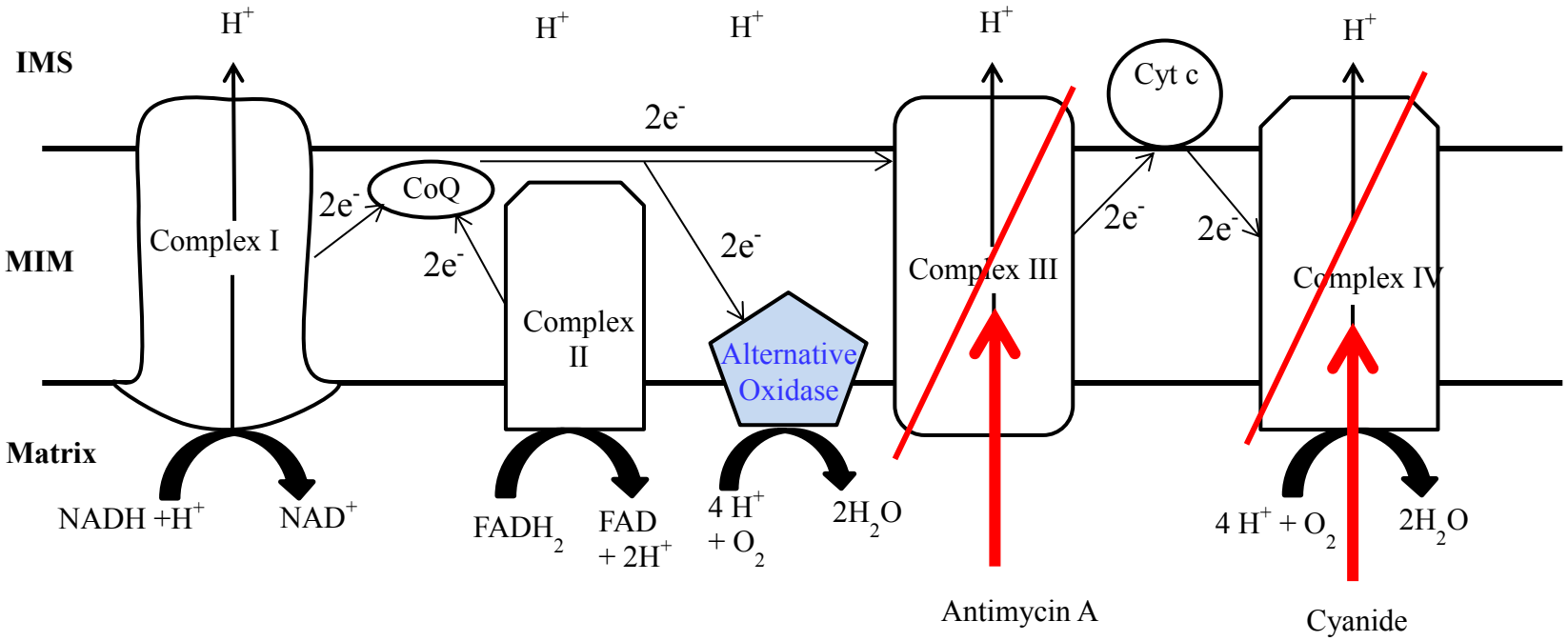

Figure 4. AOX in the sETC. AOX associates with the inner leaflet of the MIM, accepts electrons from ubiquinol (CoQ) and passes them directly to molecular oxygen, thus bypassing complex III and Complex IV. In many organisms, AOX is only produced when the sETC is inhibited. Some organisms (e.g. plants) have AOX present in some tissues even without sETC inhibition.

In many plants (mainly in angiosperms) AOX is present as a multigene family (CONSIDINE *et al.* 2001; DJAJANEGARA *et al.* 2002; KARPOVA *et al.* 2002; SAIKA *et al.* 2002; TAKUMI *et al.* 2002; CLIFTON *et al.* 2006). These *AOX* genes are generally placed into subfamilies called AOX1 and AOX2. The AOX1 gene family is present in all angiosperms and is induced as a consequence of cellular stress. The AOX2 gene family is present only in dicot angiosperms and is expressed either constitutively or developmentally (CONSIDINE *et al.* 2002). Several gene copies of the AOX1 subfamily are present in many plants, whereas the AOX2 subfamily seems to be less expanded. For example, the Arabidopsis genome contains four AOX1 type genes (*AOX1a*, *AOX1b*, *AOX1c* and *AOX1d*) and one AOX2 type gene (*AOX2*) (CLIFTON *et al.* 2006).

Several fungi like *Podospora anserina*, *Candida maltosa* and *Candida tropicalis* have also been found to contain more than one AOX gene (MCDONALD and VANLERBERGHE 2006; MCDONALD 2008). In *N. crassa* the *aod-1* gene encodes an AOX that is inducible in response to sETC perturbation. A gene with unknown function, the *aod-3* gene, shows high sequence similarity to *aod-1,* but no evidence of the expression of this gene under standard growth or sETC impared growth was established (TANTON *et al.* 2003). No animal or eubacterial species examined to date contains more than one AOX encoding gene (MCDONALD and VANLERBERGHE 2006).

Distribution of AOX in plants seems to be ubiquitous, whereas in protists, fungi and animals the appearance of AOX is more sporadic (MCDONALD and VANLERBERGHE 2004). The reasons for this are unclear since in two closely related species, one may have AOX while the other does not. For example, *S. cerevisiae* lack AOX whereas other yeasts, such as *Candida albicans* and *Pichia stipites* do possess AOX (VEIGA *et al.* 2003;

MCDONALD 2008). The nematode *Meliodogyne hapla* has AOX whereas *C. elegans* lacks AOX (MCDONALD 2008). Eukaryotic AOX is proposed to have originated from the endosymbiotic event that gave rise to mitochondria since AOX is widespread among proteobacteria. Following the endosymbiotic event that gave rise to mitochondria AOX spread throughout eukaryotes by vertical inheritance (MCDONALD and VANLERBERGHE 2006).

1.9.2 Structure of AOX

Alternative oxidase belongs to the diiron carboxylate protein family (BENDALL and BONNER 1971; NORDLUND and EKLUND 1995; SIEDOW *et al.* 1995; BERTHOLD and STENMARK 2003; MOORE *et al.* 2013). Members of this protein family have a characteristic diiron center with two EXXH motifs coordinating the metal iron center (BERTHOLD and STENMARK 2003). Diiron carboxylate proteins contain a four α-helical bundle within which the diiron center is buried and the metal center is coordinated by conserved glutamate and histidine residues provided by the four α-helices (BERTHOLD and STENMARK 2003). An early model of AOX structure (SIEDOW *et al.* 1995) was found to have several anomalies relative to other diiron carboxylate proteins. A newer model was proposed in which the structure of Δ^9 desaturase, another diiron carboxylate protein, was used as a modelling template (ANDERSSON and NORDLUND 1999; BERTHOLD *et al.* 2000; BERTHOLD and STENMARK 2003). The structure of AOX and Δ^9 desaturase, in terms of spacing of iron ligands, was the best match in comparison to other diiorn proteins with available crystal structures at that time. This model proposed AOX was an interfacial membrane protein that interacts with the inner leaflet of the MIM and contains no transmembrane domains (TMDs). It further proposed that the α-helical domains

containing the conserved EXXH motifs also contained two conserved glutamate residues that act as terminal ligands. Based on this structure a hydrophobic pocket was predicted between helix 2 and helix 3 which was proposed to be the ubiquinol binding site of AOX (ANDERSSON and NORDLUND 1999; MOORE and ALBURY 2008). Substitution mutations of conserved amino acid residues in this region were shown to cause loss of AOX activity (ALBURY *et al.* 2010). General features of the structural model of AOX are demonstrated in Fig.5

The crystal structure of the *Trpanosoma brucei* AOX was recently determined (SHIBA *et al.* 2013). The structure showed that AOX is indeed an interfacial membrane diiron carboxylate protein and confirmed most features of the model proposed by ANDERSSON and NORDLUND (1999). AOX was found to contain six long (termed α1 to α6) and four short (termed αS1 to αS4) α-helices arranged in an antiparallel fashion (MOORE *et al.* 2013). α-helices α2, α3, α5 and α6 form the four α-helical bundle that coordinates the metal iron center. The crystal structure also revealed that the average distance between the two iron atoms in AOX is 3.16 Å. In agreement with the previous structural model, the crystal structure analysis suggested that the active site includes: a hydroxo bridge between the two iron atoms, four highly conserved glutamate residues, and two highly conserved histidine residues (MOORE *et al.* 2013). These histidine residues are involved in formation of a hydrogen bond network which has been proposed to be involved in active site stabilization. Based on the distance of the tyrosine-220 residue from the diirion center and also based on mutational analysis this tyrosine residue has been proposed to play a role in the catalytic cycle of AOX (MOORE *et al.* 2013). Based on the crystal structure, substrate binding and inhibitor binding pockets for AOX

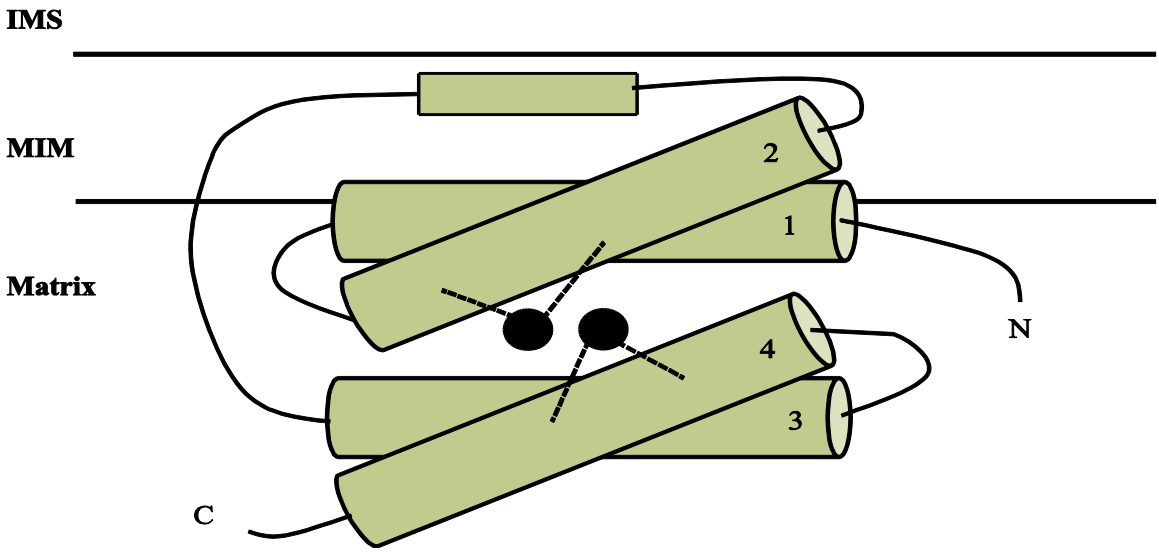

Figure 5. General features of the structural model of AOX. The model proposed by ANDERSSON and NORDLUND (1999) and modified by BERTHOLD *et al.* (2000). This model proposed AOX is an interfacial membrane protein that interacts with the inner leaflet of the MIM and contains no TMDs. The conserved EXXH motifs are present in helix 2 and 4. They coordinate the metal diiron center (iron atoms are shown as filled black circles), as shown using dotted black lines. Helix 3 and 1 provide two conserved glutamate residues that act as terminal ligands. Modified from BERTHOLD *et al.* (2000). The basics of the model are confirmed by the recently obtained crystal structure (MOORE *et al.* 2013).

were also predicted (MOORE *et al.* 2013). Over the years, using a combination of multiple sequence alignments and mutational analysis, several universally conserved residues in AOX (in addition to the ones that play an important role in coordinating the metal iron center) have been identified. These residues seem to play a role in diverse functions such as substrate binding, dimer interface, membrane binding and inter-helical interactions to name a few (MOORE *et al.* 2013).

It was previously proposed that plant AOX exists as a non-covalently linked dimer, while the fungal and protist AOX's associate with the MIM as monomers (MCDONALD 2008). In most plants the non-covalently associated monomers can become covalently linked via a reversible disulfide bond. This bond forms between cysteine residues (called CysI) in the N-terminal region of each monomer (see also section 1.9.5). Non-plant AOXs do not have this cysteine. In its oxidized form, when the disulfide bond links the two subunits, AOX is less active. When the bond is reduced, AOX is in a more active form (VANLERBERGHE *et al.* 1995; UMBACH *et al.* 2006; ALBURY *et al.* 2009). In the reduced form, the dimer can become further activated by the addition of keto acids (especially pyruvate) to CysI (UMBACH *et al.* 1994; VANLERBERGHE *et al.* 1995). The crystal structure of *T. brucei* suggested that since several residues believed to play a role in non-covalent dimer formation are highly conserved across all known AOX sequences, formation of a homodimer may be a universally conserved feature (MOORE *et al.* 2013). The α helices, α2, α3 and α4 are proposed to be involved in dimer interface formation with six universally conserved and eight highly conserved residues present within this region (MOORE *et al.* 2013). It has also been suggested that the region formed by α1, α4,

the N-terminal region of α5 and the C-terminal of α2 in both monomers of the dimer is involved in the binding of AOX to the MIM (MOORE *et al.* 2013).

1.9.3 Functions of AOX

It has been proposed that the original role of diiron carboxylate proteins was to act as an oxidase to protect early anaerobic organisms from rising oxygen levels in the atmosphere (GOMES *et al.* 2001). Several diiron carboxylate proteins still have the ability to catalyze conversion of oxygen to water in addition to their main cellular function (BROADWATER *et al.* 1998; GASSNER and LIPPARD 1999; GOMES *et al.* 2001). Examples of such diiron carboxylate proteins include, rubrerythrin (a NADH peroxidase involved in catalysis of hydrogen peroxide and oxygen free radicals into water (SZTUKOWSKA *et al.* 2002)); Δ^9 desaturase (catalyzes the desaturation of steryl-acetyl carrier protein to oleoyl-acetyl carrier protein in a fatty acid biosynthesis pathway (FOX *et al.* 1993)); and methane monooxygenase (catalyzes the conversion of methane to methanol (MERKX *et al.* 2001)). Thus, it has been suggested that AOX might have originated as an oxygen scavenging enzyme that has been retained over evolutionary time as an adaptation to oxygen stress (MCDONALD 2008).

AOX provides metabolic flexibility to organisms under stress and helps in maintaining a balance in the organism's carbon metabolism and energy production via electron transport (MCDONALD 2008). Under conditions that impair the sETC, AOX can allow for continued glycolysis and maintain Krebs cycle flux by ensuring continued NAD^+ generation via complex I. This, in turn, ensures continued generation of important carbon metabolites that are precursors to other molecules like amino acids, which are essential for growth and repair (VANLERBERGHE and MCINTOSH 1997; MCDONALD

2008). AOX has also been suggested to play a role in providing metabolic flexibility to certain organisms, as can be seen in proteobacterial species. Proteobacteria (e.g. *Novospingobium aromaticivorans*) can grow on a variety of carbon and energy sources. Since AOX levels in *N. aromaticivorans* were higher when grown in the presence of glucose than when grown in lactate, AOX is thought to provide the organism with the ability to handle electron transport and carbon metabolism imbalances in rapidly changing environments (STENMARK and NORDLUND 2003).

AOX also seems to provide protection from oxidative stress by lowering the levels of ROS produced from the sETC under certain conditions (MCDONALD 2008). If the sETC complexes are over reduced, large amounts of ROS are produced at complexes I and III. In several organisms, AOX seems to attenuate high ROS levels by using up excess electrons in the sETC and preventing over reduction of the complexes (VANLERBERGHE and MCINTOSH 1997; MCDONALD 2008). In support of this idea, when AOX was either overexpressed or suppressed in transgenic tobacco cultures, an inverse relationship between ROS level and AOX level was observed (MAXWELL *et al.* 1999). A similar association of decreased ROS production in the presence of high levels of AOX was found in the fungal species *Ustilago maydis* (JUÁREZ *et al.* 2006). In *P. anserina*, AOX dependent reduction of ROS levels has also been associated with increased lifespan (GREDILLA *et al.* 2006).

To defend against pathogenic organisms host cells often release ROS molecules or poisonous chemicals. For example, several plant tissues produce cyanogenic glycosides or cyanolipids, which are hydrolyzed into hydrogen cyanide following ingestion by a herbivore (POULTON 1990; BALLHORN *et al.* 2009). Plants also produce increased levels

of ROS in response to attack by fungal pathogens (HELLER and TUDZYNSKI 2011). Several pathogenic organisms seem to use AOX to evade such host defense mechanisms (MCDONALD and VANLERBERGHE 2006; MCDONALD 2008). The pathogenicity of the fungus *Cryptococcus neoformans,* which infects individuals with compromised immune systems is known to involve AOX (AKHTER *et al.* 2003; FANG and BEATTIE 2003). When the organism is grown at the host temperature of 37°C, the *AOX1* gene is upregulated, suggesting a role for AOX in infection. Supporting this idea is the observation that *AOX1* mutants were found to be significantly less virulent in this fungus (AKHTER *et al.* 2003). Similarly, in the protozoan parasite *T. brucei brucei* (known to cause sleeping sickness) the bloodstream form of the organism lacks mitochondrial cytochromes and possesses AOX which is essential for its respiration (CHAUDHURI *et al.* 2002).

AOX has also been suggested to be involved in resistance to metal toxicity, as seen by an increase in AOX capacity (maximum AOX activity as measured by estimating possible flux of electrons through AOX) in *Euglena gracilis* exposed to cadmium stress (CASTRO-GUERRERO *et al.* 2008). A 4.5 times higher capacity of AOX was observed in cells exposed to cadmium. Similarly, a cadmium induced increase in transcript levels of AOX was observed in *Arabidopsis thaliana* (KEUNEN *et al.* 2013). In animals inhabiting harsh environments AOX has been suggested to play a role in protection against harmful chemicals and toxins. One example of such a harmful environment would be marine sediments with potentially high levels of sulfide that inhibit cytochrome oxidase (complex IV) (GRIESHABER and VÖLKEL 1998; MCDONALD 2008; MCDONALD *et al.* 2009). The resistance of AOX to several known inhibitors of components of the sETC such as AA, azide, nitric oxide and sulfide would make it useful in many such harsh

environments (AZCÓN-BIETO *et al.* 1989; HUANG *et al.* 2002; BAURAIN *et al.* 2003; CHAE *et al.* 2007a).

In thermogenic plants, heat is generated in certain tissues to facilitate scent volatilization for attracting pollinators and also to allow for proper pollen tube formation (ZHU *et al.* 2011). In several thermogenic plants like the sacred lotus (*Nelumbo nucifera),* voodoo lily (*Sauromatum guttatum*), Arum lily (*Arum maculatum*) and skunk cabbage (*Symplocarpus renifolius*), it has been demonstrated that the ability to generate heat is a consequence of the activity of AOX (CRICHTON *et al.* 2005; GRANT *et al.* 2008; WAGNER *et al.* 2008; ITO-INABA *et al.* 2009). Since AOX is not involved in proton pumping across the MIM, and bypasses two sites of proton pumping, the high potential energy thus generated is dissipated as heat when the alternative pathway of respiration is used.

1.9.4 Regulation of AOX transcription

Several metabolites, chemicals and environmental conditions can stimulate the activity or expression of AOX (MCDONALD 2008). In plants, AOX activity is enhanced by treatment with ketoacids (see section 1.9.5), especially pyruvate (VANLERBERGHE *et al.* 1995; RASMUSSON *et al.* 2009; CARRÉ *et al.* 2011). The TCA cycle intermediates citrate, isocitrate, 2-oxoglutarate and malate are also linked to increased activation and increased AOX mRNA levels in plants (VANLERBERGHE *et al.* 1995; DJAJANEGARA *et al.* 2002; RASMUSSON *et al.* 2009).

ROS molecules also have an effect on AOX expression (MINAGAWA *et al.* 1992; WAGNER 1995; MAGNANI *et al.* 2007; VAN AKEN *et al.* 2009). Treatment with hydrogen peroxide led to increased expression of the inducible *AOX1* in tobacco (VANLERBERGHE and MCLNTOSH 1996), and maize (POLIDOROS *et al.* 2005). A similar observation was

seen for AOX in the fungus *Magnaporthe grisea* (YUKIOKA *et al.* 1998). In *Arabidopsis thaliana*, ROS treatment led to increased expression of the *AOX1a* (an AOX1 type gene) gene but repression of the *AOX2* gene, emphasizing the different roles played by the two subclasses of AOX genes in dicots (CLIFTON *et al.* 2005). In plants, several stresses like salinity, low temperature, ozone treatment, osmotic stress/drought and pathogen attack have also shown to induce AOX expression (SIMONS *et al.* 1999; BARTOLI *et al.* 2005; EDERLI *et al.* 2006; COSTA *et al.* 2007; PASQUALINI *et al.* 2007; WATANABE *et al.* 2008; FENG *et al.* 2013). In the eubacterium *N. aromaticivorans,* the expression levels of AOX are greatly influenced by the oxygenation status and the carbon source of the growth medium (STENMARK and NORDLUND 2003).

Exposure to respiratory chain inhibitors also causes an increase in transcript levels of AOX in many organisms. These responses have been studied using nuclear run-on experiments, northern blots, microarray analysis or real time PCR (MCDONALD 2008). AA, an inhibitor of complex III of the sETC, causes increased expression of the inducible form of AOX in soybean and *A. thaliana* (SAISHO *et al.* 1997; DJAJANEGARA *et al.* 2002). Potassium cyanide (KCN), an inhibitor of complex IV, also leads to increased expression of the *Aox1a* gene in maize (POLIDOROS *et al.* 2005). In the fungus *M. grisea,* a fungicide that inhibits complex III has also been shown to cause accumulation of AOX mRNA (YUKIOKA *et al.* 1998). Transcript levels of the *aod-1* gene in *N. crassa* also increase in cells grown in the presence of respiratory chain inhibitors (BERTRAND *et al.* 1983; TANTON *et al.* 2003). In the above cases, the increase in transcript levels also corresponds with an increase in the levels of the AOX protein as determined using western blots or activity measurements. The above examples, as well as nuclear run-on assays from

studies of *M. grisea* and *N. crassa,* suggest that AOX is regulated at the level of transcription.

In *M. grisea* and *N. crassa*, a low constitutive expression of the AOX transcript was seen in uninduced or unstimulated cultures, though no protein was observed using western blots. This suggests that, in certain organisms, AOX may also be regulated at the post-transcriptional level (YUKIOKA *et al.* 1998; TANTON *et al.* 2003). In *T. brucei* and *M. grisea,* treatment of cells with cycloheximide, an inhibitor of cytosolic protein synthesis, lead to accumulation of AOX mRNA in uninduced cells, suggesting that under normal conditions (no cycloheximide) the AOX transcript is degraded readily by an unknown protein factor. In the absence of this factor mRNA accumulation occurs, further suggestive of post-transcriptional regulation (YUKIOKA *et al.* 1998; CHAUDHURI *et al.* 2002; CLAYTON and SHAPIRA 2007).

The mechanism of transcriptional control of AOX is poorly understood. The promoter regions of the AOX-encoding genes from various organisms have been studied over the years and both positive and negative regulatory elements have been identified (POLIDOROS *et al.* 2009). A study of the promoter region of the *S. guttatum AOX1* gene revealed the presence of cis-acting regulatory transcriptional elements that could be binding sites for basic leucine zipper proteins (bZIP) and zinc finger proteins (RHOADS and MCINTOSH 1993). Analysis of the *A. thaliana AOX1a* gene also showed the presence of several regulatory elements, including two CCAAT box motifs (in *S. cerevisiae*, this motif is known to regulate the sETC complex subunits) and also seven motifs known to bind bZIP proteins (DOJCINOVIC *et al.* 2005). Similarly, several negative and positive elements have been identified in the promoter region of the

soybean *AOX1, AOX2* and *AOX2b* genes (THIRKETTLE-WATTS *et al.* 2003). A transcription factor, ABI4 (abscisic acid insensitive 4), that represses *AOX1a* by binding to the promoter region of the gene has been identified in *A. thaliana* (GIRAUD *et al.* 2009). ABI4 was previously shown to act as a transcriptional repressor in response to the chloroplast retrograde signals arising from Mg-protoporphyrin IX accumulation in the chloroplast and also from inhibition of plastid gene expression (KOUSSEVITZKY *et al.* 2007; WOODSON and CHORY 2008). Mutants lacking the *abi4* gene showed greater than four-fold increase in *AOX1a* promoter activity. These mutants could also not be induced any further by rotenone (complex I inhibitor) suggesting that the *AOX1a* gene was already fully derepressed (GIRAUD *et al.* 2009). This study also suggests that another abscisic acid signaling transcription factor, ABI3, may act as a positive regulator of *AOX1a*.

Another study in *A. thaliana* identified two transcription factors that bind to W box elements in the promoter region of *AOX1a* gene (VAN AKEN *et al.* 2013). W boxes contain the TTGAC motif which is known to be a binding site for WRKY transcription factors. Yeast one-hybrid assays using two W box regions from the *AOX1a* promoter, in addition to EMSA and mutational analysis, showed that AtWRKY40 and AtWRKY63 bind to the *AOX1a* promoter region. AtWRKY40 acts as a repressor and AtWRKY63 acts as an activator of the *AOX1a* gene. These transcription factors played similar roles with other nuclear encoded stress responsive chloroplast and mitochondrial protein encoding genes. Expression levels of *AOX1a* in *atwrky40* mutant plants grown in the presence of AA were significantly higher (>2 fold) in comparison to AA-treated wild-type plants, supporting a role for this transcription factor in limiting the expression of

AOX1a under AA-induced conditions (VAN AKEN *et al.* 2013). In *atwrky63* mutant plants treated with flg22 (a biotic stress signal), *AOX1a* induction was reduced by approximately 2 fold in comparison to the wild-type flg22 treated plants (VAN AKEN *et al.* 2013). High light treatment was also used to study the role of AtWRKY63 and AtWRKY40 in chloroplast retrograde signaling, as high light treatment induces chloroplast retrograde signaling pathways. In *atwrky40* mutants *AOX1a* transcript levels were more than two fold higher in comparison to wild-type plants subjected to high light. *atwrky40* over expressing plants did not show a significant increase or decrease in *AOX1a* expression levels (VAN AKEN *et al.* 2013). In *atwrky63* overexpressing plants, expression levels of *AOX1a* were significantly higher, by approximately 2 fold, following a high light treatment. The *atwrky63* mutant plants subjected to high light had a slight, though not statistically significant decrease in expression of *AOX1a* (VAN AKEN *et al.* 2013). These data suggested that AtWRKY63 and AtWRKY40 play a role in regulation of genes that respond to mitochondrial as well as chloroplast dysfunction. Promoter elements and transcription factors necessary for expression of *N. crassa* AOX have also been identified (see section 1.10).

1.9.5 Post-translational regulation of AOX

As discussed in section 1.9.2, AOX in all organisms likely exists as a non-covalently associated homo-dimer. However, the N-terminal region of AOX in most plants contains two highly conserved cysteine residues (called CysI and CysII) (UMBACH and SIEDOW 1993; BERTHOLD *et al.* 2000; UMBACH *et al.* 2006). Using site directed mutagenesis, it has been demonstrated that CysI is involved in disulfide bond formation between the molecules of the homodimer (RHOADS *et al.* 1998; VANLERBERGHE *et al.* 1998).

Formation of the disulfide bond to give a covalently joined dimer reduces AOX activity compared to the non-covalently associated form (UMBACH and SIEDOW 1993; MOORE *et al.* 2013)

The CysI and CysII of plant AOX's have been shown to be involved in another form of post-translational regulation involving α-keto acids (UMBACH *et al.* 2002; UMBACH *et al.* 2006; GRANT *et al.* 2009). α-keto acids like pyruvate can activate the AOX protein in several plant species (MILLAR *et al.* 1993; UMBACH *et al.* 2006; GRANT *et al.* 2009). Pyruvate activation takes place only when the AOX dimer is in its reduced state (UMBACH *et al.* 1994; VANLERBERGHE *et al.* 1995). Activation by other α-keto acids like glyoxylate, hydroxypyruvate and 2-oxoglutarate has also been demonstrated (MILLAR *et al.* 1993). Activation of AOX by pyruvate is abolished if CysI is mutated but no such effect was observed when CysII was mutated, suggesting pyruvate activation is dependent on CysI (RHOADS *et al.* 1998; VANLERBERGHE *et al.* 1998). On the other hand, activation via glyoxylate is dependent on CysII and this activation takes place only when the protein has been previously activated via pyruvate at CysI (UMBACH *et al.* 2006). In some plant AOXs, amino acid substitutions at the conserved cysteine residues have been observed. This includes a tomato (LeAOX1b) and a maize (ZmAOX3) AOX isozyme, where a serine (SerI) residue replaces CysI (KARPOVA *et al.* 2002; HOLTZAPFFEL *et al.* 2003; UMBACH *et al.* 2006). In tomato, the LeAOX1b protein seems to be insensitive to activation by α-keto acids but is activated by succinate (HOLTZAPFFEL *et al.* 2003; UMBACH *et al.* 2006; MCDONALD 2008). Studies using sacred lotus (*N. nucifera*) have also identified AOX isozymes (NnAOX1a and NnAOX1b) from the receptacles of this plant that lack CysI, which has been replaced by serine. AOX in the sacred lotus was

present in the non-covalently joined state and just as in LeAOX1b it was activated by succinate as opposed to pyruvate (GRANT *et al.* 2009). These studies suggest the presence of species-specific variations in AOX regulation at the posttranslational level (UMBACH *et al.* 2006).

Unlike plants, the animal, bacterial, fungal and protist AOX's lack the highly conserved cysteine residues. Thus, post-translational regulation as a result of covalent dimer formation or by α-keto acids is not observed in these organisms (JARMUSZKIEWICZ *et al.* 2002; MCDONALD 2008). In the fungal species *Yarrowia lipolytica* and *N. crassa,* and in the protists *Acanthamoeba castellani* and *Dictyostelium discoideum* AOX activity has been shown to be enhanced by the purine nucleoside 5' monophosphates GMP or AMP (VANDERLEYDEN *et al.* 1980; JARMUSZKIEWICZ *et al.* 2002; MEDENTSE *et al.* 2004; JARMUSZKIEWICZ *et al.* 2005).

1.10 *Neurospora crassa* AOX

The cyanide-insensitive respiratory pathway in *N. crassa* was first observed in the mitochondrial mutant [*poky*] (LAMBOWITZ and SLAYMAN 1971; RIFKIN and LUCK 1971; AKINS and LAMBOWITZ 1984). The [*poky*] mutant is characterized by high levels of cytochrome c and low levels of the cytochromes with mitochondrially encoded components, cytochrome aa_3 and *b* (LAMBOWITZ *et al.* 1972). Subsequently, it was demonstrated that impairment of the sETC by the chemical inhibitors AA (inhibits complex III), cyanide (inhibits complex IV), and chloramphenicol (Cm, inhibits mitochondrial protein synthesis) also lead to induction of cyanide-insensitive respiration in *N. crassa* (LAMBOWITZ and SLAYMAN 1971; EDWARDS *et al.* 1974; EDWARDS and ROSENBERG 1976). Although Cm does not directly inhibit a complex of the sETC, it

leads to deficiencies of complex I, III and IV since they contain mitochondrially encoded subunits. A similar effect was seen with mutations that effect components of the sETC, or growth of cells in copper (a component of complex IV) deficient medium (BORGHOUTS *et al.* 2001).

Initial attempts to understand cyanide-insensitive respiration and identify the alternative oxidase protein in *N. crassa* were carried out using mutagen based screening (BERTRAND *et al.* 1983). This led to the identification of several strains that were unable to grow in the presence of AA after mutagen treatment, suggesting the presence of mutations affecting AOX production in these strains. The mutations were found to comprise two complementation groups, *aod-1* and *aod-2*. Visualization of radio-labelled (^{35}S) proteins from mutant strains showed that 19 of the 20 mutants placed in the *aod-1* complementation group contained a radiolabelled protein that only appeared when strains were grown under AOX inducing conditions. All 4 strains in the *aod-2* complementation group did not contain the protein. This led to the suggestion that *aod-1* is the structural gene for AOX in *N. crassa* whereas *aod-2* is involved in the regulation of AOX. Later, LAMBOWITZ *et al.* (1989) identified proteins, of similar size (36.5 kDa and 37 kDa) in a *N. crassa* wild-type strain treated with Cm. Monoclonal antibodies specific to *S. guttatum* AOX were used for AOX detection in this study. The lone strain in the *aod-1* complementation group that lacked the protein was later shown to contain a frame-shift mutation in its coding region (LI *et al.* 1996). The remaining mutants are assumed to carry missense mutations.

It is now accepted that the structural gene for AOX in *N. crassa* is the nuclear *aod-1* gene. This gene contains two introns and encodes a 363 amino acid protein

corresponding to a 41.4 kDa protein which is processed to a mature 34.7 kDa protein by removal of the MTS (mitochondrial targeting sequence). LI *et al.* (1996) cloned and sequenced the *N. crassa aod-1* gene and identified potential CAAT and TATA boxes in the upstream region, as well as a transcription start site using a primer extension strategy. A possible cAMP responsive element (CRE) was also identified in the promoter region (746 bps upstream from the transcription start site) of the *aod-1* gene. However, deletion of portions of the promoter sequence showed that the CRE is not essential for AOX induction in *N. crassa* (TANTON *et al.* 2003).

Northern blot analysis of wild-type strains grown in the presence or absence of Cm suggested that AOX induction in *N. crassa* takes place at the level of transcription. High mRNA levels were observed in cells grown under Cm induced conditions while transcripts were not detectable in cells grown in non-induced conditions (LI *et al.* 1996). The idea that *N. crassa* AOX is regulated at the level of transcription was further supported by nuclear run-on experiments. *N. crassa* cultures treated with AA showed a rapid increase in transcript levels and a corresponding increase in protein levels as compared to uninduced cultures (TANTON *et al.* 2003). These nuclear run-on assays also suggested that uninduced cultures have a low constitutive expression of the AOX transcript but no corresponding AOX protein. This was later confirmed in RT-PCR experiments (CHAE *et al.* 2007b). Also, some *N. crassa* strains have been identified that readily accumulate detectable levels of *aod-1* mRNA under non-inducing conditions but lack any detectable AOX protein on western blots (TANTON *et al.* 2003; DESCHENEAU *et al.* 2005). This suggests that regulation also takes place at the post-transcriptional level. It was suggested that translation of the *aod-1* transcript may either be inhibited by a

cytosolic protein or a cytosolic protein present only in inducing conditions, plays an important role in translation of the *aod-1* transcript (TANTON *et al.* 2003).

BLAST searches of the *N. crassa* genome led to identification of a second alternative oxidase structural gene (TANTON *et al.* 2003). This gene was named *aod-3* and shows 55% identity to the *aod-1* gene. Transcription of *aod-3* was not observed on Northern blots when a wild-type strain was grown in uninduced or induced conditions using Cm. It was hypothesized that this gene may be developmentally regulated or is induced under unidentified stress conditions.

To identify additional genes involved in regulation of AOX in *N. crassa* a reporter construct containing 3.3 Kb of the upstream sequence of *aod-1* gene was fused to the tyrosinase gene coding sequence (DESCHENEAU *et al.* 2005). This construct was subsequently transformed into a tyrosinase null strain and the strain was subjected to ethyl methanesulfonate (EMS) mutagenesis. Strains unable to induce tyrosinase expression, identified as colonies that did not turn brown upon exposure to tyrosine, were potential AOX regulatory mutants. These were analyzed via complementation and genetic mapping studies, which helped identify four new AOX regulatory genes, *aod-4*, *aod-5*, *aod-6* and *aod-7*. The function and identity of the *aod-4*, *aod-6* and *aod-7* are still unknown. This screen was likely not saturated, as multiple isolates were identified at only the *aod-4* locus.

Gene rescue experiments were carried out to identify the *aod-2* and *aod-5* genes. These genes were shown to encode fungal-specific zinc cluster transcription factors (MACPHERSON *et al.* 2006; CHAE *et al.* 2007b). The C-terminal region of the gene products of these genes also possessed PAS (Per-ANT-Sim) domains. These domains are

known to act as signal sensors and are also involved in protein dimerization (TAYLOR and ZHULIN 1999; MÖGLICH *et al.* 2009). Using site-directed mutagenesis it was shown that two conserved glycine residues in the PAS domain are essential for proper functioning of the AOD2 and AOD5 proteins (CHAE *et al.* 2007b).

Initial promoter deletion studies suggested that the region 255 bp upstream of the transcription start site of the *aod-1* gene contains the regulatory element essential for proper AOX induction (TANTON *et al.* 2003). Further analysis of this region revealed the presence of the AIM (alternative oxidase induction motif) sequence. The AIM consists of two CGG repeats separated by seven base pairs and represents a typical binding site for fungal zinc cluster transcription factors (CHAE *et al.* 2007a). EMSA analysis using the AOD2 and/or AOD5 DNA binding domain, and probes containing the AIM sequence, demonstrated that AOD2 and AOD5 bind synergistically as a heterodimer to the AIM sequence (CHAE *et al.* 2007b). Pull-down assays and size exclusion chromatography using affinity purified tagged versions of the AOD2 and AOD5 proteins further supported the notion that the proteins physically interact with each other. Orthologs of the AOD2 and AOD5 proteins in *Aspergillus nidulans* (AcuM and AcuK) and *Podospora anserina* (RSE2 and RSE3) also play a role in AOX induction as well as in the induction of genes required for gluconeogenesis (SUZUKI *et al.* 2012; BOVIER *et al.* 2014).

Based on the above, the current model of AOX regulation in *N. crassa* is that when the sETC is disrupted, an as yet unknown signaling molecule (or signaling cascade) probably originating in the mitochondria, either directly or indirectly, activates the AOD2-AOD5 heterodimer bound to the promoter of the *aod-1* gene. This activation leads to enhanced transcription of the *aod-1* gene. The *aod-1* mRNA is then translated on

cytosolic ribosomes and the AOX protein is imported into mitochondria (Fig. 6). Apart from the above-mentioned regulatory factors, no other players in the AOX regulatory pathway have been characterized.

1.10.1 Knockout mutant library screening

The mutagenesis based screen described above (DESCHENEAU *et al.* 2005) was not saturated and was mainly designed to identify mutants with AOX transcriptional regulatory defects. More recently the *N. crassa* knockout mutant (KO) library (COLOT *et al.* 2006) was screened, to further identify mutants unable to produce AOX (NARGANG *et al.* 2012). This screen was based on the idea that KO mutant strains growing very poorly or not at all in the presence of AA should lack AOX. The gene knocked out in such a mutant could be involved in the proper functioning or production of AOX (NARGANG *et al.* 2012). KO strains identified as having no (or very slow) growth on medium containing AA were then grown in the presence of Cm and mitochondria were isolated. Western blot analysis of mitochondrial proteins was carried out to determine levels of AOX. Sixty-two strains were identified that had lower levels of AOX. These mutants were placed into three classes, designated, class 1, 2 and 3. Class 1 consisted of strains that had virtually no AOX under inducing conditions at one or both the time points tested. This class included previously identified genes (*aod-1, aod-2* and *aod-5* KO mutants) as well as eight new mutants. Class 2 consisted of twenty mutants with moderate reductions of AOX levels. Class 3 consists of thirty-four mutants with slight reductions in AOX levels. Subsequent to the study, an additional class 1 mutant was identified (mutant 113G8, KO of NCU03071).

Figure 6. Current model of *N. crassa* AOX regulation. A) AOX regulation in non-inducing conditions. Under non-inducing conditions, the AOD2-AOD5 heterodimer remains bound to the promoter of the *aod-1* gene and a low level of constitutive expression of the *aod-1* gene occurs. B) AOX regulation in inducing conditions. When the sETC is disrupted, an unknown signaling molecule activates the AOD2-AOD5

heterodimer. A signaling cascade may also be involved. This leads to enhanced transcription of the *aod-1* gene (beginning at the upstream region, represented by an arrow) and translation of AOX protein in the cytosol. The AOX protein is subsequently imported into mitochondria.

1.11 Objective of this study

The study of class 1 strains was thought to provide an excellent opportunity to identify genes and mechanisms involved in the functioning and regulation of AOX, as knockout of the genes in these strains lead to an absence of detectable amounts of AOX protein at 24 and/or 48 hours of growth in the presence of Cm. Two of these genes (NCU08887 and NCU01542) were studied to understand AOX function and/or regulation. Unexpected results suggested that the genes were not involved in AOX function. This led to a thorough examination of all novel class 1 mutants (Table 1) with respect to their authenticity.

The above-mentioned KO mutant screen also identified a different set of mutant strain. These showed very poor or no growth in the presence of AA but had virtually normal levels of AOX protein under inducing conditions (+Cm). It was hypothesized that these strains may lack an element essential for the proper assembly of the AOX protein or integration of AOX into the inner leaflet of the MIM. It was also possible that the genes affected in these strains played a role in post-translational modification steps to the activate the AOX protein in *N. crassa*. Such strains were termed putative 'assembly mutants'. Five such strains (Table 2) were further analyzed with the aim of identifying an assembly mutant.

Table 1. NCU numbers and gene product information for the eight mutants with severe AOX deficiencies (NARGANG *et al.* 2012).

Strains	NCU number	Gene/Protein KO
23H2	NCU08887	Hypothetical protein (major facilitator superfamily)
40E6*	NCU05600 NCU12096	Stk-33/ Serine/ Threonine protein kinase-33 Aspartyl aminopeptidase
41G7	NCU03589	Hypothetical protein
47H10	NCU00778	Sed5 vesicle protein (Transmembrane adaptor Erv26)
52D8	NCU07281	Glucose-6-phosphate isomerase (gpi-1) (phosphoglucose isomerase)
83H3	NCU08365	RNA polymerase II mediator complex component Med8
88H8	NCU01542	Hypothetical protein (HbrB like domain)
100B5**	NCU08158	Dual specificity phosphatase
113G8***	NCU03071	MAP kinase kinase kinase SskB (os-4)

* Initial analysis of the genome sequence identified a single coding sequence. This was used during construction of the KO mutant library. Subsequent analysis showed two genes in the region that were removed in the KO.

** Not examined as part of this study. Previously examined (DESAULNIERS 2013)

*** Identified after the publication of the initial KO screen (NARGANG *et al.* 2012).

Table 2. NCU numbers and gene product information for possible assembly mutants.

Strains	NCU number	Gene/Protein KO
13G11	NCU04566	Protein kinase 10
28B10	NCU08137	Hypothetical protein
85H5	NCU09803	Thioredoxin
99B8	NCU09327	Cytochrome-4/ protein phosphatase
101D3	NCU09560	Superoxide dismutase

References

AFRODITI, C., and T. KOSTAS, 2013 The mitochondrial intermembrane space: a hub for oxidative folding linked to protein biogenesis. Antioxid. Redox Signal. **19:** 54-62.

AHLQVIST, KATI J., RIIKKA H. HÄMÄLÄINEN, S. YATSUGA, M. UUTELA, M. TERZIOGLU *et al.*, 2012 Somatic Progenitor Cell Vulnerability to Mitochondrial DNA Mutagenesis Underlies Progeroid Phenotypes in Polg Mutator Mice. Cell Metab. **15:** 100-109.

AJIOKA, R. S., J. D. PHILLIPS and J. P. KUSHNER, 2006 Biosynthesis of heme in mammals. Biochim. Biophys. Acta - Mol. Cell Res. **1763:** 723-736.

AKHTER, S., H. C. MCDADE, J. M. GORLACH, G. HEINRICH, G. M. COX *et al.*, 2003 Role of alternative oxidase gene in pathogenesis of Cryptococcus neoformans. Infect. Immun. **71:** 5794-5802.

AKINS, R. A., and A. M. LAMBOWITZ, 1984 The [poky] mutant of Neurospora contains a 4-base-pair deletion at the 5' end of the mitochondrial small rRNA. Proc. Natl. Acad. Sci. USA **81:** 3791-3795.

ALBURY, M. S., C. ELLIOTT and A. L. MOORE, 2009 Towards a structural elucidation of the alternative oxidase in plants. Physiol. Plant. **137:** 316-327.

ALBURY, M. S., C. ELLIOTT and A. L. MOORE, 2010 Ubiquinol-binding site in the alternative oxidase: Mutagenesis reveals features important for substrate binding and inhibition. Biochim. Biophys. Acta - Bioenergetics **1797:** 1933-1939.

ALDRIDGE, J. E., T. HORIBE and N. J. HOOGENRAAD, 2007 Discovery of Genes Activated by the Mitochondrial Unfolded Protein Response (mtUPR) and Cognate Promoter Elements. PLoS One **2:** e874.

ANDERSSON, J. O., 2013 Gene Transfer and the Chimeric Nature of Eukaryotic Genomes, pp. 181-197 in *Lateral Gene Transfer in Evolution*, edited by U. GOPHNA. Springer New York.

ANDERSSON, M. E., and P. NORDLUND, 1999 A revised model of the active site of alternative oxidase. FEBS Lett. **449:** 17-22.

ARCHIBALD, J., 2011 Origin of eukaryotic cells: 40 years on. Symbiosis **54:** 69-86.

ARMSTRONG, M. R., V. C. BLOK and M. S. PHILLIPS, 2000 A Multipartite Mitochondrial Genome in the Potato Cyst Nematode Globodera pallida. Genetics **154:** 181-192.

AZCÓN-BIETO, J., M. RIBAS-CARBÓ, M. A. GONZÁLEZ-MELER and J. PEÑUELAS, 1989 Sulfide-Resistant Respiration in Leaves of Elodea canadensis Michx Comparison with Cyanide-Resistant Respiration. Plant Physiol. **90:** 1249-1251.

BALABAN, R. S., S. NEMOTO and T. FINKEL, 2005 Mitochondria, Oxidants, and Aging. Cell **120:** 483-495.

BALLHORN, D. J., S. KAUTZ, M. HEIL and A. D. HEGEMAN, 2009 Analyzing plant defenses in nature. Plant Signal Behav. **4:** 743-745.

BARTOLI, C. G., F. GOMEZ, G. GERGOFF, J. J. GUIAMÉT and S. PUNTARULO, 2005 Up-regulation of the mitochondrial alternative oxidase pathway enhances photosynthetic electron transport under drought conditions. J. Exp. Bot. **56:** 1269-1276.

BATUT, J., S. G. E. ANDERSSON and D. O'CALLAGHAN, 2004 The evolution of chronic infection strategies in the [alpha]-proteobacteria. Nat. Rev. Microbiol. **2:** 933-945.

BAUER, M. F., S. HOFMANN, W. NEUPERT and M. BRUNNER, 2000 Protein translocation into mitochondria: the role of TIM complexes. Trends Cell Biol. **10:** 25-31.

BAURAIN, D., M. DINANT, N. COOSEMANS and R. F. MATAGNE, 2003 Regulation of the Alternative Oxidase Aox1 Gene inChlamydomonas reinhardtii. Role of the Nitrogen Source on the Expression of a Reporter Gene under the Control of theAox1 Promoter. Plant Physiol. **131:** 1418-1430.

BECKER, T., M. GEBERT, N. PFANNER and M. VAN DER LAAN, 2009 Biogenesis of mitochondrial membrane proteins. Curr. Opin. Cell Biol. **21:** 484-493.

BECKER, T., S. PFANNSCHMIDT, B. GUIARD, D. STOJANOVSKI, D. MILENKOVIC *et al.*, 2007 Biogenesis of the mitochondrial TOM complex: Mim1 promotes insertion and assembly of signal-anchored receptors. J. Biol. Chem. **283:** 120-127.

BENDALL, D. S., and W. D. BONNER, 1971 Cyanide-insensitive respiration in plant mitochondria. Plant Physiol. **47:** 236-245.

BERMAN, S. B., F. J. PINEDA and J. M. HARDWICK, 2008 Mitochondrial fission and fusion dynamics: the long and short of it. Cell Death Differ. **15:** 1147-1152.

BERNT, M., R. MACHNÉ, A. H. SAHYOUN, M. MIDDENDORF and P. F. STADLER, 2013 Mitochondrial Genome Evolution in *eLS*. John Wiley & Sons, Ltd.

BERRIDGE, M. J., M. D. BOOTMAN and P. LIPP, 1998 Calcium - a life and death signal. Nature **395:** 645-648.

BERTHOLD, D. A., M. E. ANDERSSON and P. NORDLUND, 2000 New insight into the structure and function of the alternative oxidase. Biochim. Biophys. Acta - Bioenergetics **1460:** 241-254.

BERTHOLD, D. A., and P. STENMARK, 2003 Membrane-bound diiron carboxylate proteins. Annu. Rev. Plant Biol. **54:** 497-517.

BERTRAND, H., C. A. ARGAN and N. A. SZAKACS, 1983 Genetic control of the biogenesis of cyanide insensitive respiration in Neurospora crassa, pp. 495-507 in *Mitochondria*. Walter de Gruyter, Berlin.

BHANGOO, M. K., S. TZANKOV, A. C. Y. FAN, K. DEJGAARD, D. Y. THOMAS *et al.*, 2007 Multiple 40-kDa Heat-Shock Protein Chaperones Function in Tom70-dependent Mitochondrial Import. Mol. Biol. Cell. **18:** 3414-3428.

BLANCO, N. E., M. GUINEA-DÍAZ, J. WHELAN and Å. STRAND, 2014 Interaction between plastid and mitochondrial retrograde signalling pathways during changes to plastid redox status. Philos. Trans. R. Soc. Lond., Ser. B: Biol. Sci. **369**.

BOLDOGH, I. R., and L. A. PON, 2007 Mitochondria on the move. Trends Cell Biol. **17:** 502-510.

BORGHOUTS, C., A. WERNER, T. ELTHON and H. D. OSIEWACZ, 2001 Copper-Modulated Gene Expression and Senescence in the Filamentous Fungus Podospora anserina. Mol. Cell. Biol. **21:** 390-399.

BORKOVICH, K. A., L. A. ALEX, O. YARDEN, M. FREITAG, G. E. TURNER *et al.*, 2004 Lessons from the Genome Sequence of Neurospora crassa: Tracing the Path from Genomic Blueprint to Multicellular Organism. Microbiol. Mol. Biol. Rev. **68:** 1-108.

BOVIER, E., C. H. SELLEM, A. HUMBERT and A. SAINSARD-CHANET, 2014 Genetic and Functional Investigation of Zn2Cys6 Transcription Factors RSE2 and RSE3 in Podospora anserina. Eukaryot. Cell **13:** 53-65.

BRATIC, A., N.-G. LARSSON, XF and RAN, 2013 The role of mitochondria in aging. J. Clin. Invest. **123:** 951-957.

BROADWATER, J. A., J. AI, T. M. LOEHR, L. SANDERS and B. G. FOX, 1998 Peroxodiferric Intermediate of Stearoyl-Acyl Carrier Protein Δ9 Desaturase: Oxidase Reactivity during Single Turnover and Implications for the Mechanism of Desaturation. Biochemistry **37:** 14664-14671.

BURGER, G., M. W. GRAY and B. FRANZ LANG, 2003 Mitochondrial genomes: anything goes. Trends Genet. **19:** 709-716.

BURGER, G., and B. F. LANG, 2003 Parallels in Genome Evolution in Mitochondria and Bacterial Symbionts. IUBMB Life **55:** 205-212.

BUTOW, R. A., and N. G. AVADHANI, 2004 Mitochondrial signaling: the retrograde response. Mol. Cell **14:** 1-15.

CARLSON, E. A., V. K. RAO and S. S. YAN, 2013 From a cell's viewpoint: targeting mitochondria in Alzheimer's disease. Drug Discov. Today Ther. Strateg. **10:** e91-e98.

CARNEIRO, P., M. DUARTE and A. VIDEIRA, 2007 The External Alternative NAD(P)H Dehydrogenase NDE3 Is Localized both in the Mitochondria and in the Cytoplasm of Neurospora crassa. J. Mol. Biol. **368:** 1114-1121.

CARRÉ, J. E., C. AFFOURTIT and A. L. MOORE, 2011 Interaction of purified alternative oxidase from thermogenic *Arum maculatum* with pyruvate. FEBS Lett. **585:** 397-401.

CASTRO-GUERRERO, N., J. RODRÍGUEZ-ZAVALA, A. MARÍN-HERNÁNDEZ, S. RODRÍGUEZ-ENRÍQUEZ and R. MORENO-SÁNCHEZ, 2008 Enhanced alternative oxidase and antioxidant enzymes under Cd2+ stress in Euglena. J. Bioenerg. Biomembr. **40:** 227-235.

CHABAN, Y., E. J. BOEKEMA and N. V. DUDKINA, 2014 Structures of mitochondrial oxidative phosphorylation supercomplexes and mechanisms for their stabilisation. Biochim. Biophys. Acta - Bioenergetics **1837:** 418-426.

CHACINSKA, A., P. REHLING, B. GUIARD, A. E. FRAZIER, A. SCHULZE-SPECKING *et al.*, 2003 Mitochondrial translocation contact sites: separation of dynamic and stabilizing elements in formation of a TOM–TIM–preprotein supercomplex. EMBO J. **22:** 5370-5381.

CHAE, M. S., C. C. LIN, K. E. KESSLER, C. E. NARGANG, L. L. TANTON *et al.*, 2007a Identification of an alternative oxidase induction motif in the promoter region of the aod-1 gene in Neurospora crassa. Genetics **175:** 1597-1606.

CHAE, M. S., C. E. NARGANG, I. A. CLEARY, C. C. LIN, A. T. TODD *et al.*, 2007b Two zinc-cluster transcription factors control induction of alternative oxidase in Neurospora crassa. Genetics **177:** 1997-2006.

CHAN, D. C., 2006 Mitochondrial Fusion and Fission in Mammals. Annu. Rev. Cell. Dev. Biol. **22:** 79-99.

CHAN, D. C., 2012 Fusion and Fission: Interlinked Processes Critical for Mitochondrial Health. Annu. Rev. Genet. **46:** 265-287.

CHANDEL, N. S., 2014 Mitochondria as signaling organelles. BMC Biol. **12:** 34.

CHAUDHURI, M., R. SHARAN and G. C. HILL, 2002 Trypanosome Alternative Oxidase is Regulated Post-transcriptionally at the Level of RNA Stability. J. Eukaryot. Microbiol. **49:** 263-269.

CHEN, H., and D. C. CHAN, 2010 Physiological functions of mitochondrial fusion. Ann. N. Y. Acad. Sci. **1201:** 21-25.

CHIABRANDO, D., S. MERCURIO and E. TOLOSANO, 2014 Heme and erythropoieis: more than a structural role. Haematologica **99:** 973-983.

CIRCU, M. L., and T. Y. AW, 2010 Reactive oxygen species, cellular redox systems, and apoptosis. Free Radical Biol. Med. **48:** 749-762.

CLAPHAM, D. E., 2007 Calcium Signaling. Cell **131:** 1047-1058.

CLAYTON, C., and M. SHAPIRA, 2007 Post-transcriptional regulation of gene expression in trypanosomes and leishmanias. Mol. Biochem. Parasitol. **156:** 93-101.

CLIFTON, R., R. LISTER, K. L. PARKER, P. G. SAPPL, D. ELHAFEZ *et al.*, 2005 Stress-induced co-expression of alternative respiratory chain components in Arabidopsis thaliana. Plant Mol. Biol. **58:** 193-212.

CLIFTON, R., A. H. MILLAR and J. WHELAN, 2006 Alternative oxidases in Arabidopsis: A comparative analysis of differential expression in the gene family provides new insights into function of non-phosphorylating bypasses. Biochim. Biophys. Acta - Bioenergetics **1757:** 730-741.

COLOT, H. V., G. PARK, G. E. TURNER, C. RINGELBERG, C. M. CREW *et al.*, 2006 A high-throughput gene knockout procedure for Neurospora reveals functions for multiple transcription factors. Proc. Natl. Acad. Sci. USA **103:** 10352-10357.

CONSIDINE, M. J., D. O. DALEY and J. WHELAN, 2001 The Expression of Alternative Oxidase and Uncoupling Protein during Fruit Ripening in Mango. Plant Physiol. **126:** 1619-1629.

CONSIDINE, M. J., R. C. HOLTZAPFFEL, D. A. DAY, J. WHELAN and A. H. MILLAR, 2002 Molecular Distinction between Alternative Oxidase from Monocots and Dicots. Plant Physiol. **129:** 949-953.

CONTRERAS, L., I. DRAGO, E. ZAMPESE and T. POZZAN, 2010 Mitochondria: The calcium connection. Biochim. Biophys. Acta - Bioenergetics **1797:** 607-618.

COPELAND, J. M., J. CHO, T. LO JR, J. H. HUR, S. BAHADORANI *et al.*, 2009 Extension of Drosophila Life Span by RNAi of the Mitochondrial Respiratory Chain. Curr. Biol. **19:** 1591-1598.

COSTA, J. H., Y. JOLIVET, M.-P. HASENFRATZ-SAUDER, E. G. ORELLANO, M. DA GUIA SILVA LIMA *et al.*, 2007 Alternative oxidase regulation in roots of Vigna unguiculata cultivars differing in drought/salt tolerance. J. Plant Physiol. **164:** 718-727.

COZZOLINO, M., A. FERRI, C. VALLE and M. T. CARRÌ, 2013 Mitochondria and ALS: Implications from novel genes and pathways. Mol. Cell. Neurosci. **55:** 44-49.

CRICHTON, P. G., C. AFFOURTIT, M. S. ALBURY, J. E. CARRÉ and A. L. MOORE, 2005 Constitutive activity of Sauromatum guttatum alternative oxidase in Schizosaccharomyces pombe implicates residues in addition to conserved cysteines in α-keto acid activation. FEBS Lett. **579:** 331-336.

CRISTINA, D., M. CARY, A. LUNCEFORD, C. CLARKE and C. KENYON, 2009 A Regulated Response to Impaired Respiration Slows Behavioral Rates and Increases Lifespan in Caenorhabditis elegans. PLoS Genet. **5:** e1000450.

DESAULNIERS, A. B., 2013 The role of YVH1, a dual specificity phosphatase, in the production of alternative oxidase in the filamentous fungus Neurospora crassa pp. in *Department of Biological Sciences*. University of Alberta, Edmonton, Alberta.

DESCHENEAU, A. T., I. A. CLEARY and F. E. NARGANG, 2005 Genetic evidence for a regulatory pathway controlling alternative oxidase production in Neurospora crassa. Genetics **169:** 123-135.

DJAJANEGARA, I., P. FINNEGAN, C. MATHIEU, T. MCCABE, J. WHELAN *et al.*, 2002 Regulation of alternative oxidase gene expression in soybean. Plant Mol. Biol. **50:** 735-742.

DOJCINOVIC, D., J. KROSTING, A. HARRIS, D. WAGNER and D. RHOADS, 2005 Identification of a region of the Arabidopsis AtAOX1a promoter necessary for mitochondrial retrograde regulation of expression. Plant Mol. Biol. **58:** 159-175.

DUAN, W., 2013 Targeting Sirtuin-1 in Huntington's Disease: Rationale and Current Status. CNS Drugs **27:** 345-352.

DUDEK, J., P. REHLING and M. VAN DER LAAN, 2013 Mitochondrial protein import: Common principles and physiological networks. Biochim. Biophys. Acta - Mol. Cell Res. **1833:** 274-285.

DURIEUX, J., S. WOLFF and A. DILLIN, 2011 The Cell-Non-Autonomous Nature of Electron Transport Chain-Mediated Longevity. Cell **144:** 79-91.

DYALL, S. D., M. T. BROWN and P. J. JOHNSON, 2004 Ancient Invasions: From Endosymbionts to Organelles. Science **304:** 253-257.

EDERLI, L., R. MORETTINI, A. BORGOGNI, C. WASTERNACK, O. MIERSCH *et al.*, 2006 Interaction between Nitric Oxide and Ethylene in the Induction of Alternative Oxidase in Ozone-Treated Tobacco Plants. Plant Physiol. **142:** 595-608.

EDGAR, D., I. SHABALINA, Y. CAMARA, A. WREDENBERG, M. A. CALVARUSO *et al.*, 2009 Random Point Mutations with Major Effects on Protein-Coding Genes Are the Driving Force behind Premature Aging in mtDNA Mutator Mice. Cell Metab. **10:** 131-138.

EDWARDS, D. L., and E. ROSENBERG, 1976 Regulation of Cyanide-Insensitive Respiration in Neurospora. Eur. J. Biochem. **62:** 217-221.

EDWARDS, D. L., E. ROSENBERG and P. A. MARONEY, 1974 Induction of Cyanide-insensitive Respiration in Neurospora crassa. J. Biol. Chem. **249:** 3551-3556.

ENDO, T., and K. YAMANO, 2010 Transport of proteins across or into the mitochondrial outer membrane. Biochim. Biophys. Acta - Mol. Cell Res. **1803:** 706-714.

EPSTEIN, C. B., J. A. WADDLE, W. HALE, V. DAVÉ, J. THORNTON *et al.*, 2001 Genome-wide responses to mitochondrial dysfunction. Mol. Biol. Cell. **12:** 297-308.

FANG, J., and D. S. BEATTIE, 2003 Alternative oxidase present in procyclic Trypanosoma brucei may act to lower the mitochondrial production of superoxide. Arch. Biochem. Biophys. **414:** 294-302.

FELICIELLO, A., M. E. GOTTESMAN and E. V. AVVEDIMENTO, 2005 cAMP-PKA signaling to the mitochondria: protein scaffolds, mRNA and phosphatases. Cell. Signal. **17:** 279-287.

FENG, H., D. GUAN, K. SUN, Y. WANG, T. ZHANG *et al.*, 2013 Expression and signal regulation of the alternative oxidase genes under abiotic stresses. Acta Biochim. Biophys. Sin. **45:** 985-994.

FERRAMOSCA, A., and V. ZARA, 2013 Biogenesis of mitochondrial carrier proteins: Molecular mechanisms of import into mitochondria. Biochim. Biophys. Acta - Mol. Cell Res. **1833:** 494-502.

FINKEL, T., 2012 From sulfenylation to sulfhydration: what a thiolate needs to tolerate. Sci. Signal. **5:** pe10.

FOX, B. G., J. SHANKLIN, C. SOMERVILLE and E. MÜNCK, 1993 Stearoyl-acyl carrier protein delta 9 desaturase from Ricinus communis is a diiron-oxo protein. Proc. Natl. Acad. Sci. USA **90:** 2486-2490.

FREDERICK, R. L., and J. M. SHAW, 2007 Moving Mitochondria: Establishing Distribution of an Essential Organelle. Traffic **8:** 1668-1675.

FRIEDMAN, J. R., L. L. LACKNER, M. WEST, J. R. DIBENEDETTO, J. NUNNARI *et al.*, 2011 ER Tubules Mark Sites of Mitochondrial Division. Science **334:** 358-362.

FUJII, S., and K. TORIYAMA, 2009 Suppressed expression of retrograde-regulated male sterility restores pollen fertility in cytoplasmic male sterile rice plants. Proc. Natl. Acad. Sci. USA **106:** 9513-9518.

GABAY-LAUGHNAN, S., and K. J. NEWTON, 2005 Mitochondrial mutations in maize. Maydica **50:** 349.

GALLUZZI, L., J. M. BRAVO-SAN PEDRO and G. KROEMER, 2014 Organelle-specific initiation of cell death. Nat. Cell Biol. **16:** 728-736.

GASSNER, G. T., and S. J. LIPPARD, 1999 Component Interactions in the Soluble Methane Monooxygenase System from Methylococcus capsulatus (Bath). Biochemistry **38:** 12768-12785.

GEBERT, N., A. CHACINSKA, K. WAGNER, B. GUIARD, C. M. KOEHLER *et al.*, 2008 Assembly of the three small Tim proteins precedes docking to the mitochondrial carrier translocase. EMBO Rep. **9:** 548-554.

GELLERICH, F. N., S. TRUMBECKAITE, J. R. OPALKA, E. SEPPET, H. N. RASMUSSEN *et al.*, 2000 Function of the mitochondrial outer membrane as a diffusion barrier in health and diseases. Biochem. Soc. Trans. **28:** 164–169.

GENOVA, M., 2014 Electron Transport in the Mitochondrial Respiratory Chain, pp. 401-417 in *The Structural Basis of Biological Energy Generation*, edited by M. F. HOHMANN-MARRIOTT. Springer Netherlands.

GIRAUD, E., O. VAN AKEN, L. H. M. HO and J. WHELAN, 2009 The Transcription Factor ABI4 Is a Regulator of Mitochondrial Retrograde Expression of ALTERNATIVE OXIDASE1a. Plant Physiol. **150:** 1286-1296.

GOMES, C. M., J. LE GALL, A. V. XAVIER and M. TEIXEIRA, 2001 Could a Diiron-Containing Four-Helix-Bundle Protein Have Been a Primitive Oxygen Reductase? ChemBioChem **2:** 583-587.

GOODPASTER, B. H., 2013 Mitochondrial Deficiency Is Associated With Insulin Resistance. Diabetes **62:** 1032-1035.

GRANT, N., Y. ONDA, Y. KAKIZAKI, K. ITO, J. WATLING *et al.*, 2009 Two Cys or Not Two Cys? That Is the Question; Alternative Oxidase in the Thermogenic Plant Sacred Lotus. Plant Physiol. **150:** 987-995.

GRANT, N. M., R. E. MILLER, J. R. WATLING and S. A. ROBINSON, 2008 Synchronicity of thermogenic activity, alternative pathway respiratory flux, AOX protein content, and carbohydrates in receptacle tissues of sacred lotus during floral development. J. Exp. Bot. **59:** 705-714.

GRAY, M. W., 2012 Mitochondrial Evolution. Cold Spring Harb Perspect Biol. **4:** a011403.

GREDILLA, R., J. GRIEF and H. D. OSIEWACZ, 2006 Mitochondrial free radical generation and lifespan control in the fungal aging model Podospora anserina. Exp. Gerontol. **41:** 439-447.

GRIESHABER, M. K., and S. VÖLKEL, 1998 Animal adaptations for tolerance and exploitation of poisonous sulfide. Annu. Rev. Physiol. **60:** 33-53.

GRIFFITHS, A. J. F., R. A. COLLINS and F. E. NARGANG, 1995 Mitochondrial genetics of Neurospora, pp. 93-105 in *The Mycota II, Genetics and Biotechnology (U. Kück, Ed.)*.

GRIPARIC, L., and A. M. VAN DER BLIEK, 2001 The many shapes of mitochondrial membranes. Traffic **2:** 235-244.

GROSS, J., and D. BHATTACHARYA, 2009 Mitochondrial and plastid evolution in eukaryotes: an outsiders' perspective. Nat. Rev. Genet. **10:** 495-505.

GUTIÉRREZ-AGUILAR, M., and C. P. BAINES, 2014 Structural mechanisms of cyclophilin D-dependent control of the mitochondrial permeability transition pore. Biochim. Biophys. Acta Biochim Biophys Acta.

HACKENBROCK, C., B. CHAZOTTE and S. GUPTE, 1986 The random collision model and a critical assessment of diffusion and collision in mitochondrial electron transport. J. Bioenerg. Biomembr. **18:** 331-368.

HAMANAKA, R. B., and N. S. CHANDEL, 2009 Mitochondrial reactive oxygen species regulate hypoxic signaling. Curr. Opin. Cell Biol. **21:** 894-899.

HARBAUER, ANGELIKA B., RENÉ P. ZAHEDI, A. SICKMANN, N. PFANNER and C. MEISINGER, 2014 The Protein Import Machinery of Mitochondria—A Regulatory Hub in Metabolism, Stress, and Disease. Cell Metab. **19:** 357-372.

HARNER, M., C. KÖRNER, D. WALTHER, D. MOKRANJAC, J. KAESMACHER *et al.*, 2011 The mitochondrial contact site complex, a determinant of mitochondrial architecture. EMBO J. **30:** 4356-4370.

HEAD, B. P., M. ZULAIKA, S. RYAZANTSEV and A. M. VAN DER BLIEK, 2011 A novel mitochondrial outer membrane protein, MOMA-1, that affects cristae morphology in Caenorhabditis elegans. Mol. Biol. Cell. **22:** 831-841.

HEINEMEYER, J., H.-P. BRAUN, E. J. BOEKEMA and R. KOUŘIL, 2007 A Structural Model of the Cytochrome c Reductase/Oxidase Supercomplex from Yeast Mitochondria. J. Biol. Chem. **282:** 12240-12248.

HELLER, J., and P. TUDZYNSKI, 2011 Reactive Oxygen Species in Phytopathogenic Fungi: Signaling, Development, and Disease. Annu. Rev. Phytopathol. **49:** 369-390.

HERRMANN, JOHANNES M., 2011 MINOS Is Plus: A Mitofilin Complex for Mitochondrial Membrane Contacts. Dev. Cell **21:** 599-600.

HERRMANN, J. M., and J. RIEMER, 2010 The Intermembrane Space of Mitochondria. Antioxid. Redox Signal. **13**.

HERRMANN, J. M., and J. RIEMER, 2012 Mitochondrial Disulfide Relay: Redox-regulated Protein Import into the Intermembrane Space. J. Biol. Chem. **287:** 4426-4433.

HILL, S., and H. VAN REMMEN, 2014 Mitochondrial stress signaling in longevity: A new role for mitochondrial function in aging. Redox Biol. **2:** 936-944.

HOLTZAPFFEL, R. C., J. CASTELLI, P. M. FINNEGAN, A. H. MILLAR, J. WHELAN *et al.*, 2003 A tomato alternative oxidase protein with altered regulatory properties. Biochim. Biophys. Acta - Bioenergetics **1606:** 153-162.

HOPPINS, S., S. R. COLLINS, A. CASSIDY-STONE, E. HUMMEL, R. M. DEVAY *et al.*, 2011 A mitochondrial-focused genetic interaction map reveals a scaffold-like complex required for inner membrane organization in mitochondria. J. Cell Biol. **195:** 323-340.

HORVATH, S. E., H. RAMPELT, S. OELJEKLAUS, B. WARSCHEID, M. VANDERLAAN *et al.*, 2015 Role of membrane contact sites in protein import into mitochondria. Protein Sci. **24:** 277-297.

HOUTKOOPER, R. H., L. MOUCHIROUD, D. RYU, N. MOULLAN, E. KATSYUBA *et al.*, 2013 Mitonuclear protein imbalance as a conserved longevity mechanism. Nature **497:** 451-457.

HUANG, X., U. VON RAD and J. DURNER, 2002 Nitric oxide induces transcriptional activation of the nitric oxide-tolerant alternative oxidase in Arabidopsis suspension cells. Planta **215:** 914-923.

ITO-INABA, Y., Y. HIDA and T. INABA, 2009 What is critical for plant thermogenesis? Differences in mitochondrial activity and protein expression between thermogenic and non-thermogenic skunk cabbages. Planta **231:** 121-130.

JÄGER, R., and H. O. FEARNHEAD, 2013 Mitochondrial Regulation of Cell-Death, pp. 33-60 in *Mitochondria as Targets for Phytochemicals in Cancer Prevention and Therapy*, edited by D. CHANDRA. Springer New York.

JARMUSZKIEWICZ, W., M. CZARNA and F. SLUSE, 2005 Substrate kinetics of the Acanthamoeba castellanii alternative oxidase and the effects of GMP. Biochim. Biophys. Acta - Bioenergetics **1708**.

JARMUSZKIEWICZ, W. A., M. BEHRENDT, R. NAVET and F. E. SLUSE, 2002 Uncoupling protein and alternative oxidase of *Dictyostelium discoideum*: occurrence, properties and protein expression during vegetative life and starvation-induced early development. FEBS Lett. **532:** 459-464.

JAZWINSKI, S. M., 2013 The retrograde response: When mitochondrial quality control is not enough. Biochim. Biophys. Acta - Mol. Cell Res. **1833:** 400-409.

JAZWINSKI, S. M., and A. KRIETE, 2012 The yeast retrograde response as a model of intracellular signaling of mitochondrial dysfunction. Front. Physiol. **3:** 139.

JIA, Y., B. ROTHERMEL, J. THORNTON and R. A. BUTOW, 1997 A basic helix-loop-helix-leucine zipper transcription complex in yeast functions in a signaling pathway from mitochondria to the nucleus. Mol. Cell. Biol. **17:** 1110-1117.

JOSEPH-HORNE, T., D. W. HOLLOMON and P. M. WOOD, 2001 Fungal respiration: a fusion of standard and alternative components. Biochim. Biophys. Acta - Bioenergetics **1504:** 179-195.

JOVAISAITE, V., L. MOUCHIROUD and J. AUWERX, 2014 The mitochondrial unfolded protein response, a conserved stress response pathway with implications in health and disease. J. Exp. Biol. **217:** 137-143.

JUÁREZ, O., G. GUERRA, I. VELÁZQUEZ, O. FLORES-HERRERA, R. E. RIVERA-PÉREZ *et al.*, 2006 The physiologic role of alternative oxidase in Ustilago maydis. FEBS J. **273:** 4603-4615.

KARPOVA, O. V., E. V. KUZMIN, T. E. ELTHON and K. J. NEWTON, 2002 Differential Expression of Alternative Oxidase Genes in Maize Mitochondrial Mutants. Plant Cell **14:** 3271-3284.

KAZLAUSKAITE, A., and M. M. K. MUQIT, 2014 PINK1 and Parkin – mitochondrial interplay between phosphorylation and ubiquitylation in Parkinson's disease. FEBS J. **282:** 215-223.

KELLEY, D. E., J. HE, E. V. MENSHIKOVA and V. B. RITOV, 2002 Dysfunction of Mitochondria in Human Skeletal Muscle in Type 2 Diabetes. Diabetes **51:** 2944-2950.

KEUNEN, E., M. JOZEFCZAK, T. REMANS, J. VANGRONSVELD and A. CUYPERS, 2013 Alternative respiration as a primary defence during cadmium-induced mitochondrial oxidative challenge in Arabidopsis thaliana. Environ. Exp. Bot. **91:** 63-73.

KOEHLER, C. M., S. MERCHANT, W. OPPLIGER, K. SCHMID, E. JAROSCH *et al.*, 1998 Tim9p, an essential partner subunit of Tim10p for the import of mitochondrial carrier proteins. EMBO J. **17:** 6477-6486.

KOMEILI, A., K. P. WEDAMAN, E. K. O'SHEA and T. POWERS, 2000 Mechanism of Metabolic Control: Target of Rapamycin Signaling Links Nitrogen Quality to the Activity of the Rtg1 and Rtg3 Transcription Factors. J. Cell Biol. **151:** 863-878.

KÖRNER, C., M. BARRERA, J. DUKANOVIC, K. EYDT, M. HARNER *et al.*, 2012 The C-terminal domain of Fcj1 is required for formation of crista junctions and interacts with the TOB/SAM complex in mitochondria. Mol. Biol. Cell. **23:** 2143-2155.

KORNMANN, B., and P. WALTER, 2010 ERMES-mediated ER-mitochondria contacts: molecular hubs for the regulation of mitochondrial biology. J. Cell Sci. **123:** 1389-1393.

KOUSSEVITZKY, S., A. NOTT, T. C. MOCKLER, F. HONG, G. SACHETTO-MARTINS *et al.*, 2007 Signals from Chloroplasts Converge to Regulate Nuclear Gene Expression. Science **316:** 715-719.

KUTIK, S., D. STOJANOVSKI, L. BECKER, T. BECKER, M. MEINECKE *et al.*, 2008 Dissecting Membrane Insertion of Mitochondrial β-Barrel Proteins. Cell **132:** 1011-1024.

KUZMIN, E. V., O. V. KARPOVA, T. E. ELTHON and K. J. NEWTON, 2004 Mitochondrial respiratory deficiencies signal up-regulation of genes for heat shock proteins. J. Biol. Chem. **279:** 20672-20677.

LAKE, J. A., E. HENDERSON, M. OAKES and M. W. CLARK, 1984 Eocytes: a new ribosome structure indicates a kingdom with a close relationship to eukaryotes. Proc. Natl. Acad. Sci. USA **81:** 3786-3790.

LAMBOWITZ, A. M., J. R. SABOURIN, H. BERTRAND, R. NICKELS and L. MCINTOSH, 1989 Immunological identification of the alternative oxidase of Neurospora crassa mitochondria. Mol. Cell. Biol. **9:** 1362-1364.

LAMBOWITZ, A. M., and C. W. SLAYMAN, 1971 Cyanide-Resistant Respiration in Neurospora crassa. J. Bacteriol. **108:** 1087-1096.

LAMBOWITZ, A. M., C. W. SLAYMAN, C. L. SLAYMAN and W. D. BONNER, 1972 The electron transport components of wild type and poky strains of Neurospora crassa. J. Biol. Chem. **247:** 1536-1545.

LANG, B. F., 2014 Mitochondria and the Origin of Eukaryotes, pp. 3-18 in *Endosymbiosis*, edited by W. LÖFFELHARDT. Springer Vienna.

LAPOINTE, J., and S. HEKIMI, 2008 Early mitochondrial dysfunction in long-lived Mclk1+/-mice. J. Biol. Chem. **283:** 26217-26227.

LEE, C., K. YEN and P. COHEN, 2013 Humanin: a harbinger of mitochondrial-derived peptides? Trends Endocrinol. Metab. **24:** 222-228.

LEE, H.-C., and Y.-H. WEI, 2012 Mitochondria and Aging, pp. 311-327 in *Advances in Mitochondrial Medicine*, edited by R. SCATENA, P. BOTTONI and B. GIARDINA. Springer Netherlands.

LEE, S.-J., A. B. HWANG and C. KENYON, 2010 Inhibition of Respiration Extends C. elegans Life Span via Reactive Oxygen Species that Increase HIF-1 Activity. Curr. Biol. **20:** 2131-2136.

LEISTER, D., 2012 Retrograde signaling in plants: from simple to complex scenarios. Front. Plant. Sci. **3:** 135.

LENAZ, G., and M. GENOVA, 2012 Supramolecular Organisation of the Mitochondrial Respiratory Chain: A New Challenge for the Mechanism and Control of Oxidative Phosphorylation, pp. 107-144 in *Mitochondrial Oxidative Phosphorylation*, edited by B. KADENBACH. Springer New York.

LENAZ, G., and M. L. GENOVA, 2010 Structure and Organization of Mitochondrial Respiratory Complexes: A New Understanding of an Old Subject. Antioxid. Redox Signaling **12:** 961-1008.

LESNIK, C., Y. COHEN, A. ATIR-LANDE, M. SCHULDINER and Y. ARAVA, 2014 OM14 is a mitochondrial receptor for cytosolic ribosomes that supports co-translational import into mitochondria. Nat Commun. **5:** 5711.

LI, Q., R. G. RITZEL, L. L. MCLEAN, L. MCINTOSH, T. KO *et al.*, 1996 Cloning and analysis of the alternative oxidase gene of Neurospora crassa. Genetics **142:** 129-140.

LI, Z.-Y., Y. YANG, M. MING and B. LIU, 2011 Mitochondrial ROS generation for regulation of autophagic pathways in cancer. Biochem. Biophys. Res. Commun. **414:** 5-8.

LIAO, X., and R. A. BUTOW, 1993 RTG1 and RTG2: Two yeast genes required for a novel path of communication from mitochondria to the nucleus. Cell **72:** 61-71.

LIAO, X. S., W. C. SMALL, P. A. SRERE and R. A. BUTOW, 1991 Intramitochondrial functions regulate nonmitochondrial citrate synthase (CIT2) expression in Saccharomyces cerevisiae. Mol. Cell. Biol. **11:** 38-46.

LILL, R., 2009 Function and biogenesis of iron–sulphur proteins. Nature **460:** 831-838.

LINDSAY, J., M. D. ESPOSTI and A. P. GILMORE, 2011 Bcl-2 proteins and mitochondria—Specificity in membrane targeting for death. Biochim. Biophys. Acta - Mol. Cell Res. **1813:** 532-539.

LISTER, R., C. CARRIE, O. DUNCAN, L. H. M. HO, K. A. HOWELL *et al.*, 2007 Functional Definition of Outer Membrane Proteins Involved in Preprotein Import into Mitochondria. Plant Cell **19:** 3739-3759.

LIU, J., Q. WU, D. HE, T. MA, L. DU *et al.*, 2011 Drosophila sbo regulates lifespan through its function in the synthesis of coenzyme Q in vivo. J. Genet. Genomics **38:** 225-234.

LIU, Z., and R. A. BUTOW, 2006 Mitochondrial Retrograde Signaling. Annu. Rev. Genet. **40:** 159-185.

LOGAN, D. C., 2006 The mitochondrial compartment. J. Exp. Bot. **57:** 1225–1243.

LUTTIK, M. A. H., K. M. OVERKAMP, P. KÖTTER, S. DE VRIES, J. P. VAN DIJKEN *et al.*, 1998 The Saccharomyces cerevisiae NDE1 andNDE2 Genes Encode Separate

Mitochondrial NADH Dehydrogenases Catalyzing the Oxidation of Cytosolic NADH. J. Biol. Chem. **273:** 24529-24534.

MACPHERSON, S., M. LAROCHELLE and B. TURCOTTE, 2006 A Fungal Family of Transcriptional Regulators: the Zinc Cluster Proteins. Microbiol. Mol. Biol. Rev. **70:** 583-604.

MAGNANI, T., F. M. SORIANI, V. P. MARTINS, A. M. NASCIMENTO, V. G. TUDELLA *et al.*, 2007 Cloning and functional expression of the mitochondrial alternative oxidase of Aspergillus fumigatus and its induction by oxidative stress. FEMS Microbiol. Lett. **271:** 230-238.

MAIO, N., and T. A. ROUAULT, 2014 Iron–sulfur cluster biogenesis in mammalian cells: New insights into the molecular mechanisms of cluster delivery. Biochim. Biophys. Acta - Mol. Cell Res. **1853:** 1493-1512.

MALLIKARJUN, V., A. SRIRAM, F. SCIALO and A. SANZ, 2014 The interplay between mitochondrial protein and iron homeostasis and its possible role in ageing. Exp. Gerontol. **56:** 123-134.

MANNELLA, C. A., 2006 Structure and dynamics of the mitochondrial inner membrane cristae. Biochim. Biophys. Acta - Mol. Cell Res. **1763:** 542-548.

MANNELLA, C. A., 2008 Structural Diversity of Mitochondria. Ann. N. Y. Acad. Sci. **1147:** 171-179.

MARCHI, S., S. PATERGNANI and P. PINTON, 2014 The endoplasmic reticulum–mitochondria connection: One touch, multiple functions. Biochim. Biophys. Acta - Bioenergetics **1837:** 461-469.

MARGULIS, L., 1970 *Origin of Eukaryotic Cells*. Yale University Press, New Haven.

MARQUES, I., N. A. DENCHER, A. VIDEIRA and F. KRAUSE, 2007 Supramolecular Organization of the Respiratory Chain in Neurospora crassa Mitochondria. Eukaryot. Cell **6:** 2391-2405.

MARTIN, W., and K. V. KOWALLIK, 1999 Annotated English translation of Mereschkowsky's 1905 paper. Eur. J. Phycol. **34:** 287-295.

MARTINUS, R. D., G. P. GARTH, T. L. WEBSTER, P. CARTWRIGHT, D. J. NAYLOR *et al.*, 1996 Selective Induction of Mitochondrial Chaperones in Response to Loss of the Mitochondrial Genome. Eur. J. Biochem. **240:** 98-103.

MATUS-ORTEGA, M. G., K. G. SALMERÓN-SANTIAGO, O. FLORES-HERRERA, G. GUERRA-SÁNCHEZ, F. MARTÍNEZ *et al.*, 2011 The alternative NADH dehydrogenase is present in mitochondria of some animal taxa. Comp. Biochem. Physiol. Part D Genomics Proteomics **6:** 256-263.

MAXWELL, D. P., Y. WANG and L. MCINTOSH, 1999 The alternative oxidase lowers mitochondrial reactive oxygen production in plant cells. Proc. Natl. Acad. Sci. USA **96:** 8271-8276.

MCCLUSKEY, K., 2012 Variation in mitochondrial genome primary sequence among whole-genome-sequenced strains of Neurospora crassa. IMA Fungus **3:** 93-98.

MCDONALD, A. E., 2008 Alternative oxidase: an inter-kingdom perspective on the function and regulation of this broadly distributed'cyanide-resistant'terminal oxidase. Funct. Plant Biol. **35:** 535-552.

MCDONALD, A. E., and G. C. VANLERBERGHE, 2004 Branched Mitochondrial Electron Transport in the Animalia: Presence of Alternative Oxidase in Several Animal Phyla. IUBMB Life **56:** 333-341.

MCDONALD, A. E., and G. C. VANLERBERGHE, 2006 Origins, evolutionary history, and taxonomic distribution of alternative oxidase and plastoquinol terminal oxidase. Comp. Biochem. Physiol. Part D Genomics Proteomics **1:** 357-364.

MCDONALD, A. E., G. C. VANLERBERGHE and J. F. STAPLES, 2009 Alternative oxidase in animals: unique characteristics and taxonomic distribution. J. Exp. Biol. **212:** 2627-2634.

MCINERNEY, J. O., M. J. O'CONNELL and D. PISANI, 2014 The hybrid nature of the Eukaryota and a consilient view of life on Earth. Nat. Rev. Microbiol. **12:** 449-455.

MEDENTSE, A. G., A. Y. ARINBASAROVA, N. M. SMIRNOVA and V. K. AKIMENKO, 2004 Activation of the alternative oxidase of Yarrowia lipolytica by adenosine monophosphate. Microbiology **73:** 117-123.

MEISINGER, C., A. SICKMANN and N. PFANNER, 2008 The Mitochondrial Proteome: From Inventory to Function. Cell **134:** 22-24.

MERKX, M., D. A. KOPP, M. H. SAZINSKY, J. L. BLAZYK, J. MÜLLER *et al.*, 2001 Dioxygen Activation and Methane Hydroxylation by Soluble Methane Monooxygenase: A Tale of Two Irons and Three Proteins. Angew. Chem. Int. Ed. **40:** 2782-2807.

MICELI, M. V., J. C. JIANG, A. TIWARI, J. F. RODRIGUEZ-QUIÑONES and S. M. JAZWINSKI, 2011 Loss of Mitochondrial Membrane Potential Triggers the Retrograde Response Extending Yeast Replicative Lifespan. Front. Genet. **2:** 102.

MILLAR, A. H., J. T. WISKICH, J. WHELAN and D. A. DAY, 1993 Organic acid activation of the alternatlve oxidase of plant mitochondria. FEBS Lett. **329:** 259-262.

MINAGAWA, N., S. KOGA, M. NAKANO, S. SAKAJO and A. YOSHIMOTO, 1992 Possible involvement of superoxide anion in the induction of cyanide-resistant respiration in Hansenula anomala. FEBS Lett. **302:** 217-219.

MISHRA, P., and D. C. CHAN, 2014 Mitochondrial dynamics and inheritance during cell division, development and disease. Nat. Rev. Mol. Cell Biol. **15:** 634-646.

MÖGLICH, A., R. A. AYERS and K. MOFFAT, 2009 Structure and signaling mechanism of Per-ARNT-Sim domains. Structure **17:** 1282-1294.

MOORE, A. L., and M. S. ALBURY, 2008 Further insights into the structure of the alternative oxidase: from plants to parasites. Biochem. Soc. Trans. **36:** 1022-1026.

MOORE, A. L., W. D. BONNER JR and P. R. RICH, 1978 The determination of the proton-motive force during cyanide-insensitive respiration in plant mitochondria. Arch. Biochem. Biophys. **186:** 298-306.

MOORE, A. L., T. SHIBA, L. YOUNG, S. HARADA, K. KITA *et al.*, 2013 Unraveling the heater: new insights into the structure of the alternative oxidase. Annu. Rev. Plant Biol. **64:** 637-663.

MORRIS, J. C., M. E. DREW, M. M. KLINGBEIL, S. A. MOTYKA, T. T. SAXOWSKY *et al.*, 2001 Replication of kinetoplast DNA: an update for the new millennium. Int. J. Parasitol. **31:** 453-458.

MOSSMANN, D., C. MEISINGER and F. N. VÖGTLE, 2012 Processing of mitochondrial presequences. Biochim. Biophys. Acta - Gene Regulatory Mechanisms **1819:** 1098-1106.

MUN, J. Y., T. H. LEE, J. H. KIM, B. H. YOO, Y. Y. BAHK *et al.*, 2010 Caenorhabditis elegans mitofilin homologs control the morphology of mitochondrial cristae and influence reproduction and physiology. J. Cell. Physio. **224:** 748-756.

MURPHY, M. P., 2009 How mitochondria produce reactive oxygen species. Biochem. J. **417** 1–13.

NARGANG, F. E., K. ADAMES, C. RÜB, S. CHEUNG, N. EASTON *et al.*, 2012 Identification of Genes Required for Alternative Oxidase Production in the Neurospora crassa Gene Knockout Library. G3 (Bethesda) **2:** 1345-1356.

NEUPERT, W., and J. M. HERRMANN, 2007 Translocation of Proteins into Mitochondria. Annu. Rev. Biochem. **76:** 723-749.

NG, S., I. DE CLERCQ, O. VAN AKEN, S. R. LAW, A. IVANOVA *et al.*, 2014 Anterograde and Retrograde Regulation of Nuclear Genes Encoding Mitochondrial Proteins during Growth, Development, and Stress. Mol. Plant **7:** 1075-1093.

NORDLUND, P., and H. EKLUND, 1995 Di-iron—carboxylate proteins. Curr. Opin. Struct. Biol. **5:** 758-766.

O'MALLEY, M. A., 2010 The first eukaryote cell: an unfinished history of contestation. Studies Histor. Philos. Biol. Biomed. Sci. **41:** 212-224.

OSELLAME, L. D., T. S. BLACKER and M. R. DUCHEN, 2012 Cellular and molecular mechanisms of mitochondrial function. Best Pract. Res. Clin. Endocrinol. Metab. **26:** 711-723.

OSMAN, C., D. R. VOELKER and T. LANGER, 2011 Making heads or tails of phospholipids in mitochondria. J. Cell Biol. **192:** 7-16.

OWEN, O. E., S. C. KALHAN and R. W. HANSON, 2002 The Key Role of Anaplerosis and Cataplerosis for Citric Acid Cycle Function. J. Biol. Chem. **277:** 30409-30412.

PAGLIARINI, D. J., S. E. CALVO, B. CHANG, S. A. SHETH, S. B. VAFAI *et al.*, 2008 A Mitochondrial Protein Compendium Elucidates Complex I Disease Biology. Cell **134:** 112-123.

PAPA, S., P. MARTINO, G. CAPITANIO, A. GABALLO, D. DE RASMO *et al.*, 2012 The Oxidative Phosphorylation System in Mammalian Mitochondria, pp. 3-37 in *Advances in Mitochondrial Medicine*, edited by R. SCATENA, P. BOTTONI and B. GIARDINA. Springer Netherlands.

PAPIĆ, D., K. KRUMPE, J. DUKANOVIC, K. S. DIMMER and D. RAPAPORT, 2011 Multispan mitochondrial outer membrane protein Ugo1 follows a unique Mim1-dependent import pathway. J. Cell Biol. **194:** 397-405.

PARSONS, M. J., and D. R. GREEN, 2010 Mitochondria in cell death. Essays Biochem. **47:** 99–114.

PASCHEN, S. A., T. WAIZENEGGER, T. STAN, M. PREUSS, M. CYRKLAFF *et al.*, 2003 Evolutionary conservation of biogenesis of [beta]-barrel membrane proteins. Nature **426:** 862-866.

PASQUALINI, S., F. PAOLOCCI, A. BORGOGNI, R. MORETTINI and L. EDERLI, 2007 The overexpression of an alternative oxidase gene triggers ozone sensitivity in tobacco plants. Plant, Cell Environ. **30:** 1545-1556.

PASSOS, J. F., G. SARETZKI, S. AHMED, G. NELSON, T. RICHTER *et al.*, 2007 Mitochondrial dysfunction accounts for the stochastic heterogeneity in telomere-dependent senescence. PLoS Biol. **5:** e110.

PATTI, M.-E., and S. CORVERA, 2010 The Role of Mitochondria in the Pathogenesis of Type 2 Diabetes. Endocr. Rev. **31:** 364-395.

PFANNER, N., M. VAN DER LAAN, P. AMATI, R. A. CAPALDI, A. A. CAUDY *et al.*, 2014 Uniform nomenclature for the mitochondrial contact site and cristae organizing system. J. Cell Biol. **204:** 1083-1086.

PIZZO, P., I. DRAGO, R. FILADI and T. POZZAN, 2012 Mitochondrial Ca2+ homeostasis: mechanism, role, and tissue specificities. Pflug. Arch. Eur. J. Phy. **464:** 3-17.

POLIDOROS, A. N., P. V. MYLONA and B. ARNHOLDT-SCHMITT, 2009 Aox gene structure, transcript variation and expression in plants. Physiol. Plant. **137:** 342-353.

POLIDOROS, A. N., P. V. MYLONA, K. PASENTSIS, J. G. SCANDALIOS and A. S. TSAFTARIS, 2005 The maize alternative oxidase 1a (Aox1a) gene is regulated by signals related to oxidative stress. Redox Rep. **10:** 71-78.

POULTON, J. E., 1990 Cyanogenesis in Plants. Plant Physiol. **94:** 401-405.

RASMUSSON, A. G., A. R. FERNIE and J. T. VAN DONGEN, 2009 Alternative oxidase: a defence against metabolic fluctuations? Physiol. Plant. **137:** 371-382.

RASMUSSON, A. G., K. L. SOOLE and T. E. ELTHON, 2004 Alternative NAD (P) H dehydrogenases of plant mitochondria. Annu. Rev. Plant Biol. **55:** 23-39.

REINDERS, J., R. P. ZAHEDI, N. PFANNER, C. MEISINGER and A. SICKMANN, 2006 Toward the Complete Yeast Mitochondrial Proteome: Multidimensional Separation Techniques for Mitochondrial Proteomics. J. Proteome Res. **5:** 1543-1554.

RHOADS, D., 2011 Plant Mitochondrial Retrograde Regulation, pp. 411-437 in *Plant Mitochondria*, edited by F. KEMPKEN. Springer New York.

RHOADS, D. M., and L. MCINTOSH, 1993 The salicylic acid-inducible alternative oxidase gene aox1 and genes encoding pathogenesis-related proteins share regions of sequence similarity in their promoters. Plant Mol. Biol. **21:** 615-624.

RHOADS, D. M., A. L. UMBACH, C. R. SWEET, A. M. LENNON, G. S. RAUCH *et al.*, 1998 Regulation of the cyanide-resistant alternative oxidase of plant mitochondria. Identification of the cysteine residue involved in alpha-keto acid stimulation and intersubunit disulfide bond formation. J. Biol. Chem. **273:** 30750-30756.

RIBEIRO, S., and G. B. GOLDING, 1998 The mosaic nature of the eukaryotic nucleus. Mol. Biol. Evol. **15:** 779-788.

RICH, P. R., and A. L. MOORE, 1976 The involvement of the protonmotive ubiquinone cycle in the respiratory chain of higher plants and its relation to the branchpoint of the alternate pathway. FEBS Lett. **65:** 339-344.

RIFKIN, M. R., and D. J. L. LUCK, 1971 Defective Production of Mitochondrial Ribosomes in the Poky Mutant of Neurospora crassa. Proc. Natl. Acad. Sci. USA **68:** 287-290.

RIVERA, M. C., and J. A. LAKE, 2004 The ring of life provides evidence for a genome fusion origin of eukaryotes. Nature **431:** 152-155.

RIZZUTO, R., D. DE STEFANI, A. RAFFAELLO and C. MAMMUCARI, 2012 Mitochondria as sensors and regulators of calcium signalling. Nat. Rev. Mol. Cell Biol. **13:** 566-578.

ROUSSEAU-GUEUTIN, M., A. LLOYD, A. SHEPPARD and J. TIMMIS, 2012 Gene Transfer to the Nucleus, pp. 147-171 in *Organelle Genetics*, edited by C. E. BULLERWELL. Springer Berlin Heidelberg.

RUNKEL, E. D., R. BAUMEISTER and E. SCHULZE, 2014 Mitochondrial stress: Balancing friend and foe. Exp. Gerontol. **56:** 194-201.

RUSTIN, P., T. BOURGERON, B. PARFAIT, D. CHRETIEN, A. MUNNICH *et al.*, 1997 Inborn errors of the Krebs cycle: a group of unusual mitochondrial diseases in human. Biochimica et Biophysica Acta (BBA) - Molecular Basis of Disease **1361:** 185-197.

SACCONE, C., 2011 Mitochondrial Genome. eLS.

SAGAN, L., 1967 On the origin of mitosing cells. J. Theor. Biol. **14:** 225-IN226.

SAIKA, H., K. OHTSU, S. HAMANAKA, M. NAKAZONO, N. TSUTSUMI *et al.*, 2002 AOX1c, a novel rice gene for alternative oxidase; comparison with rice AOX1a and AOX1b. Genes Genet. Syst. **77:** 31.

SAISHO, D., E. NAMBARA, S. NAITO, N. TSUTSUMI, A. HIRAI *et al.*, 1997 Characterization of the gene family for alternative oxidase from Arabidopsis thaliana. Plant Mol. Biol. **35:** 585-596.

SAXTON, W. M., and P. J. HOLLENBECK, 2012 The axonal transport of mitochondria. J. Cell Sci. **125:** 2095-2104.

SCHEFFLER, I. E., 2008 *Mitochondria*. J. Wiley and Sons, Inc., Hoboken, New Jersey, 462.

SCHIEBER, M., and N. S. CHANDEL, 2014 ROS Function in Redox Signaling and Oxidative Stress. Curr. Biol. **24:** R453-R462.

SCHMIDT, O., N. PFANNER and C. MEISINGER, 2010 Mitochondrial protein import: from proteomics to functional mechanisms. Nat. Rev. Mol. Cell Biol. **11:** 655-667.

SCHMITT, S., H. PROKISCH, T. SCHLUNCK, D. G. CAMP, U. AHTING *et al.*, 2006 Proteome analysis of mitochondrial outer membrane from Neurospora crassa. Proteomics **6:** 72-80.

SCHONBAUM, G. R., W. D. BONNER, B. T. STOREY and J. T. BAHR, 1971 Specific inhibition of the cyanide-insensitive respiratory pathway in plant mitochondria by hydroxamic acids. Plant Physiol. **47:** 124-128.

SCHROEDER, E. A., N. RAIMUNDO and G. S. SHADEL, 2013 Epigenetic silencing mediates mitochondria stress-induced longevity. Cell Metab. **17:** 954-964.

SCHULTZ, B. E., and S. I. CHAN, 2001 Structures and proton-pumping strategies of mitochondrial respiratory enzymes. Annu. Rev. Biophys. Biomol. Struct. **30:** 23-65.

SEKITO, T., J. THORNTON and R. A. BUTOW, 2000 Mitochondria-to-nuclear signaling is regulated by the subcellular localization of the transcription factors Rtg1p and Rtg3p. Mol. Biol. Cell. **11:** 2103-2115.

SHAPIRO, T. A., and P. T. ENGLUND, 1995 The structure and replication of kinetoplast DNA. Annu. Rev. Microbiol. **49:** 117-143.

SHIBA, T., Y. KIDO, K. SAKAMOTO, D. K. INAOKA, C. TSUGE *et al.*, 2013 Structure of the trypanosome cyanide-insensitive alternative oxidase. Proc. Natl. Acad. Sci. USA **110:** 4580-4585.

SHLOMAI, J., 2004 The structure and replication of kinetoplast DNA. Curr. Mol. Med. **4:** 623-647.

SIEDOW, J. N., A. L. UMBACH and A. L. MOORE, 1995 The active site of the cyanide-resistant oxidase from plant mitochondria contains a binuclear iron center. FEBS Lett. **362:** 10-14.

SIMONS, B. H., F. F. MILLENAAR, L. MULDER, L. C. VAN LOON and H. LAMBERS, 1999 Enhanced Expression and Activation of the Alternative Oxidase during Infection of Arabidopsis withPseudomonas syringae pv tomato. Plant Physiol. **120:** 529-538.

SMALL, W. C., and L. MCALISTER-HENN, 1998 Identification of a Cytosolically Directed NADH Dehydrogenase in Mitochondria of Saccharomyces cerevisiae. J. Bacteriol. **180:** 4051-4055.

SONG, Z., H. CHEN, M. FIKET, C. ALEXANDER and D. C. CHAN, 2007 OPA1 processing controls mitochondrial fusion and is regulated by mRNA splicing, membrane potential, and Yme1L. The Journal of Cell Biology **178:** 749-755.

STEHLING, O., and R. LILL, 2013 The Role of Mitochondria in Cellular Iron–Sulfur Protein Biogenesis: Mechanisms, Connected Processes, and Diseases. Cold Spring Harb Perspect Biol. **5:** a011312.

STENMARK, P., and P. NORDLUND, 2003 A prokaryotic alternative oxidase present in the bacterium Novosphingobium aromaticivorans. FEBS Lett. **552:** 189-192.

STOJANOVSKI, D., P. BRAGOSZEWSKI and A. CHACINSKA, 2012 The MIA pathway: A tight bond between protein transport and oxidative folding in mitochondria. Biochim. Biophys. Acta - Mol. Cell Res. **1823:** 1142-1150.

STRAUSS, M., G. HOFHAUS, R. R. SCHRÖDER and W. KÜHLBRANDT, 2008 Dimer ribbons of ATP synthase shape the inner mitochondrial membrane. EMBO J. **27:** 1154-1160.

SUZUKI, Y., S. L. MURRAY, K. H. WONG, M. A. DAVIS and M. J. HYNES, 2012 Reprogramming of carbon metabolism by the transcriptional activators AcuK and AcuM in Aspergillus nidulans. Mol. Microbiol. **84:** 942-964.

SWEETLOVE, L. J., K. F. M. BEARD, A. NUNES-NESI, A. R. FERNIE and R. G. RATCLIFFE, 2010 Not just a circle: flux modes in the plant TCA cycle. Trends Plant Sci. **15:** 462-470.

SZTUKOWSKA, M., M. BUGNO, J. POTEMPA, J. TRAVIS and D. M. KURTZ JR, 2002 Role of rubrerythrin in the oxidative stress response of Porphyromonas gingivalis. Mol. Microbiol. **44:** 479-488.

TAIT, S. W. G., and D. R. GREEN, 2010 Mitochondria and cell death: outer membrane permeabilization and beyond. Nat. Rev. Mol. Cell Biol. **11:** 621-632.

TAKUMI, S., M. TOMIOKA, K. ETO, N. NAYDENOV and C. NAKAMURA, 2002 Characterization of two non-homoeologous nuclear genes encoding mitochondrial alternative oxidase in common wheat. Genes Genet. Syst. **77:** 81-88.

TANTON, L. L., C. E. NARGANG, K. E. KESSLER, Q. LI and F. E. NARGANG, 2003 Alternative oxidase expression in Neurospora crassa. Fungal Genet. Biol. **39:** 176-190.

TAYLOR, B. L., and I. B. ZHULIN, 1999 PAS domains: internal sensors of oxygen, redox potential, and light. Microbiol. Mol. Biol. Rev. **63:** 479-506.

TAYLOR, S. S., P. ZHANG, J. M. STEICHEN, M. M. KESHWANI and A. P. KORNEV, 2013 PKA: lessons learned after twenty years. Biochimica et Biophysica Acta (BBA)-Proteins and Proteomics **1834:** 1271-1278.

THIRKETTLE-WATTS, D., T. C. MCCABE, R. CLIFTON, C. MOORE, P. M. FINNEGAN *et al.*, 2003 Analysis of the Alternative Oxidase Promoters from Soybean. Plant Physiol. **133:** 1158-1169.

TIMMIS, J. N., M. A. AYLIFFE, C. Y. HUANG and W. MARTIN, 2004 Endosymbiotic gene transfer: organelle genomes forge eukaryotic chromosomes. Nat. Rev. Genet. **5:** 123-135.

TOKARZ, P., and J. BLASIAK, 2014 Role of mitochondria in carcinogenesis. Acta Biochim. Pol.

TOUZET, P., and E. H. MEYER, 2014 Cytoplasmic male sterility and mitochondrial metabolism in plants. Mitochondrion **19, Part B:** 166-171.

TRAVEN, A., J. M. S. WONG, D. XU, M. SOPTA and C. J. INGLES, 2001 Interorganellar communication Altered nuclear gene expression profiles in a yeast mitochondrial DNA mutant. J. Biol. Chem. **276:** 4020-4027.

TRIFUNOVIC, A., A. WREDENBERG, M. FALKENBERG, J. N. SPELBRINK, A. T. ROVIO *et al.*, 2004 Premature ageing in mice expressing defective mitochondrial DNA polymerase. Nature **429:** 417-423.

UMBACH, A. L., M. A. GONZÀLEZ-MELER, C. R. SWEET and J. N. SIEDOW, 2002 Activation of the plant mitochondrial alternative oxidase: insights from site-directed mutagenesis. Biochim. Biophys. Acta - Bioenergetics **1554:** 118-128.

UMBACH, A. L., V. S. NG and J. N. SIEDOW, 2006 Regulation of plant alternative oxidase activity: A tale of two cysteines. Biochim. Biophys. Acta - Bioenergetics **1757:** 135-142.

UMBACH, A. L., and J. N. SIEDOW, 1993 Covalent and noncovalent dimers of the cyanide-resistant alternative oxidase protein in higher plant mitochondria and their relationship to enzyme activity. Plant Physiol. **103:** 845-854.

UMBACH, A. L., J. T. WISKICH and J. N. SIEDOW, 1994 Regulation of alternative oxidase kinetics by pyruvate and intermolecular disulfide bond redox status in soybean seedling mitochondria. FEBS Lett. **348:** 181-184.

VAN AKEN, O., E. GIRAUD, R. CLIFTON and J. WHELAN, 2009 Alternative oxidase: a target and regulator of stress responses. Physiol. Plant. **137:** 354-361.

VAN AKEN, O., B. ZHANG, S. LAW, R. NARSAI and J. WHELAN, 2013 AtWRKY40 and AtWRKY63 Modulate the Expression of Stress-Responsive Nuclear Genes Encoding Mitochondrial and Chloroplast Proteins. Plant Physiol. **162:** 254-271.

VAN DER BLIEK, A. M., Q. SHEN and S. KAWAJIRI, 2013 Mechanisms of Mitochondrial Fission and Fusion. Cold Spring Harb Perspect Biol. **5:** pii: a011072.

VAN DER GIEZEN, M., 2011 Mitochondria and the Rise of Eukaryotes. Bioscience **61:** 594-601.

VAN DER LAAN, M., M. BOHNERT, N. WIEDEMANN and N. PFANNER, 2012 Role of MINOS in mitochondrial membrane architecture and biogenesis. Trends Cell Biol. **22:** 185-192.

VANDERLEYDEN, J., C. PEETERS, H. VERACHTERT and H. BERTRAND, 1980 Stimulation of the alternative oxidase of Neurospora crassa by Nucleoside phosphates. Biochem. J. **188:** 141-144.

VANLERBERGHE, G. C., D. A. DAY, J. T. WISKICH, A. E. VANLERBERGHE and L. MCINTOSH, 1995 Alternative Oxidase Activity in Tobacco Leaf Mitochondria (Dependence on Tricarboxylic Acid Cycle-Mediated Redox Regulation and Pyruvate Activation). Plant Physiol. **109:** 353-361.

VANLERBERGHE, G. C., and L. MCINTOSH, 1997 Alternative oxidase: From gene to function. Annu. Rev. Plant Physiol. Plant Mol. Biol. **48:** 703-734.

VANLERBERGHE, G. C., L. MCINTOSH and J. Y. H. YIP, 1998 Molecular localization of a redox-modulated process regulating plant mitochondrial electron transport. Plant Cell **10:** 1551-1560.

VANLERBERGHE, G. C., and L. MCLNTOSH, 1996 Signals regulating the expression of the nuclear gene encoding alternative oxidase of plant mitochondria. Plant Physiol. **111:** 589-595.

VEIGA, A., J. D. ARRABAÇA and M. C. LOUREIRO-DIAS, 2003 Cyanide-resistant respiration, a very frequent metabolic pathway in yeasts. FEMS Yeast Res. **3:** 239-245.

VON DER MALSBURG, K., JUDITH M. MÜLLER, M. BOHNERT, S. OELJEKLAUS, P. KWIATKOWSKA *et al.*, 2011 Dual Role of Mitofilin in Mitochondrial Membrane Organization and Protein Biogenesis. Dev. Cell **21:** 694-707.

WAGNER, A. M., 1995 A role for active oxygen species as second messengers in the induction of alternative oxidase gene expression in Petunia hybrida cells. FEBS Lett. **368:** 339-342.

WAGNER, A. M., K. KRAB, M. J. WAGNER and A. L. MOORE, 2008 Regulation of thermogenesis in flowering Araceae: the role of the alternative oxidase. Biochim. Biophys. Acta - Bioenergetics **1777:** 993-1000.

WALLIN, I. E., 1923 The Mitochondria Problem. Am. Nat. **57:** 255-261.

WATANABE, C. K., T. HACHIYA, I. TERASHIMA and K. O. NOGUCHI, 2008 The lack of alternative oxidase at low temperature leads to a disruption of the balance in carbon and nitrogen metabolism, and to an up-regulation of antioxidant defence systems in Arabidopsis thaliana leaves. Plant, Cell Environ. **31:** 1190-1202.

WATANABE, K. I., Y. BESSHO, M. KAWASAKI and H. HORI, 1999 Mitochondrial genes are found on minicircle DNA molecules in the mesozoan animal Dicyema1. J. Mol. Biol. **286:** 645-650.

WEST, A. P., G. S. SHADEL and S. GHOSH, 2011 Mitochondria in innate immune responses. Nat. Rev. Immunol. **11:** 389-402.

WESTERMANN, B., 2008 Molecular Machinery of Mitochondrial Fusion and Fission. J. Biol. Chem. **283:** 13501-13505.

WOESE, C. R., 1987 Bacterial evolution. Microbiol. Rev. **51:** 221-271.

WONG, W., and J. D. SCOTT, 2004 AKAP signalling complexes: focal points in space and time. Nat. Rev. Mol. Cell Biol. **5:** 959-970.

WOODSON, J. D., and J. CHORY, 2008 Coordination of gene expression between organellar and nuclear genomes. Nat. Rev. Genet. **9:** 383-395.

WU, M., A. KALYANASUNDARAM and J. ZHU, 2013 Structural and biomechanical basis of mitochondrial movement in eukaryotic cells. Int. J. Nanomedicine **8:** 4033-4042.

XU, X., C. C. CHUA, J. GAO, R. C. HAMDY and B. H. L. CHUA, 2006 Humanin Is a Novel Neuroprotective Agent Against Stroke. Stroke **37:** 2613-2619.

YANG, D., Y. OYAIZU, H. OYAIZU, G. J. OLSEN and C. R. WOESE, 1985 Mitochondrial origins. Proc. Natl. Acad. Sci. USA **82:** 4443-4447.

YANG, W., and S. HEKIMI, 2010 A Mitochondrial Superoxide Signal Triggers Increased Longevity in *Caenorhabditis elegans*. PLoS Biol. **8:** e1000556.

YLIKALLIO, E., and A. SUOMALAINEN, 2012 Mechanisms of mitochondrial diseases. Ann. Med. **44:** 41-59.

YOGEV, O., S. KARNIELY and O. PINES, 2007 Translation-coupled Translocation of Yeast Fumarase into Mitochondria in Vivo. J. Biol. Chem. **282:** 29222-29229.

YONEDA, T., C. BENEDETTI, F. URANO, S. G. CLARK, H. P. HARDING *et al.*, 2004 Compartment-specific perturbation of protein handling activates genes encoding mitochondrial chaperones. J. Cell Sci. **117:** 4055-4066.

YOULE, R. J., and M. KARBOWSKI, 2005 Mitochondrial fission in apoptosis. Nat. Rev. Mol. Cell Biol. **6:** 657-663.

YOUNG, J. C., N. J. HOOGENRAAD and F. U. HARTL, 2003 Molecular Chaperones Hsp90 and Hsp70 Deliver Preproteins to the Mitochondrial Import Receptor Tom70. Cell **112:** 41-50.

YUKIOKA, H., S. INAGAKI, R. TANAKA, K. KATOH, N. MIKI *et al.*, 1998 Transcriptional activation of the alternative oxidase gene of the fungus Magnaporthe grisea by a respiratory-inhibiting fungicide and hydrogen peroxide. Biochim. Biophys. Acta - Gene Struct. Expr. **1442:** 161-169.

ZERBES, R. M., M. BOHNERT, D. A. STROUD, K. VON DER MALSBURG, A. KRAM *et al.*, 2012 Role of MINOS in Mitochondrial Membrane Architecture: Cristae Morphology and Outer Membrane Interactions Differentially Depend on Mitofilin Domains. J. Mol. Biol. **422:** 183-191.

ZHU, C., X. WANG, J. DEINUM, Z. HUANG, J. GAO *et al.*, 2007 Cyclophilin A participates in the nuclear translocation of apoptosis-inducing factor in neurons after cerebral hypoxia-ischemia. J. Exp. Med. **204:** 1741-1748.

ZHU, Y., J. LU, J. WANG, F. CHEN, F. LENG *et al.*, 2011 Regulation of Thermogenesis in Plants: The Interaction of Alternative Oxidase and Plant Uncoupling Mitochondrial Protein. J. Integr. Plant Biol. **53:** 7-13.

ZICK, M., R. RABL and A. S. REICHERT, 2009 Cristae formation—linking ultrastructure and function of mitochondria. Biochim. Biophys. Acta - Mol. Cell Res. **1793:** 5-19.

Chapter 2: Materials and Methods

2.1 Growth of *N. crassa* strains

All strains used in this study are listed in Table 3. The methods of DAVIS and DE SERRES (1970) were used for culturing and handling *N. crassa* strains. Unless otherwise noted, strains were grown at 30°C on standard Vogel's medium with addition of supplements as required. The standard components of Vogel's are described in DAVIS and DE SERRES (1970). The medium contains inorganic salts, 1.5% sucrose as the carbon source, trace elements and biotin. Our lab abbreviates the medium as VSuTB. When conidia were required, strains were grown in 250 mL Erlenmeyer flasks (termed "conidia flasks") containing 50 mL of Vogel's medium made solid with 1.5% agar. Following inoculation of conidia onto the center of the medium in the flask, they were incubated for two to three days at 30°C, followed by incubation at room temperature in a well-lit room for another four to five days. Conidia were used three to fourteen days after formation. Working stains were maintained in test tubes containing slants of VSuTB plus any required supplements.

Liquid cultures were set up by collecting conidia from conidia flasks using sterile dH_2O. Harvested conidia were then used to inoculate liquid VSuTB in baffled flasks, followed by incubation at 30°C with constant shaking for the desired time. When required, conidia were counted using a hemocytometer and $2X10^6$ conidia were added per mL of Vogel's medium. Whenever required, inhibitors were added at the following concentrations: Cm at 2 mg/mL, AA at 0.5 µg/mL, bleomycin (Bm) at 1 µg/mL, and hygromycin B at 0.19 Units/L (each mg of hygromycin consists of 396 units of activity) (EDM Chemicals Inc., San Diago, CA).

Table 3. Strains used for the duration of this study.

Strains	Comments	Origin
NCN251	Lab wild-type strain, mating type *A*	F.E. Nargang Lab (FGSC #2489)
1C4	*aod-5* replaced by Hyg^R cassette, mating type A (genotype: *aod-5)*	KO mutant library (FGSC# 11228)
96H9	*aod-1* replaced by Hyg^R cassette, mating type A (genotype: *aod-1)*	KO mutant library (FGSC# 18947)
EN-14-34	*aod-2* mutant, mating type A (genotype*: E3, aod-2, al-1)*	Cleary, I., F.E. Nargang lab
76-26	Mating type *a* (genotype: *his-3 fpa*^{R})	R.L. Metzenberg
13G11	NCU04566 replaced by Hyg^R cassette, mating type *a*	KO mutant library (FGSC# 12420)
28B10	NCU08137 replaced by Hyg^R cassette, mating type *A*	KO mutant library (FGSC# 16091)
85H5	NCU09803 replaced by Hyg^R cassette, mating type *A*	KO mutant library (FGSC# 18375)
99B8	NCU09327 replaced by Hyg^R cassette, mating type *A*	KO mutant library (FGSC# 18995)
101D3	NCU09560 replaced by Hyg^R cassette, mating type *a*	KO mutant library (FGSC# 21068)
23H2	NCU08887 replaced by Hyg^R cassette,	KO mutant library

	mating type *A*	(FGSC# 15957)
40 E6	NCU05600 replaced by Hyg^R cassette, mating type *a*	KO mutant library (FGSC# 13805)
41G7	NCU03589 replaced by Hyg^R cassette, mating type *A*	KO mutant library (FGSC# 13924)
47H10	NCU00778 replaced by Hyg^R cassette, mating type *a*	KO mutant library (FGSC# 16938)
52D8	NCU07281 replaced by Hyg^R cassette, mating type *A*	KO mutant library (FGSC# 14469)
83H3	NCU08365 replaced by Hyg^R cassette, mating type *a*	KO mutant library (FGSC# 18277)
88H8	NCU01542 replaced by Hyg^R cassette, mating type *a*	KO mutant library (FGSC# 19221)
113G8	NCU03071 replaced by Hyg^R cassette, mating type *a*	KO mutant library (FGSC# 18202)
NCN184, [*poky*]	Mitochondrial mutant, 4 bp mtDNA deletion, mating type *a* (genotype*: nic-1, al-2*)	H. Bertrand
N Myc-1 (to 21)	Transformants, generated by transforming 23H2 with pBS520 *AscI* 23H2_5' NI_Myc	This study
C HA-1 (to 19)	Transformants, generated by transforming 23H2 with pBS520 *AscI* 23H2_3' NI_HA	This study
88H8-C-HA-1 (to	Transformants, generated by transforming	This study

25)	88H8 with pBS520 *AscI* 88H8 predicted gene containing 3' HA	
23-1-(F1-F12, M1-M15,S1-S5)*	Cross progeny strains from a 23H2 X 76-26 cross	This study
23-2-(F1-F12, M1-M15,S1-S5)	Cross progeny strains from a 23H2 X 76-26 cross	This study
40-1-(F1-F12, M1-M13, S1-S5)	Cross progeny strains from a 40E6 X NCN251 cross	This study
40-2-(F1-F12, M1-M13, S2-S5)	Cross progeny strains from a 40E6 X NCN251 cross	This study
41-1-(F1-F12, M1-M15, S1-S5, H1-12, H14, HS3- HS6)**	Cross progeny strains from a 41G7 X 76-26 cross	This study
41-2-(F1-F12, M1-M15, S1-S6, H1-15, HS2, HS3, HS5, HS6)	Cross progeny strains from a 41G7 X 76-26 cross	This study
47-1-(F1-F10, M1-M15, S1-S5, H1, H5-H8, H10-H15, HS2, HS3, HS5)	Cross progeny strains from a 47H10 X NCN251 cross	This study
47-2-(F1-F10, M1-M15, S1-S3, S5, H1-	Cross progeny strains from a 47H10 X NCN251 cross	This study

H15, HS2, HS5)		
52-1-(F1-F10, M1-M15, S2-S5,H3, H6, H9, H11, HS2)	Cross progeny strains from a 52D8 X 76-26 cross	This study
52-2-(F1-F10, M1-M15, S2, S5, H6-H8, H11)	Cross progeny strains from a 52D8 X 76-26 cross	This study
83-1-(F1-F12, M1-M7, M9-M15, S1-S6, H1-H15,HS2)	Cross progeny strains from a 83H3 X NCN251 cross	This study
83-2-(F1-F13, M2-M10, M12-M15,S1-S5, H1-H6, H8-H15)	Cross progeny strains from a 83H3 X NCN251 cross	This study
88-1-(F1, F3-F7, F9, F10, F15, M1, M5-M10, S2, S4)	Cross progeny strains from a 88H8 X NCN251 cross	This study
88-2-(F1-F15, M2, M5-M10)	Cross progeny strains from a 88H8 X NCN251 cross	This study
88-N-(F1-F3, F6, F9, F10-12, F14-F16, F18)	Cross progeny strains from a 88H8 X NCN251 cross	This study
113-1-(F1, F4-F12, M1-M15, S1 - S4,	Cross progeny strains from a 113G8 X NCN251 cross	This study

H1-H9, H13, H15, HS3)		
113-2-(F1-F6, F8-F10, M1, M3-M15, S1-S4, H1-H3, H5-H8, H10-H13, H15, HS2, HS3	Cross progeny strains from a 113G8 X NCN251 cross	This study

*Cross progeny were denoted as F if they were generated from ascospores that germinated faster than the other ascospores on Vogel's sorbose-containing plates, M if they were generated from ascospores germinating slower than the F category, S if they were generated from very slowly germinating ascospores.

**H, denotes strains that were generated from germinating ascospores that were activated and plated on Vogel's sorbose-containing plates with hygromycin added.

2.2 Growth rate measurements

For a crude estimation of growth rate, strains of interest were allowed to conidiate on VSuTB slants. Conidia from slants were picked using a sterile inoculating needle, and inoculated at the center of VSuTB agar plates (with appropriate antibiotics added as required). Plates were incubated at 30°C for two to three days. Linear growth from the site of inoculation was measured every 24 hr.

2.3 Mitochondrial isolation

Cultures were grown in liquid medium for specific times (24 or 48 hr) at 30°C and harvested by vacuum filtration. When required, Cm was added at a concentration of 2 mg/mL to the culture prior to inoculation. Mitochondria were isolated from harvested *N. crassa* mycelium by differential centrifugation, using the procedure described by NARGANG and RAPAPORT (2007). Isolated mitochondria samples were either used immediately or placed at -80°C until required.

2.4 Isolation of whole cell extracts

For preparation of whole cell extracts, strains of interest were grown in liquid medium at 30°C for 24 hr and/or 48 hr, following which, mycelium was collected by vacuum filtration. 1 g of mycelium was ground using a mortar and pestle with 1 mL of SEMP (0.25M sucrose; 1 mM EDTA (ethylenediaminetetraacetic acid); 10 mM 4-morpholinepropanesulfonic acid (MOPS), 0.2 mM phenylmethylsulfonyl fluoride (PMSF)) buffer containing 2% SDS (sodium dodecyl sulfate) and 1 g of sand (Sigma-Aldrich, St. Louis, MO). This slurry was centrifuged at 3600 x g for 10 min in a Sorvall RC-5C Plus centrifuge SA-600 rotor (Sorvall, Mandel Scientific, Guelph, ON), following

which the supernatant was collected and proteins in the sample were quantified using the BCA protein assay kit (Pierce, Rockford, IL).

2.5 Growth of *E. coli* cells, transformation of competent *E. coli* cells and plasmid DNA isolations

E. coli cells were grown in LB medium (Lysogeny broth: 10g/L tryptone, 5g/L yeast extract, 5g/L NaCl, 1g/L glucose), at 37°C with constant shaking as per the protocol of SAMBROOK and RUSSELL (2001). When *E. coli* cells were grown on LB agar plates, cells were placed in a gravity convection incubator at 37°C for 18-24 hr. Ampicillin (Amp) was added to the medium when needed at a concentration of 100 mg/L.

Competent XL-2 Blue *E. coli* cells were prepared following growth at 18°C using the Inoue method (SAMBROOK and RUSSELL 2001). The transformation efficiency of these competent cells was determined to be approximately $1X10^7$ cfu/µg using supercoiled plasmid DNA (pBSK II) when the transformation protocol of SAMBROOK and RUSSELL (2001) was used. When required, transformants of interest were picked and inoculated into LB Amp broth. After overnight growth, plasmid DNA was reisolated using the GeneJET plasmid miniprep kit (Thermo Scientific, Waltham, MA). The manufacturer's instructions were followed to isolate plasmid from 5 mL of liquid culture grown overnight.

2.6 Agarose gel electrophoresis and isolation of DNA from gels

DNA of interest was separated via electrophoresis through 1% agarose gels. The gel was placed on a UV transilluminator, bands of interest were cut out of the gel using a scalpel and were placed in a microfuge tube. Three volumes of 6M sodium iodide was added to the gel pieces. This mixture was incubated at 65°C for 15 min to melt the agar

slabs and the dissolved mixture was added to GeneJET spin columns (Thermo Scientific, Waltham, MA) to bind DNA from the solution. The column was then washed twice with the washing buffer supplied by the manufacturer of the kit and DNA was eluted in 40-50 μL of sterile milliQ water.

2.7 Ethanol precipitation of DNA

To precipitate DNA from a solution, 1/10 volume of 3M sodium acetate and 2 volumes of ice cold 95% ethanol were added to the solution containing DNA. This mixture was incubated at -20°C for 2 hr to overnight, and then spun at 16,000 x g for 15 min in a tabletop microcentrifuge. The supernatant was discarded and the pellet was washed twice with ice cold 70% ethanol and allowed to air dry for 30 min. The pellet was then resuspended in the desired amount of sterile milliQ water.

2.8 PCR amplification and mutagenesis

PCR amplification and site-directed mutagenesis were carried out based on the protocols of SAMBROOK and RUSSELL (2001). The PCR amplification primers used were designed with the help of the software Primer Premier (Version 5, Premier Biosoft International) or the NCBI primer design tool (National Centre for Biotechnology Information). Pfu DNA polymerase (Thermo Scientific) was used for all reactions.

2.9 Genomic DNA isolation

N. crassa genomic DNA was isolated using a procedure modified from WENDLAND *et al.* (1996). VSuTB liquid media was inoculated with conidia from the strain of interest. Cultures were grown with shaking at 30°C for 24 to 72 hr depending on the growth rate of the strain. Mycelium was harvested by vacuum filtration, wrapped in foil and placed

on ice. Typically, 2 gm of mycelium was used per isolation. For each gram, 1.5 g of sand (Sigma-Aldrich, St. Louis, MO) and 2 mL of "new isolation buffer" (10 mM EDTA, pH 8.0; 1% SDS; 100 mM Tris-HCl, pH 8.0) was added. This mixture was kept on ice at all times. The mycelium was ground into a fine slurry of even consistency using a mortar and pestle. This slurry was then transferred into a tube for a Sorvall RC-5C Plus centrifuge SA-600 rotor (Sorvall, Mandel Scientific, Guelph, ON) and additional new isolation buffer was added to the slurry to bring up the volume to 10 mL. The tube was then covered with parafilm and shaken vigorously, then inverted slowly for 1 min. It was then placed into a 70°C water bath for 1 hr, following which the tube was placed on ice for 10 min. 0.64 mL of 8 M potassium acetate pH 4.3 was added to the mixture and, following shaking, the tube was placed on ice for another 1 hr. The mixture was then centrifuged at 28,000 x g at 4°C in a Sorvall SA-600 rotor for 15 min. The supernatant was transferred to a fresh centrifuge tube and an equal volume of isopropanol was added. Following mixing, the tubes were placed on ice for 15 min to allow for precipitation of DNA, and then centrifuged at 14,000 x g for 15 min to pellet the DNA. The pellet was rinsed twice with 70% ethanol and allowed to air dry for 30 min. The pellet was resuspended in 400 µL of 1 mM EDTA pH 8, after which the solution was transferred to a microfuge tube and 200 µL of Hi Salt buffer (100 mM sodium chloride; 25 mM Tris-HCl, pH 7.4; 2 mM EDTA) and 15 µL of boiled RNase A (10 mg/mL) were added to the tube. After incubation at 37°C for 30 min the mixture was extracted with an equal volume of water equilibrated phenol:chloroform (1:1). Genomic DNA was then precipitated by addition of 1/10 volume of 3 M sodium acetate and 2 volumes of 95% ethanol. The DNA was pelleted at 16,000 x g for 20 min, washed with 70% ethanol and

allowed to air dry at room temperature for 30 min. The pellet was resuspended in 50-400 μL of sterile milliQ water and the concentration of gDNA was determined using a NanoDrop 1000 Spectrophotometer (Thermo Scientific, Waltham, MA) at the Molecular Biology Services Unit (MBSU), Department of Biological Sciences.

2.10 Genetic crosses and isolation of progeny

Crosses were set up using the basic procedure described by DAVIS and DE SERRES (1970) with modifications. The parent chosen to serve as the female (the wild-type strain NCN251*A* or 76-26*a his-3*) was inoculated on a sterile filter paper (serving as the sole carbon source) placed on low nitrogen Westergaard's medium petridish. When 76-26 was used as the female parent, histidine was added to the medium at a concentration of 15 mg/L, as this strain is auxotrophic for histidine. The plates were incubated for two days at 30°C and then placed in the dark for ten days at room temperature to allow formation of protoperithecia. The male strains (class one knockout mutants being tested, see section 1.10) were allowed to conidiate in slants of VSuTB medium. Conidia from these slants were harvested with sterile dH_2O and spread on the plates containing female protoperithecia. The lids of the plates were replaced by clean sterile lids at this time. The plates were then placed in the dark at room temperature for ten more days, to allow fertilization and formation of ascospores, and then moved to a well-lit area for 5 days to allow for ejection of ascospores. A sterile wooden applicator, dipped in sterile distilled water, was used to harvest ascospores off the lid of the crossing plates. These ascospores were placed in 1 mL sterile dH_2O and incubated at room temperature overnight, following which they were heat activated at 60°C for 45 min. Aliquots of the ascospore suspension were plated on Vogel's sorbose-containing plates and incubated at 30°C

overnight to allow for colony formation (DAVIS and DE SERRES 1970). A dissecting microscope was then used to identify germinated ascospores. These germinated ascospores were individually picked onto slants and allowed to conidiate. These cross progeny were then used for further analysis.

2.11 Southern blotting and hybridization

Genomic DNA was digested overnight with appropriate restriction enzymes and then precipitated. The DNA was resuspended in milliQ water and quantified using the Qubit Flourometer (Life Technologies, Burlington, ON). 10-15 μg of digested DNA was electrophoresed on 0.8% agarose gels (20 cm X 14.5 cm) at 50-60 V until the dye front migrated approximately 15 cm.

The gel was then photographed alongside a fluorescent ruler following which excess lanes and regions of the gel were trimmed off. The gel was processed according to the Southern blotting protocol of SAMBROOK and RUSSELL (2001) and was transferred to a positively charged nylon membrane (Immobilon NY+, Millipore Corporation, Etobicoke, ON). Following transfer, the membrane was blotted dry, soaked in 2XSSC (saline sodium citrate buffer: 0.03 M trisodium citrate and 0.3 M sodium chloride, pH 7.5) for 5 min, and baked in a 80°C oven for 2 hr for crosslinking DNA onto the nylon membrane.

The nylon membrane was soaked in pre-hybridization solution (5X SSC, 1% blocking reagent (Supplied with the DIG (digoxigenin) DNA labelling and detection kit, Roche Applied Science, Indianapolis, IN), 0.1% N-laurylsacrosine and 0.02% SDS) and pre-hybridized in a 65°C rotating hybridization incubator (Tyler research instruments, Edmonton, AB) for 1 hr. DIG labelled DNA probe specific to parts of the Hyg^R gene cassette was created using the DIG DNA labelling and detection kit (Roche Applied

Science, Indianapolis, IN) as per the manufacturer's instructions. The labelled probe was denatured at 95°C for 10 min followed by chilling on ice for 10 min. The probe was then added to 50 mL of pre-hybridization solution (preheated to 65°C) to make the hybridization solution. The membrane was placed in the hybridization solution at 65°C in the rotating incubator overnight. Stringency washes and probe detection was carried out as per the direction of the kit manufacturer.

2.12 SDS-PAGE (sodium dodecyl sulfate - polyacrylaminde gel electrophoresis) and western blotting

SDS-PAGE gels (12.5% polyacrylamide gels; 29:1 acrylamide: bisacrylamide) were prepared as described by SAMBROOK and RUSSELL (2001). Mitochondrial proteins for electrophoresis were prepared by resuspending 30 μg of mitochondrial proteins in cracking buffer (0.06 M Tris-HCl, pH 6.7, 2.5% SDS, 0.01% β-mercaptoethanol, 5% sucrose). Following electrophoresis, proteins were electro-blotted onto nitrocellulose membrane. The membrane was then placed in blocking buffer (5% skimmed milk powder in TBST (0.02M Tris HCl, pH 7.5; 0.15M NaCl; 0.5% Tween)) for 1 hr at room temperature with constant shaking. The blocking solution was poured off and the membrane was incubated with primary antibody milk (consisting of antibody raised in rabbits diluted in blocking buffer containing 0.02% sodium azide) for 1 hr with constant shaking. The membrane was then washed thrice with TBST for 5 min and incubated with the secondary antibody solution (consisting of a 1:3000 dilution of goat anti-rabbit antibody HRP-conjugate solution (BioRad, Mississauga, ON) in 50 mL blocking buffer) for 1 hr with shaking at room temperature. The membrane was then washed twice with TBST, once with TBS (TBST buffer without Tween) and finally with dH_2O for 5 min

each. The LumiGLO chemiluminescent detection assay (Mandel Scientific Company Inc., Guelph, ON) was used for antibody detection with Kodak XAR film.

2.13 Carbonate extraction

The procedure of WIDEMAN *et al.* (2010) was used for carbonate extraction. 30-50 µg of the mitochondrial pellet was resuspended in 50 µL of sterile dH_2O and transferred to an ultracentrifuge tube for the TLA55 rotor (Beckman Coulter, Mississauga, ON). 1 mL of freshly prepared 100 mM sodium carbonate (Na_2CO_3) was added to the mitochondria. The pH of $NaCO_3$ was either adjusted to 11.0 using 1 M NaOH, or used directly at approximately 10.8. The contents of the tube were gently mixed and then placed on ice for 30 min. The tube was then centrifuged in a TLA55 rotor of the Beckman Optima MAX ultracenrifuge (Beckman Coulter, Mississauga, ON) at 125,000 x g for 1 hr at 4°C. The pellet fraction was resuspended in cracking buffer and either loaded immediately on a SDS-PAGE gel or stored at -80°C until further use. The supernatant fraction was collected in a separate microfuge tube. To precipitate proteins in this fraction, 210 µL of 72% TCA (Trichloroacetic acid) was added and the mixture was placed on ice for 1 hr followed by a 15 min spin at 160,000 x g in a Beckman Coulter TLA55 rotor ultracentrifuge. Following this, the supernatant was discarded and 1 mL of acetone was added to the pellet. The tube was then shaken for 5 min and centrifuged for 5 min at 16,000 x g. The acetone was removed, the pellet dried at 37°C for 30 min and then resuspended in cracking buffer. The sample was either loaded onto an SDS-PAGE gel or stored at -80°C until further use.

2.14 Cytochrome spectra

Cytochrome spectra were obtained as described previously by BERTRAND and PITTENGER (1969). Briefly, mitochondrial pellets were suspended in 1mL of SEMP, and lysed using 1 mL of a solution containing 10 mM MOPS; pH 7.2 and 5% sodium deoxycholate. The solution was mixed by gentle pipetting and centrifuged at 16,000 x g for 5 min. The supernatant was divided equally into two cuvettes. The reference in one cuvette was fully oxidized by addition of a few crystals of potassium ferricyanide. The sample in the other cuvette was reduced by addition of a few crystals of sodium dithionite. A Biochrom Ultrospec 3100 pro spectrophotometer (GE Healthcare, Mississauga, ON) was used to obtain difference spectra (sample vs a reference) over wavelengths 500 to 650 nm. The spectra were then traced and scanned into Adobe Photoshop.

2.15 Transformation of *N. crassa* by electroporation and purification of transformants

Transformation of *N. crassa* was achieved by electroporation as described by HOPPINS *et al.* (2007). Transformants were selected in the presence of appropriate antibiotics added to agar plates. Single transformant colonies were picked using sterile glass pasture pipettes and transferred onto half strength antibiotic VSuTB slants. Upon conidiation, these transformants were subjected to another round of single colony isolations on full-strength antibiotic plates. Single colony transformants generated in this manner were then allowed to conidiate on VSuTB slants lacking antibiotics and were used for further analysis.

2.16 Spot growth tests

For spot growth test analysis, conidia from each strain were collected in 1 to 5 mL of sterile dH_2O. The conidia were counted using a microscope and a hemocytometer and adjusted to a concentration of $1X10^4$ conidia/µL. This suspension was serially diluted so as to have suspensions with concentrations of $1X10^3$, $1X10^2$ and $1X10^1$ conidia/µL. 10 µL of each dilution was spotted onto Vogel's sorbose-containing plates with addition of desired antibiotics and nutritional supplements. These plates were incubated at 30°C for two to three days.

2.17 DNA Sequencing and analysis of sequencing data

DNA sequencing was carried out using the protocol and reagents of the Big Dye Terminator cycle sequencing kit (Life Technologies, Burlington, ON). Initially, the sequencing reaction and PCR runs were carried out in the Nargang lab and the sequence profile determination was carried out by the MBSU of the Biological Sciences Department using a 3730 DNA Analyzer (Applied Biosystems, Foster City, CA). Towards the later stages of this thesis, the PCR reactions were also carried out at the MBSU. Software including DNAMAN version 6.0.3.99 (Lynnon Biosoft, Vaudreuil, QB) and FinchTV version 1.4 (Geospiza Inc., Seattle, WA) were used for sequence alignment and analysis.

2.18 RNA isolation, cDNA synthesis and qPCR

To ensure all glassware, forceps, mortars, pestles and aluminum foils were free of RNase contamination they were baked in an oven overnight (for at least 18 hr) at 240°C prior to use. For each strain of interest, four biological replicates were grown for each condition being tested. One liter baffled flasks containing 250 mL liquid VSuTB medium

was inoculated with $1X10^6$ conidia/mL. These flasks were incubated in a shaking incubator at 30°C for 16 hr (without Cm) or 18 hr (with added Cm). Mycelium was harvested by vacuum filtration and 100 mg of mycelium was weighed and flash frozen in liquid nitrogen. RNA was isolated from these flash frozen mycelial pads using the Qiagen RNeasy Plant Mini system following the manufacture's protocol (Qiagen, Mississauga, ON).

The quality and integrity of isolated RNA was assessed using a Bioanalyzer 2100 nano chip (Agilent technologies, Mississauga, ON). If the quality of the RNA was sufficiently good (RNA integrity number (RIN) > 8), cDNA was synthesized using 1 μg RNA per reaction and Superscript III reverse transcriptase (Invitrogen, Carlsbad, CA). This cDNA was used for the qPCR reactions. The qPCR reactions were performed using a StepOnePlus RT-PCR system (Applied Biosystems, Foster City, CA) using 5 ng of cDNA and 200 nM primer per reaction, in a 96 well plate set up. The β-tubulin gene was used as an endogenous control for the ΔΔCt quantification assay.

2.19 PCR analysis of KO strains

A PCR amplification strategy was used to verify the proposed gene KO in mutants of interest. PCR amplification was carried out using wild-type or mutant genomic DNA. When the size of the target gene was 3 Kb or less, only one primer pair was used for PCR amplification (Fig.7A). When target genes of interest were >3 Kb, they proved difficult to amplify using a single primer pair. Therefore, multiple primer pairs (e.g. F1 and R1; F2 and R2; F3 and R3 (F, forward primer; R, reverse primer)) were used to amplify target genes from the wild-type strain. Primer pair (F1 and R3), outside the replacement region was used to amplify the region of interest in the knockout mutant since it should contain

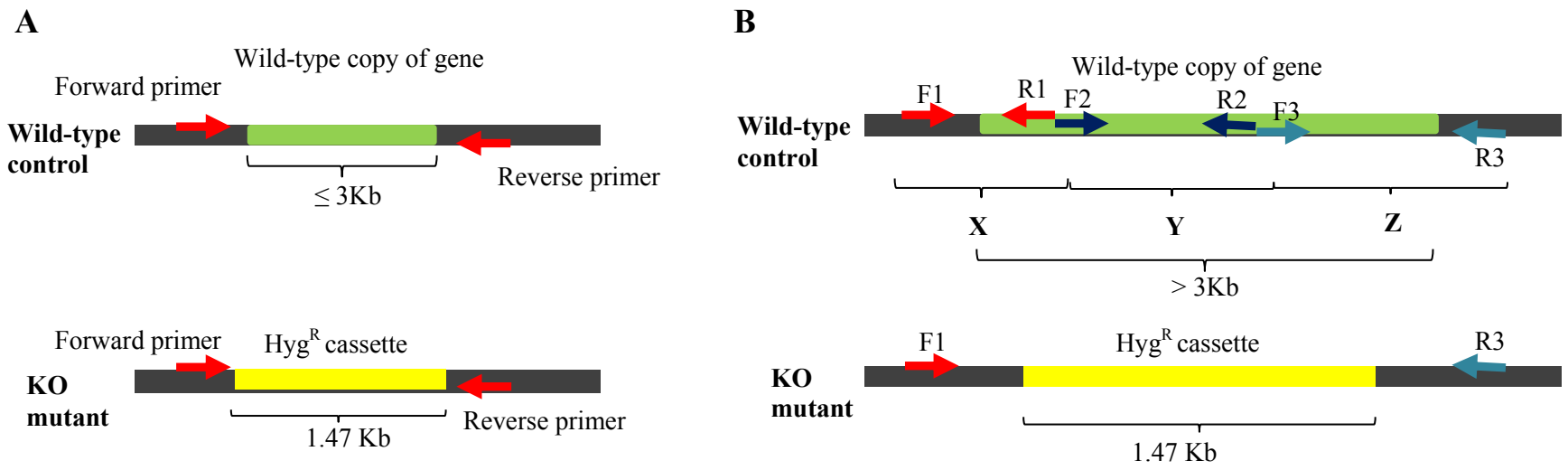

Figure 7. Generalized schematic of primer design strategy for KO mutant verification. A) Schematic diagram of primer design strategy for verifying KO mutants in which the target gene was ≤ 3Kb. In these cases, only one primer pair was used for PCR amplification (shown as red arrows). B) Schematic diagram of primer design strategy for KO mutants in which the target gene was >3Kb. Since these genes proved difficult to amplify using a single primer pair, multiple primer pairs (i.e. F1 and R1 (red arrows); F2 and R2 (dark blue arrows); F3 and R3 (light blue arrows)) were used to amplify target genes from the wild type strain. Primer pair (F1 and R3), outside the replacement region was used to amplify the region of interest in the KO mutant since it should contain the smaller Hyg^R cassette. Figure describing specific gene amplification strategies are given in section 3.2.3.1. X, Y and Z represent PCR amplified fragments. F, Forward primer, R, Reverse primer.

the smaller Hyg^R cassette (Fig. 7B). When products from both the endogenous gene and the disruption were predicted to be of similar size, a restriction enzyme that cut one of the products (but not the other) was used to differentiate between them. Based on the size of the target gene or the Hyg^R cassette, the size of the expected PCR product could be predicted.

2.20 Cloning of NCU08887 (NcMFS) and NCU01542 (NcHbrB)

The gene NCU08887 was previously cloned into the pBS520 *Asc*I vector (K. Adames, Nargang lab). The cloning strategy involved: PCR amplification of the gene from cosmid pMOCosX G2X6 (obtained from the Fungal Genetics Stock Center (FGSC)) (ORBACH 1994). The region amplified contained: 495 bp upstream of the start codon, the coding sequence of the gene (4284 bp), and 608 bp downstream of the stop codon. Cloning the gene of interest into the pBS520 *Asc*I vector, mutagenesis of the *Not*I site in the coding sequence of the gene, and insertion of *Not*I sites at the 3' or the 5' end of the coding sequence by mutagenesis for insertion of epitope tags (3XHA or 3XMyc) is described in the results (see section 3.2.1.2). The SnapGene software (GSL Biotech LLC, Chicago, IL, USA) was used for generation of plasmid models.

A portion of the NCU01542 gene was previously cloned into the pBS520 *Asc*I vector (A.B. Desaulniers, Nargang lab). The construct contained 601 bp upstream of the initially predicted start codon, 3468 bp of the initially predicted coding sequence (start codon to stop codon) and 566 bp downstream of the stop codon. It was later determined that this construct lacked part of the N-terminal coding sequence of the gene (119 bp at the 5' end, see section 3.2.2.2 and 3.2.2.3). Therefore, a 1.7 kb fragment containing part of the coding sequence (995 bp) and 744 bp upstream of the corrected start codon was PCR

amplified from cosmid pMOCosX X18A9 (obtained from the Fungal Genetics Stock Center (FGSC)) (ORBACH 1994) and was cloned into the previously created construct. Details are shown in the results, section 3.2.2.2 and 3.2.2.3. The SnapGene software (GSL Biotech LLC, Chicago, IL, USA) was used for creation of plasmid models.

2.21 Plasmids and oligonucleotides

All the plasmids and oligonucleotides relevant to this thesis are listed in Table 4 and Table 5 respectively.

Table 4. List of plasmids used in this study.

Plasmid name	Comment(s)	Origin
pBS520 *Asc*I	Bluescript vector, Amp and Bm resistance genes (Amp^R and Bm^R), *Not*I site mutagenized to *AscI* site	F.E. Nargang, Nargang lab
pBS520 *Asc*I 23H2_3' *N*I_HA	NCU08887 (along with 495 bp upstream and 605 bp downstream sequence) cloned into pBS520 *Asc*I, 3XHA tag added before stop codon	K. Adames, Nargang lab
pBS520 *Asc*I 23H2_5' *N*I_Myc	NCU08887 (along with 495 bp upstream and 605 bp downstream sequence) cloned into pBS520 *Asc*I, 3XMyc tag added after start codon	K. Adames, Nargang lab
pBS520 *Asc*I 88H8_3' *N*I_HA	NCU01542 (along with 601 bp upstream and 566 bp downstream sequence) cloned into pBS520 *Asc*I, 3XHA tag added before stop codon	A.B. Desaulniers, Nargang lab
pBS520 *Asc*I 88H8_3' *N*I_Myc	NCU01542 (along with 601 bp upstream and 566 bp downstream sequence) cloned into pBS520 *Asc*I, 3XMyc tag added before stop codon	A.B. Desaulniers, Nargang lab

pBS520 *Asc*I 88H8_5' *N*I_HA	NCU01542 (along with 601 bp upstream and 566 bp downstream sequence) cloned into pBS520 *Asc*I, 3XHA tag added after start codon	A.B. Desaulniers, Nargang lab
pBS520 *Asc*I 88H8_5' *N*I_Myc	NCU01542 (along with 601 bp upstream and 566 bp downstream sequence) cloned into pBS520 *Asc*I, 3XMyc tag added after start codon	A.B. Desaulniers, Nargang lab
pBS520 *Asc*I 88H8 predicted complete gene untagged	1.7 kb insert directionally cloned into pBS520 *Asc*I bd 88H8_5' *N*I_HA to assemble predicted functional copy of NCU01542 (along with 744 bp upstream sequence)	This study
pBS520 *Asc*I 88H8 predicted complete gene containing 3'HA	1.7 kb insert directionally cloned into pBS520 *Asc*I 88H8_3' *N*I_HA to assemble 3' 3XHA tag containing predicted functional copy of NCU01542 (along with 744 bp upstream sequence)	This study
pBS520 *Asc*I 88H8 predicted complete gene containing 3'Myc	1.7 kb insert directionally cloned into pBS520 *Asc*I 88H8_3' *N*I_Myc to assemble 3' 3XMyc tag containing predicted functional copy of NCU01542 (along with 744 bp upstream sequence)	This study

pBSK II	Plasmid used for testing transformation efficiency of XL-2 Blue *E. coli* cells	N. Go, Nargang lab
p-*aod-2* Hyg	Plasmid used for creation of Hyg^R gene probe used for Southern blot analysis	Z. Qi, Nargang lab

Table 5. Oligonucleotides relevant to this study.

Primer name	Comment(s)	Sequence
23H2 aod-1 F (2)	Forward primer to PCR amplify *aod-1* gene	5' - AAGATGCCCGATGAAGATGAGG - 3'
23H2 aod-1 R (2)	Reverse primer to PCR amplify *aod-1* gene	5' - CAACTTGGTCCAAAAACGCCT - 3'
23H2 aod-2 F1 (2)	Forward primer to PCR amplify *aod-2* gene-set 1	5' - TGGTTGCGGTCAACAGACTT - 3'
23H2 aod-2 R1 (2)	Reverse primer to PCR amplify *aod-2* gene-set 1	5' - TCATGTGCTAAGGCAGCCAA - 3'
23H2 aod-2 F2 (2)	Forward primer to PCR amplify *aod-2* gene-set 2	5' - AAAGGCTGGCTCGGAATCAA - 3'
23H2 aod-2 R2 (2)	Reverse primer to PCR amplify *aod-2* gene-set 2	5' - GTTGCTCGGAAGTGAGACCA - 3'
23H2 aod-5 F1 (2)	Forward primer to PCR amplify *aod-5* gene-set 1	5' - CAGAGATTCCACTTTGCGGC - 3'
23H2 aod-5 R1 (2)	Reverse primer to PCR amplify *aod-5* gene-set 1	5' - AGCACCCTTCTTTCTGACGG - 3'
23H2 aod-5 F2 (2)	Forward primer to PCR amplify *aod-5* gene-set 2	5' - CTCACGGTCGACCACAAAGT - 3'
23H2 aod-5 R2 (2)	Reverse primer to PCR amplify *aod-5* gene-set 2	5' - GGAAAGTTGGCGATACGGGA - 3'

23H2 aod-5 F3 (2)	Forward primer to PCR amplify *aod-5* gene-set 3	5' - CATGCCAACGGTGCATCAAA - 3'
23H2 aod-5 R3 (2)	Reverse primer to PCR amplify *aod-5* gene-set 3	5' - ATGAACCCAGCGAAGCAGTC - 3'
aod-1 seq 1	*aod-1* sequencing primer	5' - ACAAAAACCATCAGTTCGCC - 3'
aod-1 seq 2	*aod-1* sequencing primer	5' - GCAGAGCTTTAGCATCCAC - 3'
aod -1 seq 3	*aod-1* sequencing primer	5' - GCGACTGGTGTTCCGTTTC - 3'
aod-1 seq 4	*aod-1* sequencing primer	5' - CTCAAGCGAGTTCCATTACA - 3'
aod-1 seq 5	*aod-1* sequencing primer	5' - TGTTCTATGGAGCCCTACG - 3'
aod-1 seq 6	*aod-1* sequencing primer	5' - GGGGCGTTAATCATACATTG - 3'
aod-2 seq 1	*aod-2* sequencing primer	5' - GCCGACAAATCGTGGACAAG - 3'
aod-2 seq 2	*aod-2* sequencing primer	5' - CCAAGCCATCACTCAAAGGT - 3'
aod-2 seq 3	*aod-2* sequencing primer	5' - AGAGAGCCATTTTCCCGAGA - 3'
aod-2 seq 4	*aod-2* sequencing primer	5' - ACGGGAACAGAAGCCACGG - 3'
aod-2 seq 5	*aod-2* sequencing primer	5' - AGAGCGTGCTTGGGACTTCG - 3'
aod-2 seq 6	*aod-2* sequencing primer	5' - GATAGGGAAGCCCGCGAGTA - 3'
aod-2 seq 7	*aod-2* sequencing primer	5' - AGAGTCGAACGTGAGATACTGGG - 3'
aod-5 seq 1	*aod-5* sequencing primer (N. Go, Nargang lab)	5' - ACCCCACGATGATGCTAATG - 3'
aod-5 seq 2	*aod-5* sequencing primer (N. Go, Nargang lab)	5'- TCTATGTCGCCGTCGTCCTA -3'

aod-5 seq 3	*aod-5* sequencing primer (N. Go, Nargang lab)	5' - GTTTGATAAGCGACTTCCTG - 3'
aod-5 seq 4	*aod-5* sequencing primer (N. Go, Nargang lab)	5' - TGGCACTAACTCGGATACTC - 3'
aod-5 seq 5	*aod-5* sequencing primer (N. Go, Nargang lab)	5' - ACTGGAAAGAGATGGTAAGC - 3'
aod-5 seq 1 new	*aod-5* sequencing primer	5' - GGTCTTTCCAATGTTGTGAG - 3'
aod-5 seq 2 new	*aod-5* sequencing primer	5' - GCAGGGCATTGGGCTGATTGA - 3'
aod-5 seq 3 new	*aod-5* sequencing primer	5' - CTCGGTTTTGCTTCTTGCC - 3'
aod-5 seq 4 new	*aod-5* sequencing primer	5' - CGCAATAGTTTGTTACCAGG - 3'
aod-5 seq 5 new	*aod-5* sequencing primer	5' - CAGCAAGTCCAGTGAGAATACGA - 3'
aod-5-seq 2.5	*aod-5* sequencing primer	5' - TGCAGCAACACAATTAGGAT - 3'
23H2 aod-5-2 seq fwd	Forward primer for confirmation of mutation in *aod-1* gene in 23H2 and 88H8	5' - CCGAGGTCACTACCAAGGACGA - 3'
23H2 aod-5-2	Reverse primer for	5' -GGGGAGCATCGTGGAGATACTTT

seq rev	confirmation of mutation in *aod-1* gene in 23H2 and 88H8	- 3'
seq primer-23H2	Primer for confirmation of mutation in *aod-1* gene in 23H2 and 88H8	5' -TCTCAAACTTTTCGTCGCTCCACT - 3'
113G8 2F 4	Forward primer to PCR amplify NCU03071 set 1	5' - GTGCGGCAAGAGAAGAAACG - 3'
113G8 2R 4	Reverse primer to PCR amplify NCU03071 set 1	5' - GCGCGCATTCAATAGTCTGG - 3'
113G8 1F 4	Forward primer to PCR amplify NCU03071 set 2	5' - GCACGGACCAAACTGGACTA - 3'
113G8 1R 4	Reverse primer to PCR amplify NCU03071 set 2	5' - AAGGCCTCATCATTGGAGCC - 3'
113G8 3F 4	Forward primer to PCR amplify NCU03071 set 3	5' - GGCTGCCAACCCAGACTATT - 3'
113G8 3R 4	Reverse primer to PCR amplify NCU03071 set 3	5' - CGTGTCGAACCGAGCCTAAT - 3'
40E6 F-2100	Forward primer to PCR amplify NCU05600 set 1 (K. Adames, Nargang lab)	5' - GGAGGCGACGCCTTGGCAGCACAT G - 3'
40E6 R-2200	Reverse primer to PCR amplify NCU05600 set 1	5' - GTACGAAGATCCCCGTGCCGTTTGG

	(K. Adames, Nargang lab)	- 3'
40E6 F-4000	Forward primer to PCR amplify NCU05600 set 2 (K. Adames, Nargang lab)	5' - TCGCGCAGGTCTACAGGGCCAAGC T - 3'
40E6 R-4200	Reverse primer to PCR amplify NCU05600 set 2 (K. Adames, Nargang lab)	5' - CTCGACACCAGGGTGCAGCACTTTG - 3'
40E6-F	Forward primer to PCR amplify NCU05600 set 3 (K. Adames, Nargang lab)	5' - GGCATTGTTGGGCAGTGCGACTTTG - 3'
40E6-2R	Reverse primer to PCR amplify NCU05600 set 3 (K. Adames, Nargang lab)	5' - GGGCATGACACGCTTGGGGCCATC G - 3'
41G6-f	Forward primer to PCR amplify NCU03589 (K. Adames, Nargang lab)	5' - CTCATCATCGCCCACTGCAC - 3'
41G6-2r	Reverse primer to PCR amplify NCU03589 (K. Adames, Nargang lab)	5' - GGGAATCCGCTGCTGTTGCCACAG - 3'
52D8-Fwd (2nd)	Forward primer to PCR amplify NCU03589 (K. Adames, Nargang lab)	5' - GGCGATCAACGGGGAGCGAGTGAC - 3'
52D8-Rev	Reverse primer to PCR	5' -

(2nd)	amplify NCU03589 (K. Adames, Nargang lab)	CCACATGGTTCAGCCTAGCCGGTGG C - 3'
88H8-F (beau)	Forward primer to PCR amplify NCU01542 set 1 (A.B. Desaulniers, Nargang lab)	5' - CCCACGCAGAGGGCTCCAGGGAGT - 3'
88H8-R2640	Reverse primer to PCR amplify NCU01542 set 1 (K. Adames, Nargang lab)	5' - GGCACCGCCTTGGTTATGAGCCGTG - 3'
88H8-F2640	Forward primer to PCR amplify NCU01542 set 2 (K. Adames, Nargang lab)	5' - TTCCTCTCCGGTCCCAGTTCCTACC - 3'
88H8-R Beau (1542 - reverse)	Reverse primer to PCR amplify NCU01542 set 2 (A.B. Desaulniers, Nargang lab)	5' - TTCTTACATGGCGCGCCCTGCTGCC T - 3'
47H10-f	Forward primer to PCR amplify NCU00778 (K. Adames, Nargang lab)	5' - TGAACCGTCACGGTCCGCCC - 3'
47H10-r	Reverse primer to PCR amplify NCU00778 (K. Adames, Nargang lab)	5' - GCGGACAGAAGAAGCGACCA - 3'
83H3-f	Forward primer to PCR	5' - AACCGCCAAGCCGGAGGAGG - 3'

	amplify NCU08365 (K. Adames, Nargang lab)	
83H3-r	Reverse primer to PCR amplify NCU08365 (K. Adames, Nargang lab)	5' - GACCCGCCATCACCGTGCTG - 3'
23H2-2F	Forward primer to PCR amplify NCU08887 set 1 (K. Adames, Nargang lab)	5' - GGGGGAAACGAAAGGGTTGATCTAC - 3'
23H2-R2400	Reverse primer to PCR amplify NCU08887 set 1(K. Adames, Nargang lab)	5' - CCTAAAGCGGGCGCGAGCGAGGCGG - 3'
08887-sequene-4	Forward primer to PCR amplify NCU08887 set 2 (K. Adames, Nargang lab)	5' - CCTCTGCTACTACGCCTTTG -3'
23H2-R4200	Reverse primer to PCR amplify NCU08887 set 2 (K. Adames, Nargang lab)	5' - CCGATTAAGAGGGAGGAATGTAGTG - 3'
08887-sequence-8	Forward primer to PCR amplify NCU08887 set 3 (K. Adames, Nargang lab)	5' - CTCCCATCCTCACCCTCCGT -3'
23H2-2R	Reverse primer to PCR amplify NCU08887 set 3	5' - TGTTCCCGGCGTAACTCCCAAGACG

	(K. Adames, Nargang lab)	- 3'
NCU01542 5'	Forward primer to cone NCU01542 (K. Adames, Nargang lab)	5'-TATATATATAGGCGCGCCCGTCCGTCCCCATCGACCGTGTCC - 3'
NCU01542 reverse	Reverse primer to cone NCU01542 (N. Go, Nargang lab)	5' -TTCTTACATGGCGCGCCCTGCTGCCTCTGCGTTCGTATGTGG - 3'
NotI removal 1	Mutagenesis primer used for 1st *NotI* site removal (A.B. Desaulniers, Nargang lab)	5' -CCATACCCTTGCTGCCACAGCGGCTGCGAACGTGGTGTTCCCCCG - 3'
NotI removal 2	Mutagenesis primer used for 2nd *NotI* site removal (A.B. Desaulniers, Nargang lab)	5' -CCTCAAACTCAACTGGCTCGGCCGAGGCCGCACCGGTCGCAACAG -3'
NotI 5'	Primer for adding *NotI* site after start to make 5' tag containing clones (A.B. Desaulniers, Nargang lab)	5' - /5Phos/CGTCGCGCGCAACGAGACATGGCGGCCGCTCCGCCAGCCACATTGCTGC-3'
NotI 3'	Primer for adding *NotI* site before stop to make 3' tag containing clones	5' - /5Phos/CCTCAAACTCAACTGGCTCGGCCGAGGCCGCACCGGTCGCAACCA G -3'

	(A.B. Desaulniers, Nargang lab)	
88H8 *BstX*I mutagenesis	Primr to mutagenize *BstXI* site to clone extra fragment into incomplete 88H8 clone	5'-/5Phos/GTGGATGGTGACGAAACCTCTGGAGAGATGGGCACTTGGACTTGGGATGGGG -3'
88H8 *Afl*II site insertion	Inserting an *Afl*II site (mutagenesis) into previously cloned incomplete gene so as to add in extra fragment	5'-/5Phos/CAAGAGCGGCGGTCCGATGAGCCCTCCCATCTTAAGCTTGACAGAGGCGAG -3'
88H8 Fwd primer(*BstX*I)	Forward primer for PCR amplification of additional fragment (with *BstX*I site)	5'-AAATATAACCACCGCGGTGGGGAACACTTTAGGGCGATCTAG -3'
88H8 Rev Primer (*Afl*II)	Reverse primer for PCR amplification of additional fragment (with *Afl*II site)	5'-CGCGCTCGCCTCTGTCAAGCTTAAGATGGGAG -3'
88H8Insert*NotI* -5'tag new start	Mutagenesis primer for adding *NotI* site after start to make 5' tag containing clones	5'-/5Phos/CAGAAGCAAGCAAACAATCAATGGCGGCCGCCAACCCATGAGTGGAAGAGG -3'
88H8Insert*Not*I -5'tag bd	Mutagenesis primer for adding *Not*I site after start	5'-/5Phos/CAAACAATCAATGCAACCCA

	to make 5' tag containing clones (with beaus proposed start)	TGGCGGCCGCAGTGGAAGAGGAAC CCCCG -3'
88H8 seq 1	Sequencing primer (A.B. Desaulniers, Nargang lab)	5' - GGGTAGGCGTACACTCGGGC - 3'
88H8 seq 2	Sequencing primer (A.B. Desaulniers, Nargang lab)	5' - CCACAACGGCCTCGCCGGAA -3'
88H8 seq 3	Sequencing primer (A.B. Desaulniers, Nargang lab)	5' - GGCCTACAGATCCCACAGCC - 3'
88H8 seq 4	Sequencing primer (A.B. Desaulniers, Nargang lab)	5' - CCGCTTGATCCCTGCTCTTG - 3'
88H8 seq 5	Sequencing primer (A.B. Desaulniers, Nargang lab)	5' - CCTCCATGTCCAACCCCGTT - 3'
88H8 seq 6	Sequencing primer (A.B. Desaulniers, Nargang lab)	5' - CCCCCACTCCTCCACGGGCA - 3'
88H8 seq 7	Sequencing primer (A.B. Desaulniers, Nargang lab)	5' - CCGGTCGCAACAGAAGGGGC - 3'
NCU08887-5'	PCR amplification primer to clone NCU08887, forward primer (K. Adames, Nargang lab)	5' - CAGCTAGCGAGGCGCGCCGTGATG GATGATGTATCTGGACCAC - 3'
NCU08887-3'	PCR amplification primer to clone NCU08887,	5' - AGTCAGGCTAGGCGCGCCTGGCTG

	reverse primer (K. Adames, Nargang lab)	GTGATGGAAGGACGCAGCC -3'
NCU08887-5'-*Not*I	Mutagenesis primer used for *Not*I site removal (K. Adames, Nargang lab)	5' - /5Phos/ CTCTTTCCCCCACGCCAGCAGCAGC CGCCTCCACCGCACACCCACACCC - 3'
8887 *Not*I removal-sequence	Sequencing primer to check if *Not*I site has been mutaganized (K. Adames, Nargang lab)	5' - GTGCCACGAACCGGCACCAC - 3'
*Not*I insertion-5'	Primer to Add *Not*I site after start to make 5' tag containing clones (K. Adames, Nargang lab)	5' - /5Phos/ TACTTCCAAAGCTTATGATGGCGGC CGCTCCTCTACTGATGCAATTAC - 3'
*Not*I insertion-3'	Primer to add *Not*I site before stop to make 3' tag containing clones (K. Adames, Nargang lab)	5' - /5Phos/ GGTTTGTTGTTGGGAATCAAGCGGC CGCTGATGGGGCTGTGATAGGGA - 3'
08887-sequence -1	Sequencing primer (K. Adames, Nargang lab)	5' - TACTTTTGAGCTGACTGCAT - 3'
08887-sequence-2	Sequencing primer (K. Adames, Nargang lab)	5' - TCACAGCACCACCAGTGCTT - 3'
08887-	Sequencing primer (K.	5' AGAAGACGCCCGTACACTCC- 3'

sequence-3	Adames, Nargang lab)	
08887-sequence-4	Sequencing primer (K. Adames, Nargang lab)	5' - CCTCTGCTACTACGCCTTTG -3'
08887-sequence-5	Sequencing primer (K. Adames, Nargang lab)	5' - TTATACATGATGCTGATGCT - 3'
08887-sequence-6	Sequencing primer (K. Adames, Nargang lab)	5' - ATACCCCGCTGAACATCAAT - 3'
08887-sequence -8	Sequencing primer (K. Adames, Nargang lab)	5' - CTCCCATCCTCACCCTCCGT -3'
08887-sequence-9	Sequencing primer (K. Adames, Nargang lab)	5' - TTATTGGTTTGGGGGTTTTG -3'
08887-sequence-4.5	Sequencing primer (K. Adames, Nargang lab)	5' - GGGAGGAGGATCGTGTTGGT - 3'
08887-sequence-5 reverse	Sequencing primer (K. Adames, Nargang lab)	5' - AGCATCAGCATCATGTATAA -3'
aod-1 qPCR primer F	qPCR forward primer for *aod-1* (Z.Qi, Nargang lab)	5’ – GGGGCGTTAATCATACATTGA - 3’
aod-1 qPCR primer R	qPCR reverse primer for *aod-1*(Z.Qi, Nargang lab)	5’ – AGTCGCTCACAAACGGATTC – 3’
β-tubulin qPCR primer F	qPCR forward primer for β-tubulin (Z.Qi, Nargang lab)	5’ – GCCTCCGGTGTGTACAATG – 3’

β-tubulin qPCR primer R	qPCR forward primer for β-tubulin (Z.Qi, Nargang lab)	5’ – CGGAAGCCTCGTTGAAGTAG – 3’

References

BERTRAND, H., and T. H. PITTENGER, 1969 Cytoplasmic Mutants Selected from Continuously Growing Cultures of Neurospora crassa. Genetics **61:** 643-659.

DAVIS, R., and F. DE SERRES, 1970 Genetic and microbiological research techniques for Neurospora crassa. Methods Enzymol. **17A:** 79-143.

HOPPINS, S. C., N. E. GO, A. KLEIN, S. SCHMITT, W. NEUPERT *et al.*, 2007 Alternative splicing gives rise to different isoforms of the Neurospora crassa Tob55 protein that vary in their ability to insert beta-barrel proteins into the outer mitochondrial membrane. Genetics **177:** 137-149.

NARGANG, F. E., and D. RAPAPORT, 2007 Neurospora crassa as a model organism for mitochondrial biogenesis. Methods Mol. Biol. **372:** 107-123.

ORBACH, M. J., 1994 A cosmid with a Hy^R marker for fungal library construction and screening. Gene **150:** 159-162.

SAMBROOK, J., and D. W. RUSSELL, 2001 *Molecular Cloning: A laboratory manual*. Cold Spring Harbor Laboratory Press, Cold Spring Harbor, N.Y.

WENDLAND, J., K. B. LENGELER and E. KOTHE, 1996 An instant preparation method for nucleic acids of filamentous fungi. Fungal Genet. Newsl. **43:** 54-55.

WIDEMAN, J. G., N. E. GO, A. KLEIN, E. REDMOND, S. W. LACKEY *et al.*, 2010 Roles of the Mdm10, Tom7, Mdm12, and Mmm1 proteins in the assembly of mitochondrial outer membrane proteins in Neurospora crassa. Mol. Biol. Cell. **21:** 1725-1736.

Chapter 3: Results

3.1 Analysis of possible assembly mutants

Screening of the *N. crassa* KO mutant library identified several mutants with varying degrees of AOX deficiency (NARGANG *et al.* 2012). Some of the KO strains were found to have very poor or no growth in the presence of AA, but had wild-type levels (or near wild-type levels) of AOX in their mitochondria under Cm inducing conditions. One possible explanation for these data was that AOX protein was produced and imported into the mitochondria, but was not properly assembled into a functional protein. Thus, the KO strains could be assembly mutants affecting such processes as iron integration, unknown but required post-translational modifications, or integration of AOX into the MIM.

3.1.1 Preliminary tests to confirm phenotypes of possible assembly mutants

I chose five such mutant strains to analyze as possible assembly mutants, based on the severity of the AA sensitivity in these strains (as reported previously (NARGANG *et al.* 2012)). Four of these strains (13G11, 28B10, 85H5 and 101D3) had no growth and one strain (99B8) grew very slowly on AA-containing plates. All these strains were previously found to have AOX levels either slightly lower or comparable to wild-type levels on western blots following growth in the presence of Cm. As a first step, I wished to confirm the growth test and western blot data obtained during the large scale KO mutant library screen. Table 6 contains growth test data for the five KO mutant strains on standard Vogel's medium plates with or without addition of AA. Consistent with the previous observations, these KO mutant strains have very little to no growth on AA

Table 6. Growth test data for possible KO assembly mutant strains and the wild-type control.

Strain number	NCU number	Mating type	Gene description*	Growth on plates at 48 hrs**	
				AA-	AA+
Wild-type control	NCN251	A	N/A	4.2***	4.2
13G11	NCU04566	a	Protein kinase 10	4.2	0
28B10	NCU08137	A	Hypothetical protein	4.2	0
85H5	NCU09803	A	Thioredoxin	4.2	0
99B8	NCU09327	A	Cytochrome-4	4.2	0.2
101D3	NCU09560	a	Superoxide dismutase	4.2	0

* From the BROAD Institute Neurospora genome website and fungidb.org.

** Measured in cm from the point of inoculation at the center of the plate.

***This number represents the radius of the plate. Thus, at the 48 hr time point, the strain of interest, inoculated at the center of the plate, completely covered the surface of the plate.

containing plates and grow at normal rates on standard medium. It should be noted that previous work gave similar results for strains with mutations in *aod-1* the AOX structural gene (LI *et al.* 1996; DESCHENEAU *et al.* 2005).

The strains were then grown in the presence of Cm for 24 and 48 hr to determine if AOX was inducible. Levels of AOX in these strains were examined by subjecting mitochondrial proteins to SDS-PAGE followed by western blot analysis. As shown in Fig. 8, AOX is present in all strains. The levels seem to be slightly lower than the control (NCN251) in some strains (13G11, 28B10 and 85H5) but comparable to the control in the other strains. Thus, these data confirm that the strains selected for analysis as possible assembly mutants, have very poor or no growth in the presence of AA even though they have substantial AOX levels under conditions that induce the expression of the enzyme.

One possibility for an AOX assembly defect would be an inability of the protein to be properly inserted into the MIM. This was tested using carbonate extraction experiments. A schematic overview of this technique is outlined in Fig. 9. In general, peripheral membrane proteins, associated with the membrane via electrostatic interactions, can be removed from the membrane by treatment with sodium carbonate at pH 11.0. However, this treatment does not disrupt the interaction of integral membrane proteins that contain hydrophobic trans-membrane domains inserted into the membrane lipid bilayer. Thus, integral membrane proteins partition with the membrane fraction (pellet) upon centrifugation while peripheral membrane proteins are present in the supernatant fraction (along with soluble proteins) (FUJIKI *et al.* 1982a; FUJIKI *et al.* 1982b). Past results with interfacial membrane proteins (like AOX) have shown that

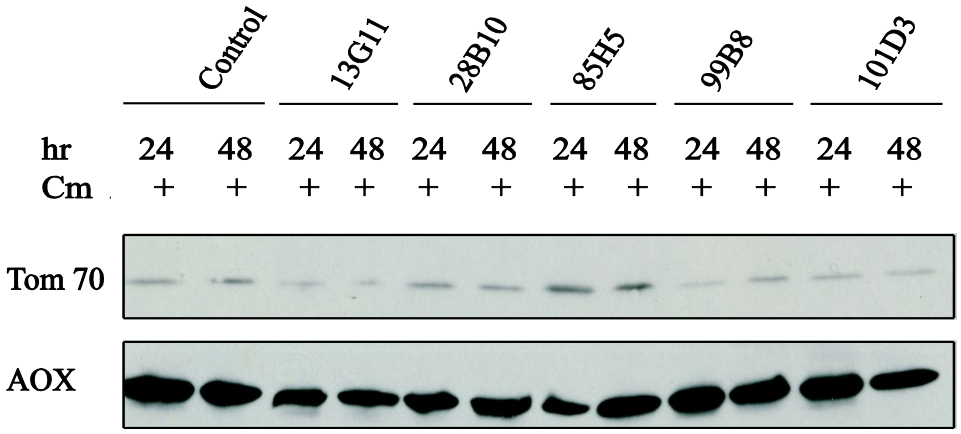

Figure 8. AOX levels in strains selected for analysis of AOX assembly. The five KO mutant strains (13G11, 28B10, 85H5, 99B8 and 101D3) selected for study as possible AOX assembly mutants were subjected to growth in the presence of Cm. Liquid cultures of these strains and a control (wild-type strain NCN251) were grown for 24 and 48 hr in the presence of the inhibitor. Mitochondria were then isolated and mitochondrial proteins were subjected to SDS-PAGE and western blotting using antibodies against Tom70, as a loading control, and AOX as indicated.

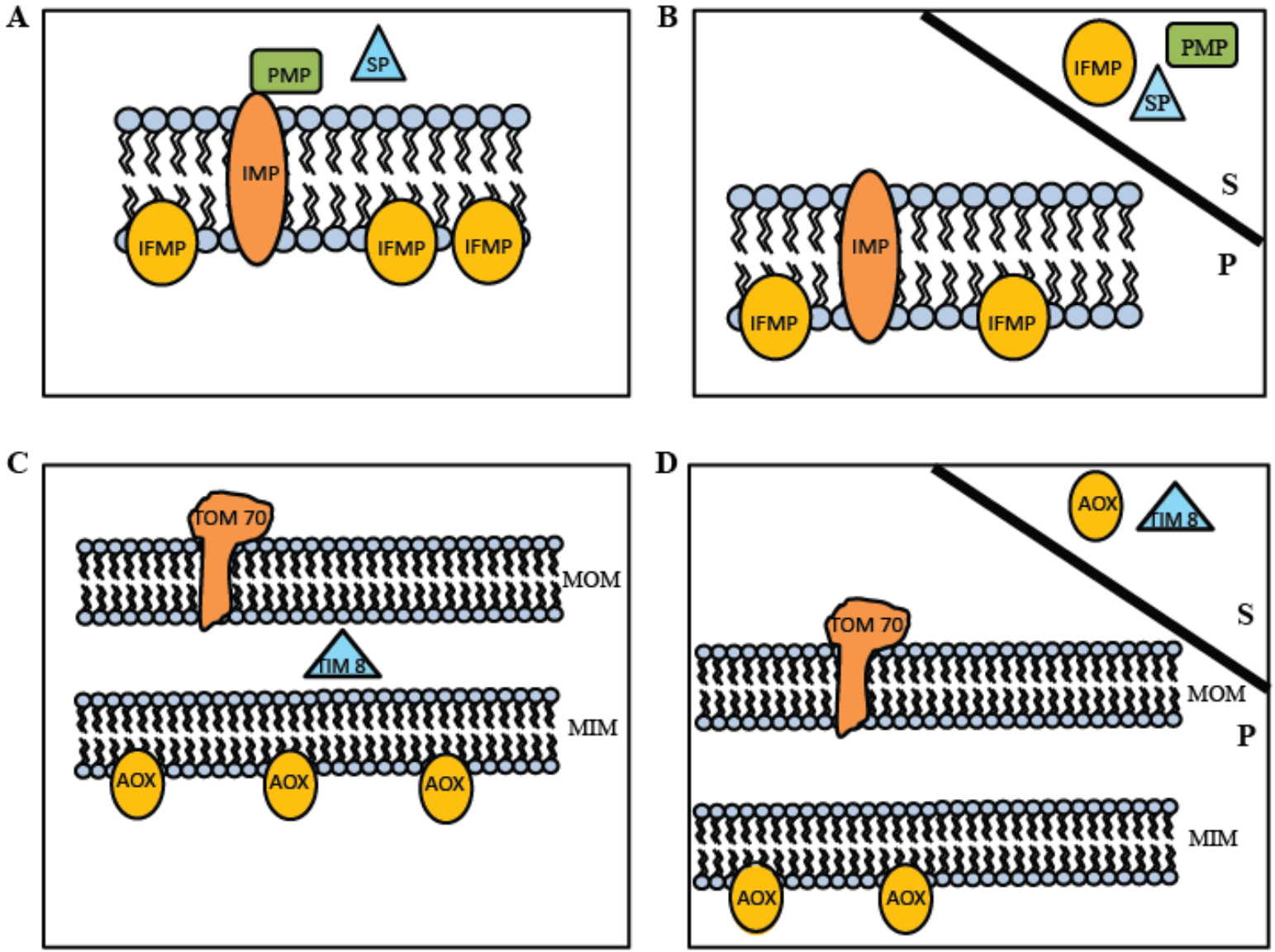
A
PMP
SP
IMP
IFMP
IFMP
IFMP
B
IFMP
PMP
SP
S
P
IMP
IFMP
IFMP
C
TOM 70
MOM
TIM 8
MIM
AOX
AOX
AOX
D
AOX
TIM 8
S
TOM 70
MOM
P
MIM
AOX
AOX

Figure 9. Basic schematic of carbonate extraction. A) A general membrane system with its associated proteins (IMP, integral membrane protein; PMP, peripheral membrane protein; SP, soluble protein and IFMP, interfacial membrane protein). B) Upon treatment of the membrane system with 0.1M sodium carbonate (pH 11.0), followed by centrifugation, the pellet fraction (P) should contain the integral membrane protein and some proportion of the interfacial membrane proteins. The soluble protein, some of the interfacial membrane proteins and the peripheral membrane protein are present in the supernatant fraction (S). C) *N. crassa* mitochondrial membrane proteins examined in this study. Tom70 is an integral membrane protein of the MOM, Tim8 is a soluble protein of the IMS whereas AOX is an interfacial membrane protein of the MIM. D) Upon carbonate treatment, the majority of Tom70 is expected to partition into the pellet fraction, Tim8 is expected to be present in the supernatant fraction whereas AOX is expected to be present in both the pellet and supernatant fraction.

these proteins fractionate to both the supernatant and pellet fraction (JANSSEN *et al.* 2002; CLAYPOOL *et al.* 2006a; SINGHA *et al.* 2009; POVELONES *et al.* 2013).

Based on the carbonate extraction results in Fig. 10, the five strains under study were divided into two subclasses. One subclass denoted 'wild-type like' consisted of strains 28B10, 99B8 and 101D3 which had an almost wild-type pattern of partitioning AOX in the pellet and the supernatant fractions. The other subclass was denoted as 'possible AOX insertion mutants' and consisted of strains 85H5 and 13G11. In the case of 13G11, at both time points tested, AOX seems to partition mostly in the supernatant fraction, unlike the pattern observed with AOX in the wild-type strain. A similar pattern was seen in 85H5 at 24 hr. This suggested that AOX may not be properly inserted into the MIM in these strains.

Unfortunately, when the carbonate extractions were done repeatedly on some of these strains, it became apparent that the data were not consistent. For example in strain 13G11, identical experiments seemed to produce a very different AOX partitioning pattern (Fig. 11). Similar variations occurred in other strains examined (not shown). These inconsistencies led us to abandon further study of assembly mutants by carbonate extraction.

3.2 Study of class I KO mutant strains

As described in section 1.10.1, a large scale screen of the *N. crassa* KO library identified eight new mutants that had no growth, or very poor growth, on AA containing medium and had virtually no AOX following growth in Cm (NARGANG *et al.* 2012). One mutant (100B5), lacking the NCU08158 gene (encoding a dual specificity phosphatase protein) was previously characterized (DESAULNIERS 2013) leaving seven new uncharacterized

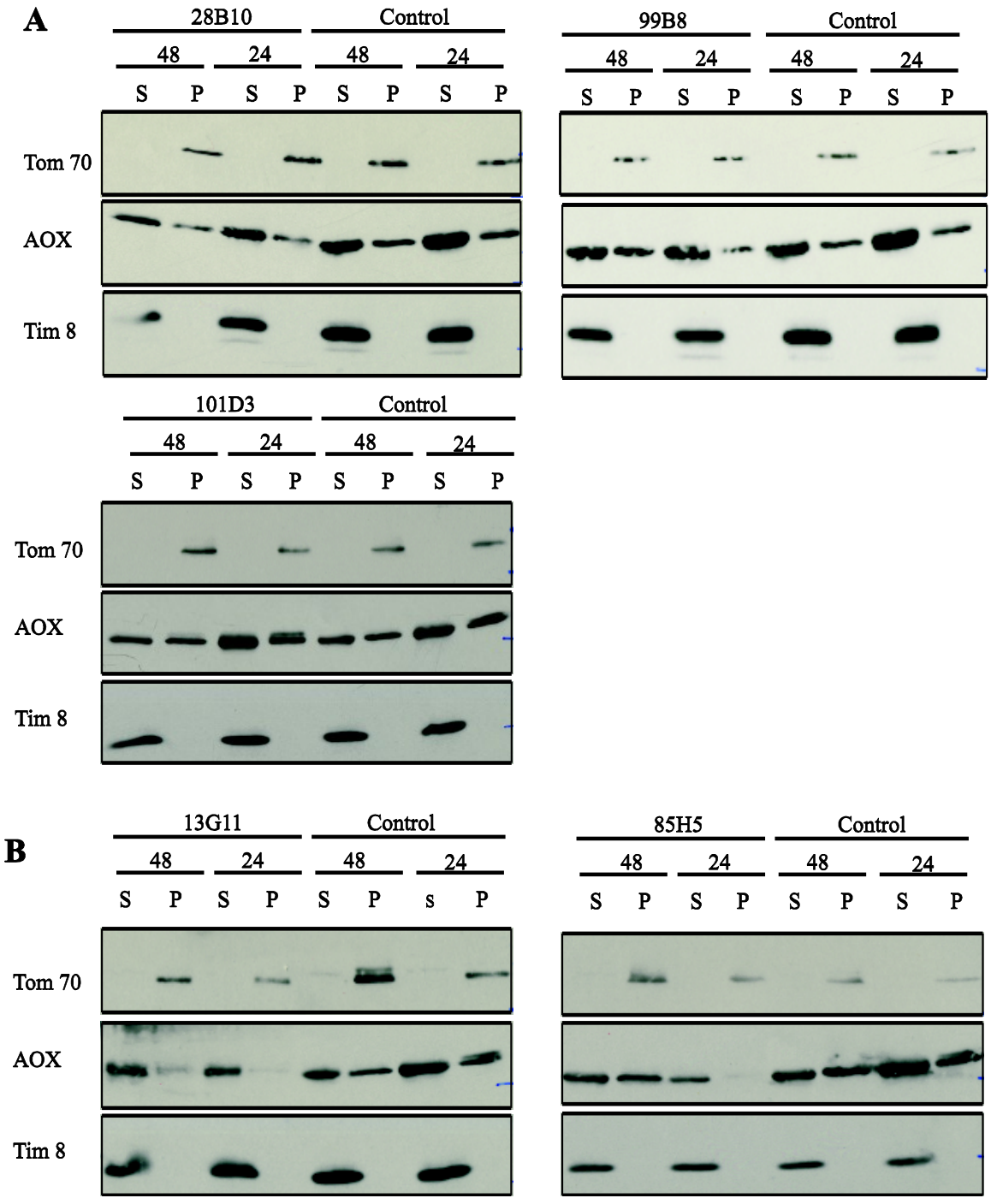

Figure 10. Carbonate extractions of putative assembly mutants. *N. crassa* strains were grown in the presence of Cm to induce AOX. Mitochondria were isolated and subjected to sodium carbonate extraction at pH 11.0. The Tom70 protein (MOM protein, present mainly in the P fraction) and the Tim8 protein (IMS protein present mainly in the

S fraction) serve as controls. A) Carbonate extraction of strains 28B10, 99B8 and 101D3. B) Carbonate extraction of strains 13G11 and 85H5. The control is the wild-type strain NCN251.

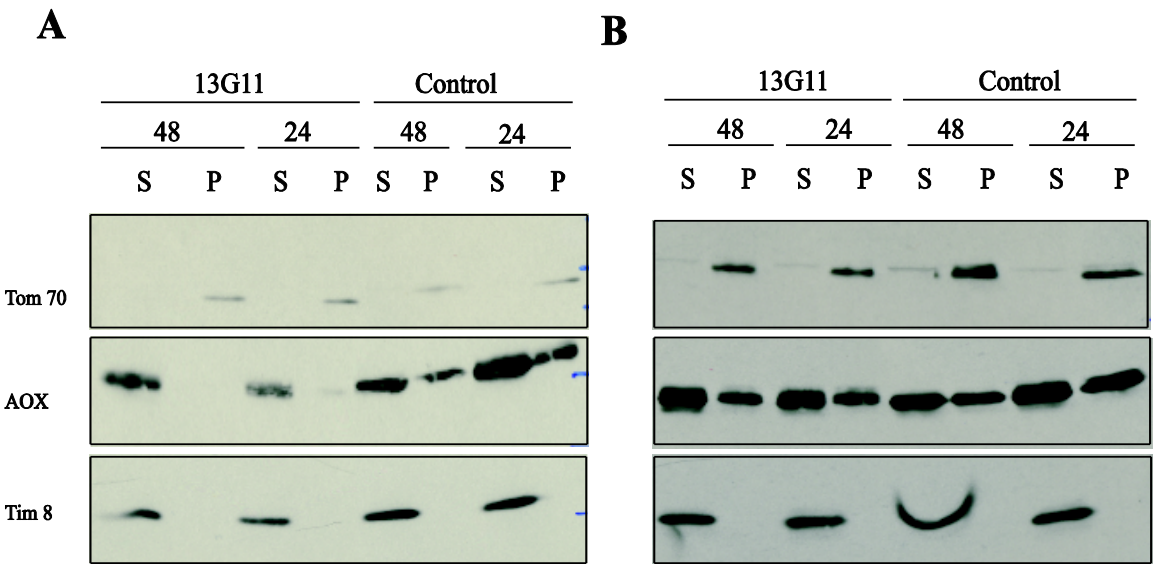

Figure 11. Inconsistencies in carbonate extraction results for strain 13G11. The AOX partitioning patterns from two identical experiments with strain 13G11. A) A separate experiment from that shown in Fig. 10B shows a similar AOX partitioning pattern as in Fig. 10B. B) An identical experiment on the same strain produces an AOX partitioning pattern that is similar to the control. The control is the wild-type strain NCN251. S, supernatant fraction; P, pellet fraction.

mutants with severe AOX deficiencies. Work in this thesis began by focusing on two mutants 23H2 (KO-NcMFS) and 88H8 (KO-NcHbrB) as these strains had good growth and conidiation on standard medium in comparison to the other class 1 KO strains. However, as described below, it became apparent that these genes were likely not involved in AOX expression. Therefore, experiments turned to assessing the integrity and authenticity of the other five class 1 KO mutant strains identified by the screen that lack AOX protein at 24 and/or 48 hr of growth in the presence of Cm. An additional KO strain, 113G8 (lacking the NCU03071 gene, encoding a MAP kinase kinase kinase protein), was included in this study. This strain was identified in our lab after the initial study, as having an AOX deficiency characteristic of other class 1 KO mutants.

3.2.1 The NCU08887 hypothetical protein (NcMFS) contains a major facilitator superfamily (MFS) domain

The gene NCU08887 encodes a 1068 amino acid long hypothetical protein (referred to in this thesis as NcMFS) annotated as containing a major facilitator superfamily (MFS) domain. Members of this superfamily are present in all kingdoms of life and are involved in the transport of small solute molecules coupled to a chemiosmotic ion gradient (PAO *et al.* 1998; REDDY *et al.* 2012). Homologs of NcMFS are found in several fungal species including *Sordaria macrospora*, *Podospora anserina* and *Chaetomium thermophilus*. However, upon performing BLAST searches, no clear homologs of this protein are observed in humans, mice, Drosophila, zebrafish and *C. elegans*.

The MFS superfamily is a large family of secondary transport proteins consisting of 76 different subfamilies (YAN 2013). The superfamily includes antiporters, symporters and uniporters that show high substrate specificity and transport substrates including:

drugs, sugars, organophosphates, metabolites, organic and inorganic anions, monocarboxylic acids and aromatic acids to name a few (PAO *et al.* 1998; REDDY *et al.* 2012; YAN 2013). Most proteins of this superfamily have either 12 or 14 transmembrane α-helical domains (TMDs) but some with more TMDs have also been observed (REDDY *et al.* 2012; YAN 2013). MFS proteins show very poor sequence similarity but all possess a common structural motif termed the MFS motif (YAN 2013).

As shown in Fig. 12, hydropathy analysis of the NcMFS protein using the WHAT 2.0 (Web based hydropathy and amphipathicity predictions (http://www.tcdb.org)) software suggested the presence of 12 transmembrane α-helical domains (TMDs). Recently, the *N. crassa* database (http://www.broadinstitute.org/annotation/genome/neurospora) has annotated the gene product of NCU08887 as a drug/toxin transport protein.

3.2.1.1 Cytochrome spectra analysis of mutant 23H2 (KO-NcMFS)

Given that the function of NCU08887 might be that of a transport protein acting on drugs or toxins it was possible that loss of the protein in the KO strain might affect entry of Cm into the cell. If Cm did not enter the cell, then no signal for AOX production would be generated. This would explain the lack of AOX in 23H2 (KO-NcMFS) following growth in Cm. An example of an antibiotic entering cells via an MFS transporter has been seen in *E. coli* and *Pseudomonas aeruginosa* where the antibiotic fosfomycin enters cells using the Glycerol-3-phosphate transporter (LEMIEUX *et al.* 2004; CASTAÑEDA-GARCÍA *et al.* 2009; SANTORO *et al.* 2011). However, it should be noted that although the scenario presented above could explain lack of AOX in 23H2 (KO-NcMFS) following growth in Cm, it would not explain why mutant 23H2 (KO-NcMFS) is unable

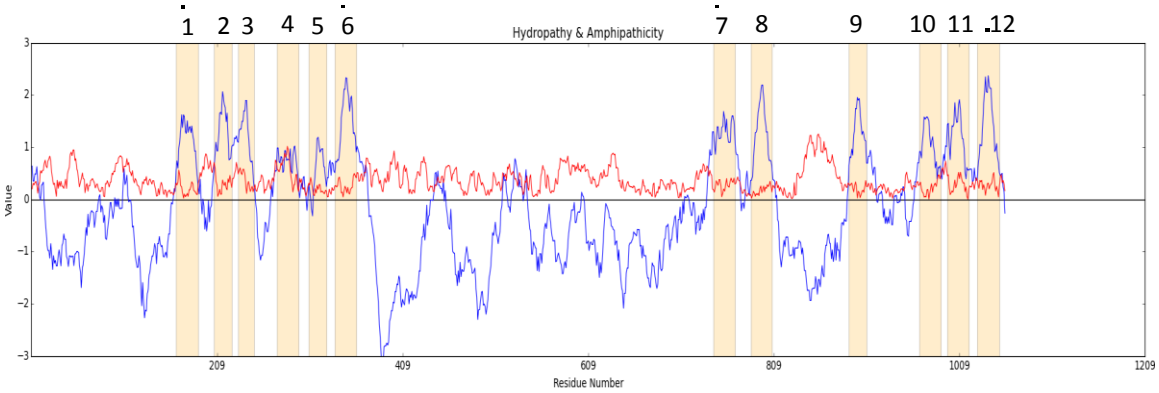

Figure 12. Hydropathy analysis of the NcMFS protein. The WHAT 2.0 software was used to determine the number of TMDs in the predicted protein product of the NCU08887 gene. The orange bars represent predicted TMDs and are numbered at the top. The blue line denotes hydropathy whereas the red line denotes amphipathicity (http://www.tcdb.org).

to grow in the presence of AA. To determine if Cm was entering cells using the NcMFS protein, cytochrome spectra analysis of mitochondria from mutant 23H2 (KO-NcMFS) and a wild-type control grown in the presence and absence of Cm was carried out. Cm inhibits mitochondrial, but not cytosolic, translation. Its effects are seen by severe reduction in the levels of cytochrome *b* and cytochrome aa_3, which have mtDNA encoded components that are poorly translated in the presence of Cm. As can be seen in Fig. 13, the cytochrome spectrum of 23H2 (KO-NcMFS) following growth in Cm lacks cytochrome *b* and aa_3, similar to the wild-type control. This demonstrates that Cm is efficiently inhibiting mitochondrial translation in this strain.

3.2.1.2 Inability to rescue KO mutant 23H2 (KO-NcMFS)

Since some MFS proteins are involved in transport of metabolites NcMFS may be involved in transport of the AOX induction signaling molecule out of the mitochondria. Once in the cytosol this signaling molecule could either enter the nucleus to directly activate the expression of AOX or act indirectly via a signaling cascade to initiate the production of AOX. Thus, the absence of NcMFS in mutant 23H2 (KO-NcMFS) would trap the AOX signaling molecule in the mitochondria and prevent AOX induction.

An initial test of this hypothesis would be to determine if the NcMFS was present in the MIM. Therefore, a rescue based approach using a gene encoding this protein with identifiable tags was used. A plasmid containing selectable markers and the NcMFS gene was previously created in the Nargang lab (K. Adames). The plasmid was further manipulated to contain either a 3XMyc tag at the N-terminal end of the coding sequence (termed N-Myc 23H2) or a 3XHA tag at the C-terminal end (termed C-HA 23H2) (Fig. 14). The tags were inserted to facilitate localization studies. The constructs were

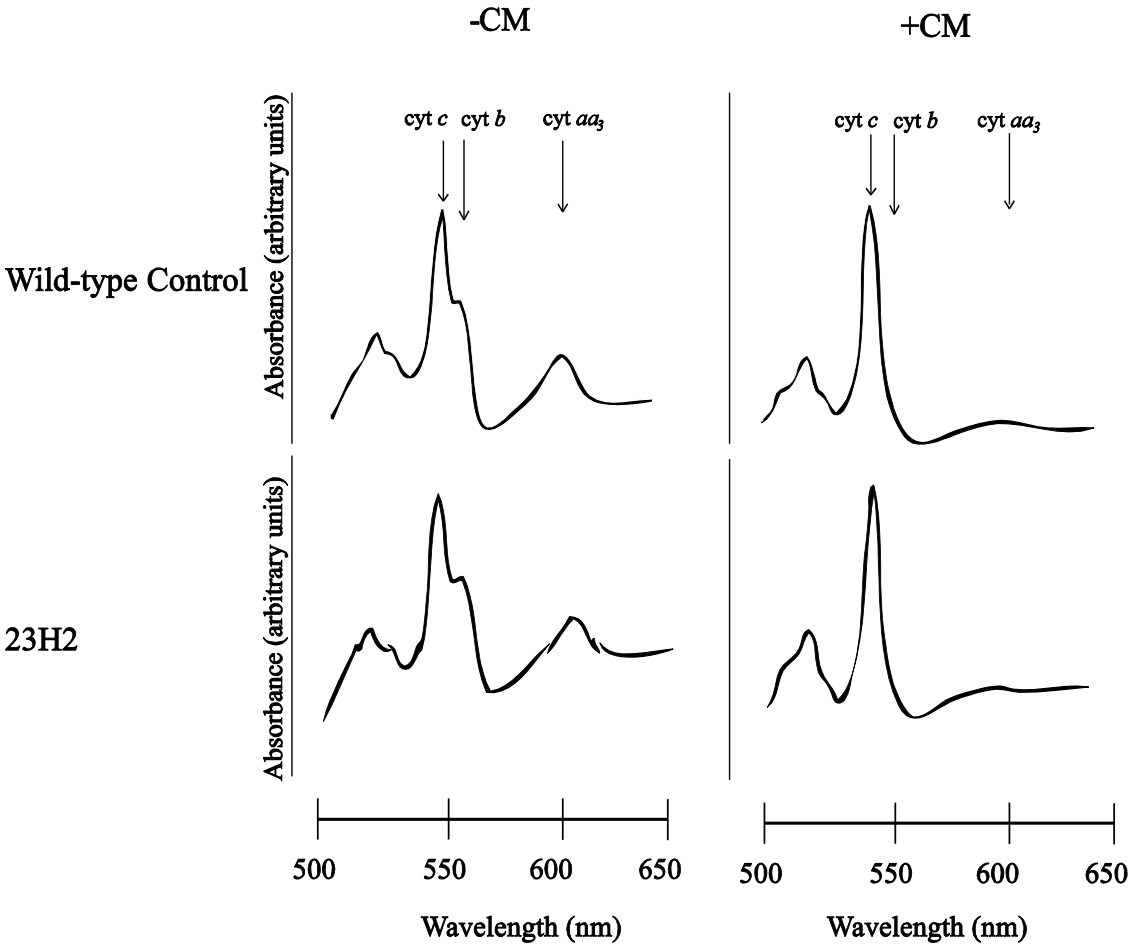

Figure 13. Cytochrome spectra of 23H2 (KO-NcMFS). The control strain (NCN251) and strain 23H2 (KO-NcMFS) were grown in the presence and absence of Cm for 24 hr. Mitochondria were isolated and processed as described in section 2.14 to obtain difference spectra (reduced sample vs oxidized reference) over wavelengths 500 to 650 nm. The Y axis represents absorbance of the sample (arbitrary units).

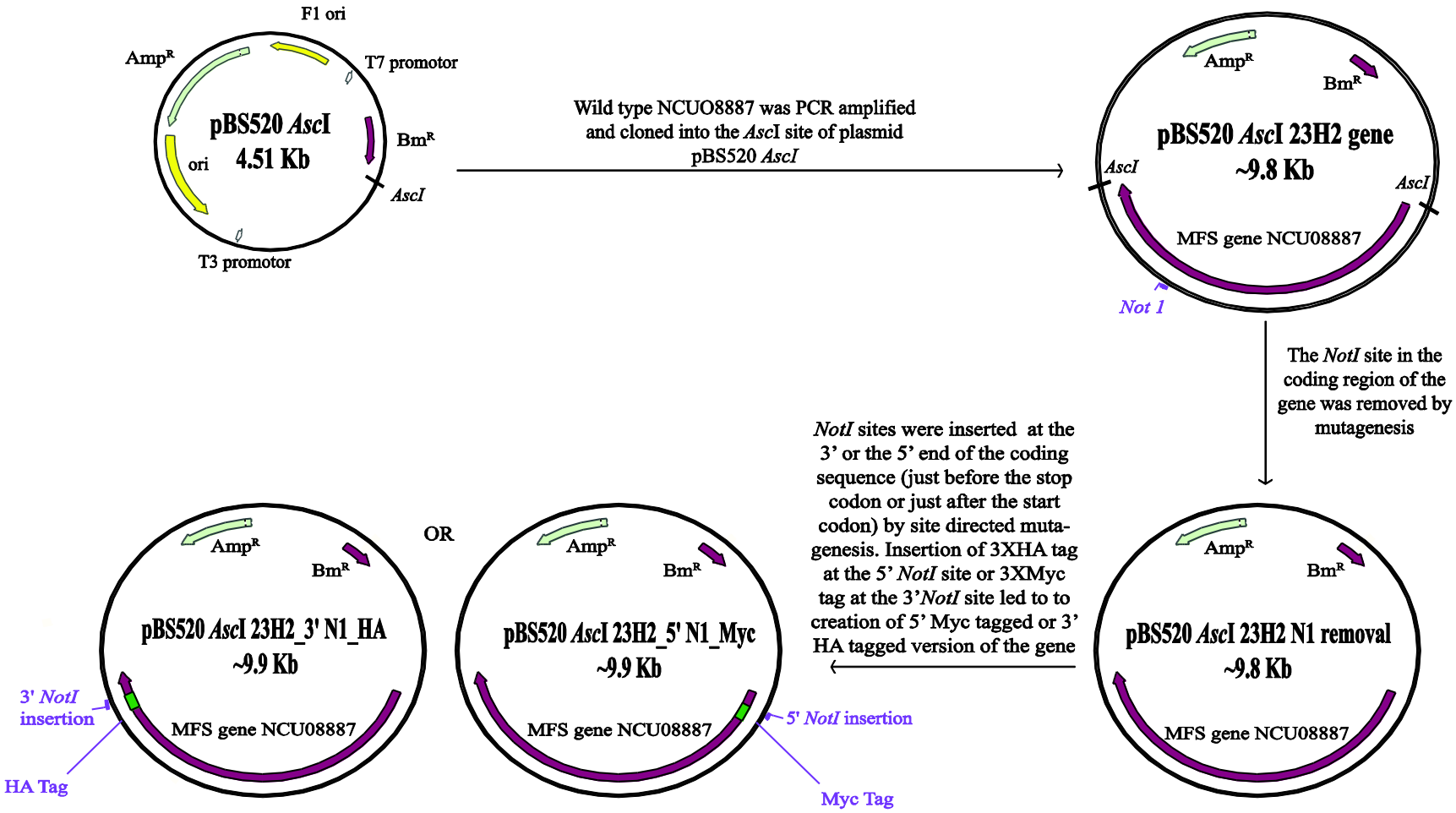
F1 ori
Amp^R
T7 promotor
pBS520 AscI
4.51 Kb
ori
Bm^R
AscI
T3 promotor
Wild type NCUO8887 was PCR amplified
and cloned into the AscI site of plasmid
pBS520 AscI
Amp^R
Bm^R
pBS520 AscI 23H2 gene
~9.8 Kb
AscI
AscI
MFS gene NCU08887
Not 1
The NotI site in the
coding region of the
gene was removed by
mutagenesis
NotI sites were inserted at the
3' or the 5' end of the coding
sequence (just before the stop
codon or just after the start
codon) by site directed muta-
genesis. Insertion of 3XHA tag
at the 5' NotI site or 3XMyc
tag at the 3'NotI site led to to
creation of 5' Myc tagged or 3'
HA tagged version of the gene
Amp^R
Bm^R
pBS520 AscI 23H2 N1 removal
~9.8 Kb
MFS gene NCU08887
OR
Amp^R
Bm^R
pBS520 AscI 23H2_3' N1_HA
~9.9 Kb
3' NotI
insertion
MFS gene NCU08887
HA Tag
Amp^R
Bm^R
pBS520 AscI 23H2_5' N1_Myc
~9.9 Kb
MFS gene NCU08887
5' NotI insertion
Myc Tag

Figure 14. Cloning strategy for NcMFS gene. The NcMFS gene (along with 495 bp upstream and 608 bp downstream from the start and stop codon, respectively) was PCR amplified from cosmid pMOCosX G2X6 and cloned into plasmid vector pBS520 *Asc*I. The plasmid contains Bm^R and Amp^R markers. A *Not*I site in the coding sequence of the NcMFS gene was removed by site directed mutagenesis without altering the amino acid specificity of the codon affected. Following this, *NotI* sites were introduced at the 3' or the 5' end of the coding sequence by mutagenesis (before the stop codon or after the start codon, respectively) for insertion of epitope tags (3XHA or 3XMyc) at these sites to create 3' 3XHA and 5' 3XMyc tagged versions of the NcMFS protein. The construction of the plasmid described above was done by K. Adames, a technician at the Nargang lab.

linearized with *Sac*I and transformed into mutant strain 23H2 (KO-NcMFS) conidia via electroporation. Transformed conidia were spread onto Bm-containing selection plates. Following a five day incubation period, 19 colonies from the C-HA 23H2 transformation plates and 21 colonies from the N-Myc 23H2 transformation plates were picked for further analysis. These transformants were subsequently purified via one round of single colony isolation and stocks were maintained on slants without Bm.

Conidia from four transformants of the N-Myc transformation (Fig. 15) and four from the C-HA transformation (Fig. 16) were spotted onto medium containing AA to determine if the AOX deficient phenotype was rescued. Surprisingly, no growth was observed for any of the tranformants, demonstrating AOX function was not restored.

Three possibilities could explain these results. First, it was conceivable that only the selected Bm^R cassette from the plasmid constructs was inserted into the genome of the transformants. However, this seemed unlikely given the usual results of similar *N. crassa* transformations and the number of transformants tested. Second, the transformed strains may not express functional NcMFS protein due to interference of the inserted tag or incomplete promoter sequence in the plasmid. The third possibility was that NcMFS may not play a role in AOX production in *N. crassa* and the AOX deficient phenotype of the strain may be due to another mutation.

To determine if tagged NcMFS was being expressed in the transformed strains, they were grown in either the presence or absence of Cm. Whole cell extracts were prepared and these were analyzed by SDS-PAGE and western blot analysis using antibodies to the protein tags. As can be seen in Fig. 17, NcMFS protein was not detected in the eight tranformants tested. Thus, the other two possibilities listed above could not be eliminated.

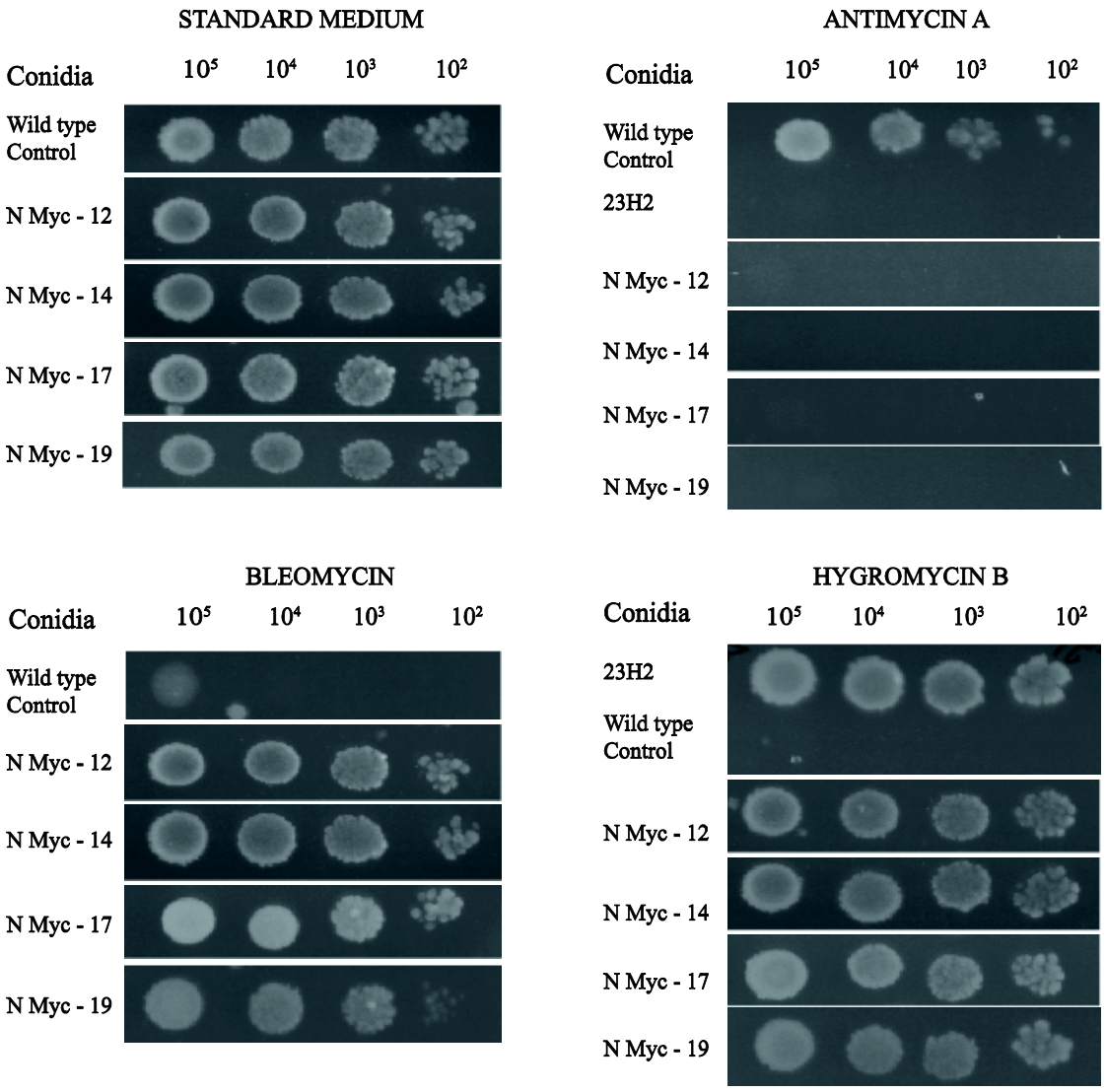

Figure 15. Growth of N-Myc tagged NcMFS transformants. 10 µL of suspension containing tenfold dilutions of conidia from the indicated strains was spotted onto standard medium with or without the indicated inhibitors. NCN251 is the wild-type control that is resistant to AA but sensitive to Bm. Bm^R gene was present on the plasmids used for transformation. The control is also sensitive to hygromycin. A Hyg^R cassette was used to disrupt genes in the KO library. The original KO strain 23H2 (KO-NcMFS) was used as a negative control for growth on AA and as a positive control for growth on hygromycin.

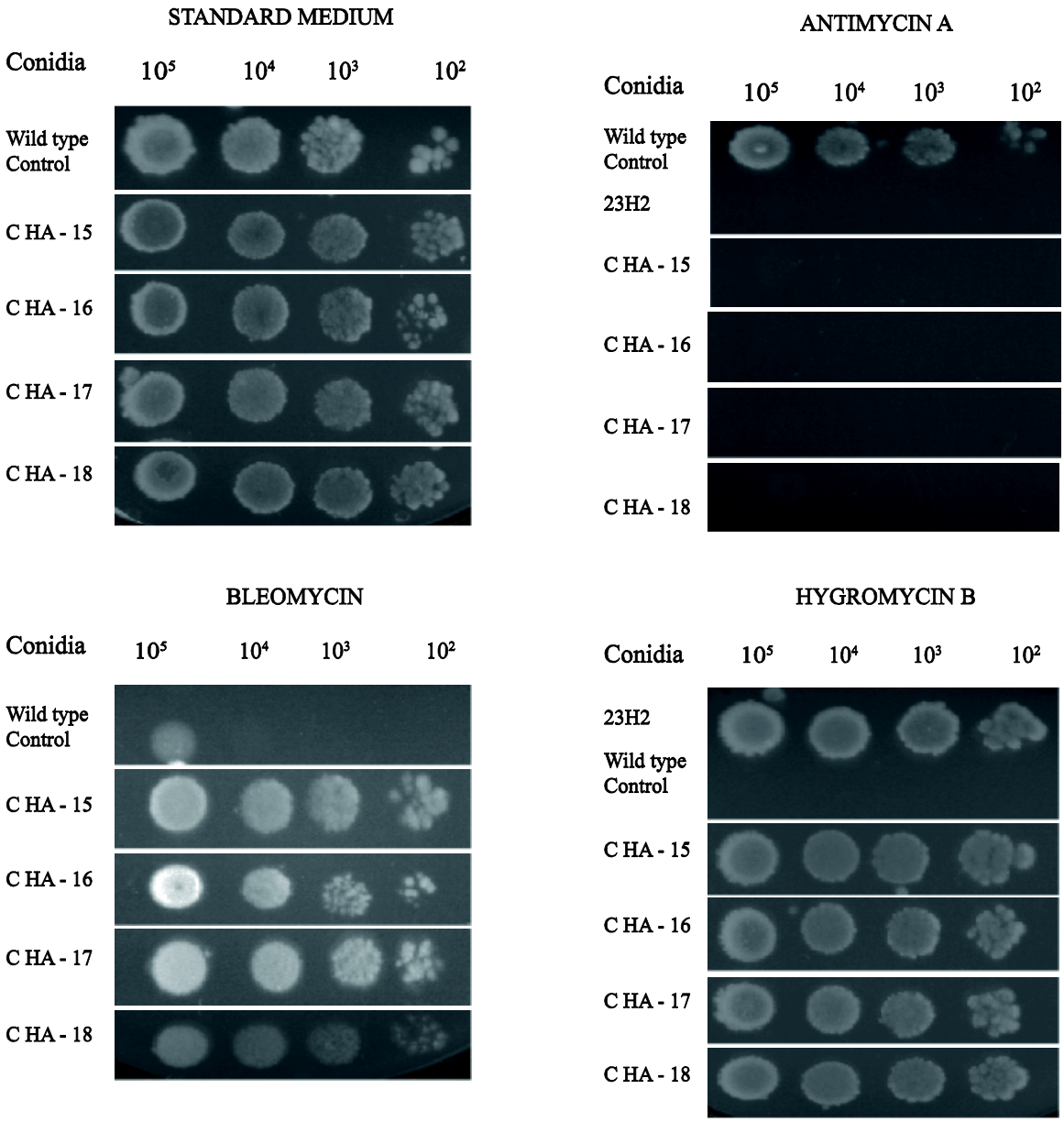

Figure 16. Growth of C-HA tagged NcMFS transformants. 10 μL suspension containing tenfold dilutions of conidia from the indicated strains was spotted onto standard medium with or without the indicated inhibitors as described in Fig. 15.

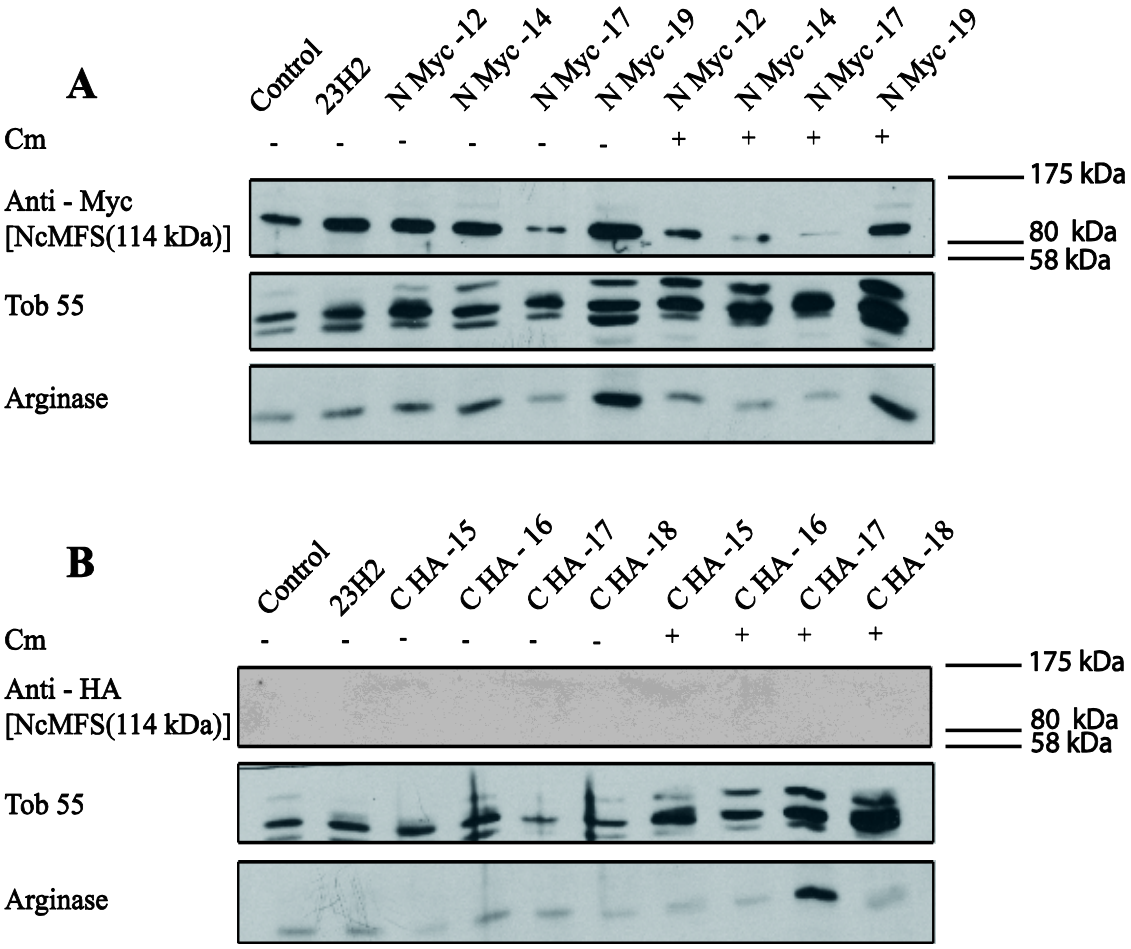

Figure 17. Examination of transformants for expression of tagged protein. A) Whole cell extracts were isolated from four N-Myc tagged NcMFS transformants grown in either the absence (-) or presence (+) of Cm. The control is the wild-type strain NCN251. Western blot analysis, using antibodies indicted on the left, was performed. The band appearing in the upper panel is a non-specific band as it is also present in the control lanes. Arginase and Tob55 serve as loading controls. B) Whole cell extracts were isolated from four C-HA tag containing transformants and analyzed as in panel A.

3.2.1.5 *aod-1* transcript levels in mutant 23H2 (KO-NcMFS)

To determine if the lack of the AOX protein in 23H2 (KO-NcMFS) is due to an effect on *aod-1* transcription, *aod-1* transcript levels in mutant 23H2 (KO-NcMFS) and in a wild-type control (NCN251) were quantified. qPCR data (Fig. 18) suggests that the *aod-1* transcript levels in these two strains are similar. This suggests that lack of AOX in strain 23H2 (KO-NcMFS) is most likely due to a post-transcriptional process.

3.2.1.4 Expression of NcMFS

While the experiments described above were being performed, RNA-seq data for a wild-type strain and class 1 mutant strain 100B5 was obtained (DESAULNIERS 2013). As shown in Fig. 19, there was virtually no transcript for the NCU08887 gene in either the wild-type or 100B5 in either the presence or absence of Cm. Even when the scale of the Y axis is lowered, virtually no transcript for this gene is observed. These data suggest that the NcMFS protein may either be expressed only at a particular developmental stage, or it may be under strict regulatory control, possibly being produced only in the presence of its specific substrate. Lack of expression either with or without Cm makes it difficult to see a role for NCU08887 in AOX production.

3.2.2 NCU01542 (NcHbrB): Hypothetical protein, with an HbrB domain

The second AOX deficient strain that I planned to investigate in this study was 88H8 (KO-NcHbrB) (section 3.2). The gene that was knocked out in this strain is NCU01542 which was initially listed at the BROAD website as encoding a 1155 amino acid protein (referred to in this thesis as NcHbrB) that contains the HbrB superfamily domain. A protein containing this domain was seen to play a role in polarized growth in *Aspergillus nidulans.* Temperature-sensitive mutants of the *A. nidulans hbrB3* gene (homolog of

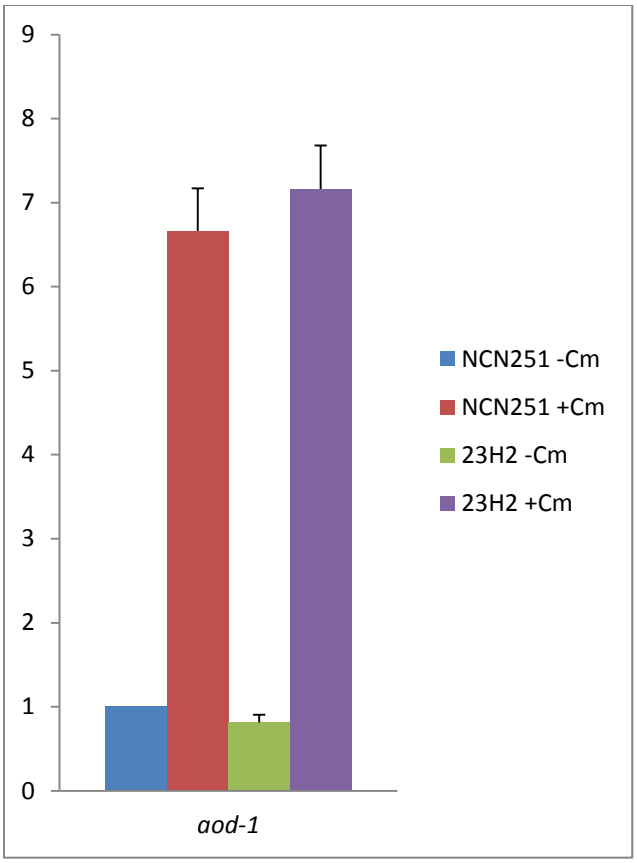

Figure 18. Transcript levels of the *aod-1* gene in mutant 23H2 (KO-NcMFS). RNA was isolated and cDNA was synthesized from the wild-type control (NCN251) and mutant 23H2 (KO-NcMFS) grown in either the presence or absence of Cm. qPCR reactions were performed using 5 ng of cDNA from each sample. β-tubulin was used as an endogenous control for the ΔΔCt quantification assay. Four biological replicates and three technical replicates were used per treatment. Error bars represent standard error.

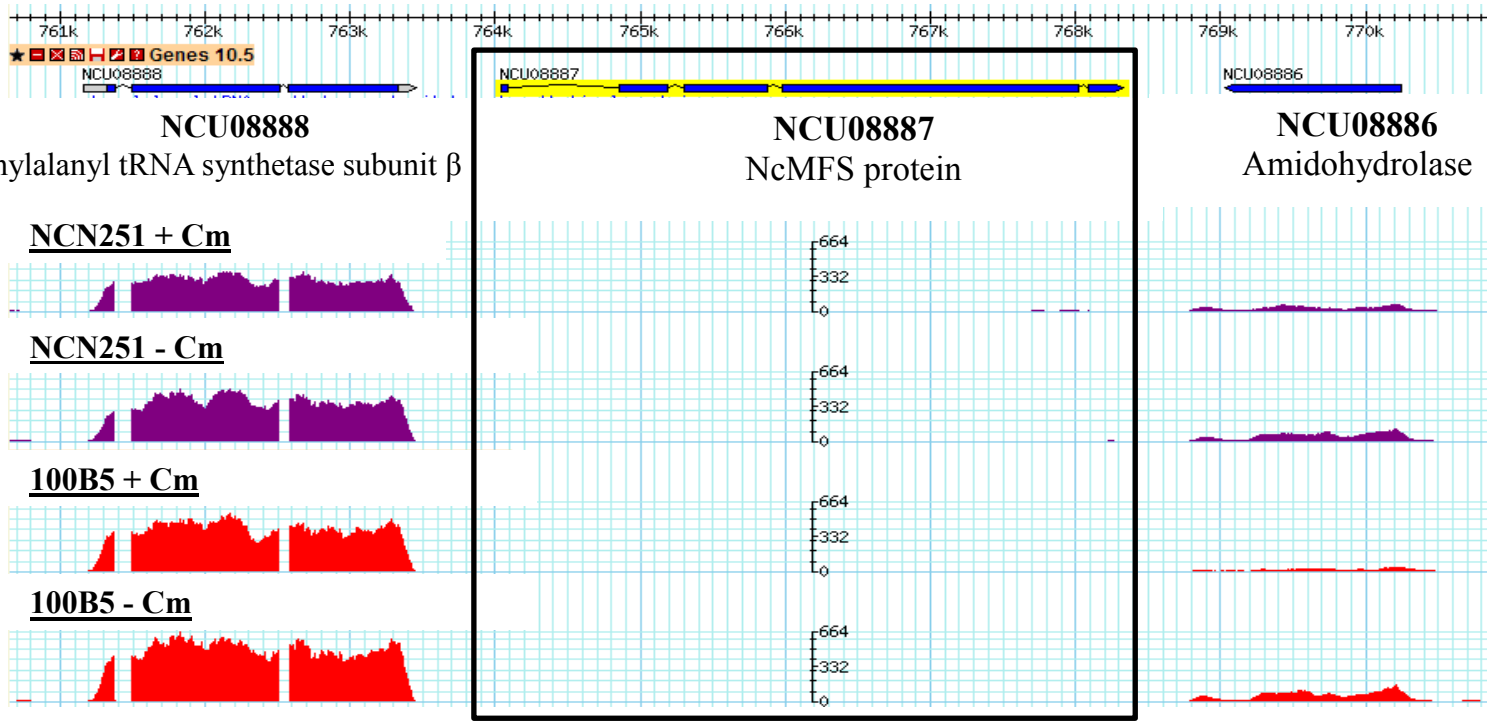

133

Figure 19. Transcription of NcMFS gene (DESAULNIERS 2013). RNA-seq was performed on wild type strain (NCN251) and the class 1 AOX mutant 100B5 (KO of NCU08158, dual specificity phosphatase protein). Both strains were grown in the presence and absence of Cm for 12 hr. RNA was isolated, cDNA libraries were created, and sequencing was performed by Delta Genomics using the Illumina platform. The number of cDNA reads were mapped onto the genome of *N. crassa* (shown in purple for the wild-type strain and in red for mutant 100B5). The box surrounds the region of the genome corresponding to the NcMFS gene. Strains and conditions are indicated on the left.

NCU01542) appear to hyperbranch as a consequence of hyperseptation at the restrictive temperature of 42°C (GATHERAR *et al.* 2004). These mutants also appear to be osmosensitive, suggesting a possible role of the hbrB domain in cell wall biogenesis. The HbrB domain appears to be fungal specific as no clear homologs of this protein are observed outside of the filamentous fungi group (GATHERAR *et al.* 2004).

3.2.2.2 Gene rescue using tagged NcHbrB

To gain insight into the role played by NcHbrB in the production of AOX, gene rescue experiments with versions of the gene designed to express tagged protein were previously attempted (A.B. Desaulniers, unpublished). The goal was to localize the tagged protein as part of an attempt to discern its function. NCU01542 (and 601 bp upstream and 566 bp downstream from the start and stop codon, respectively) was cloned into plasmid vector pBS520 *Asc*I (A.B. Desaulniers, unpublished) based on the cloning strategy depicted in Fig. 20. However, attempts to rescue the mutant phenotype of 88H8 (KO-NcHbrB) using these plasmids were unsuccessful.

A possible reason for the inability to rescue the gene defect using the original plasmids became apparent upon performing a multiple sequence alignment of NcHbrB with homologous proteins from other fungal species (*Chaetomium globosum, Thielavia terrestris, Sordaria macrospora* and *Myceliophthora thermophila*). By extending the translation of NcHbrB further into the upstream region the N-terminus of NcHbrB could be extended with good similarity to homologous proteins from other species. Thus, the alignment data (Fig. 21) suggest that the true start site might be 720 base pairs (or 240 amino acids) upstream of the initially predicted start site at the BROAD website. RNA-seq data (DESAULNIERS 2013) for the NCU01542 gene (Fig. 22) also supports the longer

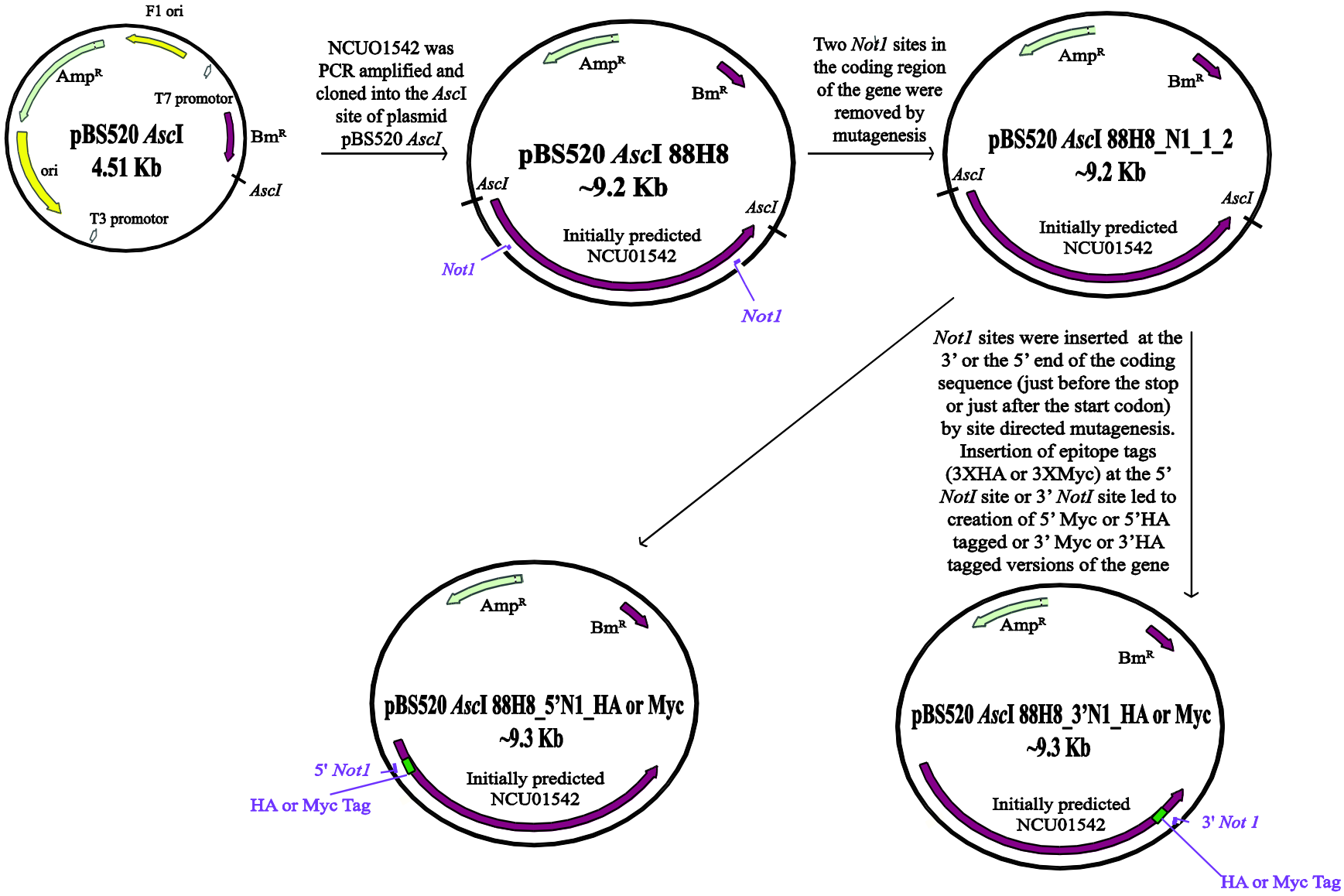
F1 ori
Amp^R
T7 promotor
pBS520 AscI
4.51 Kb
Bm^R
ori
AscI
T3 promotor
NCUO1542 was PCR amplified and cloned into the AscI site of plasmid pBS520 AscI
Amp^R
Bm^R
pBS520 AscI 88H8
~9.2 Kb
AscI
AscI
Initially predicted NCU01542
Not1
Not1
Two Not1 sites in the coding region of the gene were removed by mutagenesis
Amp^R
Bm^R
pBS520 AscI 88H8_N1_1_2
~9.2 Kb
AscI
AscI
Initially predicted NCU01542
Not1 sites were inserted at the 3' or the 5' end of the coding sequence (just before the stop or just after the start codon) by site directed mutagenesis. Insertion of epitope tags (3XHA or 3XMyc) at the 5' NotI site or 3' NotI site led to creation of 5' Myc or 5'HA tagged or 3' Myc or 3'HA tagged versions of the gene
Amp^R
Bm^R
pBS520 AscI 88H8_5'N1_HA or Myc
~9.3 Kb
5' Not1
HA or Myc Tag
Initially predicted NCU01542
Amp^R
Bm^R
pBS520 AscI 88H8_3'N1_HA or Myc
~9.3 Kb
Initially predicted NCU01542
3' Not 1
HA or Myc Tag

Figure 20. Initial cloning strategy for the NcHbrB gene. The NcHbrB gene (and 601 bp upstream and 566 bp downstream from the start and stop codon, respectively) was PCR amplified and cloned into plasmid vector pBS520 *AscI* containing a Bm^R and Amp^R marker. Two *NotI* sites in the coding sequence of the NcHbrB gene were removed by site directed mutagenesis without altering the amino acid specificity of the codon affected. Following this, *NotI* sites were introduced at the 3' or the 5' end of the coding sequence (before the stop codon or after the start codon, respectively) by mutagenesis for insertion of epitope (3XHA or 3XMyc) tags to create 3' or 5' 3XHA or 3XMyc tagged versions of the NcHbrB protein. The construction of the plasmids described above was done by A.B. Desaulniers in the Nargang lab.


New translation start
Old translation start
M.thermophila
C.globosum
T.terrestris
N. crassa
S.macrospora

```
N. crassa          ASSNSRPTDPTAPSSLYNFNLPTSPGPSSNAFKSGLDLRHGGRALREKKNKEDKSLDDAA 564
S.macrospora       ASSNSRPTDPTAPSSLYNFNLPASPGPGSNAFKSGLDLRHGGRALREKKNKEDKSLDDAA 559
                   * *****:**.******.*.** ** *.:. ***.*********:**::::::.

M.thermophila      STSGVASEWPGSSSVTSGSAAQASALYLNEPFDSHKYGLNNMTHDDAWPFLKAKLLVVFE 538
C.globosum         TASAVTSEWPGSSSVTSGSATQASTLYLNEPFDSHKYGLNNMTHDDAWPFLKAKLLVVFE 538
T.terrestris       STSGIGSEWPGSSAVGSGSGALGPALYLNEPFDSHKYGLNNMTHDDAWPFLKAKLLVVFE 531
N. crassa          SSYNPGGDWPGPSSVSSATGNLASALFHNEPFDSQKFGLNNMTLDDAWPFLRAKLLVIFE 624
S.macrospora       SSYNPGGDWPGPSSVSSASGTLASALFHNEPFDSQKFGLNNMTLDDAWPFLRAKLLVIFE 619
                   ::    .:***.*:* *.:.  ..:*: ******:*:****** *******:*****:**

M.thermophila      AEDLRLPVEDLNRVVTMHIQYCIARRSPNIIVDDLRDLLVTGFSSLDQTLRKTPEERLIP 598
C.globosum         AEDLRLPVEDLNRVVTMHIQYCLARRSPNIIVDDLRELLATGFSSLDHTLRKTPEDRLIP 598
T.terrestris       AEDLRLPVEDLNRVVTMHIQYCLARRSPNIIVDDLRELLSTGFSSLDQTLRKTPEDRLIP 591
N. crassa          AEDLRLPVEDLNRIVTMHIQYCISRRSPNIIIEDIRDFLTTGFSSLDQSLKKTPEDRLIP 684
S.macrospora       AEDLRLPVEDLNRIVTMHIQYCITRRSPNIIIEDIRDFLTTGFSSLDQSLKKTQEDRLIP 679
                   *************:********::*******::*:*::* *******::*:** *:****

M.thermophila      ALVELWIFTFTSILPYMQAVFLPLDLEFSGHGTLMSPEQARDFWGGVPVTTSSAD-ASSG 657
C.globosum         ALVELWIFTFTSILPYMQAVFLPLDLEFSGHGPLMSTEQACDFWGGIPAAASTGDGTSTV 658
T.terrestris       SLVELWIFTFTGILPYLQAVFLPLDLEFAGNGPLMSPEQARDFWGGIPATTSTSDPSSAA 651
N. crassa          ALVELWIFTFTSILPYLQAVFLPLDMEFAGNGPLMTPDQARDFWGGVPAS---------- 734
S.macrospora       ALVELWIFTFTSILPYLQAVFLPLDMEFAGNGPLMTPDQARDFWGGVPAS---------- 729
                   :**********.****:********:**:*:*.**:.:** *****:*.:

M.thermophila      SQKPGRSQSVTVAPASSVLEVRRFVLLAFRDVVILPRYETLKAMFSRLSLEFLPQSLASM 717
C.globosum         TQKPGRSHSITVSPASSVLEVRRFVLLAFRDIVILPRYDTLKAMFSRLSLEFLPQSLASM 718
T.terrestris       P------KSVSVSPASSVLEVRRFVLLAFRDIVILPRYETLKAMFSRLSLEFLPQSLASM 705
N. crassa          -------YGLSIS-ASSVLDIRRLVLLAFRDIVILPRYDTLKIMFSRLSLEFLPQSLASM 786
S.macrospora       -------FGVSIP-ASSVLDIRRLVLLSFRDIVIIPRYDTLKIMFSRLSLEFLPQNLANM 781
                          .::::. *****::**:***:***:**:***:*** ************.**.*

M.thermophila      ALASPPLPIPSPGHHNQSINQ------QLSGS-------EPHASTSLPTTLGQ------- 757
C.globosum         ALGSPPLPIPSPGYHNQSINQ------QLSNSPS-----DHYASTSLPSVLGQ------- 760
T.terrestris       ALASPPLPIPSPGYHKQSINQ------QLSGSPS-----EQHASTSLPTAFG-------- 746
N. crassa          ALSSP-VPVPTSGFQNTAHNQGGAYQPALSTSPSQESQLSLSFAGSLPATMTLGMGAGFG 845
S.macrospora       ALSSP-VPVPTSGFQNMAHNQGSVYQSALSTSPSQESQLSMSFAGSLPATMTLGMGAGFG 840
                   **.** :*:*:.*.:: : **       ** *       .   : ***:.:

M.thermophila      ---YRPGTATS-----LDPSVASYNSTGSNPFG----DSSGSGNRSRAISNVSFGSDS-- 803
C.globosum         ---YRPGTATS-----LDPSVASYNSTGSTLLG----DSSGSGNRSRAISNVSFGSDS-- 806
T.terrestris       ---YRSNPAAS-----LDPAVASYNSTGSTLLG----DSSGSGNRSRAISNVSFGSDG-- 792
N. crassa          TAPPRPNTSMSNPVPSVDPSYASYNSNGMGTAGGGGDTPPGSGNRSRTISNVSFGSDHGN 905
S.macrospora       AAPPRPNTSMSNPVGAIDPSYASYSSNGMGMGTGGGDTTPGSGNRSRTISNVSFGSDHGN 900
                       *...: *     :**: ***.*.*          ..*******:*********

M.thermophila      AAHPLRP------------------------------------------------------ 810
C.globosum         AAHPLRP------------------------------------------------------ 813
T.terrestris       PAHPLRP------------------------------------------------------ 799
N. crassa          ANRPFTPSSIQALGAASAQAAMSTPSGVGIANLNLNMSTPVQQFPLHVAPSIASIGSNSI 965
S.macrospora       GNRPFTPSSIQALGAASAQAAMSTPSGVGIANLNLNMSPPVQQFPPHVAPSITSIGSNSI 960
                     :*: *

M.thermophila      ----------------FTPSSLQHNTISAAASSTLN-LALTTTMSNTTTTSHGASSLRD- 852
C.globosum         ----------------FTPSSMN--AVTAAANSTLN-LALHTTMSNNTTASHGG------ 848
T.terrestris       ----------------RDQIVEDSKQVTDMVGRMLQCMSVLASVSVAAPVSVAATPAGQ- 842
N. crassa          HGSLRDPTGGGGGGRTADQNVEDSKQVTEMVGRMLQCMSVLASVSAPTTPS-FTSSIP--1022
S.macrospora       HGSLRDPTGG----RTADQNVEDSKQVTEMVGRMLQCMSVLASVSAPTTPSNFSSSSTSL1016
                                     :   ::  ..  *: ::: :::*  :. *

M.thermophila      ------------------------------------------------------------
C.globosum         ------------------------------------------------------------
T.terrestris       ------------------------------------------------------------
N.crassa           NQNPHSSTGNLTSYNTYSSSQDSVATTTMTNATVPASPSGSSVAGGLPPLVQTMSSPSQF1082
S.macrospora       GQNPRASTTNLSFHNTYSSSQTSVATTTMTNATVPASPSGSSAAGGLPPLVQTMSSPSQF1076
M.thermophila      ------------------------------------------------------------
```

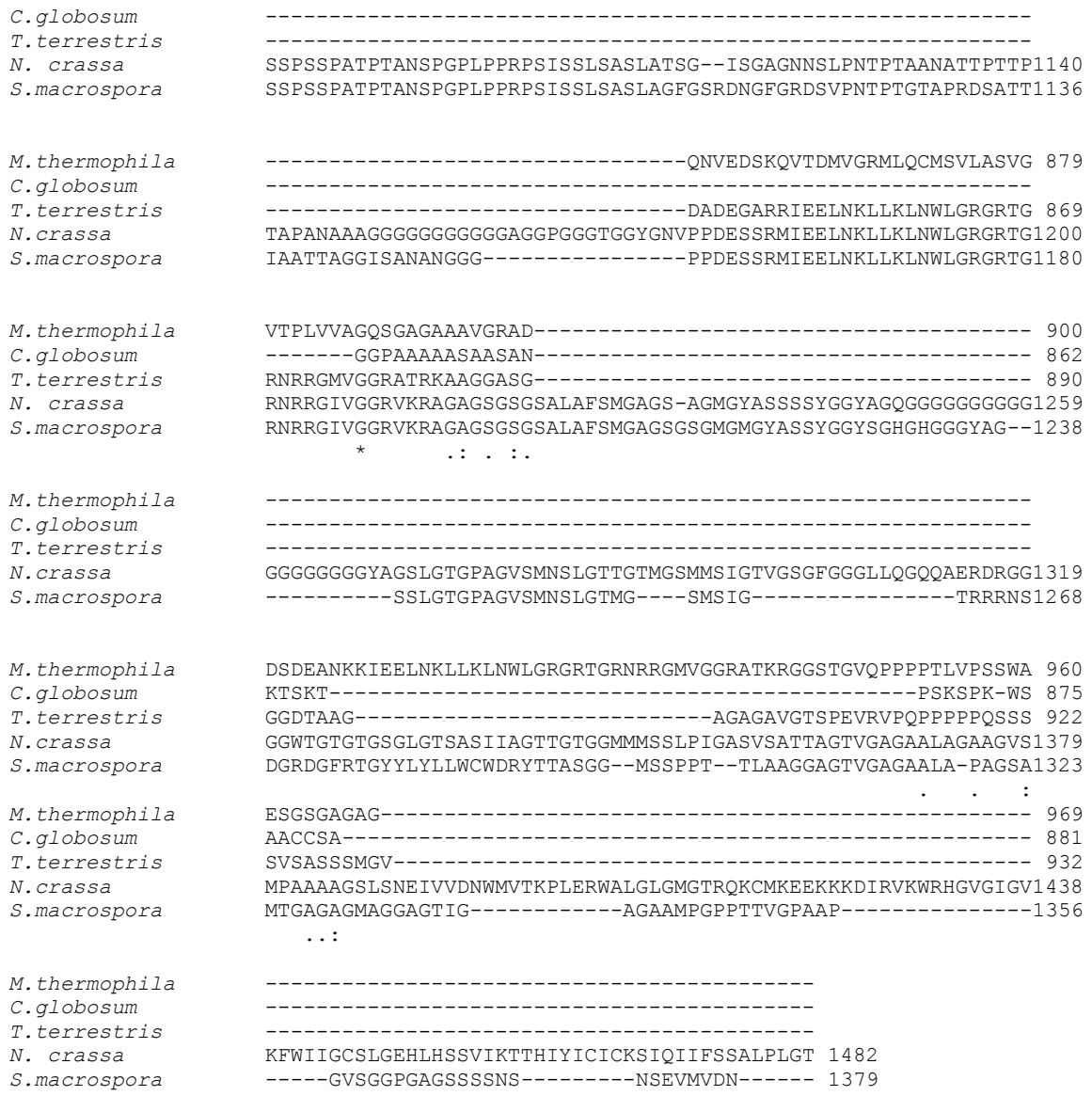

Figure 21. **Alignment of NcHbrB from various fungal species**. Hypothetical protein SMAC_02302, *Sordaria macrospora k-hell*, hypothetical protein MYCTH_2311840, *Myceliophthora thermophile*, hypothetical protein CHGG_07991, *Chaetomium globosum* CBS 148.51 and hypothetical protein THITE_2123534, *Thielavia terrestris NRRL 8126* are aligned with the *N. crassa* NcHbrB protein. The M residue in the box indicates the newly predicted translation start site for the *N. crassa* gene, whereas the M residue in the circle indicates the BROAD institute's initially predicted start site.

version of the gene predicted by the alignment. Although this could simply represent a 5'-UTR, the presence of a well conserved amino acid sequence when compared to orthologs from several species, argues for the presence of coding sequence. Thus, in the previous rescue attempts, the lack of rescue was most likely due to transformation with an incomplete gene. To correct this error, a 1.7 Kb fragment, including 995 bp of the coding region and 744 bp of upstream sequence was added to the N-terminus of the previous clone, as depicted in Fig. 23.

3.2.2.3 Inability to rescue KO mutant 88H8 (KO-NcHbrB)

Gene rescue experiments were carried out by transforming strain 88H8 (KO-NcHbrB) with the newly assembled 3' 3XHA tag containing clone (linearized with *BstX*I) carrying the predicted complete 3XHA tagged version of the NcHbrB gene. Twenty five transformants were selected following plating on Bm-containing medium. Colonies were isolated and purified by single colony isolation. These were tested for rescue of the AOX deficient phenotype by inoculating the center of AA plates with conidia from each transformant. No growth of the transformants on AA was observed, indicating no rescue of the mutant phenotype. Since selection was done for Bm, it was possible that integration of the whole plasmid had not occurred. Thus, to select for transformants resistant to AA, transformation was repeated using the 3' 3XMyc tag containing clone. Transformed conidia were directly plated onto AA containing plates. After 9 days of incubation at 30°C no colonies were observed. Rescue on AA plates for previously analyzed AOX mutants was typically seen after 5 to 7 days. These data show that

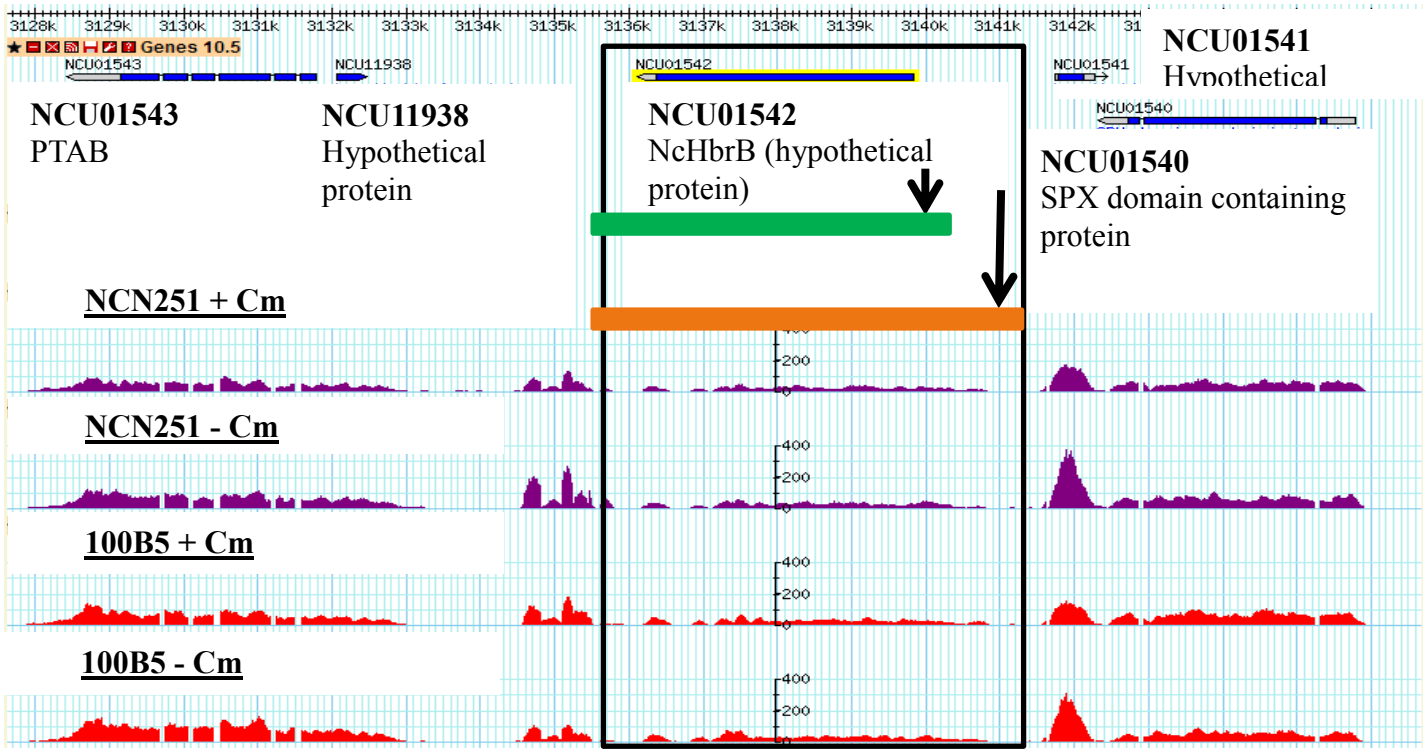

141

Figure 22. RNA-seq data for NcHbrB (DESAULNIERS 2013). The box surrounds the region of the genome corresponding to the NcHbrB gene. The short arrow indicates the location of the initially predicted translation start site. The long arrow indicates the translation start site predicted by the alignment (Fig. 21). The green open box indicates the region cloned into the original plasmids used for initial rescue experiments. The orange box indicates the region cloned in plasmids (see Fig. 23) for subsequent rescue attempts. The number of cDNA reads were mapped onto the genome of *N. crassa* (shown in purple for the wild-type strain and in red for mutant 100B5). Strains and conditions are indicated on the left.

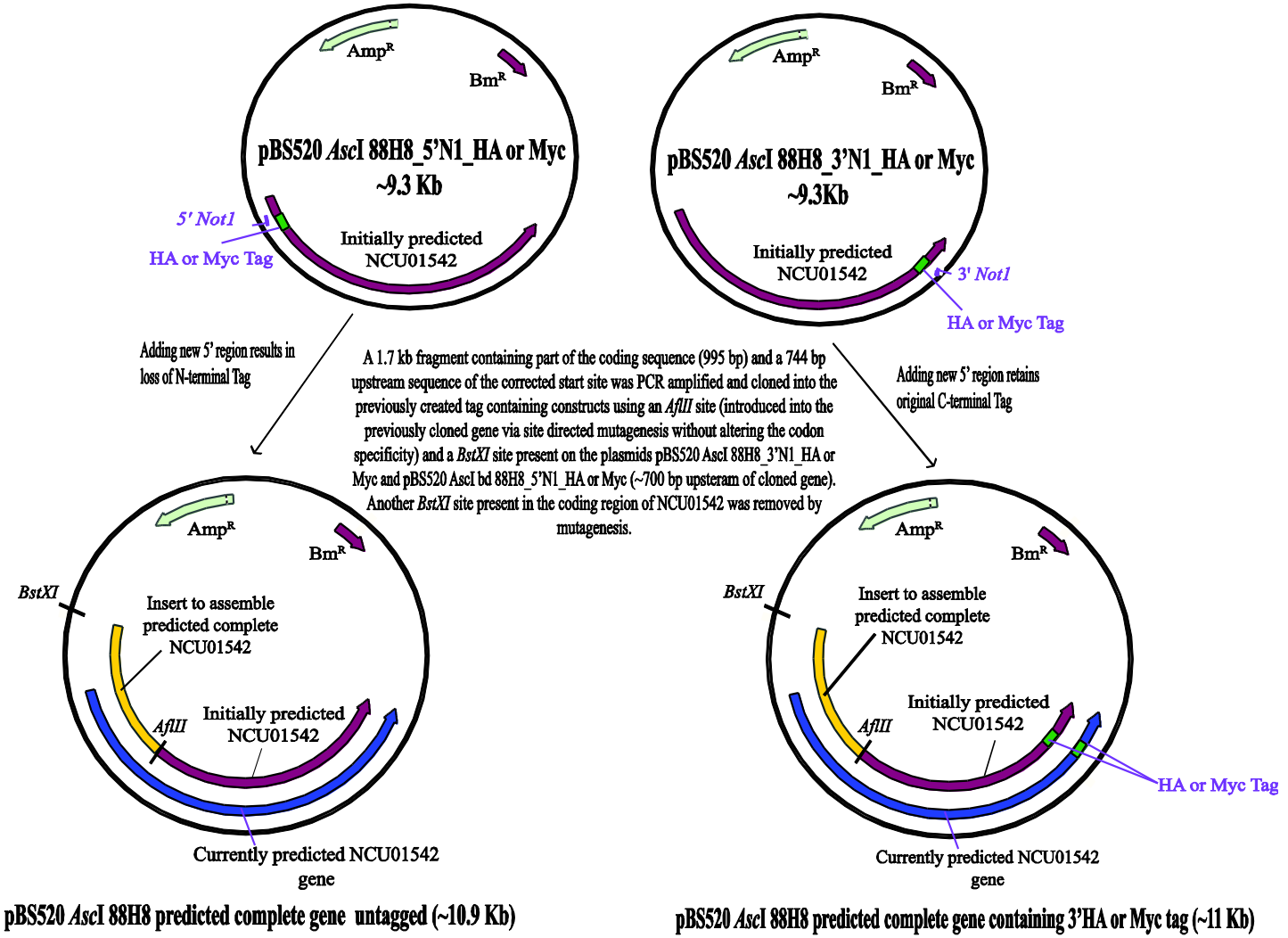
Amp^R
Bm^R
pBS520 AscI 88H8_5'N1_HA or Myc
~9.3 Kb
5' Not1
HA or Myc Tag
Initially predicted
NCU01542
pBS520 AscI 88H8_3'N1_HA or Myc
~9.3Kb
3' Not1
HA or Myc Tag
Adding new 5' region results in loss of N-terminal Tag
A 1.7 kb fragment containing part of the coding sequence (995 bp) and a 744 bp upstream sequence of the corrected start site was PCR amplified and cloned into the previously created tag containing constructs using an AflII site (introduced into the previously cloned gene via site directed mutagenesis without altering the codon specificity) and a BstXI site present on the plasmids pBS520 AscI 88H8_3'N1_HA or Myc and pBS520 AscI bd 88H8_5'N1_HA or Myc (~700 bp upsteram of cloned gene). Another BstXI site present in the coding region of NCU01542 was removed by mutagenesis.
Adding new 5' region retains original C-terminal Tag
BstXI
Insert to assemble predicted complete NCU01542
AflII
Initially predicted NCU01542
Currently predicted NCU01542 gene
pBS520 AscI 88H8 predicted complete gene untagged (~10.9 Kb)
HA or Myc Tag
pBS520 AscI 88H8 predicted complete gene containing 3'HA or Myc tag (~11 Kb)

Figure 23. Cloning strategy for assembling predicted complete NcHbrB gene. A 1.7 Kb insert containing 995 bp of the newly predicted coding sequence and 744 bp upstream of the newly predicted translation start site was PCR amplified from cosmid pMOCosX X18A9 and digested with *BstX*I and *Afl*II (*BstX*I and *Afl*II sites has been introduced into the ends of the PCR amplification product to facilitate subsequent directional cloning). The previously designed plasmid clone carrying a 3' 3XHA or 3' 3XMyc tags and the previously designed plasmid clone carrying 5' 3XHA tagged version of the NcHbrB gene (as described in Fig. 20) were also digested with *BstXI* and *AflII*. This allowed directional cloning of the insert into the preexisting plasmid clones. Thus, an untagged version of the complete gene and 3' 3XHA and 3' 3XMyc tagged versions of the complete NcHbrB gene were obtained.

transfomants believed to express epitope tagged version of NcHbrB are unable to rescue the mutant phenotype of 88H8 (KO-NcHbrB), suggesting that this protein, like NcMFS, may not play a role in AOX production.

3.2.2.5 *aod-1* transcript levels in mutant 88H8 (KO-NcHbrB)

qPCR was done to determine if the lack of the AOX protein in mutant 88H8 (KO-NcHbrB) was the result of lack of *aod-1* transcription in Cm induced conditions. As shown in Fig. 24, the *aod-1* transcript levels in mutant 88H8 (KO-NcHbrB) were comparable to that of the wild-type control in both the presence and absence of Cm. This suggests that lack of AOX in strain 88H8 (KO-NcHbrB) is most likely due to a post-transcriptional process.

3.2.3 Verifying the integrity of eight AOX deficient mutant strains

As described above, attempts to rescue two of the class 1 AOX mutants (23H2 (KO-NcMFS) and 88H8 (KO-NcHbrB)) that were identified in the large scale screen of *N. crassa* KO library were unsuccessful. This led us to suspect that the strains being used did not carry the specific KO assigned to them. Therefore, further research into the integrity of all eight uncharacterized class 1 (severely AOX deficient) mutant strains was undertaken. This included seven of the eight original class one mutants (23H2, 40E6, 41G7, 47H10, 52D8, 83H3, 88H8) (NARGANG *et al.* 2012), but not 100B5 which was previously characterized and could be rescued (DESAULNIERS 2013). It also included mutant 113G8 which was identified as a class 1 mutant among additional strains added to the KO library after the NARGANG *et al.* (2012) study. My initial goal was to verify that the assigned KO was actually present in the appropriate strain. Although this

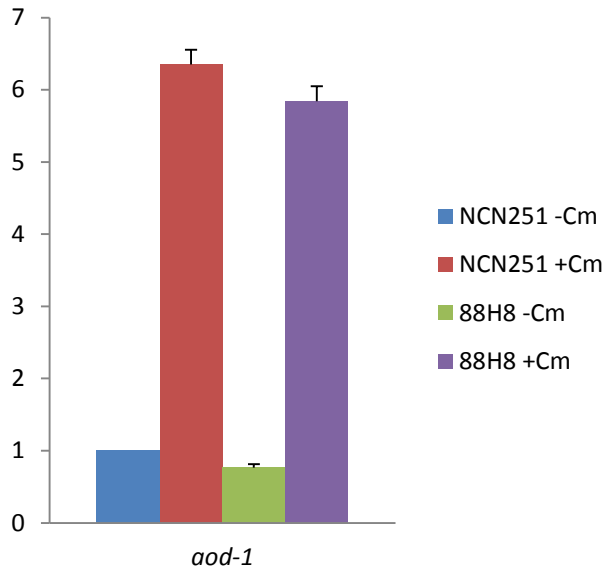

Figure 24. Transcript levels of the *aod-1* gene in mutant 88H8 (KO-NcHbrB). RNA was isolated from 88H8 (KO-NcHbrB) and the control strain (NCN251) grown either in the absence or presence of Cm. cDNA was prepared and the qPCR reactions were performed. β-tubulin was used as an endogenous control for the ΔΔCt quantification assay. Four biological and three technical replicates were used per sample. Error bars represent standard error.

had been done previously for the original class 1 mutant isolates (K. Adames and F.E. Nargang, unpublished), my results prompted the need to confirm the data for the working strains being used by me in the lab.

3.2.3.1 Verification of predicted gene KO by PCR analysis

To determine the authenticity of the eight AOX deficient mutants, PCR amplification of the genes that were proposed to be knocked out in these mutants was carried out. Primers were designed outside each gene replacement region and PCR amplification was carried out using genomic DNA from a wild-type control and each mutant. The KO mutant library was created by replacing the gene of interest with a Hyg^R cassette (COLOT *et al.* 2006). Thus, based on the size of the target gene versus the Hyg^R cassette, the size of the expected PCR product could be predicted. Fig. 25 shows the primer design strategy used for the study. When the wild-type gene was greater than 3 Kb a strategy involving two or more sets of primer pairs was employed to increase PCR efficiency. All eight mutants were found to have the expected size of PCR amplification fragments for the replacement Hyg^R cassette (Fig. 26 and 27). These data show that the proposed genes were indeed knocked out in the genome of the corresponding mutants.

3.2.3.2 Genetic analysis of the AOX deficient KO strains

Since all the mutants examined appeared to be correct in terms of the expected gene KOs, I wished to determine if unknown mutations in additional genes might be the reason for the AOX deficiency phenotype. To this end, crosses were made between each of the eight AOX deficient mutants and a wild-type strain (either NCN251*A* or 76-26*a his-3*) with the aim of analyzing the phenotypes of the haploid progeny. If loss of the gene

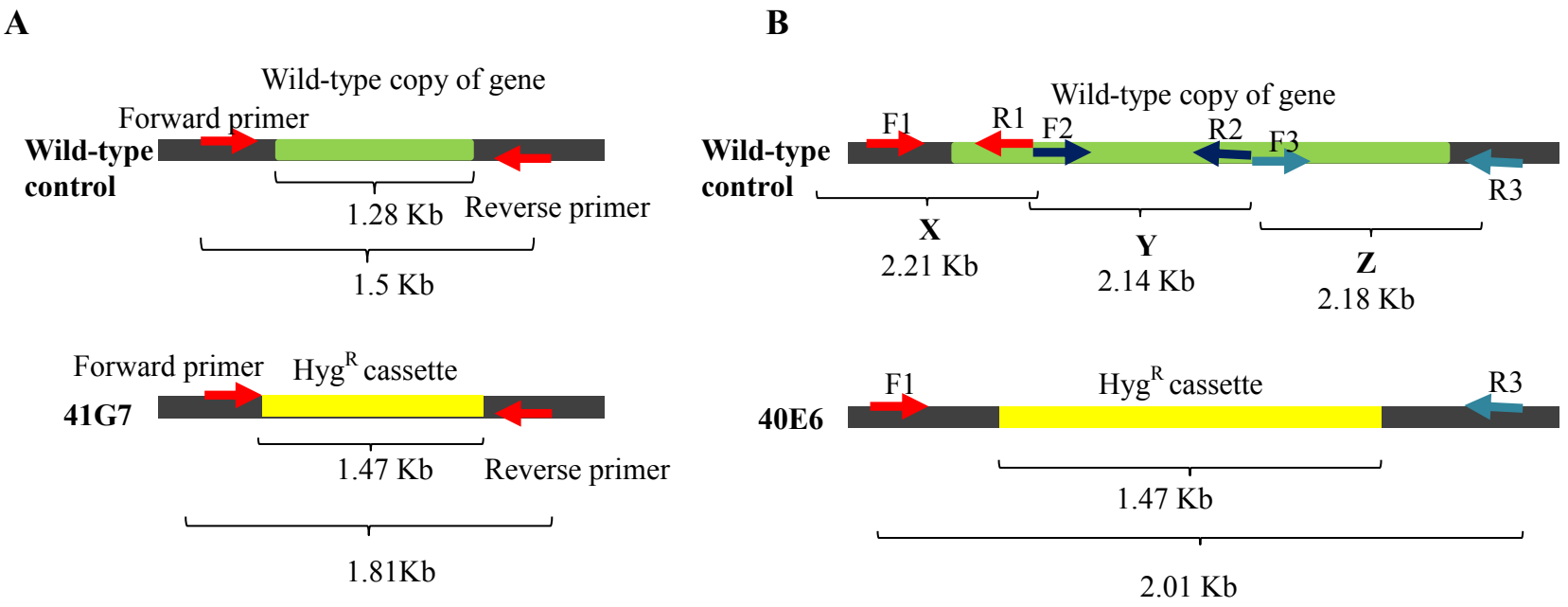

147

Figure 25. Primer design strategy for KO mutants to be verified by PCR analysis. A) Schematic diagram of primer design strategy for KO mutants in which the target gene was ≤ 3Kb. In these cases, only one primer pair (denoted as red arrows) was used for PCR amplification (strain 41G7 is used as an example, with the expected fragment sizes denoted). B) Schematic diagram of primer design strategy for KO mutants in which the target gene was >3Kb. Since these genes proved difficult to amplify using a single primer pair, multiple primer pairs (i.e. F1 and R1 (red arrows); F2 and R2 (dark blue arrows); F3 and R3 (light blue arrows)) were used to amplify target genes from the wild type strain. Primer pair (F1 and R3), outside the replacement region was used to amplify the region of interest in the KO mutant since it should contain the smaller Hyg^R cassette. X, Y and Z represent predicted PCR amplified fragments (strain 40E6 is used as an example with the sizes of expected fragments denoted). F, Forward primer, R, Reverse primer.

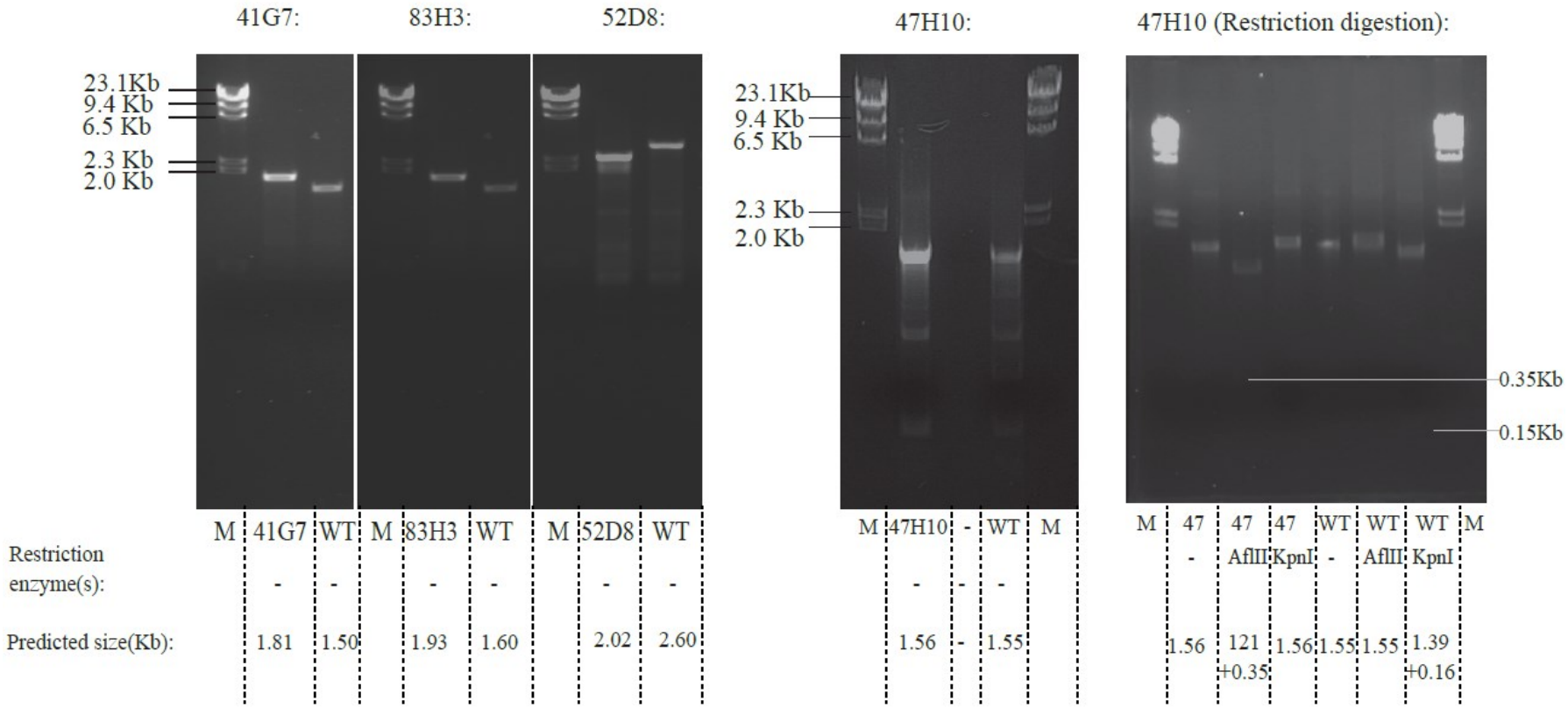

148

Figure 26. PCR amplification products for strains 41G7, 83H3, 52D8 and 47H10. PCR amplification from genomic DNA of the strains indicated at the top of the figure was done using the primer design outlined in Fig. 25A. In the case of mutant 47H10, products from both the endogenous gene and the disruption were predicted to be of similar size. Therefore, restriction enzymes that cut only one of the products were used to differentiate between them. Smaller fragments (0.35 Kb and 0.15 Kb) although not clearly visible here, were faintly visible on the gel and the change in size of the original larger fragments is indicative of successful digestion. M, marker fragments from *Hind*III digestion of λ phage (23.1 Kb, 9.4 Kb, 6.5 Kb, 2.3 Kb, 2.0 Kb); 47, 47H10; WT, wild type (NCN251) control.

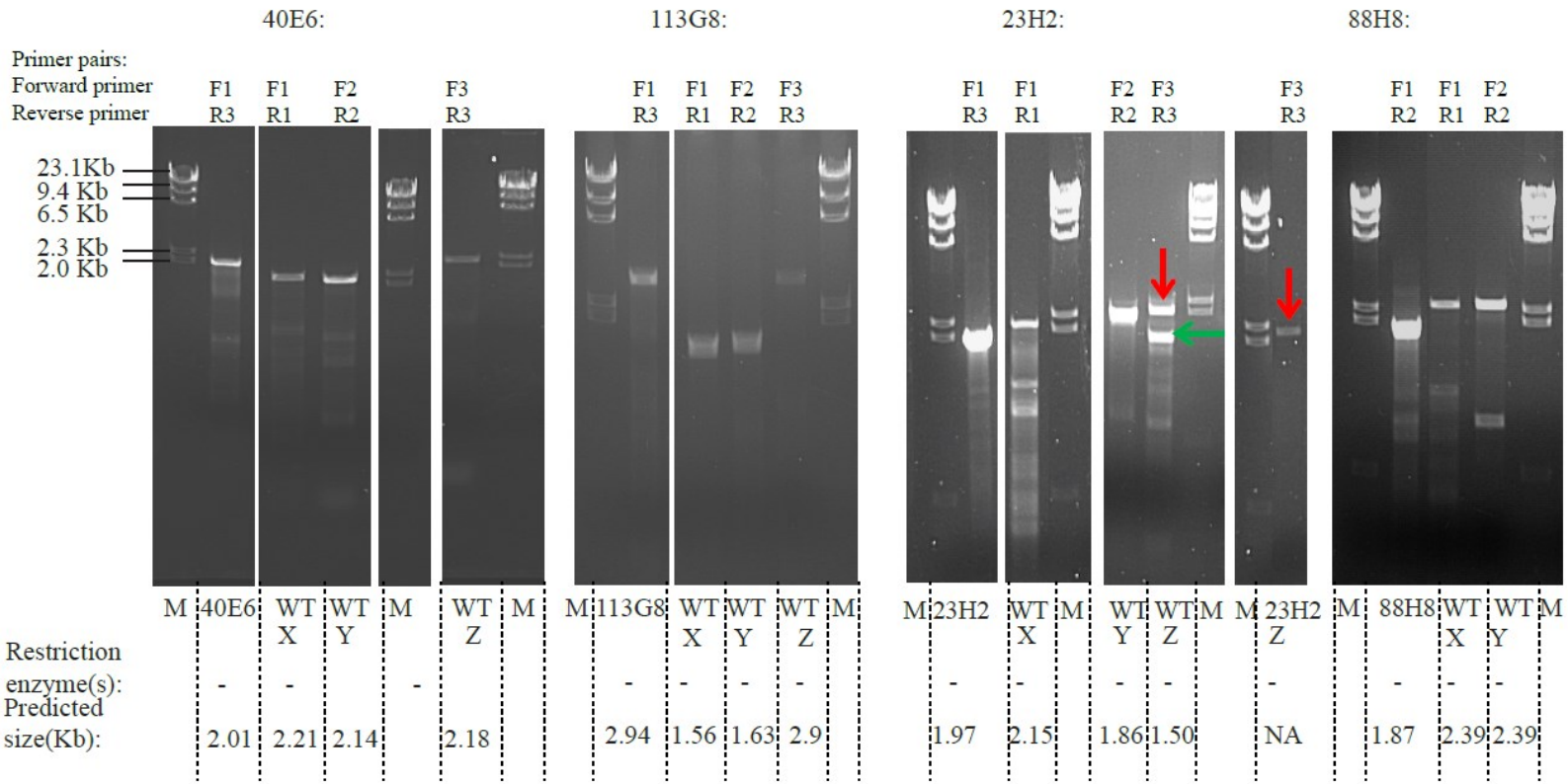

Figure 27. PCR amplification products for 40E6, 113G8, 23H2 and 88H8. Strains examined are indicated at the top of the panel. Sizes of predicted fragments are displayed below each lane. PCR confirmation for mutants 40E6, 23H2 (KO-NcMFS), 88H8 (KO-NcHbrB) and 113G8 was carried out using the primer design strategy described in Fig.25B. For 23H2, the third set of primers with wild type genomic DNA produced an additional bright band of ~2Kb (red arrow). This band was also visible (red arrow) when genomic DNA from mutant 23H2 was used as a template (negative control), suggesting that it is a non-specific band. The correct size fragment is indicated with a green arrow. M, marker fragments from *Hind*III digestion of λ phage (23.1 Kb, 9.4 Kb, 6.5 Kb, 2.3 Kb, 2.0 Kb); WT, wild type (NCN251) control.

knocked out (due to insertion of Hyg^R cassette) in each of the eight strains was causing the AOX deficiency (as determined by AA sensitivity) then the phenotypic traits of Hyg^R and AA^S (AA sensitivity), should co-segregate completely and a 50:50 ratio of the parental phenotypes of Hyg^RAA^S (mutant parent) and Hyg^SAA^R (wild-type parent) should be observed (Fig. 28). Ascospores were picked from these crosses and the progeny were tested for their resistance to hygromycin and AA.

Only one of the crosses (40E6 X wild-type strain) showed the predicted complete co-segregation of the parental phenotypes. Cross progeny of the other 7 mutants appear to have additional recombinant phenotypes (Table 7). These data suggest that the other seven strains carry a random mutation(s) or randomly inserted extra Hyg^R cassette(s) (or portion(s) thereof) in their genomes that result in the AOX deficiency. The latter may have arisen in these strains during construction of the KO mutant library.

3.2.3.3 Southern blot analysis of the eight KO mutant strains analyzed

To address the possibility that additional Hyg^R cassettes were incorporated into the genome of the mutants during the integration of the cassette for the KO procedure (COLOT *et al.* 2006), Southern blot analysis was carried out with a DIG labelled DNA probe against the Hyg^R gene cassette (Fig. 29). Using the known gene sequence and selected restriction enzymes, predicted fragment sizes for the Hyg^R cassette in each mutant were determined (Table 8). As seen in the Southern blots (Fig. 30 and Fig. 31), all eight AOX deficient mutants appear to have one band corresponding to the predicted size fragment. Though other bands are present, they are non-specific as they are also present in the negative control groups. Thus, it appears that no obvious additional insertion of Hyg^R cassettes or portions of the cassette occurred during generation of the KO's.

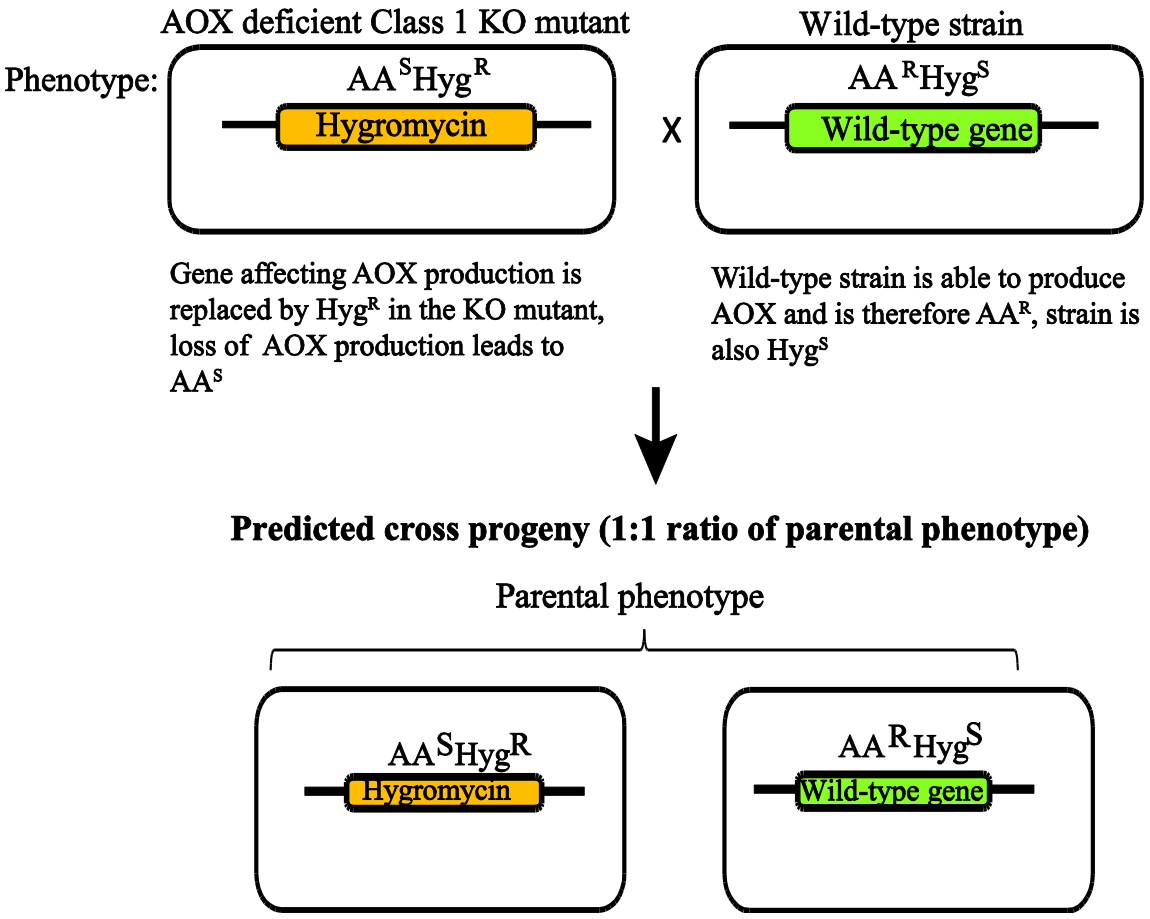

Figure 28. Predicted cosegregation of hygromycin resistance (Hyg^R) and AA sensitivity (AA^S). The class 1 KO mutants are predicted to have a gene affecting AOX production replaced by a hygromycin resistance cassette (leading to the Hyg^R and AA^S phenotype). Mutant strains were crossed with a wild-type strain (NCN251*A* or 76-26*a his-3)*, that carries no Hyg^R cassette and produces normal levels of AOX, and therefore is Hyg^S and AA^R. Cross progeny are expected to have a 1:1 ratio of parental phenotype (i.e. AA^S Hyg^R or AA^R Hyg^S).

Table 7. Cross progeny analysis.

Strain	Phenotypes of ascospores and number of ascospores with each phenotype (% of those examined)				Total ascospores examined
	Expected parental phenotype		Unexpected recombinant phenotype		
	$Hyg^{R}AA^{S}$* (% of analyzed progeny)	**$Hyg^{S}AA^{R}$** (% of analyzed progeny)	**$Hyg^{R}AA^{R}$** (% of analyzed progeny)	**$Hyg^{S}AA^{S}$** (% of analyzed progeny)	
23H2	12 (19%)	15 (23%)	14 (22%)	23 (36%)	64
40 E6	21 (36%)	38 (64%)	0 (0%)	0 (0%)	59
41G7	9 (9%)	44 (44%)	46 (45%)	2 (2%)	101
47H10	6 (9%)	52 (58%)	30 (33%)	0 (0%)	90
52D8	8 (12%)	53 (81%)	3 (5%)	1 (2%)	65
83H3	5 (6%)	55 (60%)	31 (34%)	0 (0%)	91
88H8	12 (24%)	12 (24%)	12 (24%)	14 (28%)	50
113G8	17 (21%)	54 (65%)	11 (13%)	1 (1%)	83

*R, resistant; S, sensitive

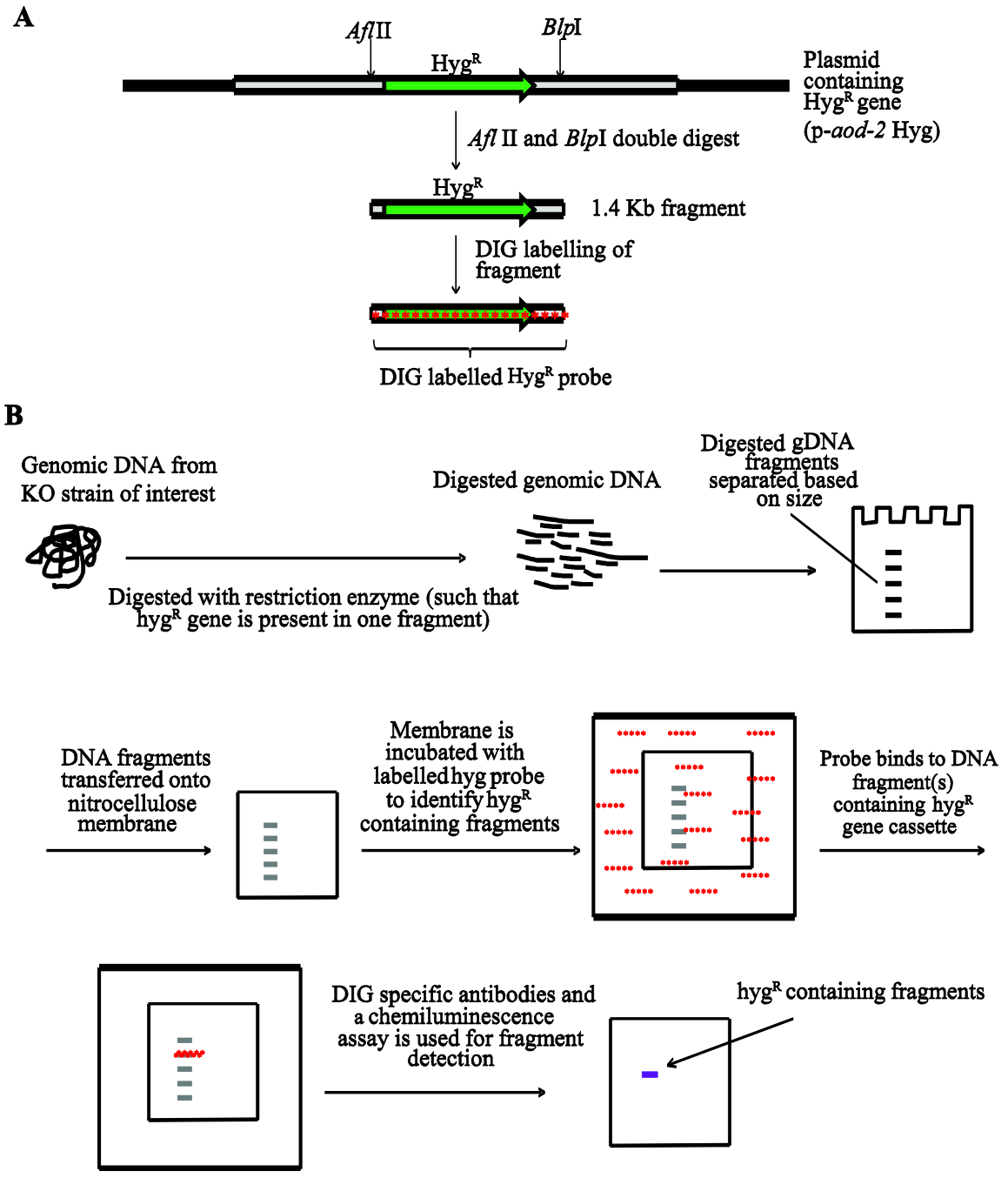

Figure 29. Schematic representation of Southern blot strategy. A) Creation of the Hyg^R cassette probe. The probe used for Southern blot analysis was prepared by isolation of a Hyg^R containing restriction fragment from a plasmid (p-*aod-2* Hyg) followed by DIG labelling of this fragment. B) Genomic DNA from each mutant and a wild-type control (NCN251) was digested with an appropriate restriction enzyme selected for each

gene to produce a known size restriction fragment based on the genome sequence. Digested genomic DNA was electrophoresed on agarose gels, and transferred to nitrocellulose membrane. The membrane was incubated with the labelled Hyg^R cassette probe followed by washing and detection of bound probe using DIG specific antibody and a chemiluminescence based assay.

Table 8. Restriction enzymes used for Southern blots.

Strains	Restriction enzyme used for digesting gDNA	Predicted hygromycin containing fragment size (Kb)
23H2	*Bcl*I	3.9
40 E6	*Stu*I	5.7
41G7	*Kpn*I	5.7
47H10	*BspH*I	5.5
52D8	*Xmn*I	4.7
83H3	*Pvu*II	5.3
88H8	*Nru*I	6.9
113G8	*BstX*I	5.0
96H9*	*Apa*I	5.7

* Control KO strain of NCU07953, the *aod-1* gene.

A

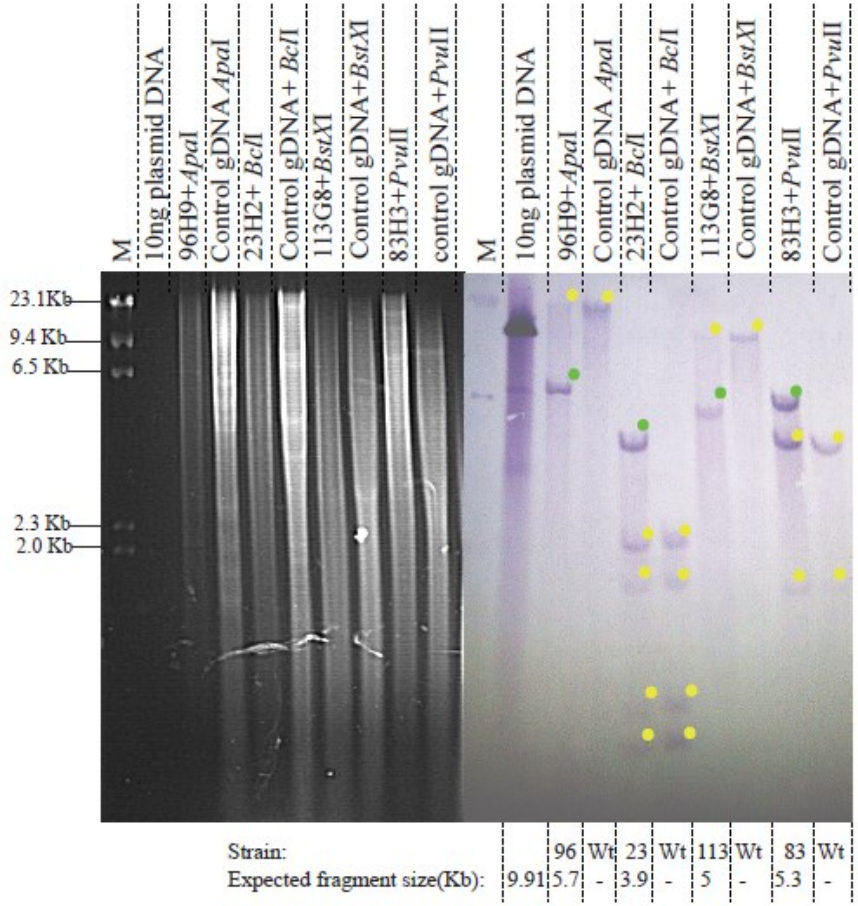
M
10ng plasmid DNA
96H9+ApaI
Control gDNA ApaI
23H2+ BclI
Control gDNA+ BclI
113G8+BstXI
Control gDNA+BstXI
83H3+PvuII
control gDNA+PvuII
23.1Kb
9.4 Kb
6.5 Kb
2.3 Kb
2.0 Kb
Strain:
Expected fragment size(Kb):
9.91
96
5.7
Wt
-
23
3.9
113
5
83
5.3

B

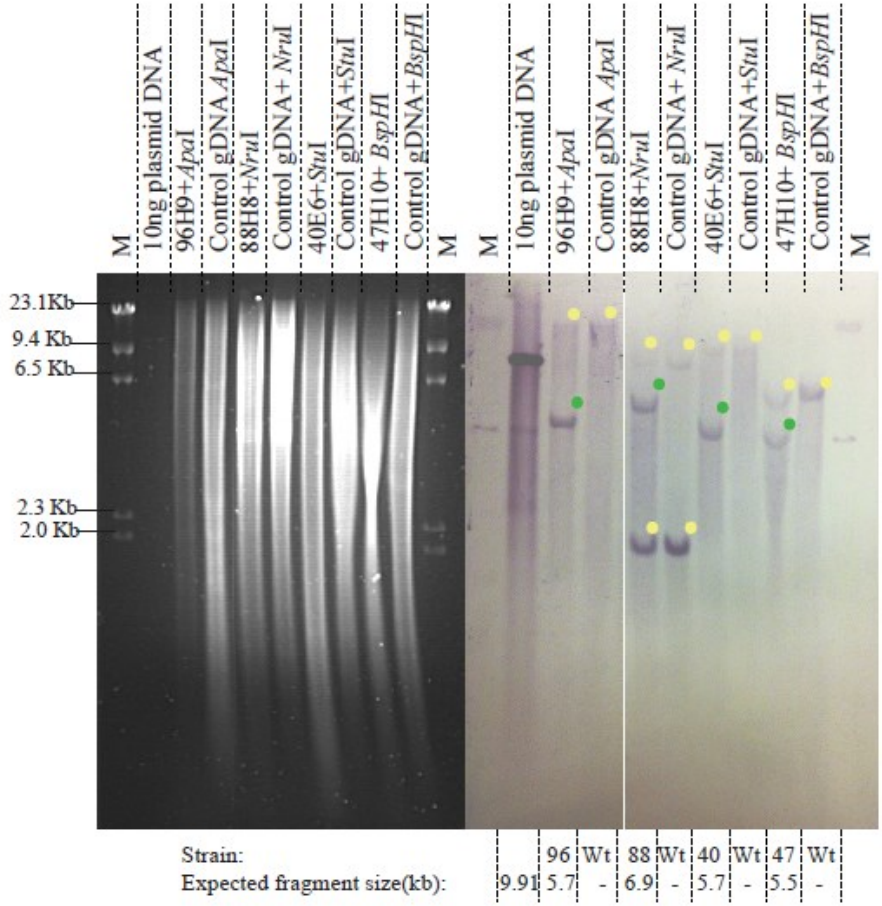
M
10ng plasmid DNA
96H9+ApaI
Control gDNA ApaI
88H8+NruI
Control gDNA+ NruI
40E6+StuI
Control gDNA+StuI
47H10+ BspHI
Control gDNA+BspHI
23.1Kb
9.4 Kb
6.5 Kb
2.3 Kb
2.0 Kb
Strain:
Expected fragment size(kb):
9.91
96
5.7
Wt
-
88
6.9
40
5.7
47
5.5

156

Figure 30. Southern blot analysis for six class 1 KO strains. Southern blots were analyzed for the presence of bands hybridizing to a Hyg^R cassette probe. In panels A and B, photos of agarose gels with digested genomic DNA are on the left with the corresponding Southern blots on the right for KO strains 23H2, 40E6, 47H10, 83H3, 88H8 and 113G8. Green dots indicate predicted fragments. The size of predicted Hyg^R containing fragments is shown below the figure. The *aod-1* KO mutant 96H9 serves as a positive control whereas wild-type control (NCN251) genomic DNA serves as a negative control. Yellow dots indicate bands present at the same position in both the negative control and mutant lanes. M, marker fragments from *Hind*III digestion of λ phage (23.1 Kb, 9.4 Kb, 6.5 Kb, 2.3 Kb, 2.0 Kb); 23, 23H2; 40, 40E6; 47, 47H10; 83, 83H3; 88, 88H8, 96, 96H9, 113, 113G8; WT, wild-type (NCN251) control; gDNA, genomic DNA.

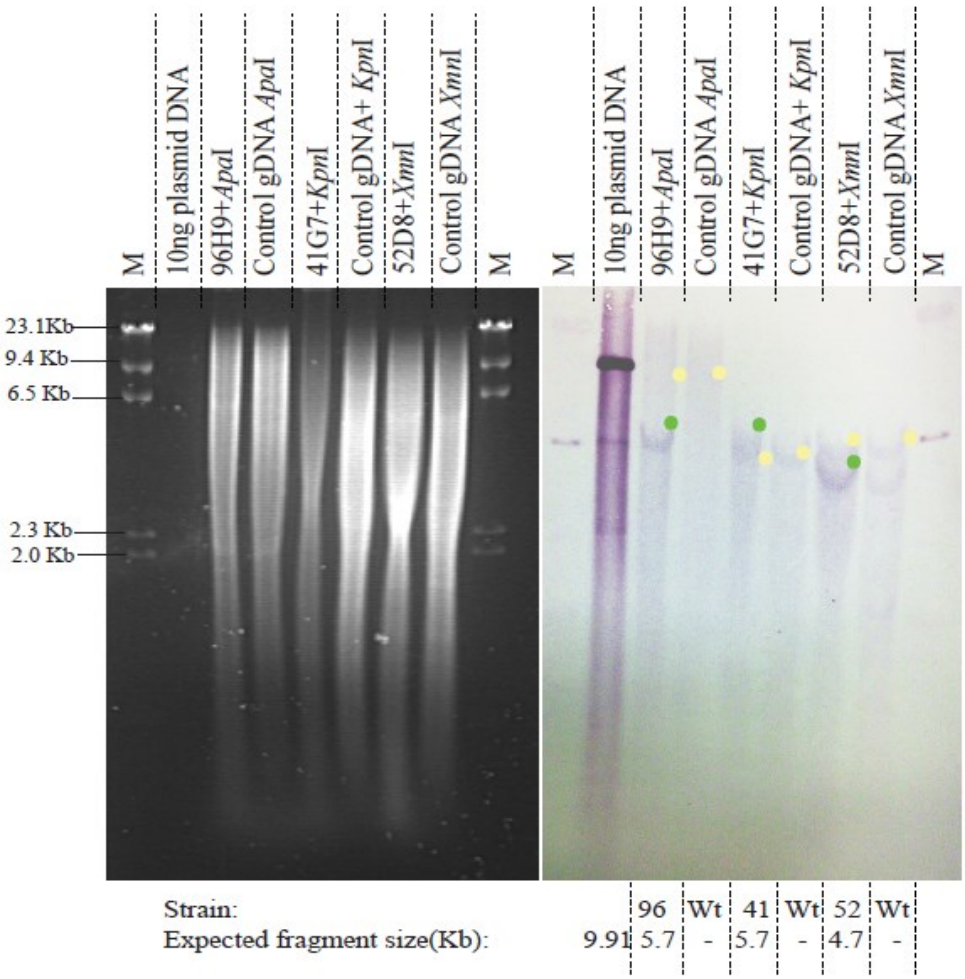

Figure 31. Southern blot analysis for two class 1 KO strains. Southern blots were analyzed as described in Fig. 30. Photos of agarose gels with digested genomic DNA are on the left with the corresponding Southern blots on the right for KO strains 41G7 and 52D8. Green dots indicate predicted fragments. The size of predicted Hyg^R containing fragments is shown below the figure. The *aod-1* KO mutant 96H9 serves as a positive control whereas wild-type control (NCN251) genomic DNA serves as a negative control. Yellow dots indicate bands present at the same position in both the negative control and mutant lanes. M, marker fragments from *Hind*III digestion of λ phage (23.1 Kb, 9.4 Kb,

6.5 Kb, 2.3 Kb, 2.0 Kb); 41, 41G7; 52, 52D8; 96, 96H9; WT, wild-type (NCN251) control; gDNA, genomic DNA.

3.2.3.4 Mutant *aod-1* gene in strains 23H2 (KO-NcMFS) and 88H8 (KO-NcHbrB)

The findings described above showed that the correct gene was knocked out in each strain and that no detectable integration of the Hyg^R cassette had occurred elsewhere in the genome of the mutants. Thus, the most obvious possibility remaining to explain lack of AOX production in these strains (except 40E6, which stands as a correct mutant, based on the genetic results) was the existence of random mutation(s) in other gene(s) that affect AOX production. At this point the best described genes known to be necessary for AOX production in *N. crassa* are the AOX regulatory genes (*aod-2* and *aod-5*) and the AOX structural gene (*aod-1*) (LI *et al.* 1996; CHAE *et al.* 2007b; CHAE and NARGANG 2009). To examine the possibility that these genes might be affected in the mutants, the *aod-1, aod-2* and *aod-5* genes from mutants 23H2 (KO-NcMFS) and 88H8 (KO-NcHbrB) were sequenced. In addition, the *aod-1* gene from mutants 40E6, 41G7, 47H10, 52D8, 83H3 and 113G8 was sequenced. A representation of each gene, the position of primers used to generate PCR products and the sequencing primers is shown in Fig. 32.

Sequencing data for strains 40E6, 41G7, 47H10, 52D8, 83H3 and 113G8 showed that these strains carry a wild-type copy of the *aod-1* gene. Sequencing data for mutants 23H3 (KO-NcMFS) and 88H8 (KO-NcHbrB) showed wild-type versions of *aod-2* and *aod-5* genes in the mutants. However, the data demonstrate the presence of a cytosine (C) insertion in the coding region of the *aod-1* gene at an identical position in both 23H2 (KO-NcMFS) and 88H8 (KO-NcHbrB) (Fig. 33). This insertion leads to the production of a frame-shift in the reading frame at codon 237 of the 363 codon *aod-1* gene, which would result in a truncated protein due to the occurrence of a stop codon after 31 codons following the frame-shift (Fig. 34). Since the AOX antibody used for western blot

analysis is specific to 122 amino acids at the C terminal end of the coding sequence, the truncated protein would not be detected by the antibody used (Fig. 34).

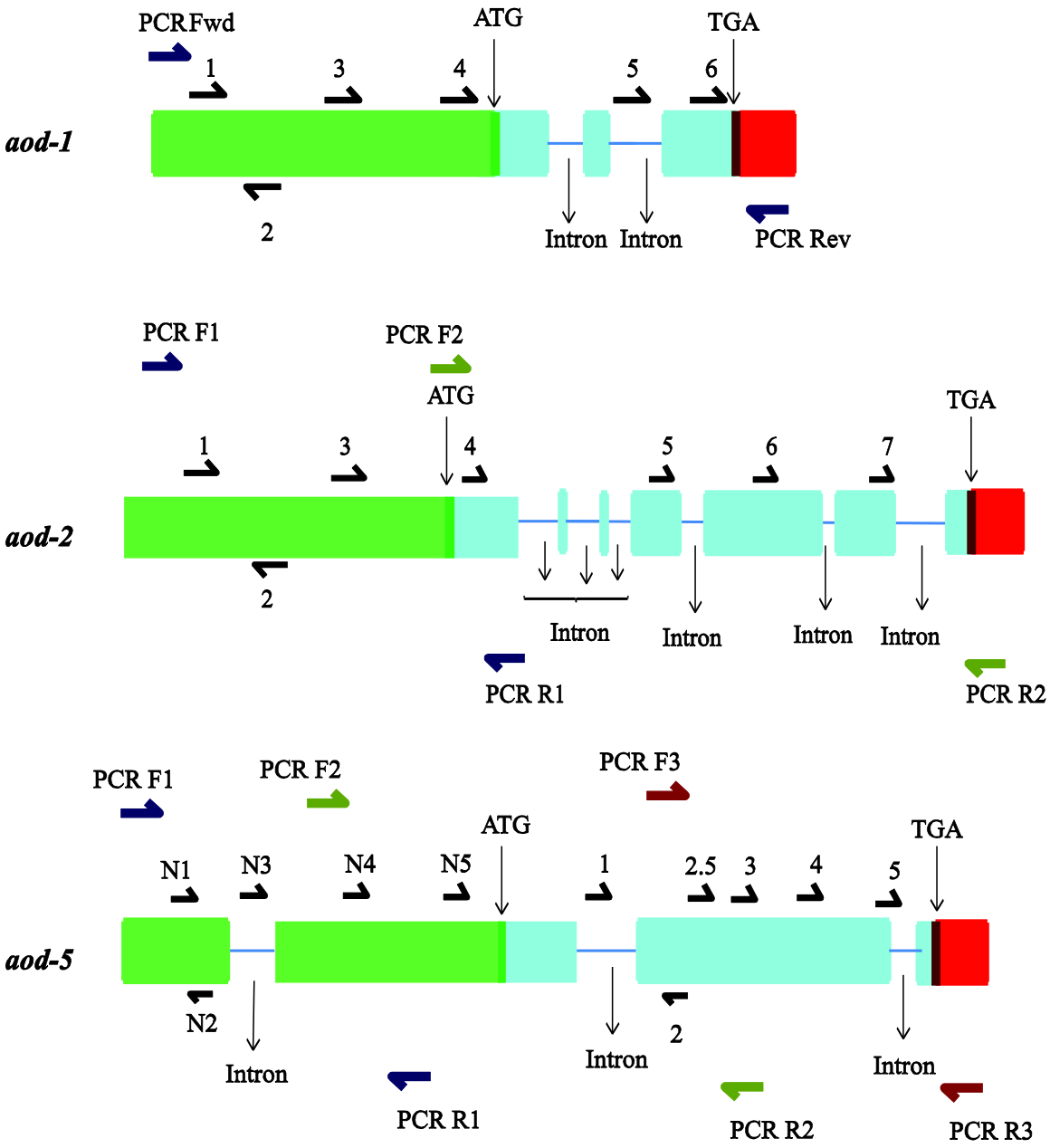

Figure 32. Sequencing strategy for the *aod-1*, *aod-2* and *aod-5* genes. The gene sequences of *aod-1, aod-2* and *aod-5* are depicted with introns as lines and exons as solid blocks. The positions of the forward (Fwd) and reverse (Rev) PCR amplification primers (used for amplifying regions to be sequenced) are indicated. The sequencing primers are

indicated by half arrows and numbers along the sequence. Green regions represent 5'UTRs whereas red regions represent 3'UTRs. Teal regions represent the coding region of each gene. The start and stop codons are indicated as ATG and TGA respectively.

```
                10        20        30        40        50        60
Wild-type  ATGAACACCCCCAAAGTAAACATACTCCACGCTCCAGGACAAGCGGCCCAACTAAGCCGT
            M  N  T  P  K  V  N  I  L  H  A  P  G  Q  A  A  Q  L  S  R
Mutant     ATGAACACCCCCAAAGTAAACATACTCCACGCTCCAGGACAAGCGGCCCAACTAAGCCGT
            M  N  T  P  K  V  N  I  L  H  A  P  G  Q  A  A  Q  L  S  R

                70        80        90       100       110       120
Wildtyp    GCCCTGATATCAACCTGCCATACTCGGCCTCTCCTGCTCGCGGGCTCTCGAGTGGCCACT
            A  L  I  S  T  C  H  T  R  P  L  L  L  A  G  S  R  V  A  T
Mutant     GCCCTGATATCAACCTGCCATACTCGGCCTCTCCTGCTCGCGGGCTCTCGAGTGGCCACT
            A  L  I  S  T  C  H  T  R  P  L  L  L  A  G  S  R  V  A  T

               130       140       150       160       170       180
Wild-type  TCCTTACATCCAACACAGACGAACCTCTCTTCCCCATCACCTCGCAATCTCTCGACAACA
            S  L  H  P  T  Q  T  N  L  S  S  P  S  P  R  N  L  S  T  T
Mutant     TCCTTACATCCAACACAGACGAACCTCTCTTCCCCATCACCTCGCAATCTCTCGACAACA
            S  L  H  P  T  Q  T  N  L  S  S  P  S  P  R  N  L  S  T  T

               190       200       210       220       230       240
Wild-type  AGCGTTACTCGACTGAAGGATTTCTTCCCGGCCAAAGAGACCGCCTATATCCGGCAGACA
            S  V  T  R  L  K  D  F  F  P  A  K  E  T  A  Y  I  R  Q  T
Mutant     AGCGTTACTCGACTGAAGGATTTCTTCCCGGCCAAAGAGACCGCCTATATCCGGCAGACA
            S  V  T  R  L  K  D  F  F  P  A  K  E  T  A  Y  I  R  Q  T

               250       260       270       280       290       300
Wild-type  CCACCCGCGTGGCCTCATCATGGATGGACAGAGGAAGAGATGACCTCGGTTGTTCCCGAG
            P  P  A  W  P  H  H  G  W  T  E  E  E  M  T  S  V  V  P  E
Mutant     CCACCCGCGTGGCCTCATCATGGATGGACAGAGGAAGAGATGACCTCGGTTGTTCCCGAG
            P  P  A  W  P  H  H  G  W  T  E  E  E  M  T  S  V  V  P  E

               310       320       330       340       350       360
Wild-type  CACCGGAAACCCGAGACTGTGGGCGATTGGCTCGCATGGAAACTCGTACGAATCTGTCGA
            H  R  K  P  E  T  V  G  D  W  L  A  W  K  L  V  R  I  C  R
Mutant     CACCGGAAACCCGAGACTGTGGGCGATTGGCTCGCATGGAAACTCGTACGAATCTGTCGA
            H  R  K  P  E  T  V  G  D  W  L  A  W  K  L  V  R  I  C  R

               370       380       390       400       410       420
Wild-type  TGGGCCACTGATATAGCGACGGGCATACGTCCAGAGCAGCAAGTTGATAAACACCACCCG
            W  A  T  D  I  A  T  G  I  R  P  E  Q  Q  V  D  K  H  H  P
Mutant     TGGGCCACTGATATAGCGACGGGCATACGTCCAGAGCAGCAAGTTGATAAACACCACCCG
            W  A  T  D  I  A  T  G  I  R  P  E  Q  Q  V  D  K  H  H  P

               430       440       450       460       470       480
Wild-type  ACGACCGCCACCAGCGCGGACAAACCTCTGACCGAAGCCCAATGGCTCGTCCGCTTCATC
            T  T  A  T  S  A  D  K  P  L  T  E  A  Q  W  L  V  R  F  I
Mutant     ACGACCGCCACCAGCGCGGACAAACCTCTGACCGAAGCCCAATGGCTCGTCCGCTTCATC
            T  T  A  T  S  A  D  K  P  L  T  E  A  Q  W  L  V  R  F  I

               490       500       510       520       530       540
Wild-type  TTCCTCGAATCCATCGCCGGCGTTCCCGGCATGGTAGCCGGCATGCTCCGCCACCTGCAC
            F  L  E  S  I  A  G  V  P  G  M  V  A  G  M  L  R  H  L  H
Mutant     TTCCTCGAATCCATCGCCGGCGTTCCCGGCATGGTAGCCGGCATGCTCCGCCACCTGCAC
            F  L  E  S  I  A  G  V  P  G  M  V  A  G  M  L  R  H  L  H

               550       560       570       580       590       600
Wild-type  TCCCTCCGCCGGCTCAAACGAGACAACGGCTGGATCGAGACTTTACTTGAAGAATCGTAC
```

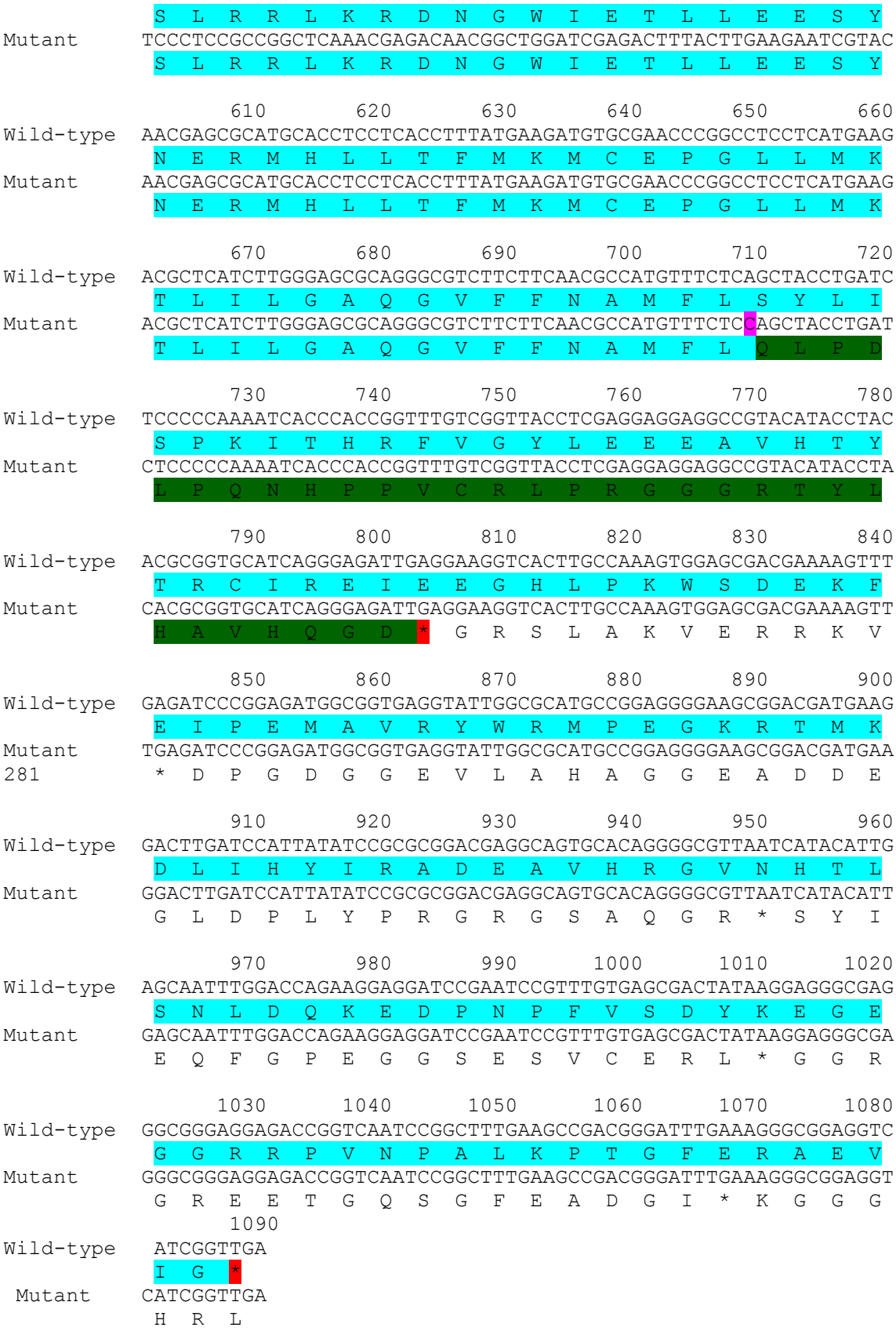
S L R R L K R D N G W I E T L L E E S Y
Mutant
TCCCTCCGCCGGCTCAAACGAGACAACGGCTGGATCGAGACTTTACTTGAAGAATCGTAC
S L R R L K R D N G W I E T L L E E S Y
610 620 630 640 650 660
Wild-type
AACGAGCGCATGCACCTCCTCACCTTTATGAAGATGTGCGAACCCGGCCTCCTCATGAAG
N E R M H L L T F M K M C E P G L L M K
Mutant
AACGAGCGCATGCACCTCCTCACCTTTATGAAGATGTGCGAACCCGGCCTCCTCATGAAG
N E R M H L L T F M K M C E P G L L M K
670 680 690 700 710 720
Wild-type
ACGCTCATCTTGGGAGCGCAGGGCGTCTTCTTCAACGCCATGTTTCTCAGCTACCTGATC
T L I L G A Q G V F F N A M F L S Y L I
Mutant
ACGCTCATCTTGGGAGCGCAGGGCGTCTTCTTCAACGCCATGTTTCTCCAGCTACCTGAT
T L I L G A Q G V F F N A M F L Q L P D
730 740 750 760 770 780
Wild-type
TCCCCCAAAATCACCCACCGGTTTGTCGGTTACCTCGAGGAGGAGGCCGTACATACCTAC
S P K I T H R F V G Y L E E E A V H T Y
Mutant
CTCCCCCAAAATCACCCACCGGTTTGTCGGTTACCTCGAGGAGGAGGCCGTACATACCTA
L P Q N H P P V C R L P R G G G R T Y L
790 800 810 820 830 840
Wild-type
ACGCGGTGCATCAGGGAGATTGAGGAAGGTCACTTGCCAAAGTGGAGCGACGAAAAGTTT
T R C I R E I E E G H L P K W S D E K F
Mutant
CACGCGGTGCATCAGGGAGATTGAGGAAGGTCACTTGCCAAAGTGGAGCGACGAAAAGTT
H A V H Q G D * G R S L A K V E R R K V
850 860 870 880 890 900
Wild-type
GAGATCCCGGAGATGGCGGTGAGGTATTGGCGCATGCCGGAGGGGAAGCGGACGATGAAG
E I P E M A V R Y W R M P E G K R T M K
Mutant
TGAGATCCCGGAGATGGCGGTGAGGTATTGGCGCATGCCGGAGGGGAAGCGGACGATGAA
281
* D P G D G G E V L A H A G G E A D D E
910 920 930 940 950 960
Wild-type
GACTTGATCCATTATATCCGCGCGGACGAGGCAGTGCACAGGGGCGTTAATCATACATTG
D L I H Y I R A D E A V H R G V N H T L
Mutant
GGACTTGATCCATTATATCCGCGCGGACGAGGCAGTGCACAGGGGCGTTAATCATACATT
G L D P L Y P R G R G S A Q G R * S Y I
970 980 990 1000 1010 1020
Wild-type
AGCAATTTGGACCAGAAGGAGGATCCGAATCCGTTTGTGAGCGACTATAAGGAGGGCGAG
S N L D Q K E D P N P F V S D Y K E G E
Mutant
GAGCAATTTGGACCAGAAGGAGGATCCGAATCCGTTTGTGAGCGACTATAAGGAGGGCGA
E Q F G P E G G S E S V C E R L * G G R
1030 1040 1050 1060 1070 1080
Wild-type
GGCGGGAGGAGACCGGTCAATCCGGCTTTGAAGCCGACGGGATTTGAAAGGGCGGAGGTC
G G R R P V N P A L K P T G F E R A E V
Mutant
GGGCGGGAGGAGACCGGTCAATCCGGCTTTGAAGCCGACGGGATTTGAAAGGGCGGAGGT
G R E E T G Q S G F E A D G I * K G G G
1090
Wild-type
ATCGGTTGA
I G *
Mutant
CATCGGTTGA
H R L

Figure 33. Nucleotide and protein sequence of the *N. crassa aod-1* gene coding region in wild-type and mutants 23H2 (KO-NcMFS) and 88H8 (KO-NcHbrB). The protein coding region of AOX from mutants and a wild-type strain is shown, with the start and stop codon marked in green and red, respectively. The respective amino acid sequences are highlighted. The wild-type *aod-1* gene encodes a 34.7 kDa protein (363 amino acids, shown in teal). The insertion of C (marked in magenta) in mutants 23H2 (KO-NcMFS) and 88H8 (KO-NcHbrB) would result in a 23.3 kDa (268 amino acids) truncated protein. In the mutants, AOX amino acids are shown in teal up to the C insertion. Following the frame-shift the amino acids are shown in dark green up to the red premature stop codon.

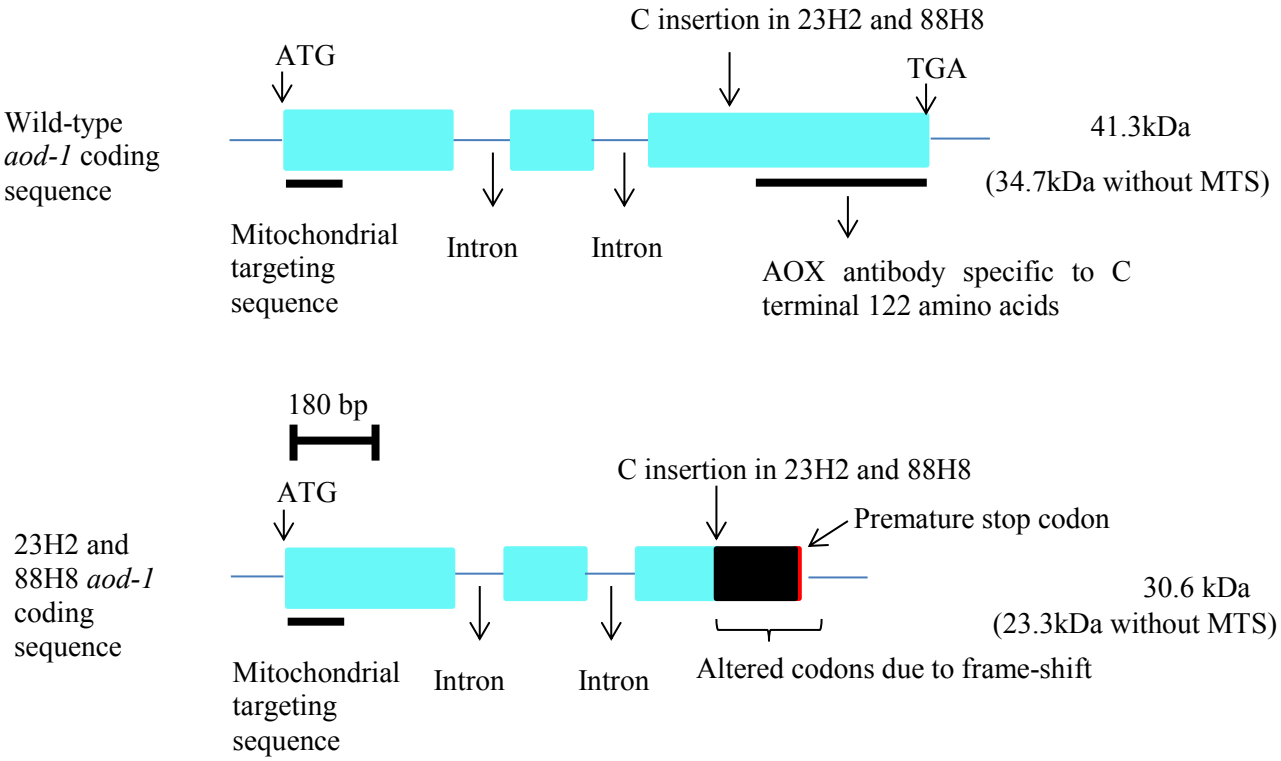

Figure 34. Position of insertion in the *aod-1* gene in mutants 23H2 (KO-NcMFS) and 88H8 (KO-NcHbrB). The *aod-1* gene from wild-type (top) and mutants 23H2 and 88H8 (bottom) are represented along with features of the gene and coding sequence. The cytosine insertion in the *aod-1* gene of mutants 23H2 and 88H8 occurs 870 nucleotides (870 bp including intronic sequence and 708 bp excluding introns) after the translation start site. The region of the protein used for antibody production is shown under the wild-type sequence. Teal boxes, exons; thin black lines, introns; black box, frame-shift altered codons; red, premature stop codon.

References

CASTAÑEDA-GARCÍA, A., A. RODRÍGUEZ-ROJAS, J. R. GUELFO and J. BLÁZQUEZ, 2009 The Glycerol-3-Phosphate Permease GlpT Is the Only Fosfomycin Transporter in Pseudomonas aeruginosa. J. Bacteriol. **191:** 6968-6974.

CHAE, M. S., C. E. NARGANG, I. A. CLEARY, C. C. LIN, A. T. TODD *et al.*, 2007 Two zinc-cluster transcription factors control induction of alternative oxidase in Neurospora crassa. Genetics **177:** 1997-2006.

CHAE, M. S., and F. E. NARGANG, 2009 Investigation of regulatory factors required for alternative oxidase production in Neurospora crassa. Physiol. Plant. **137:** 407-418.

CLAYPOOL, S. M., J. M. MCCAFFERY and C. M. KOEHLER, 2006 Mitochondrial mislocalization and altered assembly of a cluster of Barth syndrome mutant tafazzins. J. Cell Biol. **174:** 379-390.

COLOT, H. V., G. PARK, G. E. TURNER, C. RINGELBERG, C. M. CREW *et al.*, 2006 A high-throughput gene knockout procedure for Neurospora reveals functions for multiple transcription factors. Proc. Natl. Acad. Sci. USA **103:** 10352-10357.

DESAULNIERS, A. B., 2013 The role of YVH1, a dual specificity phosphatase, in the production of alternative oxidase in the filamentous fungus Neurospora crassa pp. in *Department of Biological Sciences*. University of Alberta, Edmonton, Alberta.

DESCHENEAU, A. T., I. A. CLEARY and F. E. NARGANG, 2005 Genetic evidence for a regulatory pathway controlling alternative oxidase production in Neurospora crassa. Genetics **169:** 123-135.

FUJIKI, Y., S. FOWLER, H. SHIO, A. L. HUBBARD and P. B. LAZAROW, 1982a Polypeptide and phospholipid composition of the membrane of rat liver peroxisomes: comparison with endoplasmic reticulum and mitochondrial membranes. J. Cell Biol. **93:** 103-110.

FUJIKI, Y., A. L. HUBBARD, S. FOWLER and P. B. LAZAROW, 1982b Isolation of intracellular membranes by means of sodium carbonate treatment: application to endoplasmic reticulum. J. Cell Biol. **93:** 97-102.

GATHERAR, I. M., S. POLLERMAN, N. DUNN-COLEMAN and G. TURNER, 2004 Identification of a novel gene hbrB required for polarised growth in Aspergillus nidulans. Fungal Genet. Biol. **41:** 463-471.

JANSSEN, M. J. F. W., F. VAN VOORST, G. E. J. PLOEGER, P. M. LARSEN, M. R. LARSEN *et al.*, 2002 Photolabeling Identifies an Interaction between Phosphatidylcholine and Glycerol-3-phosphate Dehydrogenase (Gut2p) in Yeast Mitochondria. Biochemistry **41:** 5702-5711.

LEMIEUX, M. J., Y. HUANG and D.-N. WANG, 2004 Glycerol-3-phosphate transporter of Escherichia coli: Structure, function and regulation. Res. Microbiol. **155:** 623-629.

LI, Q., R. G. RITZEL, L. L. MCLEAN, L. MCINTOSH, T. KO *et al.*, 1996 Cloning and analysis of the alternative oxidase gene of Neurospora crassa. Genetics **142:** 129-140.

NARGANG, F. E., K. ADAMES, C. RÜB, S. CHEUNG, N. EASTON *et al.*, 2012 Identification of Genes Required for Alternative Oxidase Production in the Neurospora crassa Gene Knockout Library. G3 (Bethesda) **2:** 1345-1356.

PAO, S. S., I. T. PAULSEN and M. H. SAIER, 1998 Major Facilitator Superfamily. Microbiol. Mol. Biol. Rev. **62:** 1-34.

POVELONES, M. L., C. TIENGWE, E. GLUENZ, K. GULL, P. T. ENGLUND *et al.*, 2013 Mitochondrial shape and function in trypanosomes requires the outer membrane protein, TbLOK1. Mol. Microbiol. **87:** 713-729.

REDDY, V. S., M. A. SHLYKOV, R. CASTILLO, E. I. SUN and M. H. SAIER, 2012 The Major Facilitator Superfamily (MFS) Revisited. FEBS J. **279:** 2022-2035.

SANTORO, A., A. R. CAPPELLO, M. MADEO, E. MARTELLO, D. IACOPETTA *et al.*, 2011 Interaction of fosfomycin with the Glycerol 3-phosphate Transporter of Escherichia coli. Biochimica et Biophysica Acta (BBA) - General Subjects **1810:** 1323-1329.

SINGHA, U. K., S. SHARMA and M. CHAUDHURI, 2009 Downregulation of Mitochondrial Porin Inhibits Cell Growth and Alters Respiratory Phenotype in Trypanosoma brucei. Eukaryot. Cell **8:** 1418-1428.

YAN, N., 2013 Structural advances for the major facilitator superfamily (MFS) transporters. Trends Biochem. Sci. **38:** 151-159.

Chapter 4: Discussion

The initial goal of this thesis, was to determine the role that thirteen genes play in the production and/or function of AOX. These genes were originally identified in a screen of the *N. crassa* KO library (NARGANG *et al.* 2012).

4.1 Analysis of possible assembly mutants

Of the thirteen genes, five (KO in mutants 13G11, 28B10, 85H5, 99B8 and 101D3) were hypothesized to be involved in the assembly of AOX into a functional protein or insertion of AOX into the MIM. KO mutants of these genes were sensitive to AA but had wild-type, or near wild-type, levels of AOX following growth in Cm (NARGANG *et al.* 2012). The predicted functions of the proteins encoded by the five genes are varied. For some, a possible relationship to AOX function is relatively straightforward. For others, this is not the case. The mechanism by which AOX associates with the MIM once the AOX preprotein enters the mitochondria is unknown. Fig. 35 shows some possible mechanisms by which AOX might assemble into the MIM.

Mutant 13G11 is a KO of protein kinase 10 (prk-10). Prk-10 belongs to the serine/threonine kinase family and is highly conserved in eukaryotes from yeast to humans. The human ortholog of prk-10 is AMPK (AMP-activated kinase) (HARDIE *et al.* 1998; GHILLEBERT *et al.* 2011). AMPK family proteins have been shown to play a role in sensing cellular energy levels in order to bring about energy homeostasis in the cell (HARDIE *et al.* 1998; HARDIE 2007). The *S. cerevisiae* homolog of prk-10, SNF1, has been found to hyperphosphorylate RDS2 (ortholog of the *N. crassa* AOD2

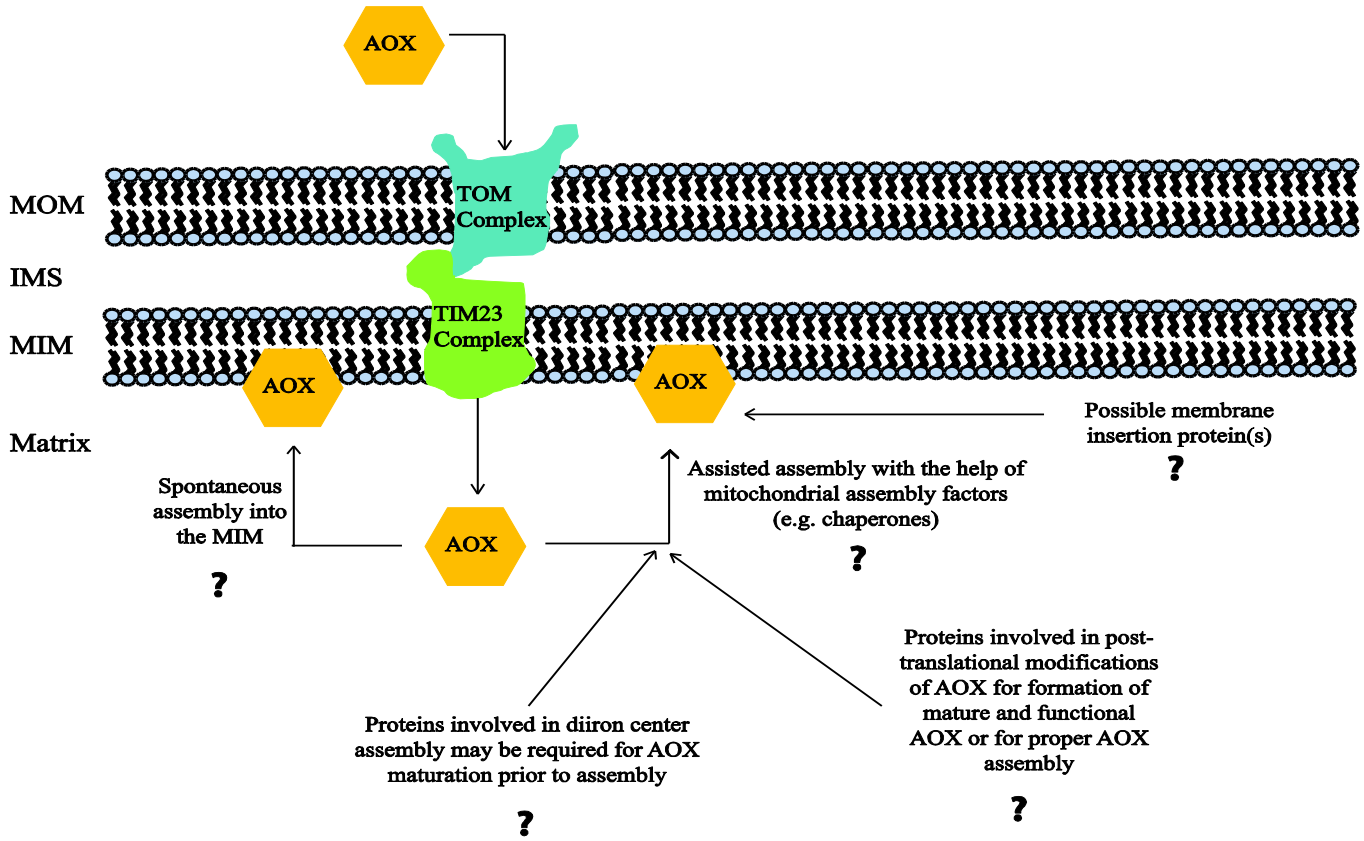

171

Figure 35. Possible mechanisms for AOX assembly into the MIM. AOX enters the mitochondria via the TOM complex and the TIM23 complex. Upon entering the matrix, it may either spontaneously assemble into the inner leaflet of the MIM, or may require unknown protein(s) and other factor(s) for assembly. These factors could include proteins involved in the assembly of the diiron center upon transport of the AOX preprotein into the matrix (possibly, the gene product of the gene KO in strain 85H5) and proteins involved in post-translational modification of AOX which might be important for protein maturation and assembly (possibly, gene products of gene KO in strain 13G11 and 99B8). Other proteins may also be required for insertion of AOX into the MIM.

protein) (SOONTORNGUN *et al.* 2007). This hyperphosphorylation of RDS2 by SNF1 leads to its activation under glucose repressing conditions. While it might be expected that the prk-10 protein similarly phosphorylates AOD2 in *N. crassa,* it is also possible that it is involved in an unknown mechanism that leads to phosphorylation of AOX or phosphorylation of a factor that is involved in the assembly of AOX into the MIM. Thus, loss of the prk-10 protein might lead to loss of AOX activity due to inactive AOX protein or due to loss of assembly into the MIM.

Mutant 28B10 is a KO of NCU08137. The BROAD website lists it as a hypothetical protein of unknown function. However, further analysis of this protein using the MITOPROT II software (CLAROS and VINCENS 1996), predicts presence of a mitochondrial targeting sequence (with a 0.9907 probability of export to mitochondria). In addition, BLAST searches suggest sequence similarity to the mitochondrial protein YMR-31 and alignment of NCU08137 with homologous proteins from several fungal and animal species showed a relationship with the YMR-31 protein from yeast (HEUBLEIN *et al.* 2014). YMR-31 was initially proposed to be a mitochondrial ribosomal protein (MATSUSHITA *et al.* 1989), but a recent study on the *S. cerevisiae* YMR-31 protein suggests that YMR-31 (now termed KGD4) is a component of the α-ketogutarate dehydrogenase protein complex and acts as a molecular adaptor to ensure proper organization of the complex (HEUBLEIN *et al.* 2014). It is difficult to suggest how a protein involved in the organization of α-ketogutarate dehydrogenase could be involved in the assembly or production of AOX.

The Neurospora genome database describes mutant 85H5 as lacking a gene encoding a thioredoxin protein (NCU09803). This protein has a thioredoxin domain at its N-

terminus and a glutaredoxin domain at its C-terminus indicating it belongs to the monothiol glutaredoxin subfamily (NARGANG *et al.* 2012). Monothiol glutaredoxins have been shown to play a role in cellular iron homeostasis maintenance (HERRERO and DE LA TORRE-RUIZ 2007; HOFFMANN *et al.* 2011). A study in *S. cerevisiae* demonstrated that depletion of monothiol glutaredoxin (*grx3/grx4*) led to impairment of iron insertion into proteins (MÜHLENHOFF *et al.* 2010; HOFFMANN *et al.* 2011). Since AOX is a diiron carboxylate protein, it was hypothesized that deletion of NCU09803 in mutant 85H5 might cause errors in AOX diiron center assembly (NARGANG *et al.* 2012).

In mutant 99B8, the gene previously described as cytochrome-4 (*Cyt-4*) has been knocked out. Mutants of this gene were originally identified in *N. crassa* as being cold-sensitive (mutants grow slowly at 25°C) and deficient in mitochondrial cytochromes *b* and aa_3 (GARRIGA *et al.* 1984; DOBINSON *et al.* 1989). The *cyt-4* mutants grew faster at 37°C (in comparison to at 25 °C, but still slower than the wild-type strain) and had cytochrome *b* (but no cytochrome aa_3) deficiency at this temperature. The Neurospora genome database describes the gene product of this gene as a phosphatase with an RNB domain (the catalytic domain of the RNase II superfamily of exoribonucleases). Proteins with this domain are known to processively hydrolyze single stranded RNA in the 3' to 5' direction and generate 5' mononucleotides (FRAZAO *et al.* 2006; BARBAS *et al.* 2008). Studies of *Cyt-4* mutants in *N. crassa* have suggested that CYT4 is a mitochondrial protein that plays a role in mitochondrial RNA splicing, processing and RNA turnover (DOBINSON *et al.* 1989; TURCQ *et al.* 1992). The CYT4 protein has been proposed to be involved in the regulation of these processes via its role as a phosphatase (TURCQ *et al.* 1992). Though it is unlikely that processing of mtRNA would directly affect AOX, it is

conceivable that the activity of a phosphatase could be required for activation or assembly of AOX.

Mutant 101D3 is a KO of a gene encoding a superoxide dismutase. The protein has been shown to be localized to the mitochondrial matrix and to utilize manganese as its metal cofactor (KEEPING *et al.* 2011; NARGANG *et al.* 2012; SARSOUR *et al.* 2013; XU *et al.* 2014). Manganese superoxide dismutases (MnSODs) are involved in detoxification of superoxide anions (SARSOUR *et al.* 2013; XU *et al.* 2014). It is difficult to suggest a direct effect of this enzyme on AOX assembly or function. However, it is conceivable that higher levels of ROS might be produced in cultures grown in AA than in Cm (see section 4.2). Absence of the MnSOD might allow accumulation of ROS in AA cultures leading to cell death. This might account for the phenotype of mutant 85H5 i.e. inability to grow in the presence of AA, but having near wild-type growth and wild-type levels of AOX when grown in the presence of Cm.

To determine if any of these five strains had a defect in the assembly of AOX into the MIM, I began by performing carbonate extractions of mitochondria. A similar approach was successfully used to study four mutants of the *S. cerevisiae* tafazzin protein (CLAYPOOL *et al.* 2006). The tafazzin protein is an interfacial membrane protein like AOX, although it is associated with the outer leaflet of the MIM and inner leaflet of the MOM, facing the IMS. Mutations in the human tafazzin gene (*TAZ*) cause the Barth syndrome. The above mentioned four *S. cerevisiae* mutants had been modelled to represent the most frequently observed amino acid changes in the tafazzin protein membrane anchor region of Barth syndrome patients (CLAYPOOL *et al.* 2006). The wild-type protein was found in both the pellet and the supernatant fraction following carbonate

extractions, with more entering the supernatant fraction as the pH of the extraction was increased from 10.9 to 12.5 (CLAYPOOL *et al.* 2006). Upon performing carbonate extractions on the four Barth syndrome model mutants, it was found that the tafazzin protein from these mutants was significantly more extractable in comparison to wild-type tafazzin, suggesting altered membrane association of the tafazzin protein in these mutants.

AOX has also been used as a control in carbonate extraction studies aimed at determining mitochondrial localization of other proteins in *T. brucei*. In one study trypanosome mitochondria were subjected to carbonate extraction at pH 11.5. The TAO (trypanosome AOX) was found exclusively associated with the pellet fraction (POVELONES *et al.* 2013). In a similar study, carbonate extraction of mitochondria at pH 11.0 showed that the majority of TAO partitioned to the pellet fraction (SINGHA *et al.* 2009).

To test the possibility of aberrant membrane association of AOX in the five KO mutant strains of interest, carbonate extractions were performed on isolated mitochondria from these strains at pH 11.0. However, inconsistent results were obtained. One possible reason for this could be that there were slight variations in the pH of the sodium carbonate used in different experiments which might affect the partitioning pattern of proteins.

An alternative technique that can be used to study membrane association of mitochondrial proteins is digitonin fractionation of mitochondria. At low concentrations, digitonin specifically disrupts the MOM, leading to loss of MOM proteins from the pellet fraction. At higher concentrations of digitionin, MIM proteins begin to be lost from the

pellet fraction (SCHMIDT *et al.* 1984). Various studies have shown that digitonin fractionation can be successfully used for analyzing the sub-mitochondrial localization of proteins (NAIR and MCGUIRE 2005; ARNOULT *et al.* 2009; CSORDÁS *et al.* 2013). Such studies use increasing concentrations of digitonin and examination of pellet and supernatant fractions with antibodies on western blots. In these studies, proteins of known sub-mitochondrial localizations are used as controls so that the placement of the protein of interest can be determined.

To my knowledge, no study has used digitonin fractionation to analyze AOX assembly. However, a study aimed at identifying the role played by the TbLOK1 protein (POVELONES *et al.* 2013), thought to be involved in maintenance of mitochondrial morphology and function in the procyclic form of *T. brucei* (ENGLUND *et al.* 2005; MOTYKA *et al.* 2006), did use this technique. AOX was examined as a control in this study and was seen to be released from the MIM at a digitonin concentration of 0.1% (POVELONES *et al.* 2013). Thus, I propose that future experiments aimed at studying the membrane association of AOX in KO mutant strains of *N. crassa* be performed using digitonin fractionation of mitochondria.

In light of my results showing that two of the class 1 KO mutants contained a mutation in the *aod-1* gene (section 3.2.3.4), another explanation should be considered as a possible basis for the phenotype in the five mutants discussed above. That is, missense mutations affecting the AOX protein could have occurred during construction of the KO library which could result in lack of AOX activity. This would result in no growth in the presence of AA. However, wild-type or near wild-type levels of inactive AOX protein might be observed following growth in Cm. Inactive AOX protein was observed in

mitochondria in early studies of *aod-1* mutants (BERTRAND *et al.* 1976; LI *et al.* 1996). The activity of AOX in these strains could be tested in respiratory studies. For cultures grown in the presence of Cm, measurements of oxygen consumption in a respirometer (TANTON *et al.* 2003; DESCHENEAU *et al.* 2005) would show whether or not any respiratory activity remained after addition of potassium cyanide (KCN) to the culture. If so, the AOX must be active, if not, the AOX detected on western blots would be deemed inactive. An alternative, or perhaps complementary approach, would be to sequence the *aod-1* gene from each of the mutants.

4.2 AA and Cm: chemical inducers of AOX

The KO mutant screening that identified the strains used in this study used AA (inhibitor of complex III of the sETC) for the initial screening and identification of strains presumed to be AOX deficient because of their inability to grow in the presence of this inhibitor (NARGANG *et al.* 2012). Following identification of such strains, Cm was used to induce AOX and the amount of AOX produced was determined using western blotting analysis, since further work with the strains could not be done using AA. Both of these inhibitors lead to AOX induction in wild-type *N. crassa,* but it is conceivable that they might use different signaling pathways and effector molecules for AOX induction.

AA inhibits sETC complex III between cytochrome *b* and c_1 (SLATER 1973; HUANG *et al.* 2005; HAN *et al.* 2009). This leads to breakdown of the mitochondrial membrane potential and production of large amounts of ROS via complexes I and III. Cm inhibits mitochondrial translation by binding to the large subunit of the mitochondrial ribosomes and inhibiting peptidyl transferase (COUTSOGEORGOPOULOS 1966; BALBI 2004). Since the mtDNA encodes subunits of the sETC complexes I, III and IV, inhibition of

mitochondrial protein synthesis leads to impairment of the sETC at several positions. Furthermore, at the concentrations commonly used, AA totally inhibits complex III, whereas a low amount of mitochondrial translation and thus formation of sETC complexes occurs in the presence of Cm. To date, the signaling pathway(s), by which these chemicals bring about their effects has not been defined. But some isolated studies in various organisms have proposed roles of certain pathways and/or effector molecules in response to the inhibitory effect of these chemicals.

A common theme in mammalian systems treated with AA or Cm seems to be the activation of MAPK signaling pathways. For example, one study aimed at testing the effect of AA and of MAPK inhibitors on calf pulmonary artery endothelial cells found that use of MAPK inhibitors on AA-treated cells augmented cell death via loss of mitochondrial membrane potential (MMP), increase in the level of ROS, and depletion of glutathione (GSH). This suggested that MAPK signaling pathways may be involved in the response to AA inhibition and may be positively involved in the response against AA in mammalian cells (HAN *et al.* 2010). Similarly, LI *et al.* (2010) found that treatment of H1299 cells (non-small-cell lung cancer cells) with Cm led to activation of the ERK (extracellular signal regulated kinase), JNK (c-Jun N-terminal kinase/stress-activated protein kinase), p38-MAPK and Atk (protein kinase B) MAP kinases. This, in turn, led to induction of MMP-13 (matrix metalloproteinase 13). Matrix metalloproteinases are zinc dependent endopeptidase proteins known to cause extracellular matrix (ECM) degradation of the cell during senescence (CHAKRABORTI *et al.* 2003).

AA leads to production of large amounts of ROS, and one study found that treatment of HeLa cells with 100 μM AA for 72 hr leads to apoptosis in 70% of the cells. Loss of

MMP, downregulation of Bcl-2 and upregulation of Bax was also observed in these AA-treated HeLa cells (PARK *et al.* 2007b). The susceptibility of AA-treated cells to apoptosis has been proposed to depend on the cell type. For example, As.4.1 juxtaglomerular cells undergo apoptosis in the presence of AA concentrations of as low as 50 nM (PARK *et al.* 2007a; PARK *et al.* 2007b).

On the other hand, treatment of cells with Cm seems to prevent apoptosis as seen in studies by YUAN and SHI (2008) and LI *et al.* (2005). In one study, HepG2 cells (human liver carcinoma cells) treated with 20 and 100 µg/mL Cm for 48 hr showed attenuation of apoptosis. This was thought to be the result of the cyclin dependent kinase inhibitor p21 (LI *et al.* 2005). Another study, aimed at understanding Cm induced leukemia development used mouse primary splenocytes treated with 500 µg/mL Cm for 1 week (YUAN and SHI 2008). This study found inhibition of activation induced cell death as a consequence of blocked FasL expression by Cm.

These data suggest that at least in mammalian cells, some differences exist in the signaling pathways activated by AA and Cm. It is possible that differences in induction of AOX by AA and Cm may also exist in *N. crassa*. Such differences could account for the observation that some strains seem to be severely deficient in AOX activity when tested on AA but seem to have near wild-type growth (and AOX levels) following growth in the presence of Cm (as is the case in KO mutant 101D3). Fig. 36 demonstrates possible differences in the ways AA and Cm could bring about their effects. However, it should be noted that on one level, the effects of the two inhibitors are very similar. Both would be expected to cause a reduction in electron transport, H^+ pumping, membrane potential, ATP synthesis, and loss of oxidation of reduced electron carriers.

4.3 Class 1 knockout mutant strain analysis

Of the thirteen genes examined in this study, the products of eight genes were hypothesized to play an essential role in the production and/or regulation of AOX. KO mutants of these genes had negligible amounts of AOX following growth for 24 and/or 48 hr in the presence of Cm. Such mutants were termed class 1 KO mutants (NARGANG *et al.* 2012).

Initially, I started working with two class 1 KO mutants, 23H2 (KO-NcMFS) and 88H8 (KO-NcHbrB). The gene knocked out in 23H2, NCU08887 (NcMFS gene), encodes a major facilitator superfamily protein, termed NcMFS. The gene knocked out in 88H8 is NCU01542 (NcHbrB gene), which encodes a protein termed NcHbrB, because it contains an HbrB domain. At the beginning of my study, the wild-type versions of the genes had been previously cloned into suitable plasmid vectors (K. Adames and A.B. Desaulniers) to be used in gene rescue experiments. Based on homology studies, I added additional sequence to the clone of the NCU01542 gene. Several attempts to rescue the AA sensitivity of mutants 23H2 (KO-NcMFS) and 88H8 (KO-NcHbrB) were made using the cloned genes, but no rescue of either mutant phenotype was ever observed. Furthermore, analysis of preliminary RNA-seq data (DESAULNIERS 2013) for NCU08887 shows virtually no transcript from this gene following growth in the presence or absence of Cm.

Even though the class 1 strains had previously been tested for carrying the correct KO by PCR analysis (K. Adames, F. E. Nargang, unpublished data), the inability to rescue mutant phenotype in 23H2 (KO-NcMFS) and 88H8 (KO-NcHbrB) led us to suspect that the strains being used as my stocks might not carry the specific KO assigned

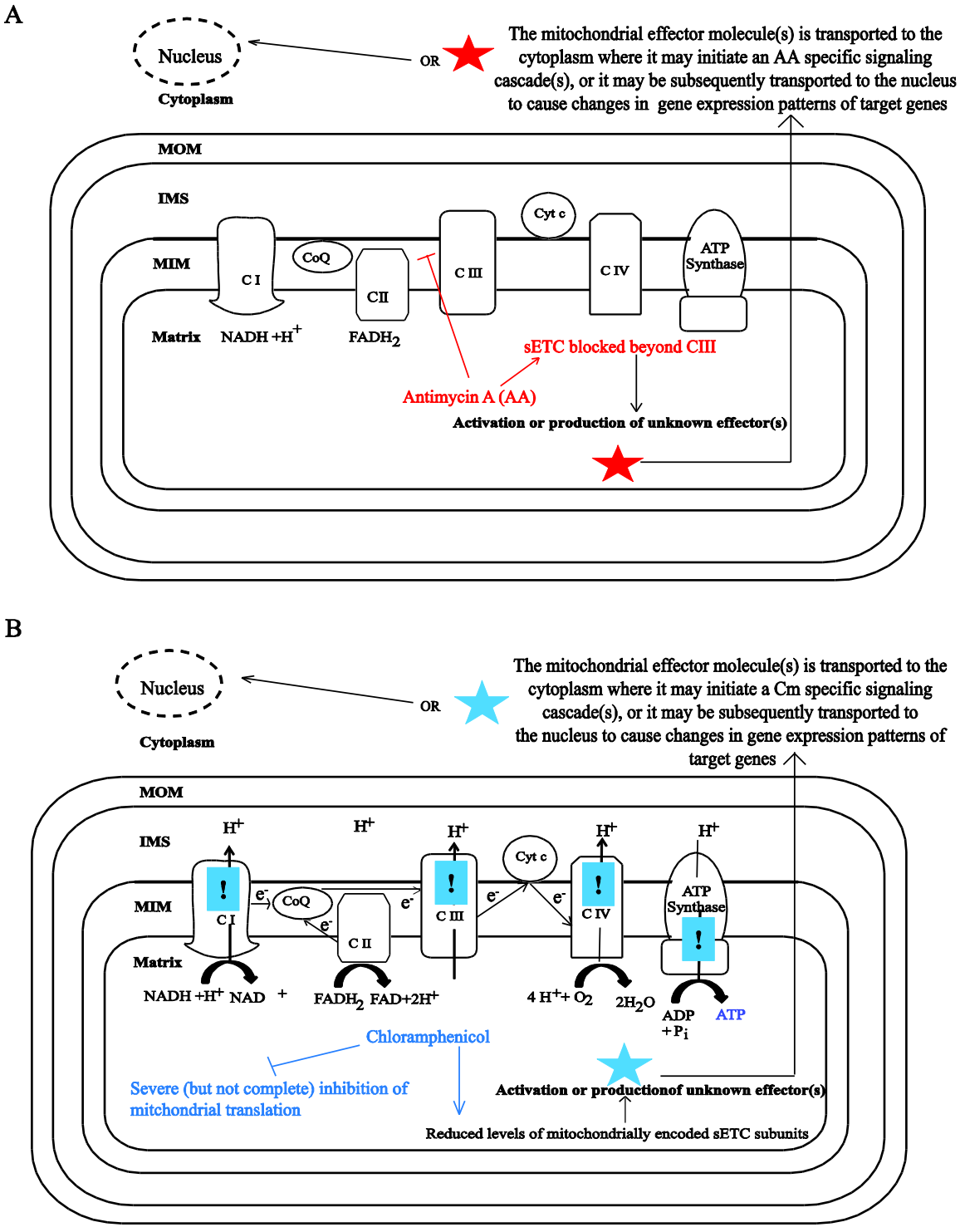

Figure 36. Possible mechanism of action of AA and Cm in AOX induction. A) AA inhibits sETC complex III activity between cytochrome *b* and c_1. This leads to blockage of electron flow along the sETC, and eventual inhibition of complex I, leading to

breakdown of the mitochondrial membrane potential. These effects may lead to activation or production of unknown effector molecule(s) (shown in red) that is transported out of the mitochondria and into the cytoplasm where it may initiate an AA specific signaling cascade(s). Alternatively, they may be transported to the nucleus where they alter the transcription levels of target genes. B) Cm binds to the large subunit of the mitochondrial ribosome which leads to a severe (but not complete) inhibition of mitochondrial translation. This causes deficiencies (represented as exclamation marks in blue boxes) of mitochondrially encoded subunits of complex I, III, IV and ATP synthase and eventual breakdown of the mitochondrial membrane potential. This may lead to activation or production of unknown effector molecule(s) (shown in blue) that is transported out of the mitochondria to achieve their effects as described for A.

to them. Thus, experiments to verify the integrity of mutants 23H2, 88H8 and six other class 1 KO mutant strains (40E6, 41G7, 47H10, 52D8, 83H3, 113G8) were carried out. In the end, my investigation included PCR amplification analysis for the correct KO (section 3.2.3.1), Southern blot analysis (section 3.2.3.3) and crossing the KO mutants with wild-type strains (section 3.2.3.2). These experiments suggested that the presence of additional secondary random mutation(s), in the genome of seven of the eight KO mutant strains tested, was responsible for the AOX deficiency observed in these strains. However, it should be noted that in case of mutant 52D8, only four out of the sixty five cross progeny analyzed had recombinant phenotypes. Thus, it could be possible that these cross progeny were mis-scored and that the gene KO in 52D8 may indeed play a role in AOX production. Another additional class 1 mutant, 100B5 (not analyzed as part of this study), was previously characterized (DESAULNIERS 2013) and the AOX deficiency was found to be due to the knocked out gene.

Once the genetic data had shown the presence of additional mutations in the strains, it seemed reasonable that these might have occurred in known AOX regulatory genes (*aod-2* and *aod-5*) or the AOX structural gene (*aod-1*). Similarly, mutations in one of the genes knocked out in the two class 1 KO mutants (40E6 and 100B5) found to be correct from the KO screen and subsequent analysis, might also account for the phenotypes. Finally, it was also conceivable that secondary mutations could be present in as yet uncharacterized AOX regulatory genes. To begin an investigation of these possibilities, the *aod-1, aod-2* and *aod-5* genes from mutants 23H2 (KO-NcMFS) and 88H8 (KO-NcHbrB) were sequenced. *aod-1* was also sequenced from mutants 40E6, 41G7, 47H10, 52D8, 83H3 and 113G8. Sequencing of *aod-1* from strains 23H2 (KO-NcMFS) and

88H8 (KO-NcHbrB) revealed the presence of an identical single nucleotide insertion (insertion of a C, 708 bp (excluding introns) after the translation start site) in the coding sequence of the gene in both mutants. The mutation resulted in a frame-shift following the insertion leading to production of a truncated protein as the result of a premature stop codon (see Fig. 33 and 34, section 3.2.3.4). The frame-shift and premature stop codon affect fifteen universally conserved AOX residues (MOORE *et al.* 2013), leading to loss of eight and changes in seven of these amino acid residues. These residues are known to play an important role in several AOX functions including dimer formation, membrane binding, and coordinating the diiron center (MOORE *et al.* 2013). Since our AOX antibody would not detect the truncated protein, it is not known if the protein fragment is present or degraded, or if degradation of the *aod-1* mRNA occurs prior to translation due to nonsense mediated decay (CONTI and IZAURRALDE 2005; SCHWEINGRUBER *et al.* 2013).

Sequencing results for *aod-2* and *aod-5* from mutants 23H2 (KO-NcMFS) and 88H8 (KO-NcHbrB) indicated the presence of wild-type sequences for these genes. Sequencing data for the *aod-1*gene from mutants 40E6, 41G7, 47H10, 52D8, 83H3 and 113G8 indicated the presence of the wild-type sequence of this gene in these mutant strains. Thus, these strains seem likely to carry secondary mutations in different genes as discussed above.

It is not entirely clear how two strains, not present on the same 96 well plate and carrying KOs of genes not linked to each other (NCU08887 (NcMFS), knocked out in 23H2, present on chromosome 5; NCU01542 (NcHbrB), knocked out in 88H8, present on chromosome 2) could have the same mutation at the same position in the *aod-1* gene.

The knockout mutant library was created by transforming conidia from Δ*mus51* or Δ*mus52* strains with Hyg^R containing knockout cassettes specific to each *N. crassa* gene (COLOT *et al.* 2006). The *mus51* and *mus52* genes encode proteins that play a role in non-homologous end joining. Elimination of their function prevents integration of transformed DNA at heterologous sites and increases the frequency of transformants with integration of exogenous DNA at homologous sites to near 100% (NINOMIYA *et al.* 2004). The initial transformants were crossed with a wild-type strain to generate homokaryons containing a wild-type copy of the *mus51* and *mus52* genes and a disruption of the gene of interest (COLOT *et al.* 2006). It is possible that a proportion of the conidia used for transformations during creation of the KO mutant library carried the *aod-1* mutation which was inherited by mutants 23H2 (KO-NcMFS) and 88H8 (KO-NcHbrB). Alternatively, conidia harboring this mutation may have contaminated the wild-type stock during the process of crossing to generate homokaryons. However, it is still not clear how this would result in the same mutation in both these mutants, but not others.

To examine the possibility that the lab bench stocks for mutant 23H2 (KO-NcMFS) and 88H8 (KO-NcHbrB) accumulated spontaneous mutations over several generations of subculturing, conidia from the freezer stock taken directly from the KO mutant library were acquired for these two strains. The *aod-1* gene was resequenced from these fresh stocks. These sequencing data confirmed the presence of the same mutation in both strains, effectively ruling out the possibility that the mutation was generated during subculturing in our lab. It is worth noting that the mutation observed in strains 23H2

(KO-NcMFS) and 88H8 (KO-NcHbrB) is not the same as any mutation found in any of the previously characterized *aod-1* mutant strains in the Nargang lab (LI *et al.* 1996).

Based on the work done in this thesis, the only strain examined that seems to be a true new class 1 KO strain is strain 40E6. Mutant 40E6 has a region encoding two genes knocked out from its genome due to an annotation error that was not corrected before the KO library was constructed. According to the Neurospora genome database, these genes encode a protein involved in ubiquinone biosynthesis (NCU05600) and an aspartyl aminopeptidase (NCU17088). A BLAST search with NCU17088 revealed that the protein is homologous to proteins of the glycoside hydrolase 71 family that contain the GH71 domain. Glycoside hydrolases are involved in hydrolysis of bonds between a carbohydrate and another compound such as another carbohydrate, a lipid or a protein (HENRISSAT 1991; CANTAREL *et al.* 2009; TYLER *et al.* 2010). When the fission yeast genome was searched for homologs of NCU17088, BLAST searches showed 30% identity to Agn2, a glucan-endo-1,3-alpha-glucosidase. Agn2 seems to play a role in hydrolysis of alpha-1,3-glucan, thereby aiding in endolysis of the ascus wall during ascospore release in *S. pombe* (DEKKER *et al.* 2004; DEKKER *et al.* 2007; ENCINAR DEL DEDO *et al.* 2009). Thus, it seems unlikely that loss of this gene affects production of AOX.

NCU05600 has been assigned the gene name *stk-33* by the Neurospora genome database. This protein contains an atypical serine threonine kinase domain (PARK *et al.* 2011; NARGANG *et al.* 2012). The closest homolog of this protein from *S. cerevisiae*, YPL109c (HomoloGene analysis, NCBI, (NARGANG *et al.* 2012)), has no known function. The human homolog of the protein ADCK2 (aarF domain containing kinase 2,

belonging to the aarF domain containing (ADC) proteins family) has been seen to play a role in breast cancer cell viability (BROUGH *et al.* 2011; NARGANG *et al.* 2012; STEFELY *et al.* 2015). Proteins belonging to the ADC family are mostly mitochondrial proteins and have been shown to play a role in ubiquinone biosynthesis (STEFELY *et al.* 2015). Both, NCU05600 and YPL109c seem to be related to Coq8 from *S. cerevisiae.* Coq8 has been shown to play a role in regulating the function of Coq3, a ubiquinone biosynthesis pathway enzyme. It has been proposed that this regulation may be direct, via phosphorylation of Coq3 by Coq8 (DO *et al.* 2001; TAUCHE *et al.* 2008; NARGANG *et al.* 2012; GONZÁLEZ-MARISCAL *et al.* 2014). Alternatively, it is possible that another intermediate protein is involved in the regulation of Coq3 activity (CHI *et al.* 2007; TAUCHE *et al.* 2008). Due to the involvement of ubiquinone in the alternative respiration pathway, it has been previously proposed that of the two genes knocked out in 40E6, NCU05600 is more likely to be involved in AOX production and/or regulation (NARGANG *et al.* 2012).

At the time of the completion of this thesis, genes known to play a role in the production and regulation of AOX include *aod-1*, *aod-2*, *aod-5*, NCU05600 and/or NCU17088 (genes knocked out in mutant 40E6) and *YVH1* (knocked out in 100B5, encodes a dual specificity phosphatase). It is interesting to note that there is a temporal pattern of AOX appearance in mutants 41G7 and 52D8 following 24 and 48 hr of growth in the presence of Cm that is similar to that of 40E6 (a verified class 1 KO mutant). AOX is reduced at 24 hr and absent at 48 hr. Thus, it is conceivable that 41G7 and 52D8 carry random mutations in the region knocked out in 40E6. This region should be sequenced

from the two strains. If this shows no mutations, then the *aod-2* and *aod-5* genes should be examined.

Strains 47H10, 83H3 and 113G8 lack AOX completely at both times. Since I have shown that the *aod-1* gene is not affected in these strains, future work should be aimed at sequencing the promoter and coding regions of the *aod-2* and *aod-5* genes from these mutants. This approach would reveal whether the secondary mutation present in these strains has disrupted one of these two known AOX regulatory genes. It would also be interesting to cross class 2 mutants identified in the KO library screen to determine if the defects observed in any of these mutants are due to the specific gene KO, or due to secondary mutations.

References

ARNOULT, D., F. SOARES, I. TATTOLI, C. CASTANIER, D. J. PHILPOTT *et al.*, 2009 An N-terminal addressing sequence targets NLRX1 to the mitochondrial matrix. J. Cell Sci. **122:** 3161-3168.

BALBI, H. J., 2004 Chloramphenicol: A Review. Pediatr Rev **25:** 284-288.

BARBAS, A., R. G. MATOS, M. AMBLAR, E. LÓPEZ-VIÑAS, P. GOMEZ-PUERTAS *et al.*, 2008 New Insights into the Mechanism of RNA Degradation by Ribonuclease II: Identification of the residue responsible for setting the RNase II end product. J. Biol. Chem. **283:** 13070-13076.

BERTRAND, H., N. A. SZAKACS, F. E. NARGANG, C. A. ZAGOZESKI, R. A. COLLINS *et al.*, 1976 The function of mitochondrial genes in Neurospora crassa. Can J Genet Cytol **18:** 397-409.

BROUGH, R., J. R. FRANKUM, D. SIMS, A. MACKAY, A. M. MENDES-PEREIRA *et al.*, 2011 Functional Viability Profiles of Breast Cancer. Cancer Discov. **1:** 260-273.

CANTAREL, B. L., P. M. COUTINHO, C. RANCUREL, T. BERNARD, V. LOMBARD *et al.*, 2009 The Carbohydrate-Active EnZymes database (CAZy): an expert resource for Glycogenomics. Nucleic Acids Res. **37:** D233-D238.

CHAKRABORTI, S., M. MANDAL, S. DAS, A. MANDAL and T. CHAKRABORTI, 2003 Regulation of matrix metalloproteinases: An overview. Mol. Cell. Biochem. **253:** 269-285.

CHI, A., C. HUTTENHOWER, L. Y. GEER, J. J. COON, J. E. P. SYKA *et al.*, 2007 Analysis of phosphorylation sites on proteins from Saccharomyces cerevisiae by electron transfer dissociation (ETD) mass spectrometry. Proc. Natl. Acad. Sci. USA **104:** 2193-2198.

CLAROS, M. G., and P. VINCENS, 1996 Computational Method to Predict Mitochondrially Imported Proteins and their Targeting Sequences. Eur. J. Biochem. **241:** 779-786.

CLAYPOOL, S. M., J. M. MCCAFFERY and C. M. KOEHLER, 2006 Mitochondrial mislocalization and altered assembly of a cluster of Barth syndrome mutant tafazzins. J. Cell Biol. **174:** 379-390.

COLOT, H. V., G. PARK, G. E. TURNER, C. RINGELBERG, C. M. CREW *et al.*, 2006 A high-throughput gene knockout procedure for Neurospora reveals functions for multiple transcription factors. Proc. Natl. Acad. Sci. USA **103:** 10352-10357.

CONTI, E., and E. IZAURRALDE, 2005 Nonsense-mediated mRNA decay: molecular insights and mechanistic variations across species. Curr. Opin. Cell Biol. **17:** 316-325.

COUTSOGEORGOPOULOS, C., 1966 On the mechanism of action of chloramphenicol in protein synthesis. Biochim. Biophys. Acta, Nucleic Acids Protein Synth. **129:** 214-217.

CSORDÁS, G., T. GOLENÁR, ERIN L. SEIFERT, KIMBERLI J. KAMER, Y. SANCAK *et al.*, 2013 MICU1 Controls Both the Threshold and Cooperative Activation of the Mitochondrial Ca2+ Uniporter. Cell Metab. **17:** 976-987.

DEKKER, N., D. SPEIJER, C. H. GRÜN, M. VAN DEN BERG, A. DE HAAN *et al.*, 2004 Role of the α-Glucanase Agn1p in Fission-Yeast Cell Separation. Mol. Biol. Cell. **15:** 3903-3914.

DEKKER, N., J. VAN RIJSSEL, B. DISTEL and F. HOCHSTENBACH, 2007 Role of the α-glucanase Agn2p in ascus-wall endolysis following sporulation in fission yeast. Yeast **24:** 279-288.

DESAULNIERS, A. B., 2013 The role of YVH1, a dual specificity phosphatase, in the production of alternative oxidase in the filamentous fungus Neurospora crassa pp. in *Department of Biological Sciences*. University of Alberta, Edmonton, Alberta.

DESCHENEAU, A. T., I. A. CLEARY and F. E. NARGANG, 2005 Genetic evidence for a regulatory pathway controlling alternative oxidase production in Neurospora crassa. Genetics **169:** 123-135.

DO, T. Q., A. Y. HSU, T. JONASSEN, P. T. LEE and C. F. CLARKE, 2001 A Defect in Coenzyme Q Biosynthesis Is Responsible for the Respiratory Deficiency in Saccharomyces cerevisiae abc1Mutants. J. Biol. Chem. **276:** 18161-18168.

DOBINSON, K. F., M. HENDERSON, R. L. KELLEY, R. A. COLLINS and A. M. LAMBOWITZ, 1989 Mutations in Nuclear Gene Cyt-4 of Neurospora Crassa Result in Pleiotropic Defects in Processing and Splicing of Mitochondrial Rnas. Genetics **123:** 97-108.

ENCINAR DEL DEDO, J., E. DUEÑAS, Y. ARNÁIZ, F. DEL REY and C. R. VÁZQUEZ DE ALDANA, 2009 β-Glucanase Eng2 Is Required for Ascus Wall Endolysis after Sporulation in the Fission Yeast Schizosaccharomyces pombe. Eukaryot. Cell **8:** 1278-1286.

ENGLUND, P. T., E. E. AGBO, M. E. LINDSAY, B. LIU, Y. LIU *et al.*, 2005 RNAi libraries and kinetoplast DNA. Biochem. Soc. Trans. **33:** 1409-1412.

FRAZAO, C., C. E. MCVEY, M. AMBLAR, A. BARBAS, C. VONRHEIN *et al.*, 2006 Unravelling the dynamics of RNA degradation by ribonuclease II and its RNA-bound complex. Nature **443:** 110-114.

GARRIGA, G., H. BERTRAND and A. M. LAMBOWITZ, 1984 RNA splicing in neurospora mitochondria: Nuclear mutants defective in both splicing and 3′ end synthesis of the large rRNA. Cell **36:** 623-634.

GHILLEBERT, R., E. SWINNEN, J. WEN, L. VANDESTEENE, M. RAMON *et al.*, 2011 The AMPK/SNF1/SnRK1 fuel gauge and energy regulator: structure, function and regulation. FEBS J. **278:** 3978-3990.

GONZÁLEZ-MARISCAL, I., E. GARCÍA-TESTÓN, S. PADILLA, A. MARTÍN-MONTALVO, T. POMARES VICIANA *et al.*, 2014 The Regulation of Coenzyme Q Biosynthesis in Eukaryotic Cells: All That Yeast Can Tell Us. Mol Syndromol. **5:** 107-118.

HAN, Y. H., H. J. MOON, B. R. YOU, S. Z. KIM, S. H. KIM *et al.*, 2009 p38 Inhibitor Intensified Cell Death in Antimycin A-treated As4.1 Juxtaglomerular Cells via the Enhancement of GSH Depletion. Anticancer Res. **29:** 4423-4431.

HAN, Y. H., B. R. YOU, H. J. MOON, S. Z. KIM, S. H. KIM *et al.*, 2010 The effects of MAPK inhibitors on antimycin A-treated calf pulmonary arterial endothelial cells in relation to cell death, reactive oxygen species and glutathione. Mol Med Rep. **3:** 161-166.

HARDIE, D. G., 2007 AMP-activated/SNF1 protein kinases: conserved guardians of cellular energy. Nat. Rev. Mol. Cell Biol. **8:** 774-785.

HARDIE, D. G., D. CARLING and M. CARLSON, 1998 THE AMP-ACTIVATED/SNF1 PROTEIN KINASE SUBFAMILY: Metabolic Sensors of the Eukaryotic Cell? Annu. Rev. Biochem. **67:** 821-855.

HENRISSAT, B., 1991 A classification of glycosyl hydrolases based on amino acid sequence similarities. Biochem. J. **280:** 309-316.

HERRERO, E., and M. A. DE LA TORRE-RUIZ, 2007 Monothiol glutaredoxins: a common domain for multiple functions. Cell. Mol. Life Sci. **64:** 1518-1530.

HEUBLEIN, M., M. A. BURGUILLOS, F. N. VÖGTLE, P. F. TEIXEIRA, A. IMHOF *et al.*, 2014 The novel component Kgd4 recruits the E3 subunit to the mitochondrial α-ketoglutarate dehydrogenase. Mol. Biol. Cell. **25:** 3342-3349.

HOFFMANN, B., M. A. UZARSKA, C. BERNDT, J. R. GODOY, P. HAUNHORST *et al.*, 2011 The Multidomain Thioredoxin-Monothiol Glutaredoxins Represent a Distinct Functional Group. Antioxid. Redox Signaling **15:** 19-30.

HUANG, L.-S., D. COBESSI, E. Y. TUNG and E. A. BERRY, 2005 Binding of the respiratory chain inhibitor antimycin to the mitochondrial bc(1) complex: a new crystal structure reveals an altered intramolecular hydrogen-bonding pattern J. Mol. Biol. **351:** 573-597.

KEEPING, A., D. DEABREU, M. DIBERNARDO and R. A. COLLINS, 2011 Gel-based mass spectrometric and computational approaches to the mitochondrial proteome of Neurospora. Fungal Genet. Biol. **48:** 526-536.

LI, C.-H., Y.-W. CHENG, P.-L. LIAO, Y.-T. YANG and J.-J. KANG, 2010 Chloramphenicol Causes Mitochondrial Stress, Decreases ATP Biosynthesis, Induces Matrix Metalloproteinase-13 Expression, and Solid-Tumor Cell Invasion. Toxicol. Sci. **116:** 140-150.

LI, C.-H., S.-L. TZENG, Y.-W. CHENG and J.-J. KANG, 2005 Chloramphenicol-induced Mitochondrial Stress Increases p21 Expression and Prevents Cell Apoptosis through a p21-dependent Pathway. J. Biol. Chem. **280:** 26193-26199.

LI, Q., R. G. RITZEL, L. L. MCLEAN, L. MCINTOSH, T. KO *et al.*, 1996 Cloning and analysis of the alternative oxidase gene of Neurospora crassa. Genetics **142:** 129-140.

MATSUSHITA, Y., M. KITAKAWA and K. ISONO, 1989 Cloning and analysis of the nuclear genes for two mitochondrial ribosomal proteins in yeast. Molec. Gen. Genet. **219:** 119-124.

MOORE, A. L., T. SHIBA, L. YOUNG, S. HARADA, K. KITA *et al.*, 2013 Unraveling the heater: new insights into the structure of the alternative oxidase. Annu. Rev. Plant Biol. **64:** 637-663.

MOTYKA, S. A., M. E. DREW, G. YILDIRIR and P. T. ENGLUND, 2006 Overexpression of a Cytochrome b5 Reductase-like Protein Causes Kinetoplast DNA Loss in Trypanosoma brucei. J. Biol. Chem. **281:** 18499-18506.

MÜHLENHOFF, U., S. MOLIK, J. R. GODOY, M. A. UZARSKA, N. RICHTER *et al.*, 2010 Cytosolic Monothiol Glutaredoxins Function in Intracellular Iron Sensing and Trafficking via Their Bound Iron-Sulfur Cluster. Cell Metab. **12:** 373-385.

NAIR, J. R., and J. J. MCGUIRE, 2005 Submitochondrial localization of the mitochondrial isoform of folylpolyglutamate synthetase in CCRF-CEM human T-lymphoblastic leukemia cells. Biochim. Biophys. Acta - Mol. Cell Res. **1746:** 38-44.

NARGANG, F. E., K. ADAMES, C. RÜB, S. CHEUNG, N. EASTON *et al.*, 2012 Identification of Genes Required for Alternative Oxidase Production in the Neurospora crassa Gene Knockout Library. G3 (Bethesda) **2:** 1345-1356.

NINOMIYA, Y., K. SUZUKI, C. ISHII and H. INOUE, 2004 Highly efficient gene replacements in Neurospora strains deficient for nonhomologous end-joining. Proc. Natl. Acad. Sci. USA **101:** 12248-12253.

PARK, G., J. A. SERVIN, G. E. TURNER, L. ALTAMIRANO, H. V. COLOT *et al.*, 2011 Global Analysis of Serine-Threonine Protein Kinase Genes in Neurospora crassa. Eukaryot. Cell **10:** 1553-1564.

PARK, W.-H., Y.-W. HAN, S.-W. KIM, S.-H. KIM, K.-W. CHO *et al.*, 2007a Antimycin A induces apoptosis in As4.1 juxtaglomerular cells. Cancer Lett. **251:** 68-77.

PARK, W. H., Y. W. HAN, S. H. KIM and S. Z. KIM, 2007b An ROS generator, antimycin A, inhibits the growth of HeLa cells via apoptosis. J. Cell. Biochem. **102:** 98-109.

POVELONES, M. L., C. TIENGWE, E. GLUENZ, K. GULL, P. T. ENGLUND *et al.*, 2013 Mitochondrial shape and function in trypanosomes requires the outer membrane protein, TbLOK1. Mol. Microbiol. **87:** 713-729.

SARSOUR, E. H., A. L. KALEN and P. C. GOSWAMI, 2013 Manganese Superoxide Dismutase Regulates a Redox Cycle Within the Cell Cycle. Antioxid. Redox Signaling **20:** 1618-1627.

SCHMIDT, B., E. WACHTER, W. SEBALD and W. NEUPERT, 1984 Processing peptidase of Neurospora mitochondria. Eur. J. Biochem. **144:** 581-588.

SCHWEINGRUBER, C., S. C. RUFENER, D. ZÜND, A. YAMASHITA and O. MÜHLEMANN, 2013 Nonsense-mediated mRNA decay — Mechanisms of substrate mRNA recognition and degradation in mammalian cells. Biochim. Biophys. Acta - Gene Regulatory Mechanisms **1829:** 612-623.

SINGHA, U. K., S. SHARMA and M. CHAUDHURI, 2009 Downregulation of Mitochondrial Porin Inhibits Cell Growth and Alters Respiratory Phenotype in Trypanosoma brucei. Eukaryot. Cell **8:** 1418-1428.

SLATER, E. C., 1973 The mechanism of action of the respiratory inhibitor, antimycin. Biochim. Biophys. Acta - Bioenergetics **301:** 129-154.

SOONTORNGUN, N., M. LAROCHELLE, S. DROUIN, F. ROBERT and B. TURCOTTE, 2007 Regulation of Gluconeogenesis in Saccharomyces cerevisiae Is Mediated by Activator and Repressor Functions of Rds2. Mol. Cell. Biol. **27:** 7895-7905.

STEFELY, JONATHAN A., ANDREW G. REIDENBACH, A. ULBRICH, K. ORUGANTY, BRENDAN J. FLOYD *et al.*, 2015 Mitochondrial ADCK3 Employs an Atypical Protein Kinase-like Fold to Enable Coenzyme Q Biosynthesis. Mol. Cell **57:** 83-94.

TANTON, L. L., C. E. NARGANG, K. E. KESSLER, Q. LI and F. E. NARGANG, 2003 Alternative oxidase expression in Neurospora crassa. Fungal Genet. Biol. **39:** 176-190.

TAUCHE, A., U. KRAUSE-BUCHHOLZ and G. RÖDEL, 2008 Ubiquinone biosynthesis in Saccharomyces cerevisiae: the molecular organization of O-methylase Coq3p depends on Abc1p/Coq8p. FEMS Yeast Res. **8:** 1263-1275.

TURCQ, B., K. F. DOBINSON, N. SERIZAWA and A. M. LAMBOWITZ, 1992 A protein required for RNA processing and splicing in Neurospora mitochondria is related to gene products involved in cell cycle protein phosphatase functions. Proc. Natl. Acad. Sci. USA **89:** 1676-1680.

TYLER, L., J. BRAGG, J. WU, X. YANG, G. TUSKAN *et al.*, 2010 Annotation and comparative analysis of the glycoside hydrolase genes in Brachypodium distachyon. BMC Genomics **11:** 1-21.

XU, Y., S. MIRIYALA, F. FANG, V. BAKTHAVATCHALU, T. NOEL *et al.*, 2014 Manganese superoxide dismutase deficiency triggers mitochondrial uncoupling and the Warburg effect. Oncogene.

YUAN, Z.-R., and Y. SHI, 2008 Chloramphenicol Induces Abnormal Differentiation and Inhibits Apoptosis in Activated T Cells. Cancer Res. **68:** 4875-4881.